PHD

Allyl and carbonyl complexes of molybdenum and tungsten.

Hill, Kathleen E.

Award date:
1982

Awarding institution:
University of Bath

ALLYL AND CARBONYL COMPLEXES OF MOLYBDENUM AND TUNGSTEN

submitted by

Kathleen E. Hill

For the Degree of Doctor of Philosophy

of the University of Bath

1982.

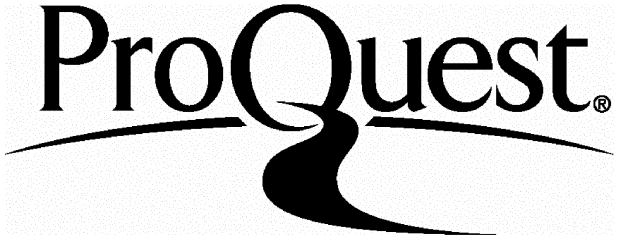

To

My Mother and my Husband.

ACKNOWLEDGEMENTS

Primarily, I would like to thank Drs. B.J. Brisdon and D.A. Edwards for their continual help and advice throughout the course of this work and for their useful suggestions during the writing of this thesis.

My thanks are also due to Dr. M. Murray of the University of Bristol and Mr. P. Benyon of JEOL (U.K.) Ltd., for the measurement of ^{13}C NMR spectra; Dr. M. Drew of the University of Reading for the structural study carried out; Mrs. V. Edwards for painstakingly typing this manuscript, and Dr. J. Charnock for assistance in proof reading the typescript.

I gratefully acknowledge the financial support for this work received from the Science Research Council.

ABSTRACT

This thesis reports an investigation of the solution properties of the compounds $[(\eta^3\text{-}C_3H_4R)M(CO)_2(MeCN)_2X]$ (R = H, M = Mo or W, X = Cl, Br or I; R = Me, M = Mo, X = Cl) and their reactions with various phosphorus and arsenic nucleophiles.

The ionisation of $[(\eta^3\text{-}C_3H_5)W(CO)_2(MeCN)_2Cl]$ to $[(\eta^3\text{-}C_3H_5)W(CO)_2(MeCN)_3]^+[(\eta^3\text{-}C_3H_5)_2W_2(CO)_4Cl_3]^-$ and free nitrile is strongly solvent dependent and slight compared with the molybdenum analogue. No autoionisation process has been detected for the bromo- or iodo- derivatives, nor for the 2-methylallyl molybdenum derivative $[(\eta^3\text{-}2\text{-}MeC_3H_4)Mo(CO)_2(MeCN)_2Cl]$. In some donor solvents solvolysis occurs resulting in the partial formation of $[(\eta^3\text{-}C_3H_4R)M(CO)_2(MeCN)_2(solvent)]^+X^-$ and/or exchange of coordinated MeCN with solvent in the neutral species. The importance of these processes in the reactions of these compounds is discussed.

The reaction of $PMePh_2$ with $[(\eta^3\text{-}C_3H_5)M(CO)_2(MeCN)_2Cl]$ (M = Mo or W) is solvent dependent. In methanol the adducts $[(\eta^3\text{-}C_3H_5)M(CO)_2(PMePh_2)_2Cl]$ are obtained whilst in acetonitrile reductive elimination of the allyl chloride occurs and the metal (O) compounds $[M(CO)_2(MeCN)(PMePh_2)_3]$ are formed. The new anions $[(\eta^3\text{-}C_3H_5)M(CO)_2(PMePh_2)Cl_2]^-$ were detected in the course of this latter reaction and have been isolated as their σ-allylphosphonium salts. Reaction of each of the compounds

$[(\eta^3\text{-}C_3H_5)Mo(CO)_2(PMePh_2)_2Cl]$, $[(\eta^3\text{-}C_3H_5)Mo(CO)_2(MeCN)_3]BF_4$, $Ph_4As[(\eta^3\text{-}C_3H_5)_2Mo_2(CO)_4Cl_3]$ and $[PMePh_2(\sigma\text{-}C_3H_5)][(\eta^3\text{-}C_3H_5)Mo(CO)_2(PMePh_2)Cl_2]$ with excess $PMePh_2$ in acetonitrile results in the final formation of the same metal (0) product $[Mo(CO)_2(MeCN)(PMePh_2)_3]$. The significance of these observations on the mechanism of the reduction of $[(\eta^3\text{-}C_3H_5)Mo(CO)_2(MeCN)_2Cl]$ is discussed.

The compounds $[M(CO)_2(MeCN)(PMePh_2)_3]$ (M = Mo or W) slowly decompose in solution to form mer-$[M(CO)_3(PMePh_2)_3]$ as isolable products. Under suitable conditions the fac-isomers can also be obtained. Both Raman and infrared spectral data have been recorded for these compounds.

Triphenylphosphine causes reduction of $[(\eta^3\text{-}2\text{-}MeC_3H_4)Mo(CO)_2(MeCN)_2Cl]$ and the $\eta^3\text{-}C_3H_5$ analogue, in both methanol and acetonitrile yielding $[Mo(CO)_2(MeCN)_2(PPh_3)_2]$. The only intermediate isolable from these reactions was $[(\eta^3\text{-}2\text{-}MeC_3H_4)Mo(CO)_2(MeCN)(PPh_3)Cl].MeCN$. Differences in the pattern of reactivity of PPh_3 compared with $PMePh_2$ are discussed in terms of steric and electronic effects.

Reactions of $[(\eta^3\text{-}C_3H_5)W(CO)_2(MeCN)_2X]$ with the ditertiary arsines $Ph_2AsCH_2CH_2AsPh_2$ (dae) and $Ph_2AsCH_2AsPh_2$ (dam) and with the secondary phosphine $PHPh_2$, yield complexes of stoichiometry $[(\eta^3\text{-}C_3H_5)W(CO)_2(L_2)X]$ (L_2 = $2PHPh_2$, X = Cl; L_2 = dae, X = Cl, Br or I) and $[(\eta^3\text{-}C_3H_5)_2W_2(CO)_4X_2(dam)]$ (X = Cl or Br). The latter compounds contain dam bridges which are readily cleaved by pyridine (py), $Ph_2PCH_2CH_2PPh_2$ (dpe), $Ph_2PCH_2PPh_2$ (dpm) or chloride ions to give $[(\eta^3\text{-}C_3H_5)W(CO)_2(L_2)X]$ (L_2 = dpm, dpe or 2py) and

$[(\eta^3\text{-}C_3H_5)_2W_2(CO)_4Cl_3]^-$ respectively. Under forcing conditions the nitrile complexes react with dpm, dpe and $PHPh_2$ to give low yields of the tungsten (0) derivatives cis-$[W(CO)_2(L_2)_2]$(L_2 = dpm, dpe or $2PHPh_2$). The molybdenum compounds $[(\eta^3\text{-}C_3H_5)Mo(CO)_2(PHPh_2)_2Cl]$ and cis-$[Mo(CO)_2(PHPh_2)_4]$ have also been prepared for comparative purposes.

Substitution of the MeCN ligands of $[(\eta^3\text{-}C_3H_4R)M(CO)_2(MeCN)_2X]$ by phosphites leads to the adducts $[(\eta^3\text{-}C_3H_4R)M(CO)_2\{P(OR')_3\}_2X]$ [R = H, M = Mo, R' = Me, X = Cl, Br or I; R = H, M = Mo, R' = Et, X = Cl or I; R = H, M = Mo, R' = i-Pr, X = Cl; R = Me, M = Mo, R' = Me, X = Cl; R = H, M = W, R' = Me or Et, X = Cl]. These compounds are stereochemically non-rigid in solution at ambient temperatures. An X-ray single crystal structure determination of $[(\eta^3\text{-}C_3H_5)Mo(CO)_2\{P(OMe)_3\}_2Cl]$ showed it to be of a structural type not previously known for this class of d^4 molybdenum(II) compounds. Its geometry is best described as a pentagonal bipyramid in which the chlorine atom and a carbonyl group are in axial positions and the allyl ligand occupies two adjacent sites in the equatorial girdle. The two dynamic cationic complexes $[(\eta^3\text{-}C_3H_4R)Mo(CO)_2\{P(OMe)_3\}_3]BF_4$ (R = H or Me) have also been characterised and shown to possess a similar pentagonal bipyramidal structure in which the chloride ion is replaced by a $P(OMe)_3$ ligand.

CONTENTS

	Page
ABSTRACT	(iv)
CONTENTS	(vii)
FIGURES	(xiii)
TABLES	(xvii)
ABBREVIATIONS	(xxi)
CHAPTER ONE: INTRODUCTION	
INTRODUCTION	1
TRANSITION METAL-ALLYL COMPOUNDS	2
(i) 1-η or η^1-allyl, 2. (ii) μ-allyl, 2. (iii) 1-3-η or η^3-allyl, 2.	
PREPARATION OF η^3-ALLYL TRANSITION METAL COMPOUNDS	8
(i) From Allyl Grignards and Related Metal Compounds, 9. (ii) Oxidative Addition of Allylic Halides to Transition Metal Compounds, 10. (iv) From Mono-olefins, 12. (v) From Conjugated Dienes, 12. (v) η^1-Allyl $\longrightarrow$ η^3-Allyl Conversions, 15. (vi) From Allenes, 16. (vii) Phase Transfer Catalysis, 17. (viii) Novel Syntheses, 20.	
STRUCTURE AND BONDING IN η^3-ALLYL TRANSITION METAL COMPLEXES.	21
BONDING	26
SPECTROSCOPIC CHARACTERISATION OF η^3-ALLYL TRANSITION METAL COMPOUNDS	32
PROTON NUCLEAR MAGNETIC RESONANCE SPECTROSCOPY	32

Coupling of the Allylic Protons to Other Nuclei, 36.
Fluxional η^3-Allyl Transition Metal Compounds, 45:
(i) syn-anti exchange, 45; (ii) syn-syn, anti-anti
exchange, 48; (iii) conformational isomerism, 51.
Base Induced η^3-Allyl Rearrangements, 53.
13-CARBON NUCLEAR MAGNETIC RESONANCE SPECTROSCOPY 56
VIBRATIONAL SPECTROSCOPY 60
η^3-ALLYL COMPLEXES OF THE GROUP VI TRANSITION METALS 66
The Reactivity of $[(\eta^3\text{-}C_3H_5)M(CO)_2(MeCN)_2X]$, 74.
CHAPTER TWO: SOLUTION PROPERTIES OF
$[(\eta^3\text{-}C_3H_4R)M(CO)_2(MeCN)_2X]$
INTRODUCTION 77
EXPERIMENTAL 80
a. Preparation of $[(\eta^3\text{-}C_3H_4R)Mo(CO)_2(MeCN)_2X]$,
(R = H, X = Cl or Br; R = Me, X = Cl), 80;
b. Preparation of $[(\eta^3\text{-}C_3H_5)M(CO)_2(MeCN)_2X]$, (M = Mo,
X = I; M = W, X = Cl, Br or I), 80. Preparation of
$[(\eta^3\text{-}C_3H_4R)M(CO)_2(MeCN)_3]BF_4$ (M = Mo or W, R = H;
M = Mo, R = Me), 81. Preparation of $Ph_4As[(\eta^3\text{-}C_3H_5)_2Mo_2(CO)_4Cl_3]$, 81; Preparation of $Ph_4As[(\eta^3\text{-}C_3H_5)_2W_2(CO)_4Cl_3]$, 82.
RESULTS AND DISCUSSION 84
The Cationic Species $[(\eta^3\text{-}C_3H_4R)M(CO)_2(MeCN)_3]^+$ as
their BF_4^- salts, 84: Solution Behaviour of
$[(\eta^3\text{-}C_3H_4R)M(CO)_2(MeCN)_3]BF_4$, 86. The Dimeric Anions
$[(\eta^3\text{-}C_3H_5)_2M_2(CO)_4Cl_3]^-$ As Their Ph_4As Salts, 96.
The Neutral Complexes $[(\eta^3\text{-}C_3H_4R)M(CO)_2MeCN)_2Cl]$
(R = H, M = Mo or W; R = Me, M = Mo), 102: Solution
Behaviour of $[(\eta^3\text{-}C_3H_5)W(CO)_2(MeCN)_2X]$, (X = Cl, Br
or I),112; Solution Behaviour of $[(\eta^3\text{-}2\text{-}MeC_3H_4)Mo(CO)_2(MeCN)_2Cl]$. (IV), 119; Solution Behaviour of

$[(\eta^3\text{-}C_3H_4R)Mo(CO)_2(MeCN)_2Cl]$ in CD_3OD, (R = H, Me), 121.

CONCLUSIONS 122

CHAPTER THREE: THE REACTIONS OF SOME DITERTIARY PHOSPHINES AND ARSINES WITH $[(\eta^3\text{-}C_3H_5)W(CO)_2(MeCN)_2X]$ (X = Cl, Br or I)

INTRODUCTION 124

EXPERIMENTAL 125

The Reaction of $[(\eta^3\text{-}C_3H_5)W(CO)_2(MeCN)_2Cl]$ with 1,2-Bis(diphenylphosphino)ethane under Forcing Conditions, 125. The Reaction of $[(\eta^3\text{-}C_3H_5)W(CO)_2(MeCN)_2Cl]$ with Bis(diphenylphosphino)methane under Forcing Conditions, 126. The Reaction of $[(\eta^3\text{-}C_3H_5)W(CO)_2(MeCN)_2X]$, (X = Cl, Br or I) with 1,2-Bis(diphenylarsino)ethane, 126. The Reaction of $[(\eta^3\text{-}C_3H_5)W(CO)_2(MeCN)_2X]$ (X = Cl or Br) with Bis(diphenylarsino)methane, 127. Reactions of $[(\eta^3\text{-}C_3H_5)_2W_2(CO)_4Cl_2(dam)]$, toluene with Other Ligands, 127: (i) With the ditertiary phosphines bis(diphenylphosphino)methane and 1,2-bis(diphenylphosphino)ethane, 127; (ii) With pyridine, 128, (iii) With tetraphenylarsoniumchloride, 128.

RESULTS AND DISCUSSION 130

The Reactions of $[(\eta^3\text{-}C_3H_5)W(CO)_2(MeCN)_2Cl]$ with the Ditertiary Phosphines bis(diphenylphosphino)methane and 1,2-bis(diphenylphosphino)ethane, 130. The Reactions of $[(\eta^3\text{-}C_3H_5)W(CO)_2(MeCN)_2X]$ with the Ditertiary Arsines bis(diphenylarsino)methane and

1,2-bis(diphenylarsino)ethane, 132: Mass Spectra, 134; ^{1}H NMR Spectra, 141; Chemical Studies, 154.

CHAPTER FOUR: THE REACTIONS OF PHOSPHITE LIGANDS WITH $[(\eta^{3}\text{-}C_3H_4R)M(CO)_2(MeCN)_2X]$

INTRODUCTION 159

EXPERIMENTAL 160

Preparation of $[(\eta^{3}\text{-}C_3H_4R)M(CO)_2\{P(OR')_3\}_2X]$, 160. Preparation of $[(\eta^{3}\text{-}C_3H_4R)Mo(CO)_2\{P(OMe)_3\}_3]BF_4$, 161. Structure Determination, 162: Crystal data, 162; Solution and Refinement, 163.

RESULTS AND DISCUSSION 165

Solid-State Structure of $[(\eta^{3}\text{-}C_3H_5)Mo(CO)_2\{P(OMe)_3\}_2Cl]$(XXII), 167. Infrared Spectra, 184. NMR Spectra 187. The Dynamic Behaviour of the Complexes $[(\eta^{3}\text{-}C_3H_4R)M(CO)_2\{P(OR')_3\}_2X]$, 202. The Preparation and Characterisation of the Complexes $[(\eta^{3}\text{-}C_3H_4R)Mo(CO)_2\{P(OMe)_3\}_3]BF_4$, (R = H or Me), 207: ^{1}H NMR Spectra, 209; ^{13}C NMR Spectra, 212; ^{31}P NMR Spectra, 215. Addendum 217.

CHAPTER FIVE: THE REACTIONS OF MONOTERTIARY PHOSPHINES AND DIPHENYLPHOSPHINE WITH $[(\eta^{3}\text{-}C_3H_4R)M(CO)_2(MeCN)_2Cl]$

INTRODUCTION 219

EXPERIMENTAL 220

Reaction of $[(\eta^{3}\text{-}C_3H_5)M(CO)_2(MeCN)_2Cl]$ with Tricyclohexylphosphine, 221. Reaction of $[(\eta^{3}\text{-}C_3H_5)M(CO)_2(MeCN)_2Cl]$ with Diphenylphosphine, 221: Preparation of $[(\eta^{3}\text{-}C_3H_5)M(CO)_2(PHPh_2)_2Cl]$, (M = Mo or W), 221; Preparation of cis-$[M(CO)_2(PHPh_2)_4]$, 221. Reaction

of [(η^3-C_3H_4R)$M(CO)_2(MeCN)_2Cl$] (R = H, M = Mo, or W; R = Me, M = Mo) with Methyldiphenylphosphine, 222: Preparation of [$M(CO)_2(MeCN)(PMePh_2)_3$] a) From [(η^3-C_3H_5)$Mo(CO)_2(MeCN)_2Cl$], 222; b) From [(η^3-C_3H_5)$W(CO)_2(MeCN)_2Cl$], 222; c) From [(η^3-C_3H_4R)$Mo(CO)_2(MeCN)_3$]BF_4 (R = H or Me), 223; d) From Ph_4As[(η^3-C_3H_5)$_2Mo_2(CO)_4Cl_3$], 223; e) From [(η^3-C_3H_5)$M(CO)_2(PMePh_2)_2Cl$], 223. Preparation of [(η^3-C_3H_4R)$M(CO)_2(PMePh_2)_2Cl$] (R = H, M = Mo or W; R = Me, M = Mo), 224. Preparation of [$PMePh_2$ (σ-C_3H_5)][(η^3-C_3H_5)$M(CO)_2$ $(PMePh_2)Cl_2$] (M = Mo or W), 225. Preparation of mer- $M(CO)_3(PMePh_2)_3$] (M = Mo or W), 225. Preparation of fac- [$M(CO)_3(PMePh_2)_3$], (i) From cis-mer- [$M(CO)_2(MeCN)(PMePh_2)_3$], 226; (ii) From mer- [$Mo(CO)_3(PMePh_2)_3$], 226. Reaction of [(η^3-2-MeC_3H_4)$Mo(CO)_2(MeCN)_2Cl$] with Triphenylphosphine: Preparation of [$Mo(CO)_2(MeCN)_2(PPh_3)_2$], 226; Preparation of [(η^3-2-MeC_3H_4)$Mo(CO)_2(MeCN)(PPh_3)Cl$]. MeCN, 227.

RESULTS AND DISCUSSION 230

Reaction of [(η^3-C_3H_5)$M(CO)_2(MeCN)_2Cl$] with Tricyclohexylphosphine, 230. Reaction of [(η^3-C_3H_5)$M(CO)_2(MeCN)_2Cl$] (M = Mo or W) with Diphenylphosphine, 231: Characterisation of the Products obtained from the Reaction of [(η^3-C_3H_5) $M(CO)_2(MeCN)_2Cl$] (M = Mo or W) with Diphenylphosphine, 234; (i) [(η^3-C_3H_5)$M(CO)_2(PHPh_2)_2Cl$] (M = Mo or W), 234; (ii) cis-[$M(CO)_2(PHPh_2)_4$] (M = Mo or W), 237.

Reactions of [(η^3-C_3H_4R)$M(CO)_2(MeCN)_2Cl$]
(R = H, M = Mo or W; R = Me, M = Mo) with
Methyldiphenylphosphine, 238.
Characterisation and Properties of the Products
obtained from the Reaction of [(η^3-C_3H_4R)
$M(CO)_2(MeCN)_2Cl$] (R = H, M = Mo or W; R = Me,
M = Mo) with Methyldiphenylphosphine, 246:
(i) [(η^3-C_3H_4R)$M(CO)_2(PMePh_2)_2Cl$] (R = H,
M = Mo or W; R = Me, M = Mo), 246;
(ii) [$PMePh_2(\sigma$-$C_3H_5)$][(η^3-C_3H_5)$M(CO)_2(PMePh_2)Cl_2$],
(M = Mo or W), 249; (iii) [$M(CO)_2(MeCN)(PMePh_2)_3$],
253. Characterisation of mer- and fac- [$M(CO)_3$
$(PMePh_2)_3$] (M = Mo or W), 256; ^{1}H NMR, 257;
Vibrational Spectra, 257: The δ(MCO) and ν(MC)
region, 263. Reactions of [(η^3-2-MeC_3H_4)$Mo(CO)_2$
$(MeCN)_2Cl$] with Triphenylphosphine, 265:
Characterisation of the Compound [(η^3-2-MeC_3H_4)
$Mo(CO)_2(MeCN)(PPh_3)Cl$].MeCN, 267; ^{1}H NMR
Spectrum, 268

APPENDICES 272

1. APPLICATION OF THE HÜCKEL MOLECULAR ORBITAL
METHOD TO THE η^3-ALLYL ENTITY 272

2. GROUP THEORETICAL TREATMENT OF SELECTED
MOLECULES AND SYSTEMS 280

1. The η^3-Allyl-Metal System: C_s Symmetry, 280
2. The Anion [(η^3-C_3H_5)$_2M_2(CO)_4Cl_3$]$^-$:
C_2 Symmetry, 285. 3. The Tricarbonyl Complexes
Mer- and Fac-[$M(CO)_3P_3$]: a) Mer-Tricarbonyls:

C_{2v} Symmetry 290; b) Fac-Tricarbonyls: C_{3v} Symmetry 293.

3. SOLVENTS, REAGENTS, PHYSICAL METHODS AND INSTRUMENTATION 295

General, 295. Solvents, 295. Reagents, 295. Infrared Spectroscopy, 296. Raman Spectroscopy, 296. Mass Spectroscopy, 296. NMR Spectroscopy, 297. Conductivity, 297. Analysis, 297. Melting Points, 297.

4. CALCULATED AND OBSERVED STRUCTURE FACTORS AND THERMAL PARAMETERS 298

REFERENCES 307

FIGURES

1.1: Jonassen's proposed bonding scheme for $[C_4H_7Co(CO)_3]$ 8

1.2: Schematic drawing of the $[(\eta^3\text{-}C_3H_5)PdCl]_2$ dimer 22

1.3: The structures of (i) $[(\eta^3\text{-}2\text{-}MeC_3H_4)Pd(PPn_3)Cl]$ and (ii) $[(\eta^3\text{-}C_3H_5)W(CO)(\eta^5\text{-}C_5H_5)(NO)I]$ 23

1.4: The general orientation of the η^3-allyl ligand to the coordination plane of the molecule 24

1.5: The π-molecular orbitals of the allyl anion 26

1.6: η^3-Allyl-transition metal bonding interactions 29

1.7: The symmetrical η^3-allyl group 33

1.8: The resonance pattern for an AM_2X_2 spin system 33

1.9: The two possible isomeric forms of $(\eta^3\text{-}1\text{-}RC_3H_4)$ 35

1.10: Largest J(P-H) occurs between atoms which are mutually trans. 40

1.11: The stereochemistries for various η^3-allyl-phosphorus donor ligand-transition metal compounds 44

1.12: Syn-anti proton exchange 45

1.13: Syn-syn, anti-anti proton exchange 48

1.14: The trigonal twist rearrangement proposed for $[(\eta^3\text{-}C_3H_5)Mo(CO)_2(P\text{-}P)X]$ Complexes 49

1.15: Symmetrical (i) and unsymmetrical (ii) isomers of $[(\eta^3\text{-}C_3H_5)Mo(CO)_2(pd)py]$ 50

1.16: The two isomeric forms of $[(\eta^3\text{-}C_3H_5)Fe(CO)_3X]$ 52

1.17: Rotation of the η^3-allyl group in its own plane in $[(\eta^3\text{-}C_3H_5)_3Rh]$ 53

1.18: Possible isomeric forms for $[(\eta^3\text{-}C_3H_5)W(CO)_4X]$ 67

1.19: The fac-arrangement of the $[(\eta^3\text{-allyl})M(CO)_2]$unit 69

1.20: The (i) symmetrical and (ii) unsymmetrical arrangements of the L_2 and X ligands in $[(\eta^3\text{-allyl})M(CO)_2L_2X]$ 72

2.1: The molecular structure of $[(\eta^3\text{-}C_3H_5)Mo(CO)_2(MeCN)_3][(\eta^3\text{-}C_3H_5)_2Mo_2(CO)_4Cl_3]$ 78

2.2: ^1H NMR spectrum of $[(\eta^3\text{-}C_3H_5)Mo(CO)_2(MeCN)_3]BF_4$ in CD_3CN 91

2.3: Variable temperature ^1H NMR spectra of $[(\eta^3\text{-}C_3H_5)W(CO)_2(MeCN)_3]BF_4$ recorded in CD_3CN 92

2.4: An intramolecular rearrangement process for $[(\eta^3\text{-}C_3H_4R)M(CO)_2(MeCN)_3]^+$ 93

2.5: Infrared spectra (ν(CO) region) of (X) in CH_3OH solution recorded (a) immediately; (b) after 10 min. 95

2.6: Solid state stereochemistry of $[(\eta^3\text{-}C_3H_5)_2Mo_2(CO)_4Cl_3]^-$ 98

2.7: Far-infrared Spectra of the Complexes $[(\eta^3\text{-}C_3H_5)Mo(CO)_2(MeCN)_2X]$ 107

2.8: Far-infrared Spectra of the Complexes $[(\eta^3\text{-}C_3H_5)W(CO)_2(MeCN)_2X]$ 108

2.9: ^1H NMR Spectra of $[(\eta^3\text{-}C_3H_5)W(CO)_2(MeCN)_2Br]$ in $(CD_3)_2CO$ at (i) $+50^oC$ and (ii) -40^oC 117

3.1: The characteristic isotope pattern for tungsten 134

3.2: Structure of the $AsC_{12}H_8$ fragment 137

3.3: ^1H NMR Spectrum of $[(\eta^3\text{-}C_3H_5)W(CO)_2(dae)X]$ in CD_2Cl_2 144

3.4: ^1H NMR Spectra for $[(\eta^3\text{-}C_3H_5)W(CO)_2(dae)I]$ recorded at (a) $\pm$ 0, (b) -60 and (c) -125^oC 145

3.5: A structure for $[(\eta^3\text{-}C_3H_5)W(CO)_2(dae)X]$, lacking a plane of symmetry 146

3.6: The molecular structure of dinuclear $[Re_2(CO)_6Cl_2(dam)]$ 148

4.1: The Molecular Structure of $[(\eta^3\text{-}C_3H_5)Mo(CO)_2\{P(OMe)_3\}_2Cl]$ 168

4.2: Disposition of the trimethylphosphite groups 177

4.3: Ligand arrangements (i) commonly observed for compounds of the type $[(\eta^3\text{-allyl})Mo(CO)_2L_2L']$ and (ii) found for $[(\eta^3\text{-}C_3H_5)Mo(CO)_2\{P(OMe)_3\}_2Cl]$. 180

4.4: The carbonyl region of the solid state infrared spectrum of $[(\eta^3\text{-}C_3H_5)Mo(CO)_2\{P(OMe)_3\}_2Cl]$ 184

4.5: Solution ($CHCl_3$) infrared spectrum (carbonyl region) of $[(\eta^3\text{-}C_3H_5)Mo(CO)_2\{P(OMe)_3\}_2Cl]$. 186

4.6: The inequivalence of P and P' to H_M and $H_{M'}$ in the solid state structure of $[(\eta^3\text{-}C_3H_5)Mo(CO)_2\{P(OMe)_3\}_2Cl]$ 194

4.7: The ^1H NMR spectrum of the syn protons of $[(\eta^3\text{-}C_3H_5)Mo(CO)_2\{P(OMe)_3\}_2Cl]$ at various temperatures between +32 and -40°C 195

4.8: The ^1H NMR spectra of the syn allylic protons of $[(\eta^3\text{-}2\text{-}MeC_3H_4)Mo(CO)_2\{P(OMe)_3\}_2Cl]$ at (a) 54°C and (b) 45°C, and the calculated theoretical spectra at (c) 54°C and (d) 45°C 199

4.9: Variation of J_{HP}, $J_{HP'}$, $J_{HH'}$ and $J_{PP'}$ with temperature for (XXV) 200

4.10: Pentagonal bipyramid to capped trigonal prism conversion 205

5.1: Diagrammatic representation of the X part of an XAA'X' spin system 235

5.2: The ^1H NMR Spectrum of $[PMePh_2(\sigma\text{-}C_3H_5)]$ $[(\eta^3\text{-}C_3H_5)Mo(CO)_2(PMePh_2)Cl_2]$ 251

5.3: Normal ν(CO) modes of $[M(CO)_3L_3]$ in C_{2v} Symmetry 259

5.4: The ^1H NMR Spectrum of (XXXXVIII) in CD_3OD at -20°C 269

5.5: The ^1H NMR Spectrum of (XXXXVIII) in CD_3OD at 60°C 270

TABLES

1.1: Examples of χ for various η^3-Allyl Transition Metal Compounds 25

1.2: Chemical Shift and Coupling Constant Data for Syn- and Anti- $[(\eta^3\text{-}1\text{-}MeC_3H_4)Co(CO)_3]$ 36

1.3: Examples of J_{Pt-H} Values for $[(\eta^3\text{-allyl})Pt]$ Compounds 38

1.4: Phosphorus-Hydrogen Coupling Constants (Hz) for some η^3-Allyl-M Complexes 42

1.5: ^{13}C NMR Chemical Shifts and Coupling Constants for η^3-Allyl Compounds 57

1.6: Numbers and Symmetries of the Normal Modes for an $[(\eta^3\text{-}C_3H_5)\text{-}M]$ Group 62

1.7: Vibrational Frequencies (cm^{-1}) and Proposed Assignments for the $\eta^3\text{-}C_3H_5\text{-}M$ Modes in Various Compounds 63

1.8: The Geometry of the $[(\eta^3\text{-allyl})M(CO)_2]$ Unit in Different structures 70

2.1: Yields and Analytical Data 83

2.2: Selected Infrared Data for the Complexes $[(\eta^3\text{-}C_3H_4R)M(CO)_2(MeCN)_3]BF_4$ 85

2.3: Solution Infrared Spectral Data [ν(CO) region] for $[(\eta^3\text{-}C_3H_4R)M(CO)_2(MeCN)_3]BF_4$ 87

2.4: ^1H NMR Data for $[(\eta^3\text{-allyl})M(CO)_2(MeCN)_3]BF_4$ Recorded at 30°C 88

2.5: Selected Infrared Data (2000-200cm^{-1}) for the Dimeric Anions $[(\eta^3\text{-}C_3H_5)_2M_2(CO)_4Cl_3]^-$ as their Ph_4As^+ salts (Nujol Mulls) 97

2.6: Solution Infrared Spectral Data [ν(CO) region]for $Ph_4As[(\eta^3\text{-}C_3H_5)_2M_2(CO)_4Cl_3]$ 99

2.7: ^{1}H NMR Data for $Ph_4As[(\eta^3\text{-}C_3H_5)_2W_2(CO)_4Cl_3]$ 101

2.8: Selected Infrared Data (4000-600cm^{-1}) for the complexes $[(\eta^3\text{-}C_3H_4R)M(CO)_2(MeCN)_2X]$ 104

2.9: Infrared spectra (400-40cm^{-1}) of the Complexes $[(\eta^3\text{-}C_3H_4R)M(CO)_2(MeCN)_2X]$ 105

2.10: The Mass Spectrum of $[(\eta^3\text{-}C_3H_5)W(CO)_2(MeCN)_2Cl]$ 110

2.11: ^{1}H NMR Data for $[(\eta^3\text{-}C_3H_5)W(CO)_2(MeCN)_2X]$ (X = Cl, Br and I) 113

2.12: ^{1}H NMR Data for $[(\eta^3\text{-}C_3H_5)W(CO)_2(MeCN)_2X]$ in $(CD_3)_2CO$ 115

2.13: ^{1}H NMR Data for $[(\eta^3\text{-}C_3H_4R)Mo(CO)_2(MeCN)_2Cl]$ Recorded at 26^{o}C 120

3.1: Yields, Melting Points and Analytical Data 129

3.2: Selected Infrared Spectral Data for the Complexes $[(\eta^3\text{-}C_3H_5)W(CO)_2(dae)X]$ (X = Cl, Br or I) 133

3.3: Tungsten-containing Ions in the Mass Spectra of $[(\eta^3\text{-}C_3H_5)W(CO)_2(dae)X]$. (Based on ^{182}W only) 136

3.4: ^{1}H NMR Data for the Complexes $[(\eta^3\text{-}C_3H_5)W(CO)_2(dae)X]$ (X = Cl, Br and I) 140

3.5: Transition Energies and Intensities for the AA' part of the Methylene Region of $Ph_2As(CH_2)_2AsPh_2$ in Complex (XVI) 142

3.6: Coupling Constants for the Methylene Protons of $Ph_2As(CH_2)_2AsPh_2$ in the Complexes $[(\eta^3\text{-}C_3H_5)W(CO)_2(dae)X]$ 143

3.7: Selected Infrared Spectral Data for the Complexes $[(\eta^3\text{-}C_3H_5)_2W_2(CO)_4X_2dam]$ (X = Cl or Br) 148

3.8: ^1H NMR Data for the Complexes $[(\eta^3\text{-}C_3H_5)_2W_2(CO)_4X_2dam]$, (X = Cl or Br) 149

3.9: Possible Arrangements of the η^3-Allyl and Carbonyl ligands for the Compounds $[(\eta^3\text{-}C_3H_5)_2W_2(CO)_4X_2dam]$ 152

3.10: ^1H NMR Data for the Complexes $[(\eta^3\text{-}C_3H_5)W(CO)_2L_2Cl]$ (L_2 = dpe, dpm or 2py) 156

4.1: Yields, Melting Points and Analytical Data 164

4.2: Atomic Coordinates (x 10^4) with Estimated Standard Deviations in Parentheses 170

4.3: Interatomic Distances (Å) and Angles (°) with Standard Deviations in Parentheses 171

4.4: Least Squares Planes with Deviations (Å) of Atoms from the Planes 175

4.5: Selected Infrared Data for the Complexes $[(\eta^3\text{-}C_3H_4R)M(CO)_2\{P(OR')_3\}_2X]$ 182

4.6: ^1H and $^{31}P\{^1H\}$ NMR Data for the Complexes $[(\eta^3\text{-}C_3H_4R)M(CO)_2\{P(OR')_3\}_2X]$ 188

4.7: ^{13}C NMR Data for the Complexes $[(\eta^3\text{-}C_3H_4R)Mo(CO)_2\{P(OMe)_3\}_2L']^{+,0}$ 190

4.8: Coalescence Temperature Ranges for the Complexes $[(\eta^3\text{-}C_3H_4R)M(CO)_2\{P(OR')_3\}_2X]$ 197

4.9: Coupling Constants for the syn Protons of the Allyl in $[(\eta^3\text{-}2\text{-}MeC_3H_4)Mo(CO)_2\{P(OMe)_3\}_2Cl]$ 198

4.10: ^1H and ^{31}P NMR Data for the Complexes $[(\eta^3\text{-}C_3H_4R)Mo(CO)_2\{P(OMe)_3\}_3]BF_4$ 210

5.1: Melting Points and Analytical Data 228

5.2: Selected Infrared Data for the Compounds $[M(CO)_2(Pcy_3)_2(MeCN)_2]$ and trans-$[M(CO)_4(Pcy_3)_2]$ 230

5.3: Selected Infrared Data for $[(\eta^3\text{-}C_3H_5)M(CO)_2(PHPh_2)_2Cl]$ and cis-$[M(CO)_2(PHPh_2)_4]$, (M = Mo or W) 232

5.4: ^1H NMR Data for the Compounds $[(\eta^3\text{-}C_3H_5)M(CO)_2(PHPh_2)_2Cl]$ (M = Mo or W) 233

5.5: Electronic Parameters and Cone Angles for Phosphorus Ligands 240

5.6: ^1H NMR and Selected Infrared Spectral Data for the Compounds $[(\eta^3\text{-}C_3H_4R)M(CO)_2(PMePh_2)_2Cl]$ 248

5.7: ^1H NMR and Selected Infrared Spectral Data for the Compounds $[PMePh_2(\sigma\text{-}C_3H_5)][(\eta^3\text{-}C_3H_5)M(CO)_2(PMePh_2)Cl_2]$ (M = Mo or W) 252

5.8: Vibrations of an $[M(CO)_3]$ Unit in C_{2v} and C_{3v} Symmetries 258

5.9: Vibrational Spectra of Solid mer- and fac-$[M(CO)_3(PMePh_2)_3]$ in the Carbonyl Region 260

5.10: Solid State Vibrational Spectra between 700-300cm^{-1} for the Complexes mer- and fac-$[M(CO)_3(PMePh_2)_3]$ (M = Mo or W) and for $PMePh_2$ (liquid) 262

ABBREVIATIONS

a	asymmetric
acac	acetylacetonate
Ar	aryl
ax	axial
bipy	2,2'-bipyridine
Bu	butyl
COC	capped octahedron
COD	cycloocta-1,5,-diene
Cp	η^5-cyclopentadienyl
CTP	capped trigonal prism
Cy	cyclohexyl
dae	1,2-bis(diphenylarsino)ethane
dam	bis(diphenylarsino)methane
dape	1-diphenylarsino-2-diphenylphosphinoethane
diars	1,2-bis(dimethylarsino)benzene
dme	1,2-dimethyloxyethane
dpe	1,2-bis(diphenylphosphino)ethane
dpm	bis(diphenylphosphino)methane
eq.	equation
Et	ethyl
hv	ultra violet radiation
m*	metastable
Me	methyl
PB	pentagonal bipyramid
pd	pentane-2,4-dionate
Ph	phenyl

phen	1,10-phenanthroline
Pr	propyl (i-iso)
py	pyridine
pz	pyrazolyl (Hpz = pyrazine; $\overbrace{CH : CHCH : NNH}$)
R	alkyl
r.t.	ambient temperature
salal	N-phenylsalicylideneiminato anion
THF	tetrahydrofuran
TMS	tetramethylsilane
ψ	molecular orbital
ϕ	atomic orbital
$\triangle$	heat
Λ	conductivity
Γ	group theoretical representation

Nuclear Magnetic Resonance (NMR):

d	doublet
J	coupling constant (Hz)
m	multiplet
p.p.m.	parts per million
q	quartet
s	singlet
t	triplet
δ	chemical shift

Infrared (IR) and Raman (R) Spectra:

br	broad
m	medium
s	strong

sh	shoulder
shp	sharp
v	very
w	weak
δ	deformation
ν	stretching vibration

CHAPTER ONE

INTRODUCTION

INTRODUCTION

Recent interest in the chemistry of transition metal-allyl complexes has undoubtedly been stimulated by the discovery of their catalytic importance [1-6]. They have been found to be extremely effective catalysts* for the stereospecific polymerisation and oligomerisation of alkenes and dienes[1, 7-10] and participate in the isomerisation[13-16], oxidation[17], hydrogenation[18,19] and carbonylation[20,21] reactions of unsaturated organic compounds. These studies, which have been carried out largely using platinum metal complexes are well documented in various review articles[1,3,7,10], and have led to the discovery of many other useful η^3-allyl complexes[22-26] including some which have been successfully employed in the synthesis of natural products[27-29].

The unusual bonding and structural aspects of η^3-allyl complexes have also attracted much attention[30-32], as has the interpretation of their often complicated spectroscopic features[33].

The work described in this thesis concerns the reactivity of the η^3-allylic complexes $[(\eta^3\text{-}C_3H_4R)M(CO)_2(MeCN)_2X]$ (where M = Mo, W, and X = halide and R = H or Me) towards various phosphorus and arsenic ligands. The spectroscopic properties of the products and their mode of formation is discussed.

* The catalytic activity of η^3-allyl complexes is often enhanced by the use of a co-catalyst such as a Lewis acid[11,12].

TRANSITION METAL-ALLYL COMPOUNDS

A transition metal-allyl compound may be classified as one of three types, depending on the mode of allyl to metal bonding involved .

(i) 1-η or η^1-allyl; in these compounds the allyl group acts as a one electron donor with a terminal carbon atom σ-bonded to the metal atom and a localised double bond between the two remaining carbon atoms as in complexes such as $[(\eta^1\text{-}C_3H_5)Nb(CS_2)(\eta^5\text{-}C_5H_5)_2]$ [35] and $[(\eta^1\text{-}C_3H_5)Mn(CO)_5]$ [36].

(ii) μ-allyl; the allyl group bridges two metal atoms, normally being σ-bonded to one through a terminal carbon atom and π-bonded to the other via the localised allyl double bond as in $[Pt(\mu\text{-}C_3H_5)acac]_2$ [37], $[(\eta^3\text{-}C_3H_5)Cr(\mu\text{-}C_3H_5)]_2$ [38] and $[Pt(\mu\text{-}C_3H_5)Cl]_4$ [37]. There is also one novel η^3-allyl complex $[Pd_3\{\mu\text{-}[\eta^3\text{-}C_3(Ph)(p\text{-}MeOC_6H_4)_2]_2\}(acac)_2]$ [39], in which symmetrical η^3-allyl ligands with equal C-C bond lengths (1.42 and 1.43Å) act as bridging ligands.

(iii) 1-3-η or η^3-allyl; the bond between the allyl group and the metal atom is delocalised and multicentric. All three carbon atoms are involved in bonding to the metal but not always equally. This is often reflected in the C-C bond lengths of the allyl ligand which may be equal or substantially different giving rise to symmetrical or unsymmetrical η^3-allyls respectively. For most

d-block transition metal compounds the mode of bonding (η^1 / η^3) of the allyl fragment is largely dependent upon the electronic requirements of the metal atom in its aim to attain a stable eighteen electron configuration, but by far the most prolific, and of most relevance to the work described in this thesis, are the η^3-allyl transition metal species.

Smidt and Hafner[40] working with $[(\eta^3\text{-}C_3H_5)PdCl]_2$ were the first to propose that the coordinated allyl group could be regarded as a delocalised π-electron system, and that its bonding to the metal could be compared to that in η^5-cyclopentadienyl-metal complexes. A year later, in 1960, Heck and Breslow[41] used ^{1}H NMR spectroscopy to show that the allyl group in (η^3-allyl)cobalt-tricarbonyl was indeed symmetrically bonded to the metal atom. To date many different forms of the η^3-allyl group have been identified. These vary from the isolated three carbon system with or without substituents at one or more of the carbon atoms, through carbocyclic rings to heteronuclear η^3-skeleton systems. Shown below are some examples of the many different types of η^3-allyl moiety whose structures have either been determined by X-ray diffraction studies or elucidated by NMR spectroscopy.

(a) Unsubstituted η^3-C_3H_5, as in $[(\eta^3\text{-}C_3H_5)_2Ru(PPh_3)_2]$[42], $[(\eta^3\text{-}C_3H_5)PdCl]_2$[43] and $[(\eta^3\text{-}C_3H_5)Co(CO)_3]$[44].

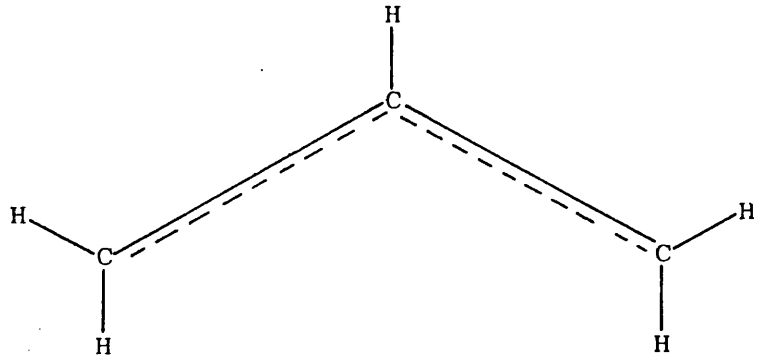

(b) Substituted (η^3-allyl) complexes[45-48].

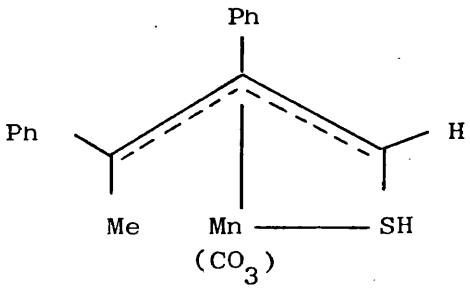

(47)

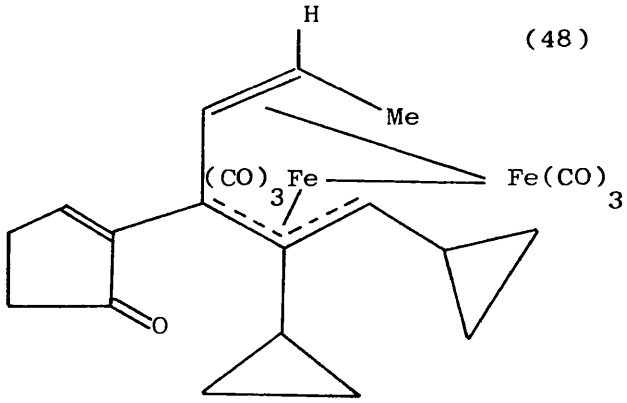

(48)

(c) η^3-allyl as part of a larger hydrocarbon system[49-51].

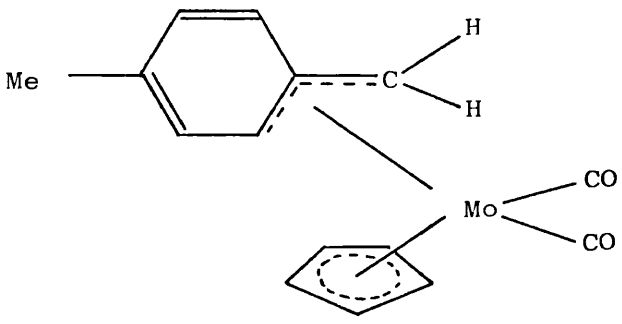

(49)

(d) Cyclic η^3-allyl systems. Examples of complexes in which part of a cyclic ligand is bound to a transition metal in a trihapto-manner may be found for a variety of ring sizes. These range from the special case of the three membered cyclopropenyl ring to the much larger and much less common seven, eight and nine-membered cyclic systems.

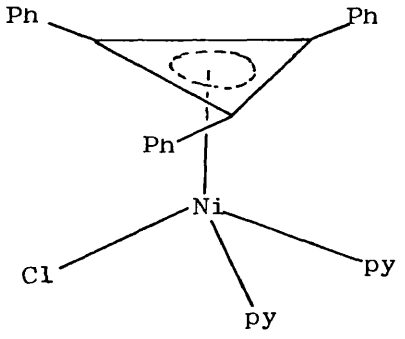

(52)

(53)

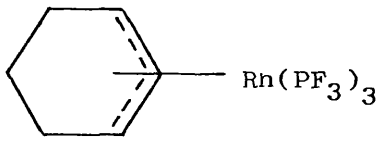

(54)

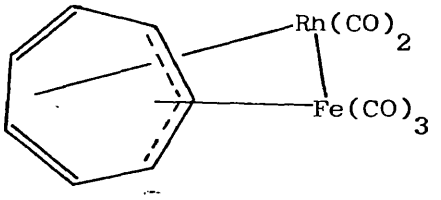

(55)

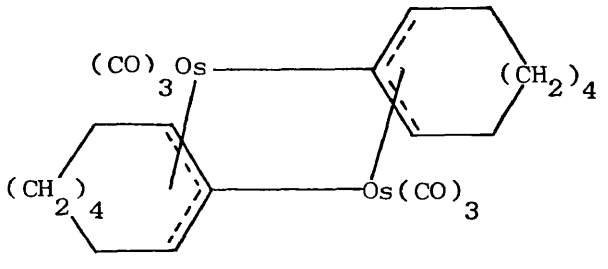

(e) The variety of heteronuclear η^3-allyl systems is also considerable as shown below:

"oxo- η^3-allyl"[57]

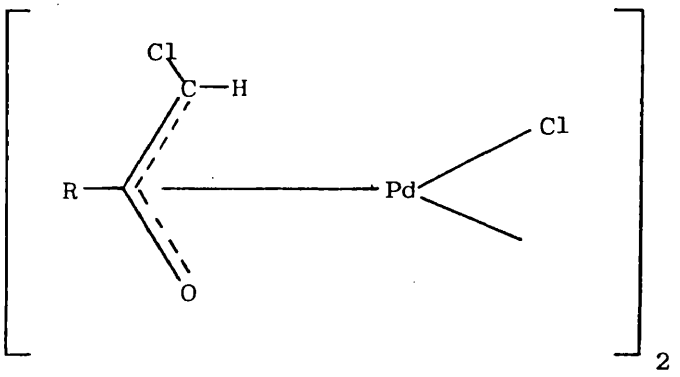

"diazoallyl"[58]

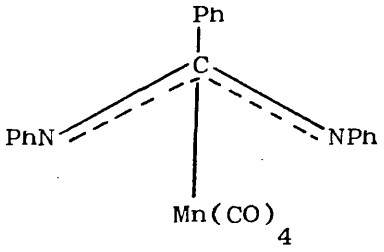

" η^3-borallyl"[59]

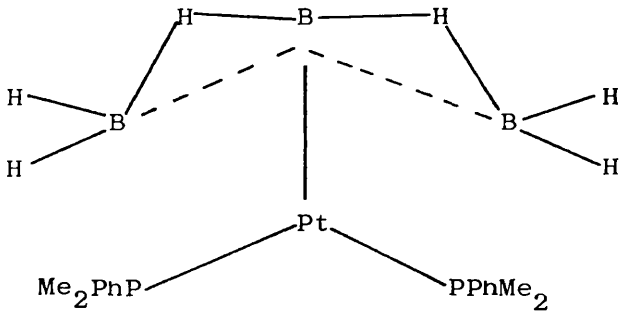

"η^3-P_3"[60]

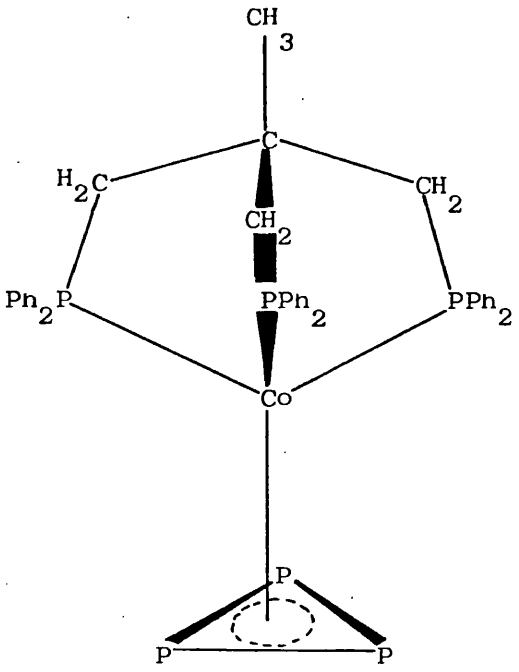

Even a novel "η^3-metallyl" moiety[61] has been suggested on the basis of X-ray diffraction studies.

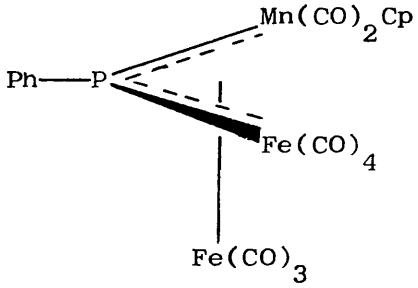

PREPARATION OF η^3-ALLYL TRANSITION METAL COMPOUNDS

The first η^3-allyl transition metal complex was probably obtained in 1952 by Pritchard[62] from the reaction between $HCo(CO)_4$ and butadiene, the product however was erroneously described as the 1:1 adduct $[C_4H_7Co(CO)_4]$ Later Jonassen[63] and co-workers discovered that the reaction was in fact accompanied by the release of one molecule of carbon monoxide, but incorrectly suggested the mode of bonding of the organic ligand to the metal to be as shown in Figure 1.1.

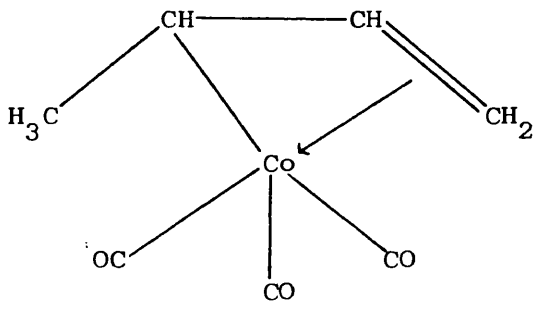

Figure 1.1: Jonassen's[63] proposed bonding scheme for $[C_4H_7Co(CO)_3]$

Illustrated below are the general methods currently employed for the preparation of these complexes, together with a number of specialised routes which have been adopted for specific compounds. The new technique of phase transfer catalysis shows an exciting potential for general applicability and is also mentioned.

(i) From Allyl Grignards and Related Metal Compounds

By far the most used method in the preparation of homoleptic η^3-allyl compounds such as $[(\eta^3\text{-}C_3H_5)_2M]$, M = Pd, Pt, Ni; $[(\eta^3\text{-}C_3H_5)_3M]$ M = V, Cr, Fe, Co, Rh, Ir; $[(\eta^3\text{-}C_3H_5)_4M]$ M = Zr, Th, Mo, W; $[(\eta^3\text{-}C_3H_5)_4M_2]$ M = Cr, Mo[1]. is the reaction of an anhydrous metal halide with an allylic Grignard reagent e.g.

$$IrCl_3 + 3C_3H_5MgCl \longrightarrow [(\eta^3\text{-}C_3H_5)_3Ir^{III}] + 3MgCl_2$$ [64]

This route may be modified to yield substituted and mixed η^3-allyl complexes e.g.

$$[(\eta^5\text{-}C_5H_5)_2Ni] \xrightarrow{C_3H_5MgBr} [(\eta^3\text{-}C_3H_5)Ni(\eta^5\text{-}C_5H_5)]$$ [65]

$$[Ni(\sigma\text{-}C_6Cl_5)(PPhMe_2)_2Cl] + CHR^1 : CR^2CH_2MgCl \rightarrow [(\eta^3\text{-}CHR^1CR^2CH_2)Ni(\sigma\text{-}C_6Cl_5)(PPhMe_2)_2]$$ [66]

($R^1 = R^2 = H$; $R^1 = H$ $R^2 = Me$; $R^1 = Me$ $R^2 = H$.)

$[(\eta^3\text{-}C_3H_5)_6Re_2]$ and $[(\eta^3\text{-}C_3H_5)_4Mo_2]$ have both been successfully isolated from reactions in which allyl-lithium has been used in place of the more conventional Grignard reagents[67]. The potential of allyl-tin reagents as allylating species has also been reported[68], and is illustrated (Scheme 1.1) by the preparation of $[(\eta^3\text{-}C_3H_5)Re(CO)_4]$. This reaction appeared to be of special significance when first published since it was believed that this complex could not be prepared via decarbonylation of $[(\eta^1\text{-}C_3H_5)Re(CO)_5]$[69]/ which is the generally accepted intermediate in these kind of reactions. On the basis of spectroscopic evidence

/ This has since been proved to be incorrect[70].

it was suggested that this reaction involves initial coordination of the olefinic linkage followed by intramolecular elimination of

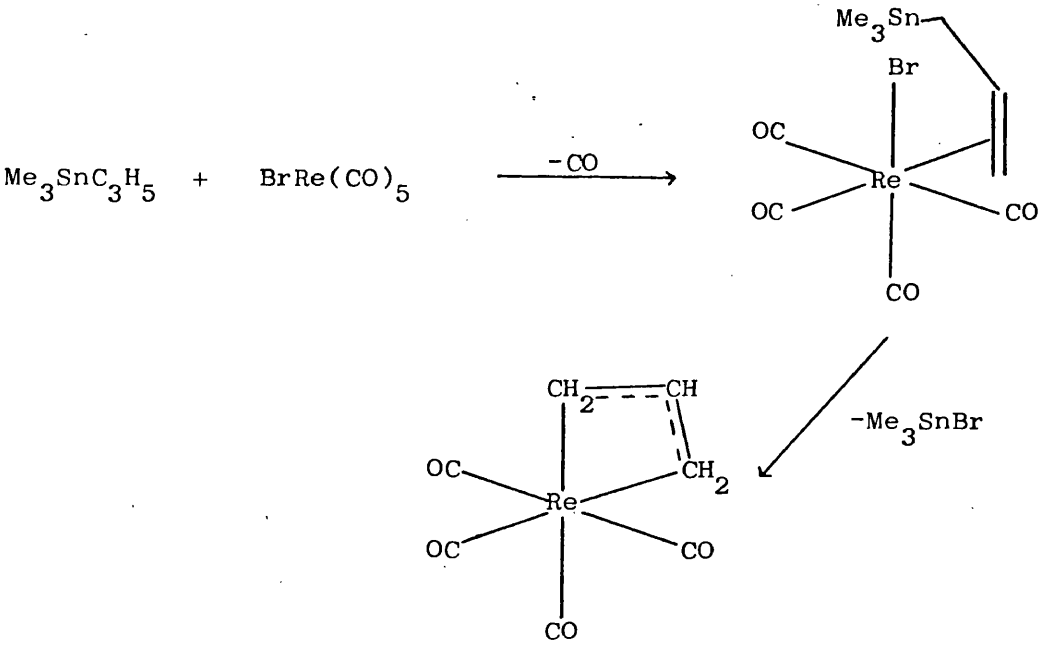

Scheme 1.1

trimethyltin halide.

(ii) Oxidative Addition of Allylic Halides to Transition Metal Compounds.

In these reactions allyl halides or pseudohalides are reacted with metal complexes in low oxidation states, often with displacement of another coordinated ligand, to produce an allyl complex in which the metal oxidation state has increased by two (the coordination number of the metal also usually increases*) e.g.

* The η^3-allyl group can be regarded to formally occupy two coordination sites - see later.

$$[Fe(CO)_5] + C_3H_5I \xrightarrow{u.v.} [(\eta^3\text{-}C_3H_5)Fe(CO)_3I] + 2CO \quad ^{71}$$

$$[Rh(PPh_3)_3Cl] + C_3H_5Cl \longrightarrow [(\eta^3\text{-}C_3H_5)Rh(PPh_3)_2Cl_2] + PPh_3 \quad ^{72}$$

$$[W(CO)_3(bipy)py] + C_3H_5Br \longrightarrow [(\eta^3\text{-}C_3H_5)W(CO)_2(bipy)Br] + py + CO \quad ^{73}$$

$$[(C_2H_4)_2Ir^{I}(CO)(PMe_2Ph)_2]BPh_4 + CH_2C(Me)CH_2Cl \longrightarrow$$

$$[(\eta^3\text{-}2\text{-}MeC_3H_4)Ir^{III}(CO)(PMe_2Ph)_2Cl]BPh_4 + 2C_2H_4 \quad ^{74}$$

Anionic metal carbonyls readily undergo this kind of reaction because of their highly nucleophilic nature, and so provide a route to η^3-allyl complexes not available by other synthetic routes e.g.

$$2\ Et_4N[Mo(CO)_5Cl] + 2C_3H_5Cl \longrightarrow$$

$$Et_4N[(\eta^3\text{-}C_3H_5)_2Mo_2(CO)_4Cl_3] + Et_4NCl + 6CO \quad ^{75}$$

$$[V(CO)_4(diars)]^- + C_3H_5Cl \xrightarrow{THF} [(\eta^3\text{-}C_3H_5)V(CO)_3(diars)] + Cl^- + CO \quad ^{76}$$

$$[Cr(CO)_3(bipy)Cl]^- + C_3H_5Cl \longrightarrow [(\eta^3\text{-}C_3H_5)Cr(CO)_2(bipy)Cl] + Cl^- + CO \quad ^{77}$$

The mechanism for the oxidative addition of organic halides to transition metals is far from established, and has been the subject of many review articles and discussions in the literature[78,79]. Proposed mechanisms for the oxidative addition of alkyl halides to low oxidation state transition metal complexes include, (a) nucleophilic attack of the metal at the carbon atom bearing the halogen[80,81],

(b) a concerted insertion of the metal into the C-X bond[82] and (c) a radical chain process[83,84]. In the addition of alkenyl halides however, initial coordination of the double bond to the metal appears to be an important first stage in the mechanism[85,86].

(iii) From Mono-olefins.

This important method has been used very extensively for making palladium complexes of the type $[(\eta^3\text{-allyl})_2Pd_2Cl_2]$[87] e.g.

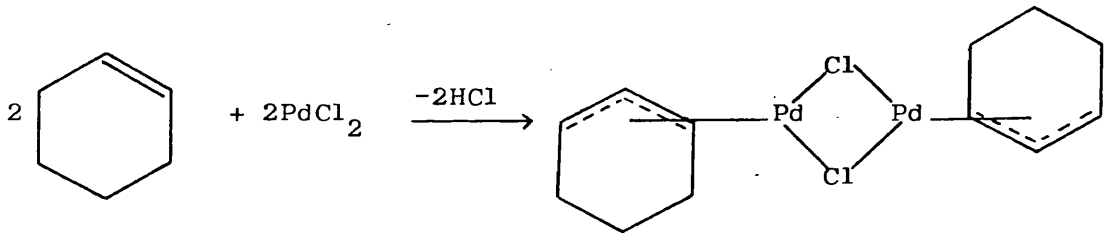

The formation of an η^3-allyl complex from a mono-olefin is thought to proceed via the initial formation of an unstable olefin-metal complex followed by loss of a hydrogen atom[89].

(iv) From Conjugated Dienes

Conjugated dienes may be used to prepare η^3-allyl compounds in a number of ways;

(a) diene insertion into transition metal-hydrides or -alkyl complexes e.g.

$$[HCo(CN)_5]^{3-} + C_4H_6 \longrightarrow [(\eta^3\text{-}1\text{-}MeC_3H_4)Co(CN)_4]^{2-} + CN^- \quad 90$$

$$[RhH(PPh_3)_4] + \quad \longrightarrow \quad + 2PPh_3 \quad 91$$

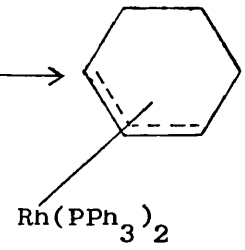

$$[PhMn(CO)_5] + CD_2 : CH\ CH : CD_2 \quad 92$$

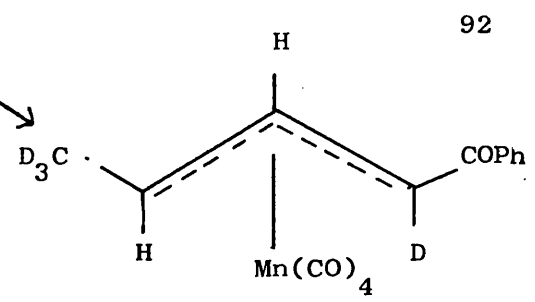

In this latter reaction the stereochemistry of the product obtained from the deutero-labelled butadiene reveals that a 1-4 hydrogen shift occurs in the formation of the η^3-allyl compound.

(b) the use of species (e.g. H, RCO, OR and OAc) which are capable of attacking the terminal carbon atom of the diene to produce the η^3-allyl entity e.g.

$$Na[Co(CO)_4] + C_4H_6 \xrightarrow[-CO]{CH_3COCl} \quad CH_2COCH_3 + NaCl \quad 93$$

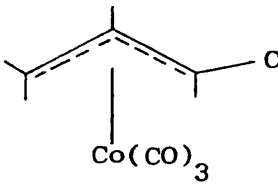

$$[PdCl_4]^{2-} + (CH_3)_2C : CHCH : CH_2 \xrightarrow{MeOH}$$

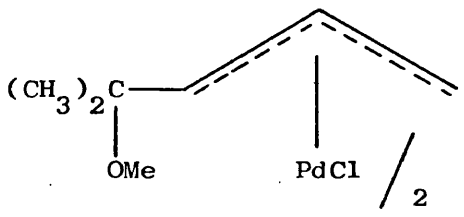

$$+ HCl + 2Cl^- \quad 94$$

With unsymmetrical dienes attack by the alkoxy group is at the most highly substituted carbon atom[94].

(c) the protonation of coordinated 1,3-dienes.

These reactions often proceed stereospecifically to produce a single geometric isomer e.g.

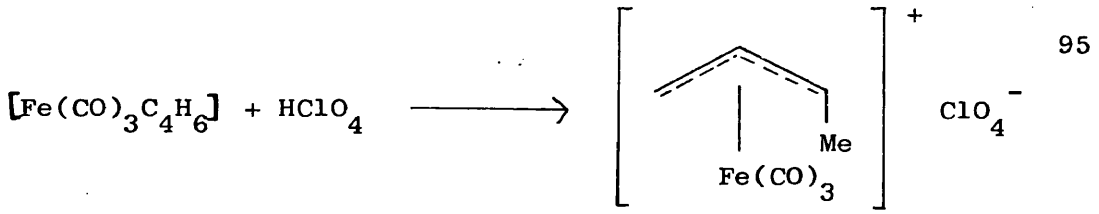

anti-isomer only [95]

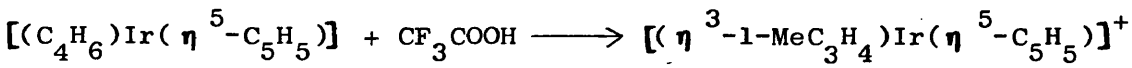

anti-isomer only [96]

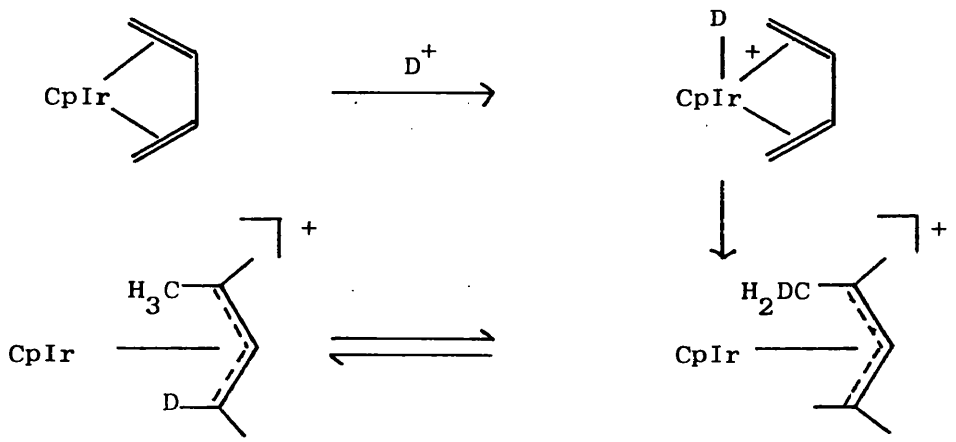

Scheme 1.2

A study of this reaction with deutero CF_3COOD has shown (as indicated in Scheme 1.2) that protonation occurs initially at the metal to produce a very short lived protonated metal cation. An equilibrium is then established in which the proton is rapidly transferred between the anti-methyl substituent of the η^3-allyl and the other end of the η^3-allyl entity.

(d) oligomerisation of conjugated dienes.

There are many examples of this type of reaction producing η^3-allylic species, several involve butadiene and the preparation of catalytically important η^3-allyl-nickel complexes e.g.

1

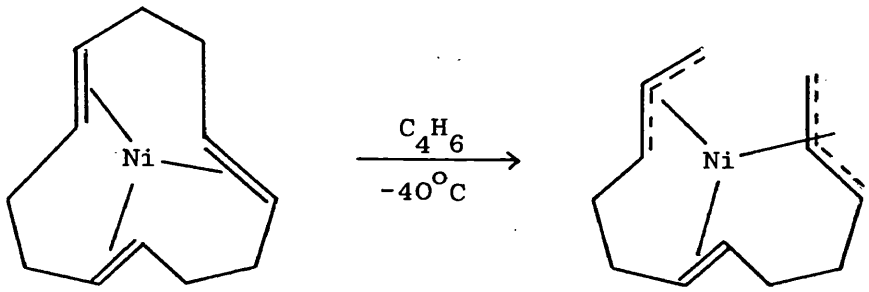

(v) η^1-Allyl $\longrightarrow$ η^3-Allyl Conversions

A coordinated η^1-allyl ligand may be converted to the η^3-mode by various methods which normally involve the simultaneous loss of two electrons from the metal coordination sphere e.g.

(a) photolysis

$$[(\eta^1\text{-}C_3H_5)Fe(CO)_2(\eta^5\text{-}C_5H_5)] \xrightarrow[-CO]{u.v.} [(\eta^3\text{-}C_3H_5)Fe(CO)(\eta^5\text{-}C_5H_5)]^{97}$$

(b) thermally

$$[(\eta^1\text{-}C_3H_5)Mn(CO)_5] \xrightarrow[-CO]{T > 80^oC} [(\eta^3\text{-}C_3H_5)Mn(CO)_4]^{98}$$

(c) by halide abstraction

$$[(\eta^1\text{-}CH_2CH : CHR)Pt(COD)Cl] + AgBF_4 \longrightarrow$$

$$[(\eta^3\text{-}1\text{-}RC_3H_4)Pt(COD)]BF_4 + AgCl \quad ^{99}$$

(100)

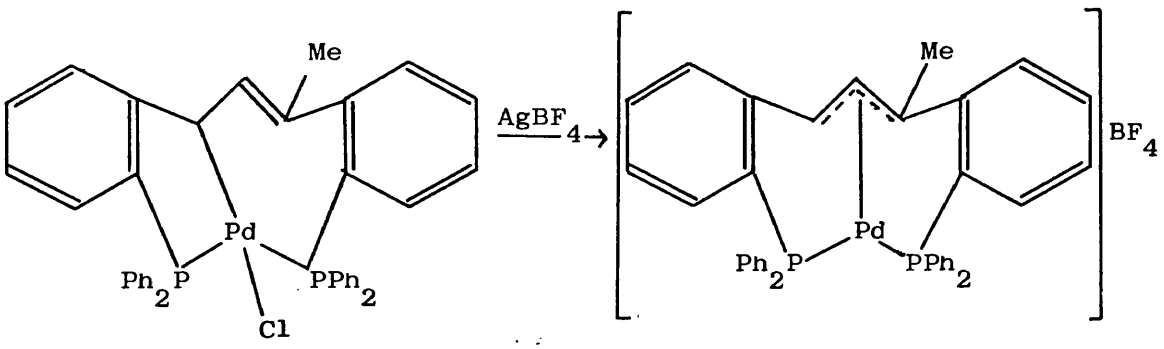

(vi) From Allenes

$$Na[Fe(CO)_2Cp] + (CF_3)_2C : C : C(CF_3)_2$$

THF (-70°C)

$$(CF_3)_2C{=}C{-}C(CF_3){=}CF_2$$

$$CpFe(CO)_2$$

hν pentane

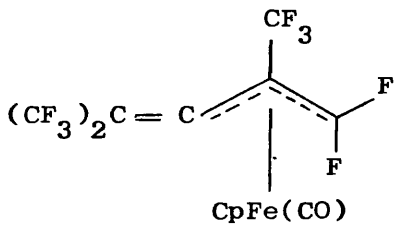

(101)

$$2[Pd(C_6H_5CN)_2Cl_2] + 2CH_2 : C : CH_2$$

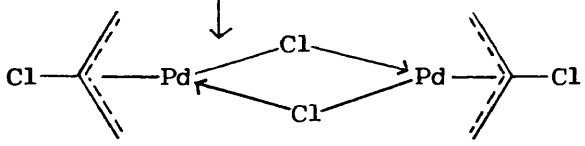

$$+ \ 4C_6H_5CN$$ 102

Conditions are often crucial in these reactions as demonstrated by the following scheme 1.3[103];

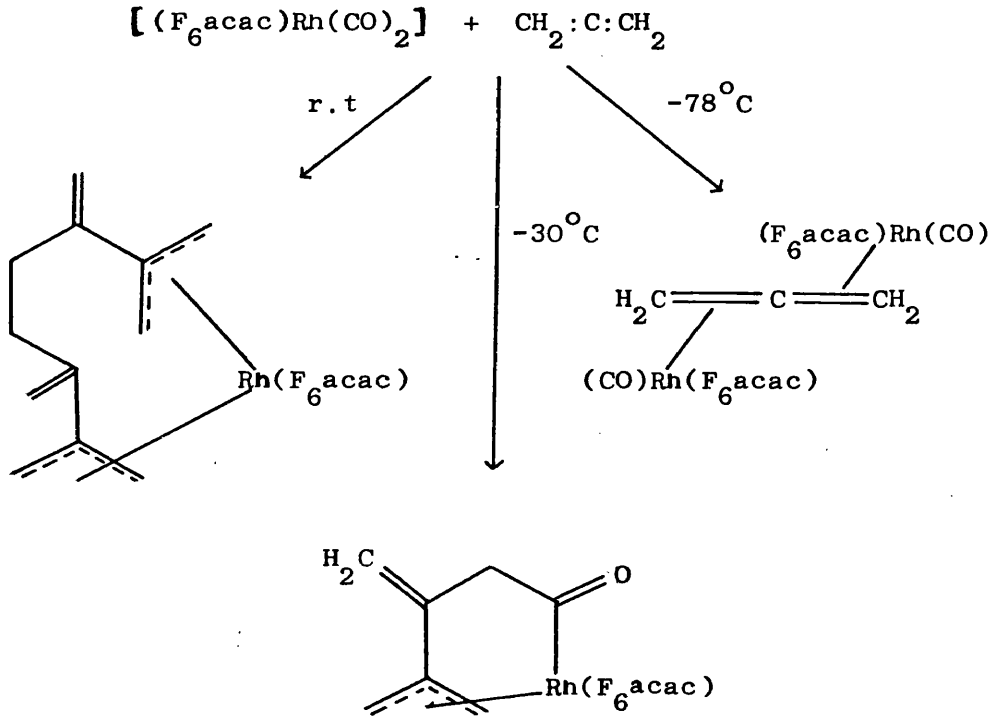

Scheme 1.3

(vii) Phase Transfer Catalysis[104]

Phase transfer catalysis is an exciting new technique which has been applied to the preparation of allyl derivatives. The advantages of this technique are the mild conditions, speed, simplicity and exceptionally good yields. Alper[105] first advocated this method for the preparation of $[(\eta^3\text{-HCRCR'CH}_2)\text{Co(CO)}_3]$ and used a two-phase system consisting of NaOH(aq) - C_6H_6 with the reaction catalysed by $PhCH_2NEt_3^+Cl^-$ as the phase transfer catalyst (see Scheme 1.4). He suggested a mechanism in which the catalyst is

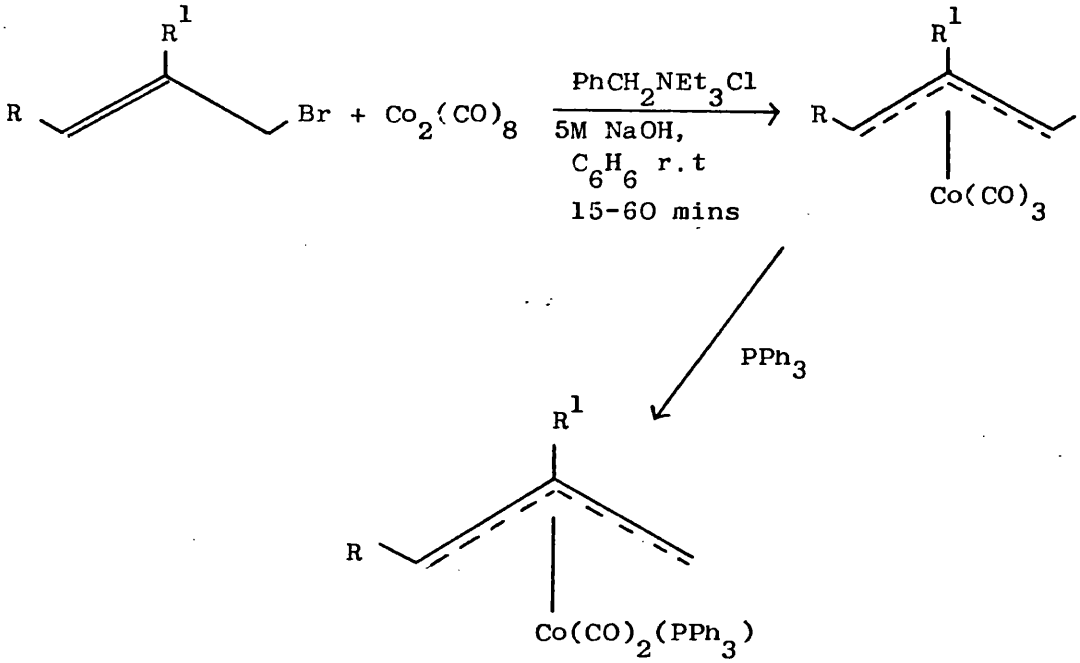

(70 - 80%)

Scheme 1.4

initially converted to the hydroxide in the aqueous phase, then transfers to the organic phase as an ion-pair and attacks the dissolved $[Co_2(CO)_8]$ forming $[Co(CO)_4]^-$ (ref. 106). Reaction of the metal carbonyl anion with allyl bromide then proceeds via the η^1-allyl intermediate finally yielding $[(\eta^3\text{-allyl})Co(CO)_3]$, and the regenerated catalyst $PhCH_2NEt_3^+Cl^-$ migrates back into the aqueous phase.

Gibson and co-workers[107] recently applied this method to the synthesis of the η^3-allyl complexes $[(\eta^3\text{-}C_3H_5)Mn(CO)_4]$, $[(\eta^3\text{-}C_3H_5)Mo(CO)_2(\eta^5\text{-}C_5H_5)]$ and $[(\eta^3\text{-}C_3H_5)Fe(CO)(\eta^5\text{-}C_5H_5)]$.

This work utilised metal carbonyl halides in organic phases of C_6H_6 or CH_2Cl_2, with $PhCH_2NEt_3^+Cl^-$ in aqueous NaOH as the phase transfer catalyst.

In contrast to the mechanism proposed by Alper, Gibson has suggested that a hydroxide ion directly attacks a carbonyl ligand of the transition metal complex so producing an intermediate containing a -COOH group which may subsequently either decarboxylate or serve to labilise the metal compound towards substitution by a second nucleophile [108]. This scheme has gained support from reactions conducted in the absence of allyl halide, in which $PhCH_2NEt_3^+[X\text{-}Mn(CO)_4\text{-}Mn(CO)_5]^-$ (X = Cl, Br) (also identified as a product from the photolysis of $[Mn_2(CO)_{10}]$ in the presence of quaternary ammonium halides[109]) was isolated in good yield after only short reaction times. A possible mechanism for the formation of this species is shown below:

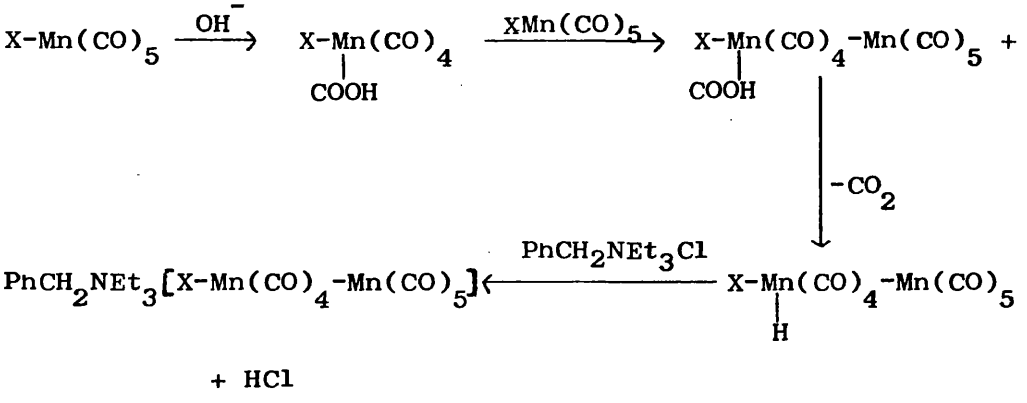

The mode of reaction of $PhCH_2NEt_3[XMn(CO)_4\text{-}Mn(CO)_5]$ with allyl halides to form $[(\eta^3\text{-}C_3H_5)Mn(CO)_4]$ is at present under study by Gibson, who does not appear to agree with Alper that an η^1-allyl-metal intermediate is formed in the reaction.

(viii) Novel Syntheses

(a) from alkynes e.g.

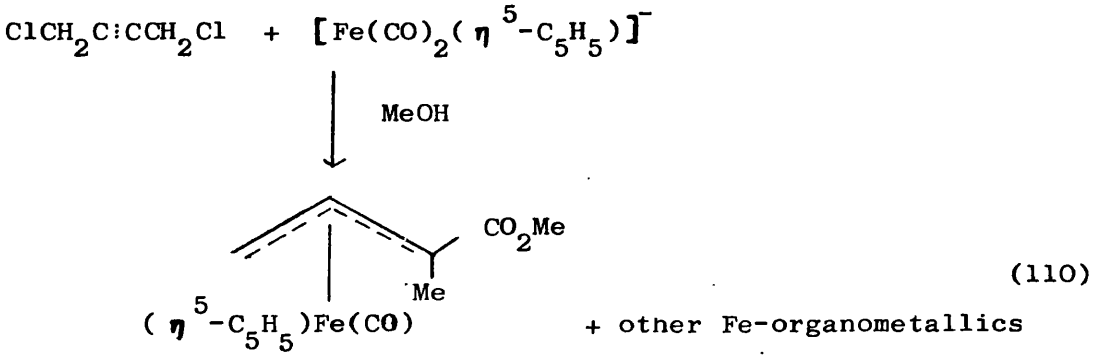

(110)

(b) Allyl halides react directly with highly reactive transition metals prepared either by alkali-metal reduction of metal salts in hydrocarbon solvent[111] or by vaporisation and cocondensation[112], e.g.

$$Pd(\text{powder}) + 2C_3H_5Br \xrightarrow{\text{r.t.}} [(\eta^3\text{-}C_3H_5)PdBr]_2 \quad (111)$$

$$Ni(\text{vapour}) + 2C_3H_5Cl \xrightarrow{-196} [(\eta^3\text{-}C_3H_5)NiCl]_2 \quad (112)$$

(c) by reactions which alter the bonding mode of coordinated organic ligands, e.g.

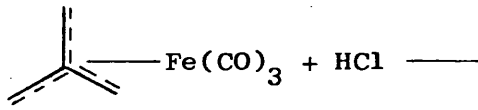

$$\rightarrow [(\eta^3\text{-}2\text{-}MeC_3H_4)Fe(CO)_3Cl] \quad (113)$$

$$2[(\eta^7\text{-}C_7H_7)Mo(CO)_2Br] \xrightarrow{NaOCH_3} [(\eta^3\text{-}C_7H_7)(\eta^7\text{-}C_7H_7)Mo_2(CO)_2(\mu\text{-}OCH_3)_3] + 2CO \quad (114)$$

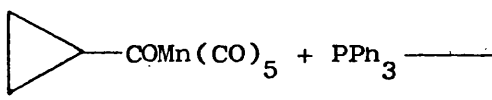

$$\rightarrow [(\eta^3\text{-}C_3H_5)Mn(CO)_3PPh_3] + 2CO \quad (115)$$

(d) allyl transfer reactions[116] e.g.

$$[(\eta^3\text{-}C_3H_5)NiCl]_2 + [Fe_2(CO)_9] \longrightarrow 2[(\eta^3\text{-}C_3H_5)Fe(CO)_3Cl] + Fe + 3CO + 2Ni \quad (117)$$

(e) isomerisations e.g.

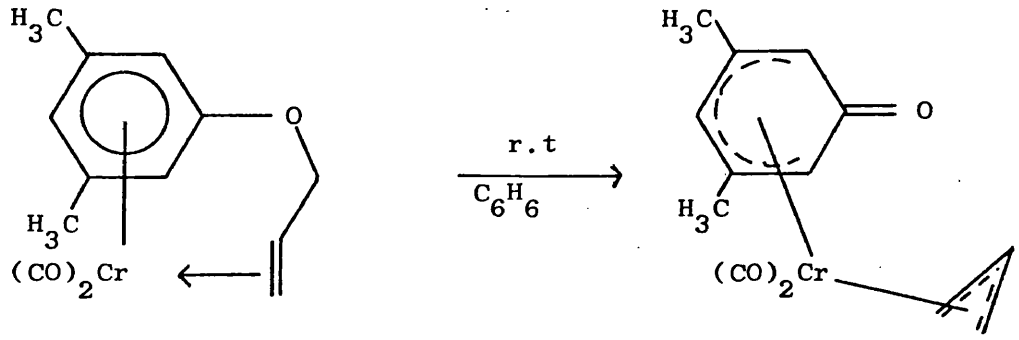

STRUCTURE AND BONDING IN η^3-ALLYL TRANSITION METAL COMPLEXES

The palladium dimer $[(\eta^3\text{-}C_3H_5)PdCl]_2$, was the first η^3-allyl transition metal complex to be examined by crystallographic methods. Preliminary investigations[119,120] were followed by two independent three dimensional analyses[121,43]. The most detailed and accurate of these conducted at -140^oC [43] showed that the three carbon and five hydrogen atoms of the allyl group form a plane orientated at an angle of 111.5 ± 0.9^o to the plane containing the $PdCl_2Pd$ bridge system.

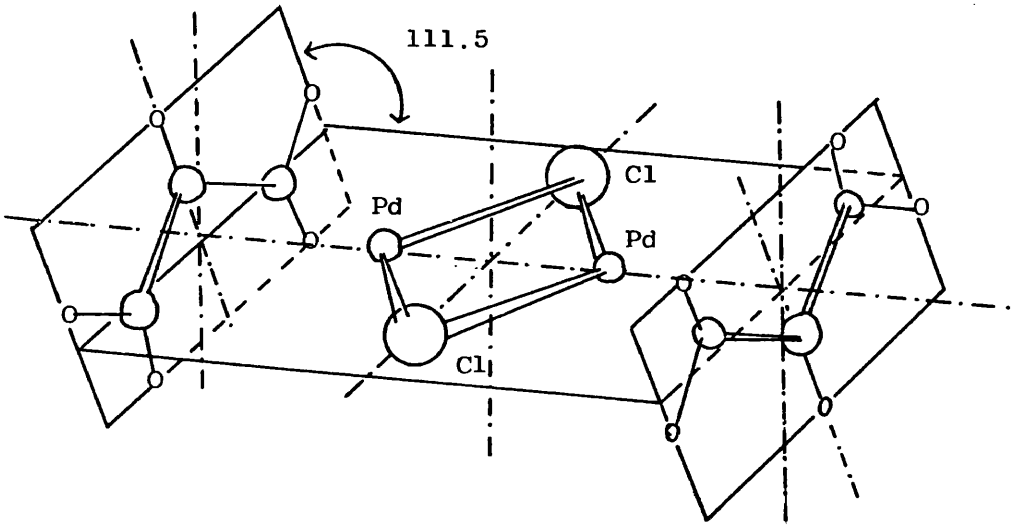

Figure 1.2: Schematic drawing of the $[(\eta^3\text{-}C_3H_5)PdCl]_2$ dimer.

The central carbon atom C(2) of the allyl is tipped away from the palladium, but the Pd-C(2) distance equals the average of the Pd-C(1) and Pd-C(3) distances. In this example - as in the majority of other such complexes - the η^3-allyl ligand is symmetrically bonded, i.e. C(1)-C(2) $\sim$ C(2)-C(3) = 1.376Å (average). However, when the chemical environment at one terminal carbon atom of the η^3-allyl ligand is grossly different from that at the other, because of ligands having different <u>trans</u> and/or steric effects, the symmetrical bonding of the η^3-allyl group may be destroyed as shown below for $[(\eta^3\text{-}2\text{-}MeC_3H_4)Pd(PPh_3)Cl]$[122] and $[(\eta^3\text{-}C_3H_5)W(CO)(\eta^5\text{-}C_5H_5)(NO)I]$[123].

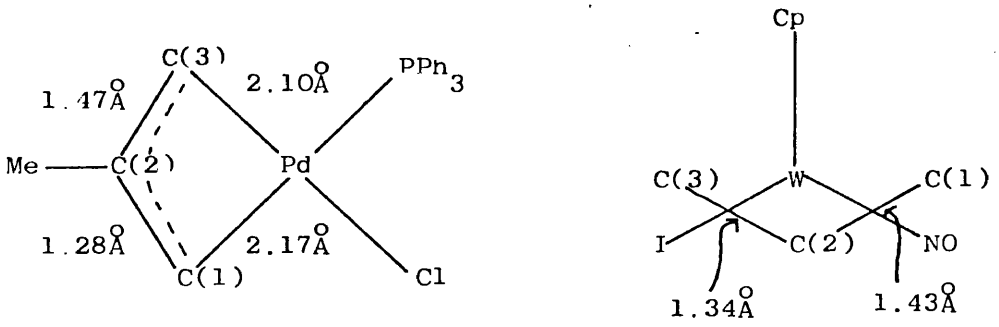

Figure 1.3: The structures of
(i) $[(\eta^3\text{-}2\text{-}MeC_3H_4)Pd(PPh_3)Cl]$ and
(ii) $[(\eta^3\text{-}C_3H_5)W(CO)(\eta^5\text{-}C_5H_5)(NO)I]$

The discovery that the plane of the η^3-allyl ligand was not in fact perpendicular to the coordination plane of the molecules - even in the symmetrically bonded palladium complex mentioned above - was somewhat unexpected (c.f. ethylene-Pd complexes in which the C-C bond is perpendicular to the coordination plane of the metal[124]) but has since come to be recognised as an inherent structural feature of these compounds where a coordination plane can be defined (Figure 1.4).

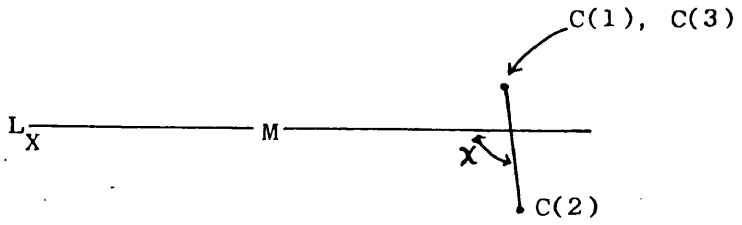

Figure 1.4: The general orientation of the η^3-allyl ligand to the coordination plane of the molecule.

C(1) and C(3) are the terminal carbon atoms of the allyl ligand which lie trans to the ligand(s) L_x. In this definition the tilt or dihedral angle χ, is the angle between the coordination plane and the plane of the allyl ligand. Table 1.1 gives values of χ for a selection of η^3-allyl metal compounds*, and as described in the next section, the allyl tilt observed, which is commonly around 111^o, can be rationalised in terms of the bonding which occurs between the allyl ligand and the transition metal.

* For a more extensive list the reader is referred to Ref. 127.

Table 1.1: Examples of χ for various η^3-Allyl Transition Metal Compounds

Compound	Ref.	Angle^o
$[(\eta^3\text{-}C_3H_5)PdCl]_2$	43	111.5[a]
	121	108[b]
$[(\eta^3\text{-}C_3H_5)Pd(OCOCH_3)]_2$	125	117
$[(\eta^3\text{-}C_3H_5)Mo(CO)_2(bipy)py]BF_4$	126	107.9
$[(\eta^3\text{-}C_3H_5)Fe(CO)_3]_2$	127	98.9
$[(\eta^3\text{-}2\text{-}MeC_3H_4)Ni(dpe)Br]$	128	106.5
$[(\eta^3\text{-}2\text{-}MeC_3H_4)Rh(AsPh_3)Cl_2]$	129	126.6
$[(\eta^3\text{-}C_3H_5)Ir(CO)(PMe_2Ph)_2Cl]PF_6$	86	126
$[(\eta^3\text{-}1\text{-}Me\text{-}2\text{-}Me\text{-}C_3H_3)Ti(\eta^5\text{-}C_5H_5)_2]$	130	124.1

[a] - determined at -140^{o}C

[b] - determined at r.t.

BONDING

After the σ-framework of the allyl entity has been constructed, a straight forward Huckel calculation (see Appendix 1) shows that the remaining unused $2p_z$ orbitals of the allyl carbon atoms can form three molecular orbitals, ψ_1, ψ_2 and ψ_3 (all symbols have their usual meaning[131]) (Figure 1.5) which may interact with the atomic orbitals of the metal.

Atomic Orbitals Molecular Orbitals

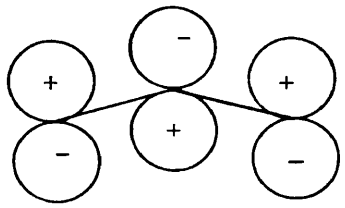

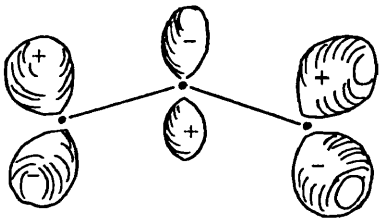

Antibonding
$E = \alpha - 2\beta$

$$\psi_3 = \tfrac{1}{2}\phi_1 - \sqrt{\tfrac{1}{2}}\phi_2 + \tfrac{1}{2}\phi_3$$

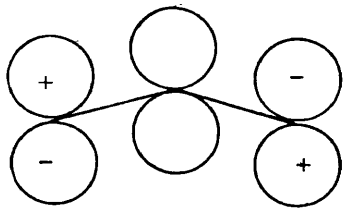

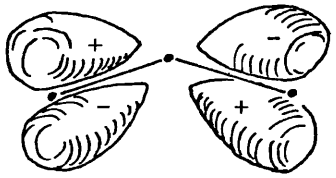

Non-bonding
$E = \alpha$

$$\psi_2 = \sqrt{\tfrac{1}{2}}(\phi_1 - \phi_3)$$

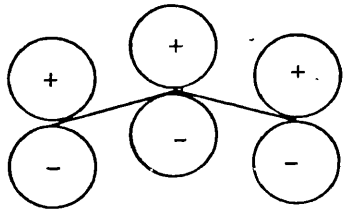

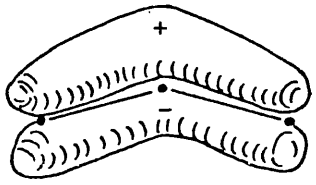

Bonding

$E = \alpha + 2\sqrt{2}\beta$

$$\psi_1 = \tfrac{1}{2}\phi_1 + \sqrt{\tfrac{1}{2}}\phi_2 + \tfrac{1}{2}\phi_3$$

Figure 1.5: The π - molecular orbitals of the allyl anion

Convention dictates that the η^3-allyl group contributes one unit to the oxidation number of the metal; the allyl anion is therefore formally a 4e donor. However, as shown in Appendix 1, the allylic system can be considered to supply 4, 3 or even 2 electrons for coordination to the metal, depending on whether it is regarded as an anion, a radical or a cation - all of which are equivalent in terms of bonding energy. In order to accommodate this flexibility when electron counting compensation is made in terms of the formal oxidation state of the metal.

Early theoretical bonding schemes[132] for the η^3-C_3H_5-M system were based solely on symmetry arguments, with the allyl plane taken to be perpendicular to the coordination plane of the metal. No explanation of the observed tilt ($\chi > 90^\circ$) was made.

In 1966 however, Kettle and Mason[30] developed a bonding scheme (Figure 1.6) which took this structural feature into account. They proposed that the bonding in these systems was the result of two distinct overlap mechanisms, which differed in the orientation of the allyl with respect to the metal and remaining ligands. Maximization of the bonding interactions from these two extreme orientations of the allyl group (I and II in Figure 1.6) produced a dihedral angle χ which was between 90° and 180°. Kettle estimated the overlap integrals for the various possible orbital interactions in the (η^3-C_3H_5)-Pd system using Slater orbitals and values of overlap integrals for $2p\pi$ - $4d\pi$ interactions based on the average of those for $2p\pi$ - $3d\pi$ and $2p\pi$ - $5d\pi$, for which suitable tabulations were available. Since the magnitude of the calculated overlap integrals concerning ψ_3, the antibonding orbital of the allyl ligand, were small compared to those involving ψ_1 and ψ_2, they were ignored. The total bonding energy of ψ_1 and ψ_2 with the atomic orbitals of Pd was considered to be composed of two terms, the first arising from the interactions which occur with the allyl in Orientation I and the second with the allyl in Orientation II, each of which was assumed to be proportional to the square of the respective overlap integrals. By maximising the total bonding energy with respect to χ Kettle predicted the values of χ at which greatest ψ_1-metal and ψ_2-metal orbital overlap would occur to be 114° and 102° respectively. On the basis that stronger bonds arise from the interaction of most suitably energetically matched orbitals,

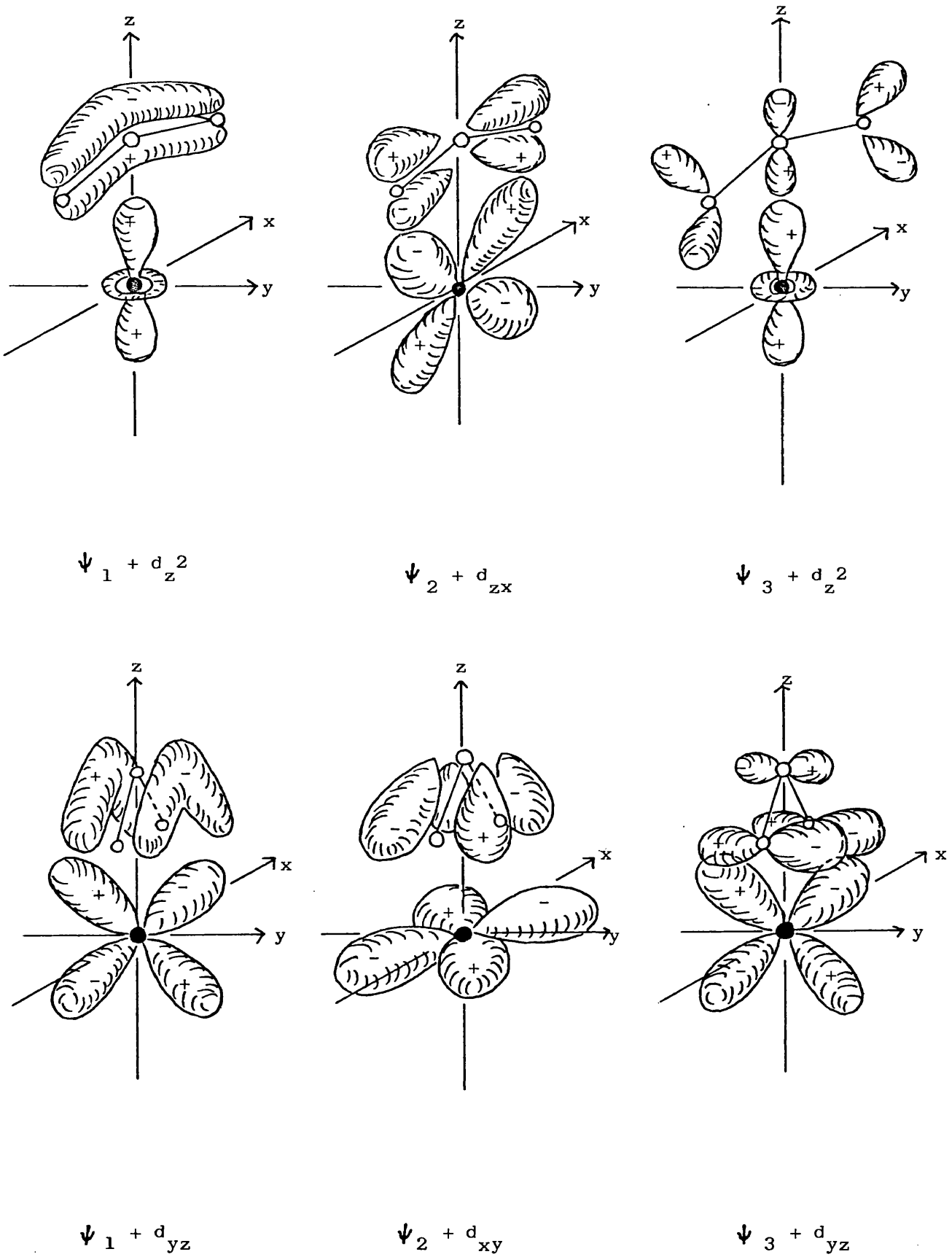

Figure 1.6 η^3-Allyl-transition metal bonding interactions.

Kettle suggested that ψ_1 - M_d interactions were largely responsible for the bonding and therefore χ to be nearer 114^o than 102^o, in fair agreement with experimentally determined values (108^o - 127^o [43,45,133-137]).

As with any theoretical treatment of a real system, necessity dictates that approximations and estimates be made, which are often not totally acceptable to all, in order to render the problem mathematically viable. Predictably then, Kettle's proposals have since received criticism. Van Leewen and Praat[131], also working with the η^3-allyl-Pd system, devised a somewhat different approach, which led to their belief that the most important bonding contribution involves ψ_2 - the non-bonding orbital of the allyl ligand. This view is based on energy considerations and has received support from other workers[138], notably Veillard[139] who carried out calculations on bis(η^3-allyl)nickel. Other semi-empirical molecular orbital calculations on the analogous palladium compound bis(η^3-allyl)palladium indicate that interactions of ψ_1 with M_s and M_p (and not M_d) are of major importance[32] (Kettle considered these interactions to be insignificant on energy grounds). The ability of the ψ_2 orbital of the allyl to act either as an electron donor or electron acceptor orbital in different compounds has also been suggested[140]. In ^{13}C NMR spectra of coordinated η^3-allyls the central carbon atom C(2) is always found at lowest field. This is consistent with the donation of electron density from the metal to the ψ_2 orbital of the allyl[141,142] [the C(2) atom contains a nodal plane in ψ_2 - see Figure 1.5]. In the uncoordinated allyl carbonium ion the terminal

carbon atoms C(1) and C(3) are electron deficient[143]. The insignificance of $M_d \rightarrow \psi_3$ back donation is yet another point of contention*[31,139], since it is accepted to be an important feature in M-olefin[144], M-allene and M-acetylene complexes[145]. In connection with this latter point, Kaduk, Poulos and Ibers[86] have recently published a compilation of structural data which shows a number of correlations between certain features of the η^3-C_3H_5-M linkage. The most interesting of these concerns the negative relationship of $\bar{C}$ (the average C-C bond lengths of the allyl group) and a parameter D', which provides a measure of the average distance from the metal atom to the centre of mass of the allyl group for metals having the same number of d electrons. (particularly for d^8 and d^4 systems). Small D' values imply strong η^3-allyl-M bonds, and these may be envisaged to arise in a number of ways;

(i) by an increase in electron transfer from the allyl bonding orbital ψ_1, to the metal atom;

(ii) by an increase in electron transfer from the allyl non-bonding orbital ψ_2 to the metal atom; or

(iii) by an increase in electron transfer from filled metal d orbitals to the empty antibonding orbital ψ_3 of the allyl;

but whilst both (i) and (iii) would be expected to involve the observed lengthening of $\bar{C}$, (ii) should not affect this parameter.

* However, it is important to note that Kettle considered these interactions to be negligible only in comparison with those of ψ_1 and ψ_2.

This, together with the fact that the general order of M - η^3-allyl bond lengths is $d^8 < d^6 < d^4$, which can be directly correlated with the expected strength of back donation from the metal ($d^8 > d^6 > d^4$) is suggested by the authors as evidence for the importance of metal to allyl back donation. Such concepts as these must be applied with care, however, for the effect of different ligands coordinated to a metal will inevitably influence the flow of electron density to and from the allyl group. Hence, although there seems to be general agreement about the types of allyl-metal interactions which are responsible for the bonding in these systems, the relative contributions of each is less well established, partly because these simple bonding schemes take no account of the considerable mixing of orbitals that must occur in systems of such low local symmetry.

SPECTROSCOPIC CHARACTERISATION OF η^3-ALLYL TRANSITION METAL COMPOUNDS.

A number of techniques have been utilized for the characterisation of η^3-allyl organometallics, the major methods being vibrational spectroscopy and probably most important, NMR spectroscopy, to which the allylic system is particularly amenable.

PROTON NUCLEAR MAGNETIC RESONANCE SPECTROSCOPY[33]

Theoretically the symmetrically bound η^3-C_3H_5 group may possess up to 5 magnetically distinct hydrogens - as shown in

Figure 1.7.

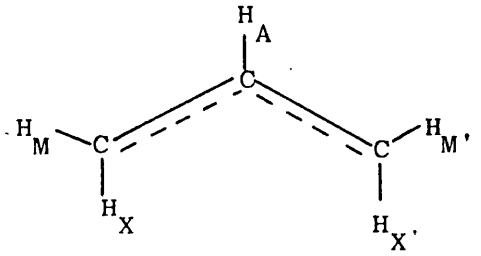

H_M and $H_{M'}$ = H_{syn}

H_X and $H_{X'}$ = H_{anti}

Figure 1.7: The symmetrical η^3-allyl group.

First order rules are applicable, but although an AMM'XX' pattern is expected, it is only rarely observed since J_{MX} and $J_{MX'}$ are small and often not detected. The majority of published spectra have therefore been explained in terms of an AM_2X_2 spin system, the form of which, together with typical values of the ^1H NMR parameters for the η^3-C_3H_5 transition metal entity, are shown in Figure 1.8.

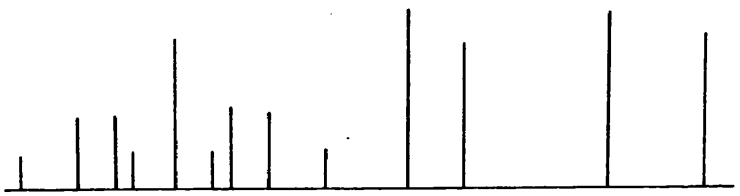

(η^3-C_3H_5)	A	M	X
range of reported chem. shift (δ)	6.5 - 4	5 - 2.5	4 - 1
Typical values (δ)	5.5	4	2.5
Typical J values (Hz)		6.9	11.9
Relative area	1	2	2

Figure 1.8: The resonance pattern for an AM_2X_2 spin system.

On the basis that trans-vic-hydrogens couple more strongly than cis-vic-hydrogens the doublet at higher field, with the larger coupling constant is assigned to the H_X protons. Such an assignment is also in agreement with the envisaged structural configuration of the η^3-C_3H_5-M entity, since if the hydrogens of the ligand lie in or near the plane of the carbon atoms the H_X protons are subject to the greatest shielding by the metal and may as a consequence be expected to occur at high fields. Although, as previously mentioned, the values of J_{MX} and $J_{MX'}$ are small, they are not zero, and under suitable high resolution conditions these second order splittings can be observed, producing a considerably more complex spectrum. Each of the bands for the M and X protons are resolved into a doublet of triplets, caused by the apparent equivalence of J_{MX} and $J_{MX'}$ which are both of the order of 1Hz. According to Karplus[146], J_{MX} is small because both protons are attached to the same carbon atom and the H_MCH_X angle is near 125° (a value consistent with sp^2 hybridisation of the carbon atom) and $J_{MX'}$ is similarly small because it is a long range coupling effect. For the same reasons $J_{X'M'} = J_{XM'} \sim 1Hz$. Theoretically the maximum number of lines possible for the A resonance is sixteen, however, in practice no more than fifteen lines have ever been successfully resolved[147].

$J_{MM'}$ and $J_{XX'}$ have not been observed for unsubstituted η^3-allyl complexes probably because they are extremely small as a result of their long separation and cis orientation. It has been possible, however, to calculate values for these coupling constants from high resolution ^1H NMR and/or ^{13}C NMR spectra of a

number of substituted η^3-allyls such as $[(\eta^3\text{-}2\text{-}ClC_3H_4)Pd(acac)]$[147] for which $J_{MM'} = 2.7 \pm 0.2$ Hz and $J_{XX'} = 0.5 \pm 0.2$ Hz.

^{1}H NMR measurements are of particular importance in the structural elucidation of η^3-allylic species, particularly those in which one or more of the hydrogens have been replaced by other groups. Whilst substitution of H_A on the central carbon atom results in simplified spectra, this is not the case when substitution of a hydrogen on one of the terminal carbon atoms occurs. Then the symmetry of the η^3-allyl group is effectively destroyed and an increase in the number of magnetically inequivalent protons occurs. In addition the unique group R can replace either a H_M or H_X proton in a $(\eta^3\text{-}1\text{-}R\ C_3H_4)M$ species and thus two isomers are possible (Figure 1.9).

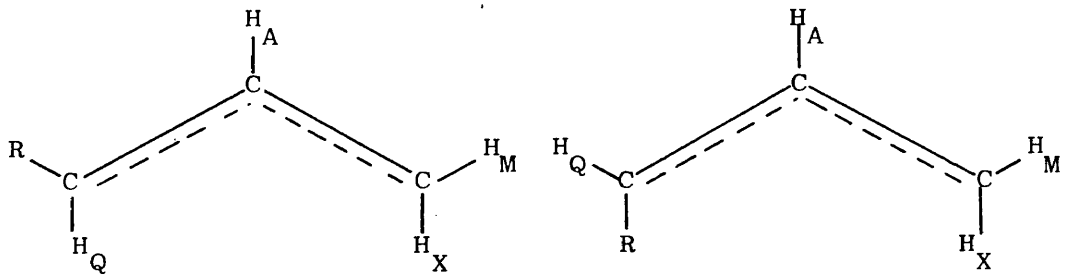

syn isomer anti isomer

Figure 1.9: The two possible isomeric forms of $(\eta^3\text{-}1\text{-}RC_3H_4)$

The chemical shift values (δ) and J values (Hz) for the two isomers of $[(\eta^3\text{-1-MeC}_3\text{H}_4)\text{Co(CO)}_3]$[148] are given in Table 1.2.

Table 1.2: Chemical Shift and Coupling Constant Data for Syn- and Anti- $[(\eta^3\text{-1-MeC}_3\text{H}_4)\text{Co(CO)}_3]$

	(δ) values (p.p.m.)			J values (Hz)	
	syn	anti		syn	anti
H_A	5.74	5.62	J_{AM}	6.3	7.1
H_M	3.54	3.92	J_{AX}	10.5	12.3
H_X	2.62	3.47	J_{AQ}	10.5	6.8
H_Q	3.78	4.89	J_{MX}	0.2	0.6
CH_3	2.24	1.89	J_{MQ}	0.2	1.6
			$J_{Q\text{-}CH_3}$	6.5	7.0

The assignments shown above were based primarily on the differences in the coupling constants, J_{AQ} of the two isomers. The higher value of 10.5Hz was attributed to trans-vic-coupling which occurs between H_A and H_Q in the syn isomer, and the lower value of 6.8Hz to cis-vic-coupling of H_A and H_Q in the anti-isomer.

Coupling of the Allylic Protons to Other Nuclei

The ^{1}H NMR spectrum of an η^3-allylic group may appear slightly more complex than that described above because of secondary splittings resulting from coupling of the allylic protons to other nuclei in the same complex. In $(\eta^3\text{-}C_3H_5)$-Pt

compounds side bands due to $J(^{195}Pt\text{-}H_{allyl})$ (^{195}Pt, $I = \frac{1}{2}$ natural abundance = 34%) are often present. As demonstrated in Table 1.3, for all reported examples $J(Pt\text{-}H_X) > J(Pt\text{-}H_M)$, but the relative magnitudes of these two parameters vary considerably, depending on the complex. Particularly notable are (a) the very small values of $J(Pt\text{-}H_M)$ when phosphorus or arsenic ligands are bonded to the metal, and (b) the difference in the two $J(Pt\text{-}H_X)$ values for compounds of the type $[(\eta^3\text{-allyl})PtAr(PPh_3)]$, when Pt coupling to the anti hydrogen H(2) trans to the phosphorus ligand is larger than that to the anti hydrogen H(3) trans to the aryl ligand. This observation has been rationalised in terms of a stronger NMR trans-influence[153] of the Ar group compared with that of PPh_3.

The variation in widths of the allylic proton resonances of rhodium η^3-allyl complexes[154] has been attributed to differences in the magnitude of the various J(Rh-H) (^{103}Rh $I = \frac{1}{2}$ natural abundance = 100%). When clearly resolved the size of $J(Rh\text{-}H_{allyl})$ at 1-2Hz,[91,155] is smaller than the analogous $J(Pt\text{-}H_{allyl})$ values, but again $J(Rh\text{-}H_X) > J(Rh\text{-}H_M)$.

Such effects as these found for platinum- and rhodium-η^3-allyl complexes are only observed for metal which possess an isotope of $I = \frac{1}{2}$ in sufficient natural abundance to produce detectable splitting of the proton resonances. Thus although $M\text{-}H_{allyl}$ coupling is theoretically feasible for η^3-allyl

Table 1.3: Examples of J_{Pt-H} Values for (η^3-allyl)Pt Compounds

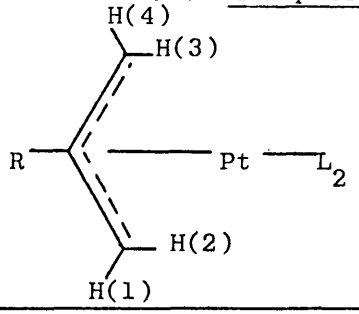

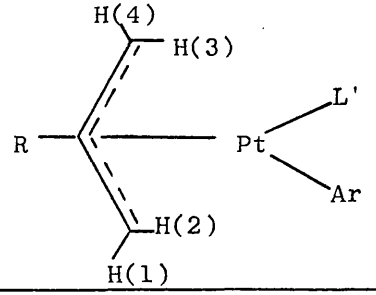

Allyl	Complex L_2	Ar	L'	$J(Pt-H)(Hz)$ H_M H(1)	H_M H(4)	H_X H(2)	H_X H(3)	R	REF.
C_3H_5	Cp			60		108		-	149
2-MeC_3H_4	Cp			61		111		34	149
2-MeC_3H_4	acac			41.5		92		81	149
2-MeC_3H_4		Cl	py[a]	31.5		78		82	149
2-MeC_3H_4	$(AsMe_3)_2$[b]			7		49		65	150
2-MeC_3H_4	$(PPhMe_2)_2$[b]			0.5		42.7		57.7	150
2-MeC_3H_4	diars[b]			9.4[c]		52.3		63.2	151
2-MeC_3H_4	dpe[b]			[d]		44.5		57.0	151
C_3H_5		C_6HCl_4	PPh_3	-		56	40	-	152
2-MeC_3H_4		C_6HCl_4	PPh_3	-		56	40	55	152
C_3H_5		C_6F_5	PPh_3	-		49	44	-	152

a - pyridine solvate, b - PF_6^- salt, c - broad signal; coupling only revealed in double resonance experiments. d - too small to be measured.

complexes of tungsten and iron neither have ever been reported, a consequence of the small natural abundance of the isotopes ^{183}W($I = \frac{1}{2}$, natural abundance 14%) and ^{57}Fe($I = \frac{1}{2}$, natural abundance 2.2%). For tungsten, the absence of such coupling effects could also be a result of their size. Values of J_{WH} for directly bonded H-W systems are only of the order of 30 - 80Hz[156] and that for the $W-CH_3$ entity merely 4Hz, thus $J(W-H_{allyl})$ which is a long range effect is, in all probability, extremely small.

The coupling of the allylic protons to metal nuclei with $I > \frac{1}{2}$ is normally destroyed by the electric quadrupole moments possessed by such nuclei[157]; thus, for example, $Re-H_{allyl}$ coupling has never been reported, indeed no J_{Re-H} has been found even for directly bonded Re-H compounds[158].

A more commonly observed phenomenon is the coupling of the allylic protons to phosphorus nuclei which are coordinated to the same metal centre. The stereochemical relationship of the phosphorus atoms to the protons on each end of the allyl group appears to influence the size of the $J(P-H_{allyl})$ coupling. Most workers suggest that largest $J(P-H_{allyl})$ coupling occurs between the hydrogen(s) of the allyl and the phosphorus atom trans to them.

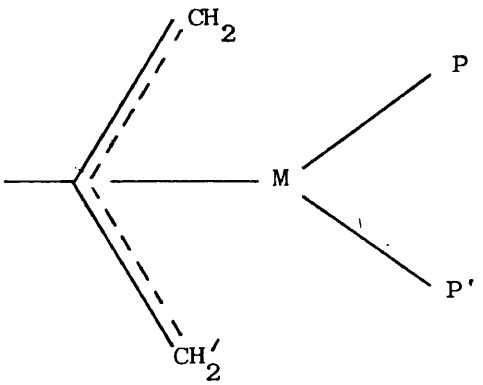

$$J(P\text{-}H') = J(P'\text{-}H) > J(P\text{-}H) = J(P'\text{-}H')$$

Figure 1.10: Largest J(P-H) occurs between atoms which are mutually trans.

This opinion is based on the work of Shaw et al[159a,159b] who studied transition metal hydrides stabilised by tertiary phosphines. They reported strongest coupling between phosphorus and hydrogen atoms in mutually trans-positions. Where η^3-allyl containing compounds possess a coordination plane defined by the allyl the metal and phosphorus ligand(s), as in square planar complexes such as $[(\eta^3\text{-}C_3H_5)Pd(PR_3)_2]$ (Figure 1.10), it appears a reasonable assumption that the sequence $J(P\text{-}H_{allyl})$ trans $>$ $J(P\text{-}H_{allyl})$ cis should apply. It is, however, more difficult to use this sequence as a general rule of thumb for compounds where no such plane is present. Recent work on compounds of the type $[(\eta^3\text{-}C_3H_5)Mo(CO)(PR_3)(\eta^5\text{-}C_5H_5)]$[160] for instance has shown the opposite trend, i.e. $J(P\text{-}H_{allyl})$ cis $>$ $J(P\text{-}H_{allyl})$ trans. Table 1.4 lists the $J(P\text{-}H_{allyl})$ parameters for a selection of compounds. As found for $J(M\text{-}H_{allyl})$, the magnitudes of $J(P\text{-}H_M)$ differ from those of $J(P\text{-}H_X)$. For complexes of V, Mo, W, Ru and Co $J(P\text{-}H_X) < J(P\text{-}H_M)$ but where the transition metals involved are Mn, Re, Rh, Ir, Pd or Pt, $J(P\text{-}H_X) > J(P\text{-}H_M)$.

These trends appear to be general for most η^3-allyl-phosphine containing compounds of the same metal, but to date there has been little attempt to explain these observations. Indeed the sole publication on this topic is by Reilley and Thyret[91], who suggested that the difference in magnitude of $J(P\text{-}H_X) \sim 6Hz$ and $J(P\text{-}H_M) \sim 0Hz$ for $[(\eta^3\text{-allyl})Rh(PPh_3)_2]$ correlates with the unsymmetrical relationship of the trans phosphorus nuclei to H_X and H_M. They assumed a dihedral angle χ between the plane of the allyl ligand and that defined by the rhodium and phosphorus nuclei to be greater than 90^o and proposed that as a consequence, each phosphorus is effectively cis to the H_M proton and trans to the H_X proton on the allylic carbon atom to which it is mutually trans. So by virtue of preferential P_{trans} coupling $J\ P\text{-}H_X(trans) > J\ P\text{-}H_M(trans)$.

A comprehensive literature search has failed to reveal any further relevant discussions as to why the order $J(P\text{-}H_X) > J(P\text{-}H_M)$ is found for some metals but the reverse for others. The magnitude of such couplings will doubtless depend on both the stereochemistry and ligand arrangements of individual compounds since both these factors will influence the orbitals involved in M-P and M-η^3-allyl bonding. However, Figure 1.11 demonstrates quite clearly that there is no simple correlation between the respective sites of the allyl and phosphorus atoms and the relative sizes of the $J(P\text{-}H_X)$ and $J(P\text{-}H_M)$ coupling observed (for example one cannot state that a criterion for $J(P\text{-}H_X) > J(P\text{-}H_M)$ is that the allyl metal and phosphorus atoms should be coplanar). It should be noted that the stereochemistries

Table 1.4: Phosphorus-Hydrogen Coupling Constants (Hz) for some η^3-Allyl-M Complexes*

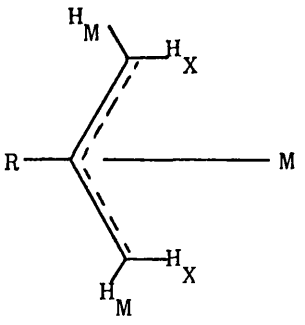

Compound	J(P-H_X)	J(P-H_M)	J(P-H_R)	REF
$[(\eta^3\text{-}C_3H_5)V(CO)_3(dpm)]$	~0	4.9[a]	~0	161
$[(\eta^3\text{-}2\text{-}MeC_3H_4)V(CO)_3(dpm)]$	~0	9.1[a]	~0	161
$[(\eta^3\text{-}C_3H_5)Mo(CO)_2(dpm)Cl]$	<1	3.3[a]	<1	162
$[(\eta^3\text{-}2\text{-}MeC_3H_4)Mo(CO)_2(bipy)(P(OPh)_3)]BF_4$	~0	2	~2	163
$[(\eta^3\text{-}C_3H_5)W(CO)_2(dpm)Cl]$	<1	3.3[a]	<1	162
$[(\eta^3\text{-}C_3H_5)Mn(CO)_3PPh_3]$	4.0	0	12.0	164
$[(\eta^3\text{-}C_3H_5)Mn(CO)_2(P(OMe)_3)_2]$	14.0[a]	1.0[a]	12.0[a]	164
$[(\eta^3\text{-}C_3H_5)Re(CO)_3PPh_3]$	4.0	0	10.8	164
$[(\eta^3\text{-}1\text{-}PhC_3H_4)Ru(PPh_3)_2H(CH_3CN)]$[b]	J_{PH_1}[c] = 5.8 $J_{P'H_2}$ = 4.5	6.4[c]	-	16
$[(\eta^3\text{-}C_3H_5)Ru(NO)(PPh_3)_2]$	6.0[a]	-	-	165
$[(\eta^3\text{-}C_3H_5)Co(CO)_2PPh_3]$	~0	2	-	166
$[(\eta^3\text{-}C_3H_5)Rh(PF_3)_3]$	4.6[d]	-[e]	0	167
$[(\eta^3\text{-}2\text{-}MeC_3H_4)Rh(PF_3)_3]$	5.9[d]	-	4.0	167
$[(\eta^3\text{-}1\text{-}PhC_3H_4)Ir(PPh_3)_2HCl]$[b]	$J_{PH(2)}$[f] = 11.3 $J_{P'H(1)}$ = 8.4	3.5[f]	-	168

...../contd.

Table 1.4: cont'd.

Compound	$J(P\text{-}H_X)$	$J(P\text{-}H_M)$	$J(P\text{-}H_R)$	REF
$[(\eta^3\text{-}1Bu^t\text{-}2\text{-}MeC_3H_3)Pd(dpe)]PF_6$ [g]	$J_{P\text{-}H(2)}$ $=J_{P'H(3)}$ $= 10$ $J_{P'H(2)}$ $= 1.5$ $J_{P\text{-}H(3)}$ < 1	$J_{P'H_4}$ $= 8$ $J_{P\text{-}H_4}$ $= 1$	–	169
$[(\eta^3\text{-}2\text{-}MeC_3H_4)Pt(PPhMe_2)_2]PF_6$	9.0 [f]	0.5 [f]	~ 0	150
$[(\eta^3\text{-}2\text{-}MeC_3H_4)Pt(dpe)]PF_6$	9.0 [f]	[e]	~ 0	151

* spectra recorded at room temperature unless otherwise stated.

a - protons coupled to 2 equivalent P nuclei

b - suggested structure

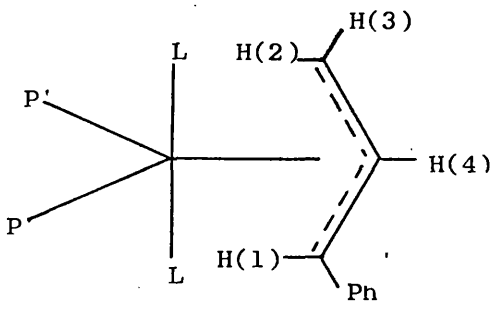

c - each proton couples to 1 P nucleus - (the workers involved suggest coupling is $J_{P_{cis}\text{-}H_{allyl}}$)

d - each proton couples to 3 equivalent P nuclei - spectrum was recorded at -50^oC

e - $J_{P\text{-}H}$ observed but too small to be accurately determined

f - protons are coupled to the one P trans nuclei

g

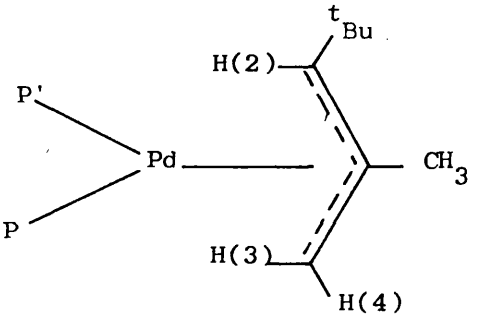

depicted for the complexes in Figure 1.11 are as determined in the solid state and it is conceivable that they may not be maintained in solution, particularly since η^3-allyl complexes are frequently stereochemically non-rigid on the NMR time scale.

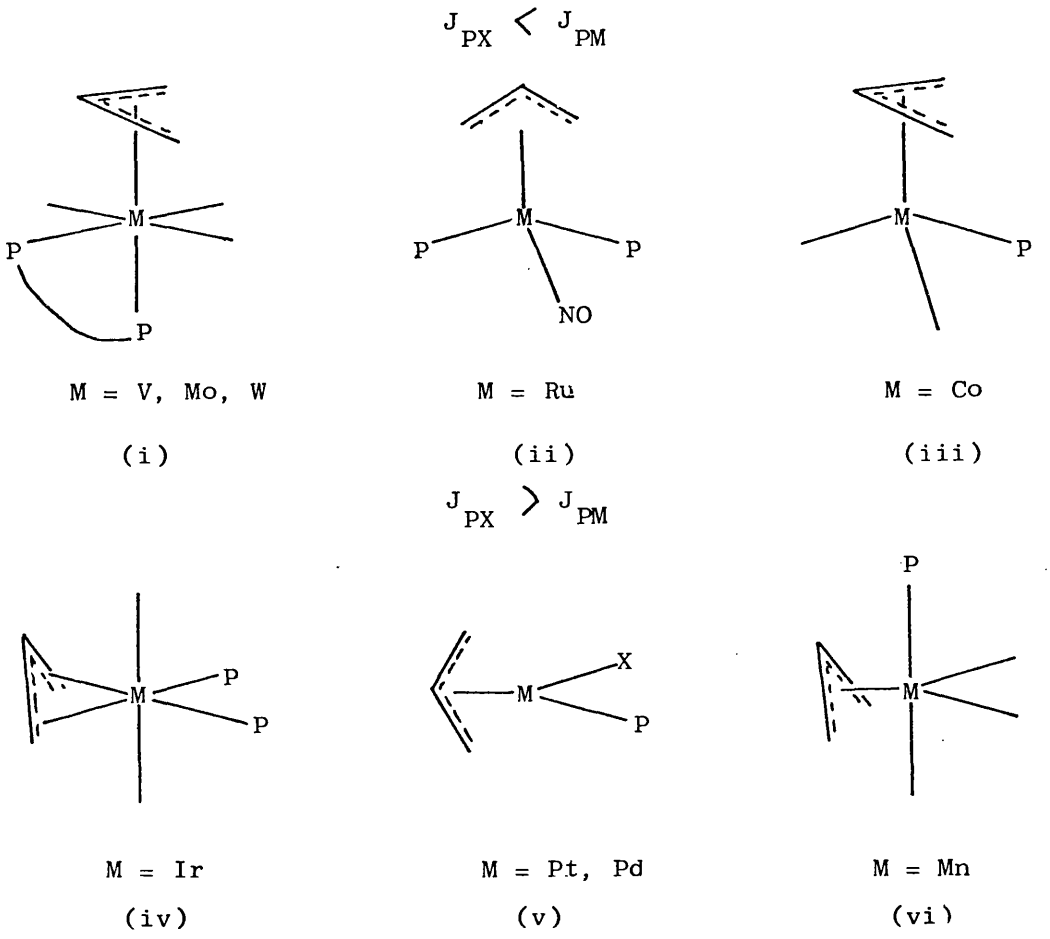

Figure 1.11: The stereochemistries for various η^3-allyl-phosphorus donor ligand-transition metal compounds*

* The stereochemistries of the η^3-allyl-phosphorus donor ligand-transition metal compounds are those which have been reported for such compounds or directly analogous species;
viz. structure type (i) has been found for $[(\eta^3\text{-}1\text{-}MeC_3H_4)V(CO)_3(diars)]$[170] and $[(\eta^3\text{-}C_3H_5)Mo(CO)_2(dpe)Cl]$[171]

(ii) has been found for $[(\eta^3\text{-}C_3H_5)Ru(NO)(PPh_3)_2]$[165]

(iii) " " " " $[(\eta^3\text{-}C_3H_5)Co(CO)_2(PPh_3)]$[172]
and is suggested for $[(\eta^3\text{-}C_3H_5)Rh(PF_3)_3]$

(iv) has been found for $[(\eta^3\text{-}1\text{-}PhC_3H_4)Ir(PPh_3)_2HCl]$[168]

(v) square planar arrangement of ligands observed for all Pd and Pt compounds of the type $[(\eta^3\text{-allyl})MLX]$[43,17]

(vi) has been found for $[(\eta^3\text{-}C_3H_5)Mn(CO)_2(P(OMe)_3)_2]$[164]
and is suggested for $[(\eta^3\text{-}C_3H_5)M(CO)_3(PPh_3)]$
M = Mn, Re.

Fluxional η^3-Allyl Transition Metal Compounds

Complexes possessing η^3-allyl groups are often fluxional. In most cases the dynamic behaviour observed may be identified as being due to one of three types of rearrangement, namely (i) syn-anti exchange, (ii) syn-syn, anti-anti exchange or (iii) interconversion between conformers. These rearrangements may involve either a motion of the η^3-allyl group itself or the non-rigidity of other parts of the molecule (e.g. pseudo-rotations).

(i) syn-anti exchange

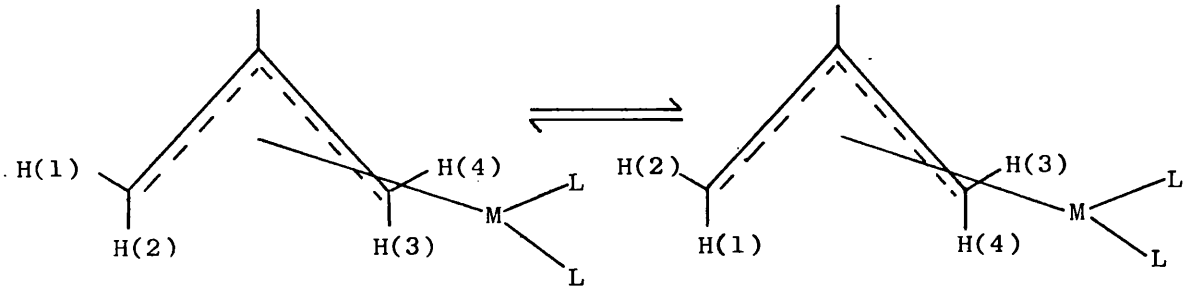

Figure 1.12. Syn-anti proton exchange

Some η^3-allylic complexes produce misleadingly simple ^{1}H NMR spectra which indicate that all the terminal hydrogens of the allyl group are equivalent. The spectra observed are those of typical AX_4 spin systems. Many isoleptic η^3-allyl complexes e.g. $[(\eta^3\text{-}C_3H_5)_4M]$ (M = $Zr^{174,175}$, Th^1) exhibit such a spectrum at and above room temperature, but a normal AM_2X_2 η^3-allylic spectrum at low temperatures. The equivalence of the terminal protons at ambient temperatures is obviously due to some rapid interchange of syn and

anti protons and a number of mechanisms have been suggested[176]. These include:-

(a) internal rotation of the CH_2 groups about the C-C bond in a short lived η^2-allylic intermediate (Scheme 1).

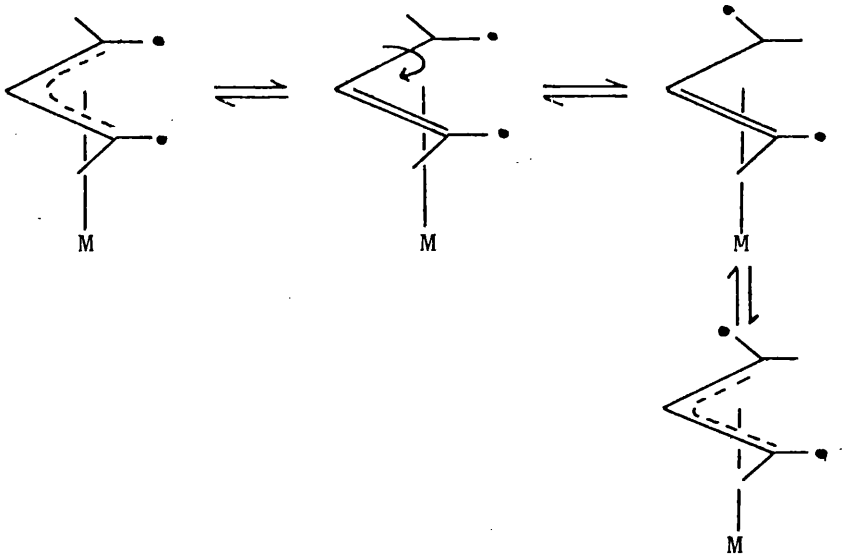

Scheme 1.5

(b) Isomerisation of the η^3-allyl system to a 1,3- η^2-allyl complex having the 3 carbon atoms of the allyl group in a common plane with the metal, followed by a return to η^3-allyl bonding (Scheme 1.6).

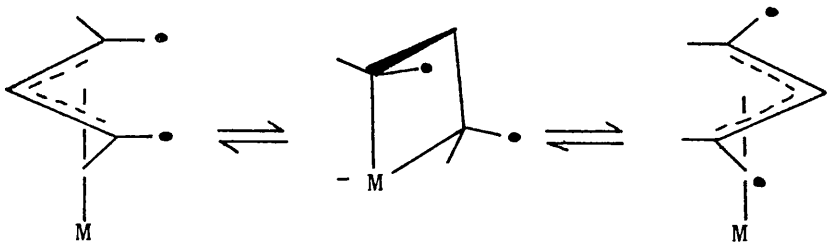

Scheme 1.6

(c) the most widely accepted mechanism involves a rapid $\eta^3 - \eta^1 - \eta^3$ interconversion for the allyl ligand. The syn and anti protons achieve equivalence by rotation about the metal-carbon single bond in the short lived η^1-allylic form, followed by reversion to an η^3-allyl complex (Scheme 1.7).

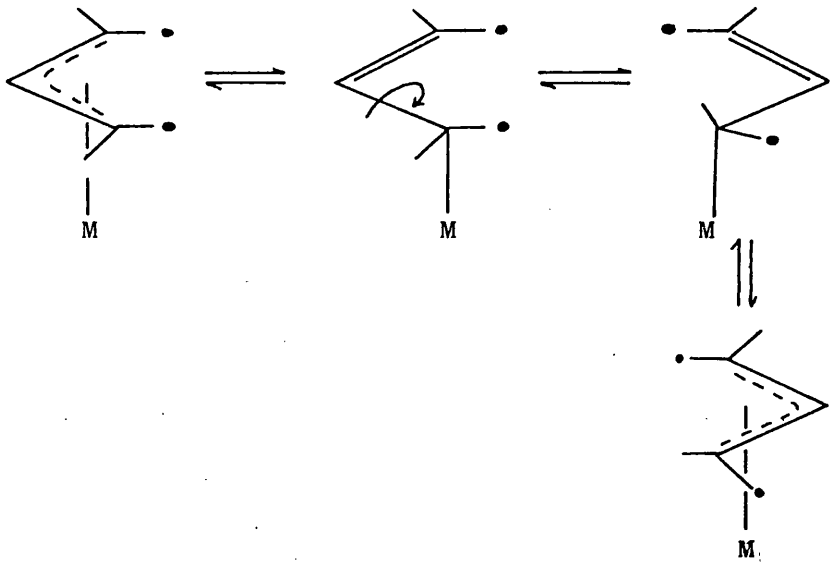

Scheme 1.7

Convincing evidence for (iii) has been obtained by Whitesides et al[177] from dynamic line shape calculations on $(\eta^3\text{-}C_3H_5)_4Zr]$ in $CFCl_3$ solutions.

Syn-anti exchange is commonly observed for non-isolepic compounds such as $[(\eta^3\text{-}2\text{-}MeC_3H_4)RhCl_2(AsPh_3)_2]$[178] and exchange may occur solely at one carbon atom as has been observed for the complex $[(\eta^3\text{-}2\text{-}MeC_3H_4)PdCl(PPhMe_2)]$[179]. The favoured mechanism in each of these examples is again an $\eta^3 - \eta^1 - \eta^3$ interconversion of the allyl ligand.

(ii) syn-syn, anti-anti exchange

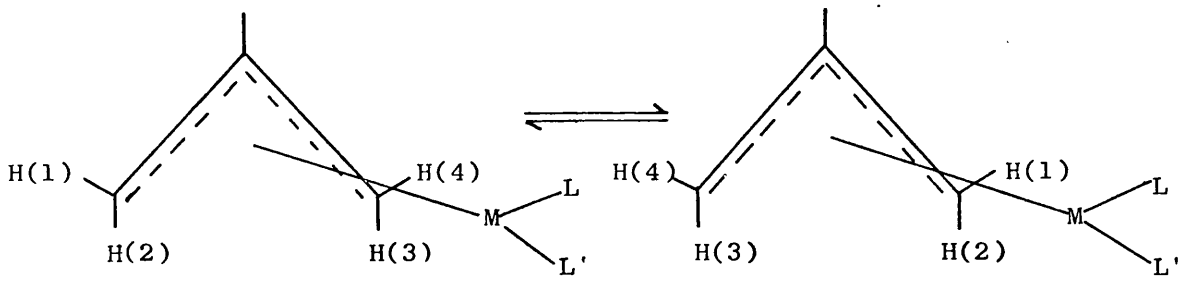

Figure 1.13 Syn-syn, anti-anti proton exchange

This type of exchange is most easily detected for complexes of low symmetry in which the terminal carbon atoms of the η^3-allyl group are inequivalent and an AGMPX spin pattern is observed in the limiting low temperature ^{1}H NMR spectrum. For complexes which exhibit syn-syn, anti-anti exchange raising the temperature results in the coalescence of the two syn proton resonances (G and M) and the two anti proton resonances (P and X) producing a normal AM_2X_2 spectrum. Syn-syn, anti-anti proton site exchange may be achieved either by a simple rotation of the allyl group about an axis passing through the metal or, alternatively, by some pseudorotation of the other ligands which by producing averaged environments for the terminal carbons of the allyl group results in the same experimental observations. In many instances it has been impossible to unequivocally establish the precise mechanism involved. However, very recently Faller et al[171] have reported the use of a combination of physical techniques, including variable

temperature ^{1}H, ^{31}P and ^{13}C NMR spectroscopies and a three-dimensional X-ray crystal structure determination, to demonstrate that the syn-syn anti-anti exchange observed in the room temperature ^{1}H NMR spectrum of $[(\eta^{3}\text{-}C_3H_5)Mo(CO)_2(dpe)X]$ (X = Cl, Br or I) is due, not to a rotation of the allyl, but to a pseudo-rotation of other ligands in the complex by a "trigonal twist" type mechanism as shown below in Figure 1.14.

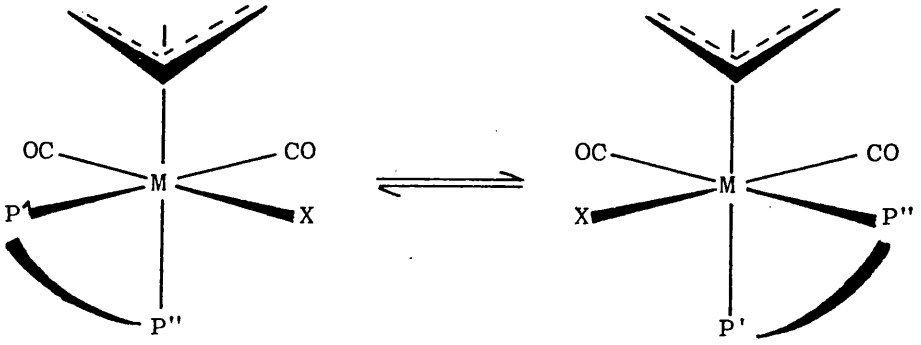

Figure 1.14. The trigonal twist rearrangement proposed for $[(\eta^{3}\text{-}C_3H_5)Mo(CO)_2(P\text{-}P)X]$ complexes.

This process involves the rotation of the triangular face formed by the halogen and the two phosphorus atoms with respect to the face formed by the allyl and two carbonyl groups. An important feature of this type of rearrangement is the limited number of permutations of sites which are allowed. This has important consequences in terms of the chirality of the molecule. Cahn et al[258] have set forth rules for the specification of chirality at metal centres in octahedral environments. According to these rules, the rearrangement depicted in Figure 1.14 illustrates a molecule interconverting between S and R configurations. Thus enantiomerisation of the metal centre results from this trigonal twist process.

Similar room temperature ^{1}H and ^{13}C NMR spectra have been reported for the related complex $[(\eta^{3}\text{-}C_3H_5)Mo(CO)_2(pd)(py)]$ which possesses a similar solid state structure with no plane of symmetry. For this species, however, two isomers ((i) and (ii) in Figure 1.15) were identified in the limiting low temperature ^{1}H NMR spectrum in $CDCl_3$, and because of this the authors suggest that

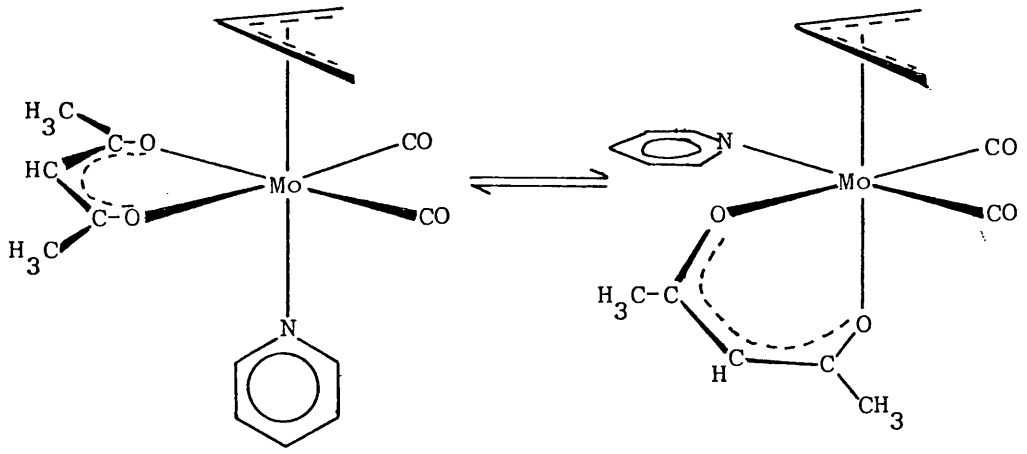

Figure 1.15: Symmetrical (i) and unsymmetrical (ii) isomers of $[(\eta^{3}\text{-}C_3H_5)Mo(CO)_2(pd)py]$

complete rotation of the trigonal face formed by the pyridine and two oxygen atoms (with respect to the $[(\eta^{3}\text{-}C_3H_5)Mo(CO)_2]$ unit) occurs[180].

Rotation of the η^{3}-allyl ligand about the allyl-metal bond has been invoked to explain the syn-syn, anti-anti exchange observed in the room temperature ^{1}H NMR spectrum of $[(\eta^{3}\text{-}C_3H_5)Mo(CO)_3(dpe)]PF_6$[181] (Scheme 1.8).

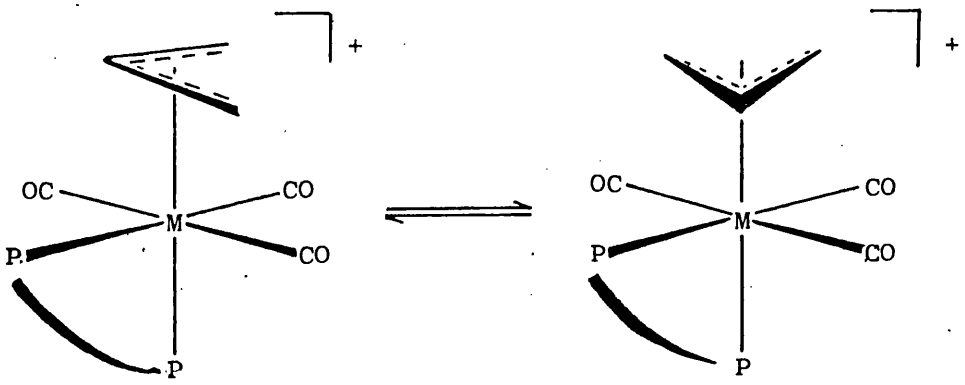

Scheme 1.8

For $[(\eta^3\text{-}C_3H_5)_2Ru(CO)_2]$[182] simultaneous exchange of the ends of both allyl groups is envisaged to occur by rotation of the two allyl groups 90° in the same direction possibly by a Ray-Dutt process (Scheme 1.9).

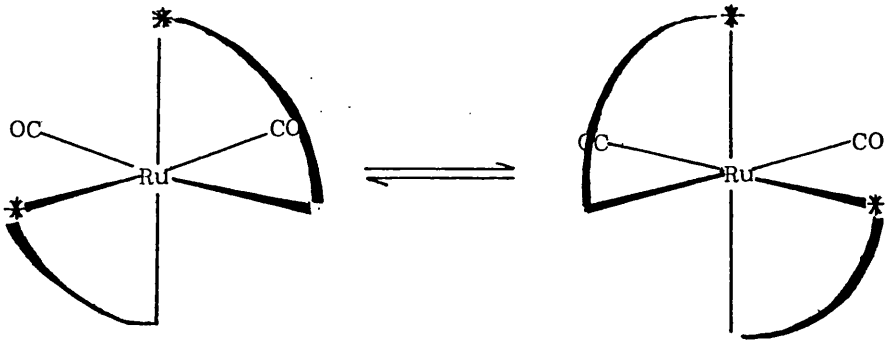

Scheme 1.9

Complexes which exhibit <u>syn-syn</u>, <u>anti-anti</u> proton exchange often also exhibit <u>syn-anti</u> proton exchange at higher temperatures, as observed for $[(\eta^3\text{-}C_3H_5)_2Ru(CO)_2]$[182] and $[(\eta^3\text{-}C_3H_5)Ir(CO)(PPh_3)_2]$[183].

(iii) <u>conformational isomerism</u>

The room temperature ^1H NMR spectrum of $[(\eta^3\text{-}C_3H_5)Fe(CO)_3X]$[184]

(X = Cl, Br, I) consists of two overlapping AM_2X_2 spin patterns indicating the presence of isomers I and II shown in Figure 1.16. (The solid state structure of $[(\eta^3\text{-}C_3H_5)Fe(CO)_3I]$[185] has been determined and is shown as I in Figure 1.16). The ratio of the

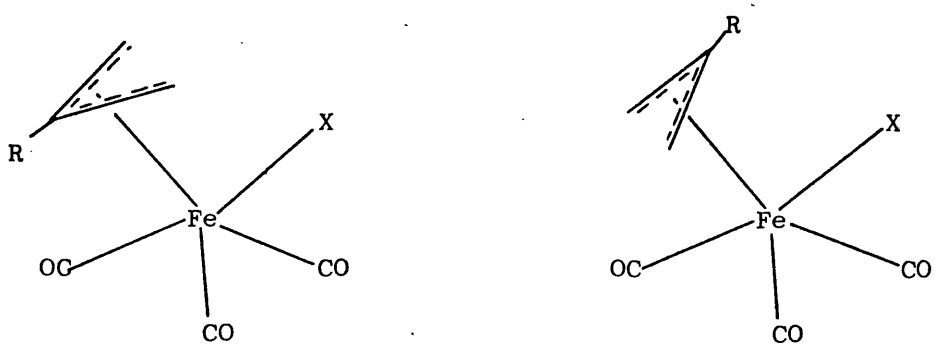

I II

Figure 1.16 The two isomeric forms of $[(\eta^3\text{-}C_3H_5)Fe(CO)_3X]$

two isomers vary between 1:1 and 1:8, depending upon the nature of the group R and the halogen X. In this instance the temperature dependence of the interconversion of the isomers could not be determined due to decomposition above +25°C, but for numerous other systems including $[(\eta^3\text{-}C_3H_5)_2Fe(CO)_2]$[184] and $[(\eta^3\text{-}C_3H_5)Mo(CO)_2(\eta^5\text{-}C_5H_5)]$[186] the two AM_2X_2 patterns of the isomers can be observed to coalesce to a single AM_2X_2 pattern in the high temperature spectra. The spectroscopic evidence is consistent with a rotation of the planar η^3-allyl moiety about the metal- η^3-allyl axis.

A particularly interesting variable temperature ^1H NMR spectrum is observed for $[(\eta^3\text{-}C_3H_5)_3Rh]$[154,155]. At -74°C three sets of AM_2X_2 patterns are observed indicating all three allyl groups are inequivalent but symmetrically bonded to the rhodium atom. At +34°C, two of the allyl groups become magnetically equivalent probably due to a rotation of the third allyl group in its own plane, as is shown in Figure 1.17.

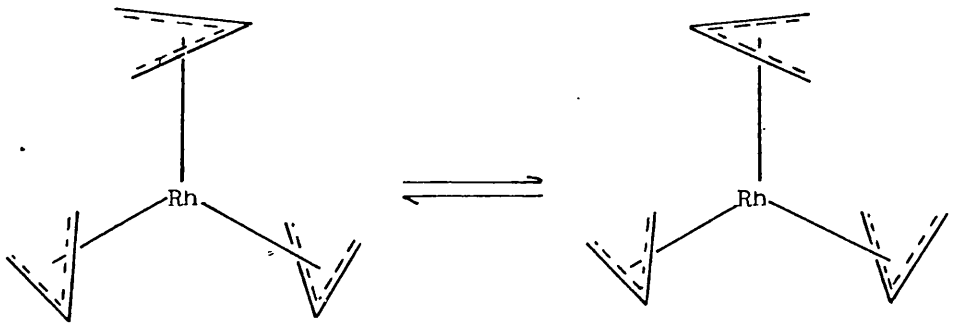

Figure 1.17: Rotation of the η^3-allyl group in its own plane in $[(\eta^3\text{-}C_3H_5)_3Rh]$

Base Induced η^3-Allyl Rearrangements

In a number of instances[33,151] the dynamic behaviour of complexes containing η^3-allyls is promoted by the presence of bases. Rearrangements of the η^3-allyl ligand which occur under these circumstances are not categorised under the headings of fluxional[187] or stereochemically non-rigid[188] η^3-allyls since the mechanisms involved can not truly be described as intramolecular.

The addition of pyridine to $[(\eta^3\text{-}2\text{-Me}\ C_3H_4)Pd(dpe)]\ PF_6$[189] in $CDCl_3$ at room temperature causes the observation of a fast syn-anti proton exchange on the ^{1}H NMR time scale. It is proposed that attack by pyridine at the palladium centre displaces one terminal carbon atom of the allyl group producing an η^1-allyl-M entity in which rotation about the carbon-carbon single bond effects syn-anti proton exchange before η^3-allyl-M bonding is recovered with loss of pyridine.

The dynamic behaviour of $[(\eta^3\text{-2-MeC}_3H_4)PdCl(PR_3)]$ in the presence of tertiary phosphines has been the subject of much discussion[138,169,176,190]. When the concentration of PR_3 is low, syn-syn, anti-anti proton exchange is observed. Vrieze[190] suggested that coordination of one molecule of PR_3 to $[(\eta^3\text{-2-MeC}_3H_4)PdCl(PR_3)]$ could conceivably produce a pentacoordinate intermediate in which a rotation of the allyl about the metal-allyl axis was a low energy process. Other workers[169] have since criticised this approach, and submitted evidence to show that the syn-syn, anti-anti proton exchanges proceed via consecutive S_N2 substitution reactions as shown in Scheme 1.10. (At higher concentrations of PR_3 ligand syn-anti exchange is also observed probably via a $\eta^3 - \eta^1 - \eta^3$ mechanism as shown in Scheme 1.11).

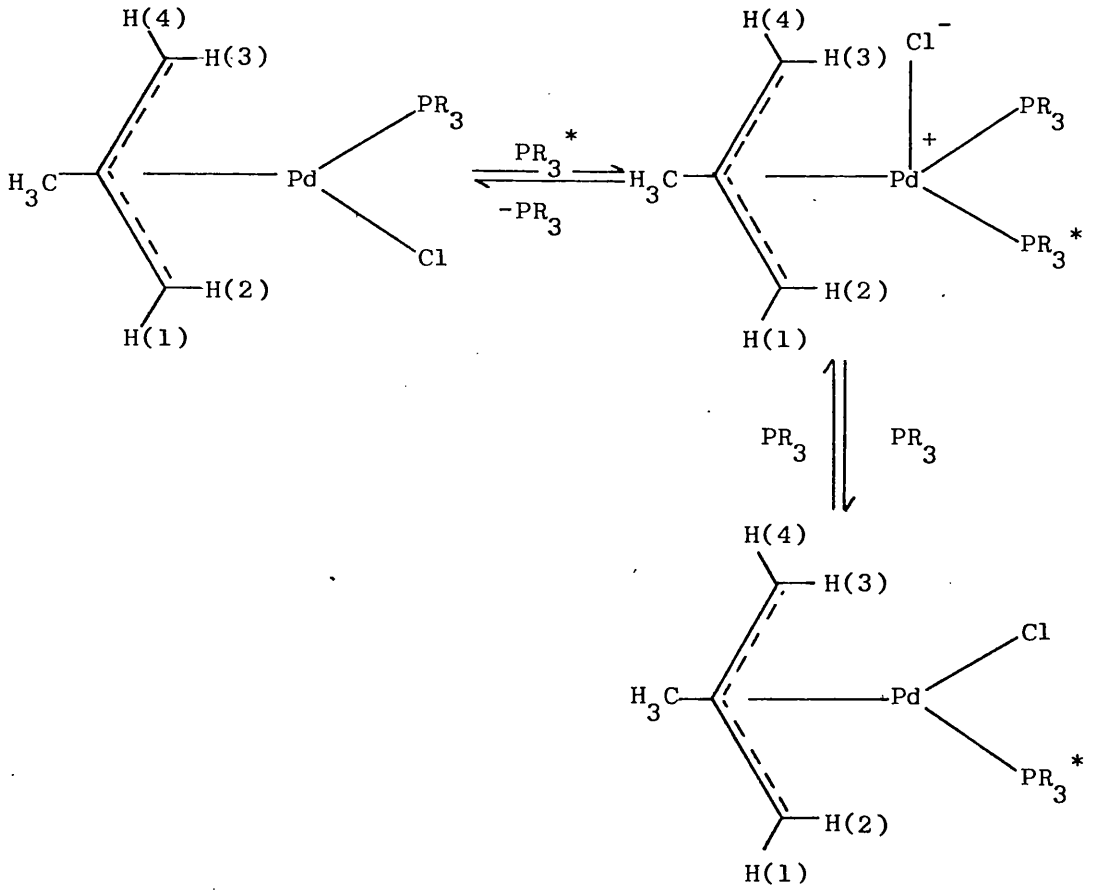

Scheme 1.10 Syn-syn exchange for $[(\eta^3\text{-}C_4H_7)PdCl(PR_3)]$ occurring at low PR_3 concentrations.

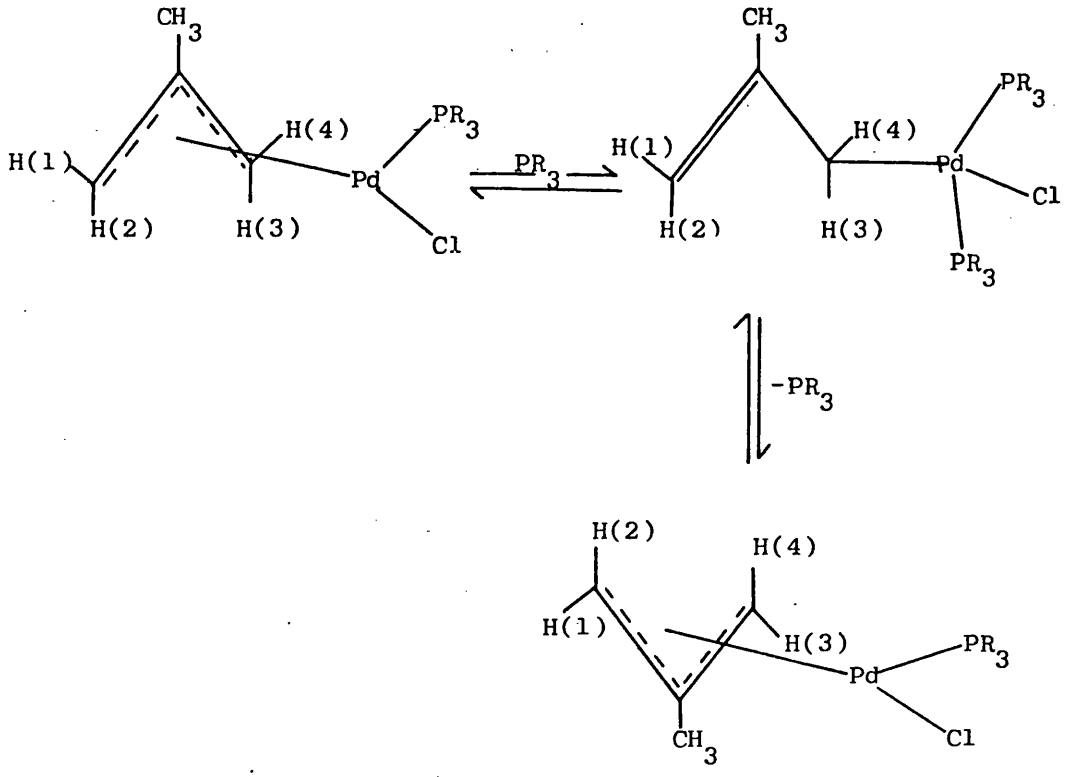

Scheme 1.11: Syn-anti exchange for $[(\eta\text{-}^{3}C_4H_7)PdCl(PR_3)]$ occurring at higher PR_3 concentrations

13-CARBON NUCLEAR MAGNETIC RESONANCE SPECTROSCOPY

It is only relatively recently that the potential of ^{13}C NMR spectroscopy as a structural tool has been fully exploited. Previously only crude instrumentation, which produced extremely poor quality spectra, was available and this seriously restricted the use of this technique. However, the improved signal-to-noise ratio now made possible by pulsed Fourier Transform and, for compounds containing carbon-hydrogen bonds, noise-decoupling techniques, has allowed the detailed study of a wider range of compounds including organometallics.

With the exception of perhaps palladium complexes relatively little data has been obtained for η^3-allyl-transition metal systems. Nevertheless ^{13}C chemical shifts of η^3-allyl ligands can be quite characteristic, as shown in Table 1.5.

For the unsubstituted derivatives, the terminal carbon atoms C(1) and C(3) have chemical shifts in the range 35-80 δ, the central carbon C(2) resonance is observed at lower field, characteristically in the range 90 - 140 δ. The deshielding effect of a methyl substituent (δ $\underline{C}$-Me occurs at lower fields than the analogous δ $\underline{C}$-H) is a commonly observed feature for these and other systems [197, 198, 200], as is the relative insensitivity of the chemical shifts to the formal charge on the complex [201].

Table 1.5: ^{13}C NMR Chemical Shifts and Coupling Constants for η^3-Allyl Compounds

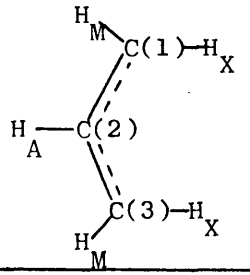

Compound[a]		Ref	^{13}C Chemical Shift (ppm; TMS = 0) C(1)	C(2)	C(3)	Coupling Constants (J in Hz)
$[(\eta^3\text{-1-Me}C_3H_4)Ti(\eta^4\text{-}C_4H_6)Cp]$[b]		191	80.9	124.4	57.7	$J(C\text{-}H_X) = J(C\text{-}H_M) = 155$
$[(\eta^3\text{-}C_3H_5)V(CO)_3dpae]$		192	53.1	88.0	53.1	
$[(\eta^3\text{-2-Me}C_3H_4)V(CO)_3dpae]$		192	55.4	105.8	55.4	
$[(\eta^3\text{-}C_3H_5)W(CO)_2dpeCl]$		171	52.2	73.0	52.2	
$[(\eta^3\text{-}C_3H_5)Mo(CO)_2dpeCl]$		171	60.4	83.7	60.4	
$[(\eta^3\text{-2-Me}C_3H_4)Mo(CO)_2(bipy)py]BF_4$		163	57.4	85.1	57.4	
$[(\eta^3\text{-}C_3H_5)Mn(CO)_4]$[c]		141	43.2	93.8	43.2	$J(C\text{-}H_X) = J(C\text{-}H_M) = 161$ $J(C\text{-}H_A) = 157$
$[(\eta^3\text{-1-Et}C_3H_4)Mn(CO)_4]$[c]		141	71.0	92.7	37.0	$J[C(1)\text{-}H_X] = J[C(1)\text{-}H_M] = 150$ $J[C(3)\text{-}H_X] = J[C(3)\text{-}H_M] = 162$ $J[C(2)\text{-}H_A] = 157$
$[(\eta^3\text{-}C_3H_5)Fe(CO)_3X]$[b,d]	X = Cl	193	59.5	100.6	59.5	
	X = Br	193	65.0	101.7	65.0	
	X = I	193	68.2	102.4	68.2	

...../cont'd.

Table 1.5 (cont'd).

Compound[a]	Ref.	^{13}C Chemical Shift (ppm; TMS = 0) C(1)	C(2)	C(3)	Coupling Constants (J in Hz).
$[(\eta^3\text{-}C_3H_5)Fe(CO)_4]BF_4$	142	56.8	99.2	56.8	$J(C\text{-}H_X) = J(C\text{-}H_M) = 163.3$ $J(C\text{-}H_A) = 165.5$
$[(\eta^3\text{-}1,1\text{-}Me_2C_3H_3)Fe(CO)_4]BF_4$	142	115.7	93.7	47.6	$J[C(3)\text{-}H_X] = J[C(3)\text{-}H_M] = 164.0$ $J[C(2)\text{-}H_A] = 161.8$
$[(\eta^3\text{-}2\text{-}MeC_3H_4)RhCpCl]$	194	59.1	107.9	59.1	$J[Rh\text{-}C(1)] = J[Rh\text{-}C(3)] = 10$ $J[Rh\text{-}C(2)] = 6$
$[(\eta^3\text{-}1\text{-}MeC_3H_4)RhCpCl]$	194	81.8	88.3	54.4	$J[Rh\text{-}C(1)] = 9$ $J[Rh\text{-}C(3)] = 10$ $J[Rh\text{-}C(2)] = 6$
$[(\eta^3\text{-}2\text{-}MeC_3H_4)RhCp(AsPh_3)]BF_4$	194	48.7	106.7	48.7	$J[Rh\text{-}C(1)] = J[Rh\text{-}C(3)] = 10$ $J[Rh\text{-}C(2)] = 6$
$[(\eta^3\text{-}1\text{-}MeC_3H_4)RhCp(PPh_3)]BF_4$	194	76.5	84.6	48.1	$J[Rh\text{-}C(1)] = J[Rh\text{-}C(3)] = 10$ $J[Rh\text{-}C(2)] = 4$
$[(\eta^3\text{-}C_3H_5)PdX]_2$ X = Cl	147	63.2	111.9	63.2	
X = Br	147	65.2	111.3	65.2	
X = I	147	68.0	110.2	68.0	
$[(\eta^3\text{-}C_3H_5)Pd(PEt_2Ph)_2]BF_4$	195	71.6	112.6	71.6	
$[(\eta^3\text{-}2\text{-}MeC_3H_4)Pd(PEt_2Ph)_2]BF_4$	195	71.0	136.3	71.0	
$[(\eta^3\text{-}C_3H_5)Pd(PPh_3)Cl]$	147	62.0	118.7	79.4	

...../cont'd.

Table 1.5 (contd)

Compound[a]		Ref.	^{13}C Chemical Shift (ppm; TMS = 0) C(1)	C(2)	C(3)	Coupling constants (J in Hz)
$[(\eta^3\text{-2-MeC}_3\text{H}_4)\text{PdCp}]$		147	47.0	112.2	47.0	$J[C(1)\text{-}H_M] = J[C(3)\text{-}H_M] = 157.3$; $J[C(1)\text{-}H_X] = J[C(3)\text{-}H_X] = 157.3$
$[(\eta^3\text{-1-MeC}_3\text{H}_4)\text{NiX}]_2$ [e]	X = Cl	196	70.0	106.9	48.0	$J[C(1)\text{-}H] = 161$; $J[C(3)\text{-}H_M] = J[C(3)\text{-}H_X] = 159$; $J[C(2)\text{-}H_A] = 163$
	X = Br	196	71.2	105.6	49.6	$J[C(1)\text{-}H] = J[C(3)\text{-}H_M] = J\ C(3)\text{-}H_X] = 161$; $J[C(2)\text{-}H_A] = 165$.
	X = I	196	76.3	105.5	52.4	$J[C(1)\text{-}H] = 161$; $J[C(3)\text{-}H_M] = J[C(3)\text{-}H_X] = 162$; $J[C(2)\text{-}H_A] = 161$.

a - determined at r.t.;

b - determined at 10°C;

c - determined at -95°C;

d - data for the major isomer;

e - δ rel. to hexamethyldisiloxane (HMDS)

Only a few spin-spin coupling constants for directly bonded ^{1}H-^{13}C have been reported for these systems; the magnitude of J(H-C) providing valuable information about the hybridisation of the carbon atoms[202]. Values of J(H-C) for these compounds normally fall in the range 155-165Hz which is consistent with sp^2 hybridisation of the allylic carbon atoms. In one detailed study[147] ^{13}C coupling to the syn protons H_M has been shown to be smaller than coupling to the anti protons H_X [$J(C-H_M)$ = 157.3Hz, $J(C-H_X)$ = 159.3Hz].

Studies of a series of square planar η^3-allyl compounds of Pd[147] and Ni[196] have shown that as the halide ligands trans to the allyl group are changed, the chemical shift of the terminal allylic carbons move to higher field in the order I < Br < Cl. This is the reverse order expected on the basis of changes in halogen electron withdrawing power, and suggests the η^3-allylic ligand in the iodine analogue is the most labile.

VIBRATIONAL SPECTROSCOPY

The absorptions due to η^3-allyl vibrations are characteristically weak, and as a consequence easily obscured by other ligand modes. Nevertheless two bands which are particularly diagnostic of the η^3-allyl group can be used in their identification, these are $\nu(CCC)_{asym}$ at $\sim 1400cm^{-1}$ and δ (CCC) at $\sim 530cm^{-1}$. In addition, the absence of a band at $\sim 1550cm^{-1}$ attributable to the ν(C=C) stretch of a carbon - carbon double bond, is useful evidence of η^3- as opposed to η^1-allyl bonding.

Partial data (especially for the modes mentioned above) have been reported for a number of compounds[203], but detailed studies (excluding a very early publication by Fritz[204]) have only recently been undertaken[70,205-212]. In the majority of cases, examination of the infrared and Raman spectra of the compounds indicates that the assignment of the internal vibrations of the η^3-allyl group may be made quite satisfactorily on the basis of C_s "local symmetry" i.e. the vibrations observed are characteristic of an isolated η^3-C_3H_5 group, there being little coupling of these modes with those from other parts of the molecule. Table 1.6 shows the eighteen normal modes of vibration (10A' + 8A") which group theory predicts for an η^3-C_3H_5 group of C_s symmetry, together with the additional 4 modes which are associated with allyl - metal skeletal vibrations. (For a group theoretical treatment of the [(η^3-C_3H_5)-M] entity see Appendix 2).

The assignments of observed bands to the various vibrational modes for a number of [(η^3-C_3H_5)-M] systems are shown in Table 1.7. These assignments have been arrived at by making use of techniques such as isotopic shift data[205,210] and polarised Raman effects[70,206-209]. Also comparisons with the vibrational spectra of hydrocarbons and co-ordinated ethylene[213-214] have been employed. For each compound the infrared spectrum has the same general form viz;

3100-2900 cm^{-1} - 5 bands assigned to the C-H stretching modes.

1500-1300 cm^{-1} - characterised by 3 bands - (usually the most intense of the spectrum)

1300-700 cm^{-1} - 9 fundamental modes expected

600-500 cm^{-1} - δ (CCC) fundamental expected

500-200 cm^{-1} - bands associated with allyl-M modes.

Table 1.6: Numbers and Symmetries of the Normal Modes for an [η^3-C_3H_5-M] Group.

Vibrational mode[a]	C_s symmetry species[b]
ν(CH)	A'
ν (CH_2)	2A' + 2A"
δ (CH_2)	A' + A"
π (CH)	A'
δ (CH)	A"
ν (CCC)	A' + A"
ρ_t (CH_2)	A' + A"
ρ_w (CH_2)	A' + A"
ρ_r (CH_2)	A' + A"
δ (CCC)	A'
ν [M-(allyl)]	2A' + A"
γ [M-(allyl)]	A"

a - ν = stretch; δ = in-plane deformation; π -out of plane deformation; ρ_t = twist; ρ_r = rock; ρ_w = wag ; γ = torsion.

b - all vibs are infrared and Raman active; A' vibs will give polarised Raman scattering, A" vibs will give depolarised Raman scattering.

Table 1.7: Vibrational Frequencies (cm^{-1}) and Proposed Assignments for the η^3-C_3H_5-M Modes in Various Compounds

$[(\eta^3\text{-}C_3H_5)PdCl]_2$ [h]	$[(\eta^3\text{-}C_3H_5)_3Ir]$ [g]	$[(\eta^3\text{-}C_3H_5)Re(CO)_4]$ [e]	$[(\eta^3\text{-}C_3H_5)Co(CO)_3]$ [c]	$[(\eta^3\text{-}C_3H_5)Mn(CO)_4]$ [a]	Assignment	$[(\eta^3\text{-}C_3H_5)Fe(CO)_2NO]$ [b]	$[(\eta^3\text{-}C_3H_5)Co(CO)_3]$ [d]	$[(\eta^3\text{-}C_3H_5)PdBr]_2$ [f]
3065w	3052m	3075w	3086w	3073m	$\nu(CH_2)A''$	3082ms	3078m	
3030vwbr	3012sh	3015w	3022w	3018m	$\nu(CH)A'$	3048w	3056sh	
2997vvw		2965vw	2970sh	2972w	$\nu(CH_2)A'$	3016ms	3014m	
	2990m			2962m	$\nu(CH_2)A''$	2932w	2955w	
		2935vw	2940w		$\nu(CH_2)A'$	2968ms	2922w	
1488w	1496m	1495m	1485m	1499s	$\delta(CH_2)_aA''$	1387s	1385s	1461s
1461ms	1455m	1463m	1476m	1464s	$\delta(CH_2)_sA'$	1466s	1469s	1383s
1385ms	1383m	1397w	1388m	1397m	$\nu(CCC)_aA''$	1492s	1484s	1491w
1299w	1216m	1214m	1225m	1215s	$\pi(CH)A'$	1229s	1224s	913w
1195w	1181m	1140w	1186m	1150w	$\delta(CH)A''$	1202s	1186m	1193w
1024m		1025vw	1071m	1020m	$\nu(CCC)_sA'$	966ms	950ms	1024s
1000wm	999s	1004m		1009m	$\rho_t(CH_2)_sA'$	1018s	1017s	998m
		978vw	927m [i]	980w	$\rho_t(CH_2)_aA''$	752ms	772s	767m

Table 1.7: Vibrational Frequencies (cm^{-1}) and Proposed Assignments for the η^3-C_3H_5-M Modes in Various Compounds

$[(\eta^3\text{-}C_3H_5)PdCl]_2$ [h]	$[(\eta^3\text{-}C_3H_5)_3Ir]$ [g]	$[(\eta^3\text{-}C_3H_5)Re(CO)_4]$ [e]	$[(\eta^3\text{-}C_3H_5)Co(CO)_3]$ [c]	$[(\eta^3\text{-}C_3H_5)Mn(CO)_4]$ [a]	Assignment	$[(\eta^3\text{-}C_3H_5)Fe(CO)_2NO]$ [b]	$[(\eta^3\text{-}C_3H_5Co(CO)_3]$ [d]	$[(\eta^3\text{-}C_3H_5PdBr]_2$ [f]
968ms	967m [i]	923m	950m	922m	$\rho_w(CH_2)_sA'$	926s	927sh	968s
943s	940w 929s 916s	872m	934m	886m	$\rho_w(CH_2)_aA''$	916s	932s	943vs
	895s	774vw	805w	785m	$\rho_r(CH_2)_aA''$	722w	735vw	1230w
766wmbr	793m	797w	775m	773w	$\rho_r(CH_2)_sA'$	778ms	812mw	767m
510m	598m 585m			523w	δ (CCC)A'	561sh	555vs	512s
402wm		377vs	375m	417m	ν [M-(allyl)]$_a$A''	335m	340m	403m
381wbr		395msh	410w	389m	ν [M-(allyl)]$_a$A'	417ms	415mw	379sh
366wm		332m	362m	331s	ν [M-(allyl)]$_s$A'	365ms	376s	369w

[a] - CS_2 solution (CCl_4 used in cut off regions) see ref. 207; [b] - Liquid film see ref. 210; [c] - liquid film see ref. 208; [d] - liquid film see ref. 211; [e] - melt see ref. 70; [f] - KBr disc 1500-500 cm^{-1} nujol mulls below 500 cm^{-1} see ref. 205; [g] - KBr disc see ref. 209; [h] - in nujol mulls see ref. 206; [i] - only observed in Raman spectrum.

The most striking point of contention between various workers is the assignment of the three bands in the 1500-1300cm^{-1} region of the spectra. Whilst these three bands are without doubt attributable to the modes $\delta(CH_2)_a A''$; $\delta(CH_2)_s A'$; and $\nu(CCC)_a A''$, only the A' mode (which is polarised in the Raman spectra) has been unequivocally assigned to the intermediate band at $\sim$ 1470cm^{-1} *. Paliani[210] has suggested that for $[(\eta^3\text{-}C_3H_5)Fe(CO)_2NO]$ the higher frequency band at $\sim$1500cm^{-1} corresponds to the skeletal $\nu(CCC)_a A''$ mode since it was scarcely influenced by deuteration, and Nakamoto proposed a similar, although unsupported, assignment for $[(\eta^3\text{-}RC_3H_4)PdX]_2$ (R = H, CH_3; X = Cl, Br)[205]. Davison and co-workers[207] however, are of the opinion that it is the band at lowest frequency ($\sim$1390cm^{-1}) which should be ascribed to $\nu(CCC)_a A''$. This latter interpretation of the spectra of $[(\eta^3\text{-}C_3H_5)Mn(CO)_4]$, is based on two points; firstly, the band at $\sim$1390cm^{-1} was considered to be too low to be assigned to the $\delta(CH_2)A''$ mode[203], and secondly, the Mn-allyl bond which is strong could reasonably be expected to cause a large perturbation of the bonding in the allyl group, producing a significant lowering of the $\nu(CCC)_a A''$ mode to that observed in $C_3H_5^-$ (which is found at 1535cm^{-1} [215]).

As shown in Table 1.7 there is little consistency between the various publications concerning the frequency assignments in the 1300-700 cm^{-1} region. This is understandable perhaps, since many

* This assignment effectively disproves an earlier assignment of this mode by Nakamoto[205].

vibrations of the same symmetry species occur within this fairly restricted frequency range, and as a result extensive coupling of modes is expected. Any assignments made therefore, can only be approximate indicating the mode considered to make the major contribution to a particular band.

η^3-ALLYL COMPLEXES OF THE GROUP VI TRANSITION METALS

Numerous η^3-allyl complexes of the Group VI transition metals have been prepared and characterised. These range from the 'pure allyl' or so-called isoleptic complexes such as $[(\eta^3\text{-}C_3H_5)_3Cr]$[1] and $[(\eta^3\text{-}C_3H_5)_4M]$ (M = Mo, W)[1] to those containing a wide variety of mixed ligands such as $[(\eta^3\text{-}C_3H_5)M(NO)CpI]$ (M = Mo[216] or W[123]). Particularly relevant to the work described in this thesis are the η^3-allyldicarbonyl complexes of general formula $[(\eta^3\text{-}C_3H_5)M(CO)_2L_2X]^{n\pm,o}$ where (L_2 = bidentate nitrogen, oxygen, phosphorus or arsenic, or two monodentate nitrogen or phosphorus, donor ligands and X = halides, pseudohalides, monodentate Lewis bases etc.). Compounds of this type possess interesting structural features and some have been found to be catalytically active in the polymerisation of dienes[217].

The parent unsubstituted carbonyl compounds i.e. $[(\eta^3\text{-}C_3H_5)M(CO)_4X]$ have proved to be very difficult to synthesise[218], indeed only the tungsten-bromide and -iodide analogues[219] have, as yet, been successfully prepared. These were isolated from U.V. photolysis of $W(CO)_6$ and the allyl halide in sealed and evacuated pyrex tubes. The chloride analogue could not be prepared by this route, but an incompletely characterised compound, formulated as $[(\eta^3\text{-}C_3H_5)W_2(CO)_6Cl_3]$ from analytical and mass spectral data, was obtained.

Both the infra-red and ^{1}H NMR spectra of $[(\eta^3\text{-}C_3H_5)W(CO)_4X]$, (X = Br, I) are consistent with the co-existence of two isomers (such as (i) and (ii) in Figure 1.18) in solution at room temperature.

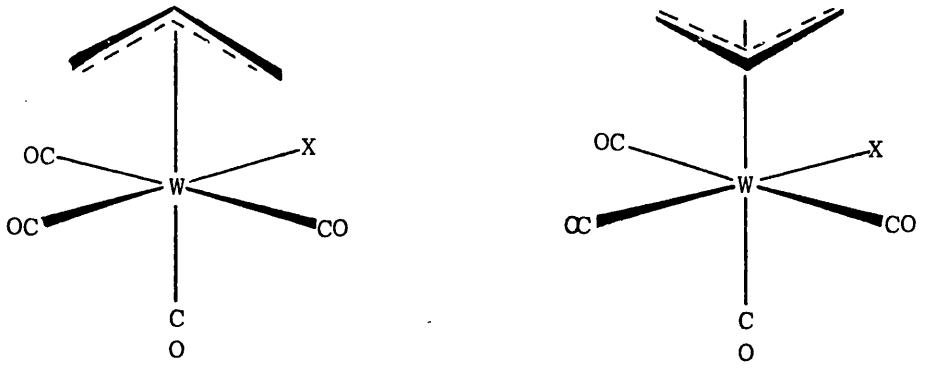

Figure 1.18: Possible isomeric forms for $[(\eta^3\text{-}C_3H_5)W(CO)_4X]$

Although detailed variable temperature ^{1}H NMR studies were not possible (due to the thermal instability of the species), interconversion of the two conformational isomers was indicated to occur above 80°C. In contrast to the parent compounds substituted derivatives of the type $[(\eta^3\text{-}C_3H_5)M(CO)_2L_2X]$ (X = halide or pseudohalide) are readily prepared. Essentially four routes have been used:

(a) Allyl oxidation of $[Mo(CO)_4L_2]$[73,221,222] and $[M(CO)_3L_2Y]$ (M = Mo, W)[73,220,221]

(b) Reaction of $M(CO)_6$, (M = Mo or W in some cases), allyl halides or pseudohalides and a donor ligand such as diamines[220], diethers[217], or acetonitrile[222].

(c) Bridge splitting reactions of $Et_4N[(\eta^3\text{-2-Me}C_3H_4)_2Mo_2(CO)_4Cl_3]$ with pyridine, 2,2'-bipyridine and 1,2-diaminoethane[223]

and (d) Reaction of $[M(CO)_3L_2X]^-$ anions (M = Cr, Mo or W) with allyl compounds[77,220,224].

Reaction (d) is especially important since it is the preferred route for the tungsten complexes which are formed only very slowly by routes (a) and (b) and, in addition, provides the only known route to the chromium analogues[77].

The resultant dicarbonyl complexes are stable to further CO displacement even by boiling pyridine[73]. Halide replacement however, may be readily effected by other anions such as SCN^- or $SC_6F_5^-$ [73], or Lewis bases such as PPh_3, $AsPh_3$ or C_5H_5N [163] in the presence of BF_4^- or BPh_4^-.

Crystal structure determinations have been performed on several compounds of the type $[(\eta^3\text{-allyl})M(CO)_2L_2X]$[126,171,180,217,225-229], but studies have mainly been restricted to the molybdenum compounds. Notably consistent features in their respective geometries are, firstly the basically octahedral environment for the metal, (that is if the allyl group is regarded as occupying one co-ordination site*), and secondly the fac-arrangement of the η^3-allyl and two cis-carbonyl ligands (see Figure 1.19). These features are common to all sterically non-hindered species† containing the

* While the allyl group can be considered as formally bidentate from a purely structural point of view it can be described as bi- or uni-dentate, depending on in what terms the geometry of the complex is best explained. The structure of the $[(\eta^3\text{-}C_3H_5)M(CO)_2L_2X]$ complexes is usually described as pseudo-octahedral, however, there is really little to choose from between this description and that of a capped trigonal prism with the bidentate allyl occupying the unique edge.

† The exception is $[(\eta^3\text{-}p\text{-}CH_3C_6H_4CH_2)Mo(CO)_2Cp]$[49] in which the presence of the bulky ring substituent on the allyl group doubtless creates a very strong steric preference for the structure with the η^3-allyl group rotated through 180° to that shown in Figure 1.19.

$[(\eta^3\text{-allyl})M(CO)_2]^{n\pm,o}$ (M = Mo, W) unit for which structures have been determined[126,171,180,216,217,225-241] prior to this work (see Chapter 4).

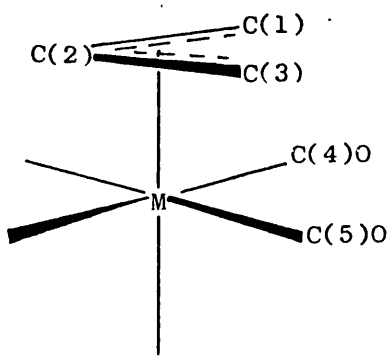

Figure 1.19: The fac-arrangement of the $[(\eta^3\text{-allyl})M(CO)_2]$ unit.

The constancy of the $[(\eta^3\text{-allyl})Mo(CO)_2]$ unit in the solid state is also quite striking as demonstrated in Table 1.8 which lists a selection of pertinent crystallographic parameters. Some authors consider the orientation of the η^3-allyl group with its terminal carbon atoms lying above and close to the cis-carbonyl ligands, to be energetically favourable and as such partially responsible for the relatively high stability of these complexes compared with other Mo(II) derivatives[180].

Another point of interest concerning the geometry of these complexes is that they may either adopt a structure with a plane of symmetry (hereafter referred to as "symmetrical" structure) or a structure without a plane of symmetry (termed the "unsymmetrical" structure). In the frequently encountered symmetrical structure the η^3-allyl group occupies the site trans to the unidentate ligand X,

Table 1.8: The Geometry of the $[(\eta^3\text{-allyl})M(CO)_2]$ Unit in Different Structures*

Compound†	Ref.	Str‡	C(1)-C(2)	C(2)-C(3)	C(1)-C(2)-C(3)	M-C(1)	M-C(2)	M-C(3)	Mean of M-C(4) & M-C(5)	C(4)-M-C(5)
$[(\eta^3\text{-}C_3H_5)Mo(CO)_2(dme)(CF_3CO_2)]$	217	S	1.45	1.45	114	2.34	2.16	2.34	1.90	79
$[(\eta^3\text{-}C_3H_5)W(CO)_2(dme)(CF_3CO_2)]$	217	S	1.36	1.36	123	2.29	2.07	2.29	1.84	75
$[(\eta^3\text{-}C_3H_5)Mo(CO)_2(bipy)NCS]$	225	S	1.46	1.42	116	2.29	2.20	2.35	1.93	78
$[(\eta^3\text{-}C_4H_7)Mo(CO)_2(phen)NCS]$	226	S	1.45	1.40	117	2.32	2.27	2.35	1.97	83
$[(\eta^3\text{-}C_3H_5)Mo(CO)_2(bipy)py]BF_4$	126	S	1.37	1.47	111	2.31	2.28	2.29	1.99	78
$[(\eta^3\text{-}C_3H_5)W(CO)_2(C_6H_{11}NCH.NCHC_6H_{11})Br]$	227	S	1.43	1.43	114	2.33	2.20	2.33	1.99	80
$[(\eta^3\text{-}C_4H_7)Mo(CO)_2(C_6H_{11}NCH.NCHC_6H_{11})Cl]$	228	S	1.42	1.42	112	2.33	2.27	2.33	1.98	81
$[(\eta^3\text{-}C_3H_5)Mo(CO)_2(pd)py]$	180	U	1.40	1.37	115	2.30	2.20	2.31	1.95	80
$[(\eta^3\text{-}C_3H_5)Mo(CO)_2(salal)py]$	229	U	1.37	1.42	115	2.32	2.24	2.34	1.91	79
$[(\eta^3\text{-}C_3H_5)Mo(CO)_2(dpe)Cl]$	171	U	1.40	1.40	116	2.34	2.22	2.35	1.96	78
$[(\eta^3\text{-}C_4H_7)Mo(CO)_2(MeGa(3,5\text{-}Me_2pz)_2OH)]$	230	U	1.40	1.41	114	2.33	2.26	2.36	1.92	76
$[(\eta^3\text{-}C_4H_7)Mo(CO)_2(Me_2Ga(3,5\text{-}Me_2pz)(OCH_2CH_2NH_2)]$	231	U	1.39	1.40	116	2.33	2.37	2.32	1.93	79
$[(\eta^3\text{-}C_3H_5)Mo(CO)_2\ MeGa(N_2C_3H_3)_3]$	232	S	1.38	1.37	116	2.36	2.23	2.34	1.94	81
$[(\eta^3\text{-}C_3H_5)Mo(CO)_2\ PhB(pz)_3]$	233	S	1.42	1.42	116	2.37	2.22	2.34	1.92	79
$[(\eta^3\text{-}C_7H_7)Mo(CO)_2\ PhB(pz)_3]$	233	S	1.41	1.39	121	2.37	2.23	2.42	1.94	82
$[(\eta^3\text{-}C_4H_7)Mo(CO)_2\ HB(pz)_3]$	234	S	1.42	1.42	113	2.34	2.26	2.36	1.96	82

...../contd.

Table 1.8 (contd)

	Ref.	Str≠	C(1)-C(2)	C(2)-C(3)	C(1)-C(2)-C(3)	M-C(1)	M-C(2)	M-C(3)	'Mean of M-C(4) & M-C(5)	C(4)-M-C(5)
$[(\eta^3\text{-}C_3H_5)Mo(CO)_2\ Et_2B(pz)_2\ (Hpz)]$	235	S	1.39	1.41	117	2.34	2.26	2.35	1.95	81
$[(\eta^3\text{-}C_3H_5)Mo(CO)_2\ HHB(3,5\text{-}Me_2pz)_2]$	236	U	1.42	1.35	118	2.33	2.21	2.36	1.95	80
$[(\eta^3\text{-}C_7H_7)Mo(CO)_2(Et(CHHCH_3)B(pz)_2]$	237	U	a							
$[(\eta^3\text{-}2\text{-}PhC_3H_4)Mo(CO)_2\ Et.(CHHCH_3)\ B(pz)_2]$	238	U	1.41	1.39	114	2.35	2.26	2.31	1.94	80
$[(\eta^3\text{-}C_4H_7)Mo(CO)_2\ Ph_2B(pz)_2]$[b]	239		1.43	1.40	115	2.33	2.28	2.36	1.89	80
$[(\eta^3\text{-}C_3H_5)W(CO)_2Cl_2PPh_3]\ NEt_4$	240	S	1.47	1.41	114	2.33	2.20	2.35	1.94	76
$[(\eta^3\text{-}C_3H_5)Mo(CO)_2(MeCN)_3]^+$	241	S	1.47	1.47	117	2.36	2.25	2.35	1.95	82
$[(\eta^3\text{-}C_3H_5)_2Mo_2(CO)_4Cl_3]^-$	241	S	1.38	1.46	118	2.38	2.23	2.30	1.94	82
			1.41	1.45	113	2.32	2.18	2.35	1.93	78
$[(\eta^3\text{-}C_3H_5)Mo(CO)_2Cp]$	216		1.38	1.38	121	2.36	2.24	2.36	1.95	83
Average values										
$[(\eta^3\text{-}C_3H_5)Mo(CO)_2L_3]$			1.41	1.41	116	2.34	2.24	2.34	1.94	80
$[(\eta^3\text{-}C_3H_5)W(CO)_2L_3]$			1.42	1.40	117	2.32	2.16	2.32	1.92	77

* - Carbon atom numbering system shown in Figure 1.19; ≠ - Donor atom underlined where not obvious;
≠ - Structural type S = symmetrical U = unsymmetrical (see text); a - Refined structural data not available;
b - No sixth co-ordination atom; c - All values fall within ± 5% of the average values except structure reported in Ref. 231 whose M-C(2) length falls within 6% of the average value.

and the donor atoms from the bidentate, L_2, lie approximately co-planar with the cis-dicarbonyl groups (as shown in Figure 1.20(i)).

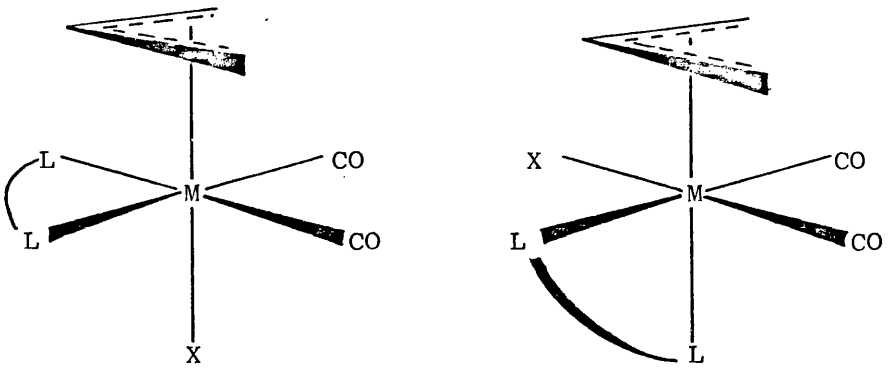

(i) (ii)

Figure 1.20: The (i) symmetrical and (ii) unsymmetrical arrangements of the L_2 and X ligands in $[(\eta^3\text{-allyl})M(CO)_2L_2X]$.

Few complexes adopt the alternative lower symmetry structure Figure 1.20(ii) but these include $[(\eta^3\text{-}C_3H_5)Mo(CO)_2(pd)py]$[180]. $[(\eta^3\text{-}C_3H_5)Mo(CO)_2(dpe)Cl]$[171] and $[(\eta^3\text{-}C_3H_5)Mo(CO)_2(salal)py]$[229]. Each of these complexes possess a chiral metal centre the chirality of which may be designated (S) or (R) in accordance with the octahedral sequence and chirality rules[258].

No explanation has been offered yet as to why these compounds should exhibit this particular ligand distribution, but the choice of bidentate ligand is most probably significant. It is perhaps noteworthy that in two of the examples quoted i.e. $[(\eta^3\text{-}C_3H_5)Mo(CO)_2(dpe)Cl]$[171] and $[(\eta^3\text{-}C_3H_5)Mo(CO)_2(pd)py]$[180], the chelating ligands pd and dpe both possess a considerable capacity to accept electron density from the metal ion. Sites particularly unfavourable for

ligands of this type will be those trans to the synergically bonded carbonyl ligands and this would presumably destabilise the structure of higher symmetry.

Such a low symmetry structure has also been found for the related compounds $[(\eta^3\text{-allyl})Mo(CO)_2(\text{tridentate})]$ containing the anionic bis(pyrazolyl)borato ligand[236-238], where the sixth co-ordination site is completed by a C(B)-H-Mo bridge or remains vacant[239] (the bis-[230] and mono-[231](pyrazolyl)gallato ligands have been shown to behave similarly). In each of these latter examples the η^3-allyl group is sited trans to a pyrazolyl nitrogen atom in preference to other nitrogen or oxygen donor atoms of the tridentate ligand, an arrangement which has been claimed to allow greater steric freedom for the η^3-allyl group[242]. Finally a combination of steric and electronic factors is probably responsible for the unsymmetrical structure of $[(\eta^3\text{-}C_3H_5)Mo(CO)_2(\text{salal})py]$[229] where the nitrogen and oxygen donor atoms of the bidentate N-phenylsalicylideneiminato(salal) ligand are sited trans to η^3-allyl and CO ligands respectively.

A number of compounds with the stoichiometry $[(\eta^3\text{-allyl})M(CO)_2L_2X]$ (M = Mo, W; X = Cl., Br, I) have been successfully prepared from the compounds $[(\eta^3\text{-allyl})M(CO)_2(MeCN)_2X]$ by replacement of the weakly bonded nitrile ligands by phosphorus[162,222,243] arsenic[244] and nitrogen[222, 243, 245, 246] ligands. These compounds have also proved to be of considerable synthetic importance in the preparation of many other M(II)[222, 247, 248] and M(O)[247,249-251] compounds and since they have been used extensively throughout the work described in this thesis will be discussed in more detail.

The Reactivity of $[(\eta^3\text{-}C_3H_5)M(CO)_2(MeCN)_2X]$

In 1968, Hayter[222] published an extremely efficient synthesis of $[(\eta^3\text{-allyl})M(CO)_2(MeCN)_2X]$ (M = Mo, W; X = Cl, Br; allyl = C_3H_5, C_4H_7, C_3H_4Cl, C_6H_9 or C_3Ph_3) which for the molybdenum compounds simply consisted of refluxing the reagents $Mo(CO)_6$, allyl halide and acetonitrile, together. (For the tungsten derivatives a slightly more involved synthetic route was required in which $[(CH_3CN)_3W(CO)_3]$[252] was initially isolated and then reacted with allyl halide). The acetonitrile of these complexes was reported to be readily replaced by bidentate ligands such as 2,2'-bipyridine, 1,10-phenanthroline and 1,2-bis(diphenylphosphino)ethane. Further investigations, mainly concerning the reactivity of $[(\eta^3\text{-}C_3H_5)Mo(CO)_2(MeCN)_2Cl]$ were conducted by Dieck and co-workers[249, 250, 253] who showed that in reactions with monodentate phosphine ligands PR_3 (R = Ph or n-Bu), the allyl group was eliminated as allylphosphonium halide and the vacant co-ordination sites occupied by further phosphine ligands to give the zero-valent cis-dicarbonyl complexes $[Mo(CO)_2(MeCN)_2LL']$ L = L' = PPh_3; L = L' = $P(n\text{-}Bu)_3$; L = MeCN, L' = $P(n\text{-}Bu)_3$. Dieck stressed that the Mo(0) products were formed in a variety of solvents (methanol, anisole, mesitylene, benzene) and that under no conditions could he obtain any indication that the acetonitrile ligands could be displaced to give complexes of the type $[(\eta^3\text{-}C_3H_5)Mo^{II}(CO)_2(PR_3)_2Cl]$. These latter species were perhaps the ones which Dieck had expected to isolate, since, as stated earlier, simple MeCN replacement by 1,2-bis(diphenyl - phosphino)ethane had been observed and the tungsten analogues $[(\eta^3\text{-}C_3H_5)W^{II}(CO)_2(PPh_3)_2X]$ (X = Br, I) had already been reported,

albeit prepared by a different route[219]:-

$$[(\eta^3\text{-}C_3H_5)W^{II}(CO)_4X] \xrightarrow{PPh_3} [(\eta^3\text{-}C_3H_5)W^{II}(CO)_2(PPh_3)_2X]$$

Recently, however, Hohmann[251] has shown that it is not possible to prepare these latter species by the reaction of PR_3 (R = Ph, n-Bu) with $[(\eta^3\text{-}C_3H_5)W(CO)_2(MeCN)_2X]$. He obtained, as Dieck did for the molybdenum analogues, only M(0) compounds of the type $[W(CO)_2(PR_3)_2(MeCN)L]$ (R = Ph, L = MeCN; R = n-Bu, L = PR_3). Further work by Brisdon[162] has shown that under mild conditions (at room temperature), reaction with 1,2-bis(diphenylphosphino)methane also causes MeCN displacement, as does the monodentate phosphine $HPPh_2$[254] which has subsequently been reported by Dieck. It therefore appears that the reaction of $[(\eta^3\text{-}C_3H_5)M(CO)_2(MeCN)_2X]$ (M = Mo, W; X = Cl, Br) with phosphines under mild conditions can follow one of two routes (A) or (B) Scheme 1.12.

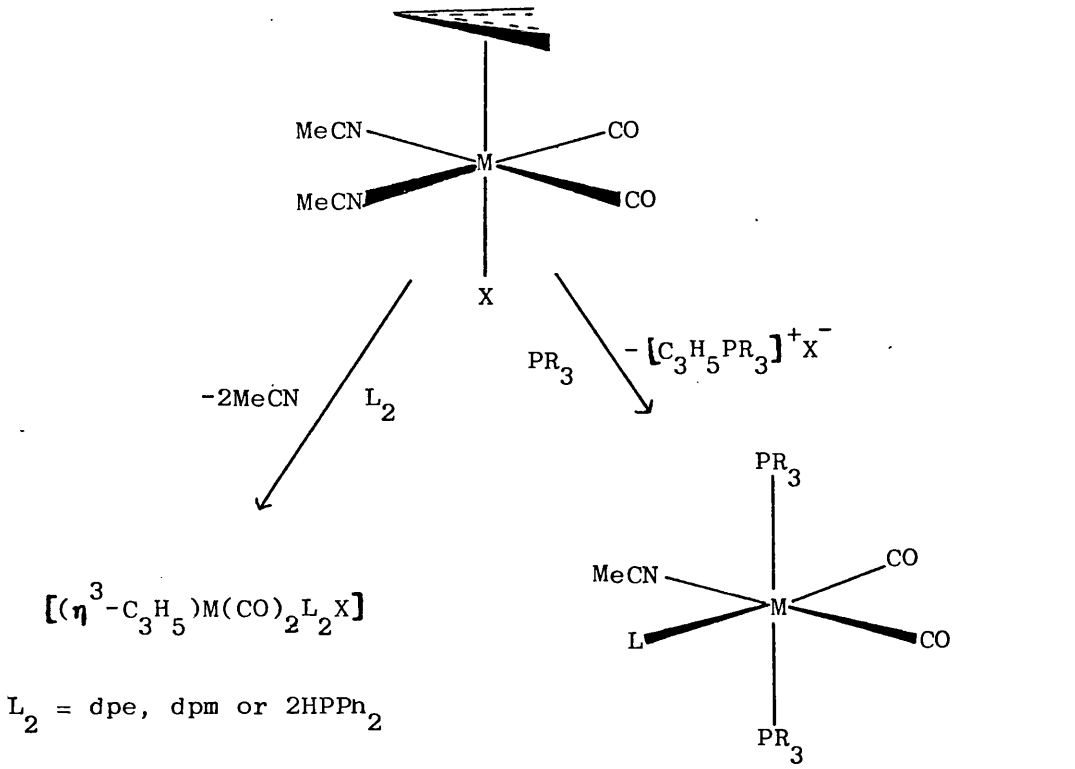

Scheme 1.12.

Fundamentally, the routes (A) and (B) differ in the site of nucleophilic attack by the phosphorus ligands. In (A) attack has evidently occurred at the metal centre whilst in (B) it has occurred at the co-ordinated allyl ligand. By using considerably more forcing conditions (boiling acetonitrile or acetone) Brisdon[244] has observed that both 1,2-bis(diphenylphosphino)-ethane and 1,2-bis(diphenylphosphino)methane react with $[(\eta^3\text{-}C_3H_5)Mo(CO)_2(MeCN)_2X]$ (X = Cl, Br, I) to effect allyl halide elimination with the production of the Mo(0) complexes cis-$[Mo(CO)_2(L_2)_2]$ (L_2 = dpm, dpe). However, in this reaction the substituted products $[(\eta^3\text{-}C_3H_5)Mo(CO)_2L_2X]$, ($L_2$ = dpe or dpm), are formed before reduction occurs, unlike the monodentate tertiary phosphine reactions where no intermediate Mo(II) complex of the type $[(\eta^3\text{-}C_3H_5)Mo(CO)_2(PR_3)_2Cl]$ could be obtained even under extremely mild conditions[244,255].

The work described in this thesis has been ultimately concerned with the collection of relevant experimental data in an effort to rationalise the differing reactivities of various phosphorus and arsenic donor ligands towards $[(\eta^3\text{-}C_3H_4R)M(CO)_2(MeCN)_2X]$ (M = Mo, W; R = H; X = Cl, Br, I; M = Mo, R = Me, X = Cl). Of crucial importance to this work are the rather unique solution properties of the complexes $[(\eta^3\text{-}C_3H_5)M(CO)_2(MeCN)_2X]$ (M = Mo; X = Cl, Br) which have recently been reported by Brisdon and Cartwright[256,257]. The significant features of these complexes, together with those of the tungsten analogues and $[(\eta^3\text{-}2\text{-}MeC_3H_4)Mo(CO)_2(MeCN)_2Cl]$, are described in Chapter Two.

CHAPTER TWO

SOLUTION PROPERTIES OF

$[(\eta^3\text{-}C_3H_4R)M(CO)_2(MeCN)_2X]$

INTRODUCTION

Although Dieck[243] had previously reported that the ^1H NMR spectra of the species $[(\eta^3\text{-}C_3H_5)Mo(CO)_2(MeCN)_2X]$ (X = Cl or Br) in CD_3CN and $CDCl_3$, were as expected i.e. an AM_2X_2 pattern for the symmetrically bonded $\eta^3\text{-}C_3H_5$ group and a singlet for two equivalent MeCN ligands, Brisdon and Cartwright[257] were unable to repeat these findings. The spectra that they obtained [in CD_3CN, $CDCl_3$ and $(CD_3)_2CO$] were considerably more complex and could only be interpreted on the basis that at least three distinct $\eta^3\text{-}C_3H_5$ entities were present in the solutions. After eliminating possible sources of discrepancy, such as hydrolysis, impurities and dimer formation[243], they realised that one of the sets of η^3-allyl signals was characteristic of the anion $[(\eta^3\text{-}C_3H_5)_2Mo_2(CO)_4X_3]^-$ (ref. 75). This observation led to the speculation that the spectra were indicative of the presence of an equilibrium involving the neutral species $[(\eta^3\text{-}C_3H_5)Mo(CO)_2(MeCN)_2X]$ and a positive and negative ion which were formed on dissociation in solution;

$$3[(\eta^3\text{-}C_3H_5)M(CO)_2(MeCN)_2X] \rightleftharpoons [(\eta^3\text{-}C_3H_5)M(CO)_2(MeCN)_3]^+ + [(\eta^3\text{-}C_3H_5)_2M_2(CO)_4X_3]^- + 3MeCN \qquad (2.1)$$

This autoionisation was calculated to be most extensive for the chloro-complex, particularly in CD_3CN and $(CD_3)_2CO$, (K, 7×10^3 mol^2/dm^2). For the corresponding bromo-complex a similar but less pronounced degree of ionisation was observed (K, $(CD_3)_2CO$, 7×10^{-2} mol^2/dm^2), but there was no indication that the iodo-complex behaved in a similar way. Traces of $[(\eta^3\text{-}C_3H_5)Mo(CO)_2(MeCN)_3]^+$ detected in CD_3CN solutions of the iodo-complex were attributed to a simple solvolytic process:

$$[(\eta^3\text{-}C_3H_5)Mo(CO)_2(MeCN)_2I] + MeCN \longrightarrow [(\eta^3\text{-}C_3H_5)Mo(CO)_2(MeCN)_3]^+ + I^- \qquad (2.2)$$

The absence of any anionic allyl species in these solutions was not regarded as particularly surprising since earlier work had indicated that the iodide ion is unable to stabilise a halogen-bridged anion of the type $[(\eta^3\text{-}C_3H_5)_2M_2(CO)_4X_3]^-$ (M = Mo or W) [223].

Dieck[243] had also reported that attempted recrystallisations of $[(\eta^3\text{-}C_3H_5)Mo(CO)_2(MeCN)_2X]$ (X = Cl or Br but not I) from hot benzene solutions, resulted in the formation of what he proposed was a neutral halogeno-bridged dimeric species $[(\eta^3\text{-}C_3H_5)Mo(CO)_2(MeCN)X]_2$. However, Brisdon, Cartwright and Drew[241] showed (by a single crystal X-ray study on the chloro-derivative) that the correct formulation for this "dimeric" species was in fact $[(\eta^3\text{-}C_3H_5)Mo(CO)_2(MeCN)_3]^+$ $[(\eta^3\text{-}C_3H_5)_2Mo_2(CO)_4X_3]^-$ (isolated in the crystalline form as the benzene solvate).

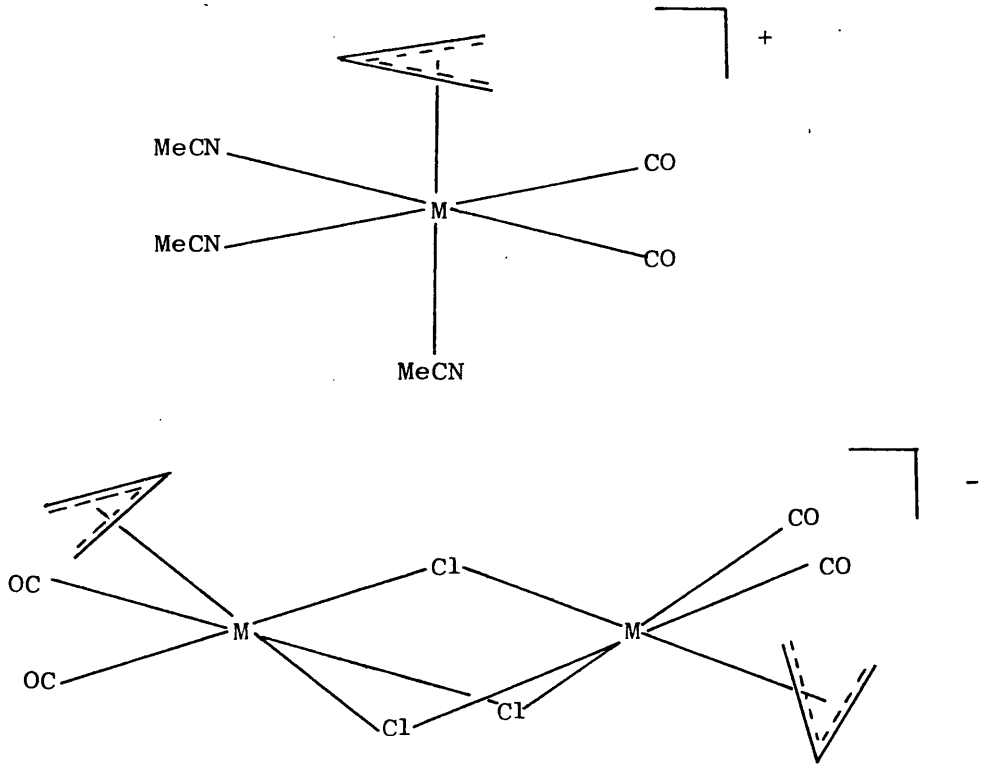

Figure 2.1. The molecular structure of $[(\eta^3\text{-}C_3H_5)Mo(CO)_2(MeCN)_3][(\eta^3\text{-}C_3H_5)_2Mo_2(CO)_4Cl_3]$.

This is fully consistent with their proposed ionisation of the neutral bis-MeCN compounds, and demonstrates that in the presence of a large excess of a non-coordinating solvent such as benzene, the ionic product preferentially crystallises out.

This chapter describes the preparation and characterisation of the starting materials $[(\eta^3\text{-}C_3H_4R)M(CO)_2(MeCN)_2X]$ (R = H, M = Mo or W, X = Cl, Br or I; and R = Me, M = Mo, X = Cl), which have been used throughout the work in this thesis. Also incorporated here is an extension of the work by Brisdon and Cartwright[257] on the solution properties of these compounds to include the η^3-2-methylallylmolybdenum and η^3-allyltungsten analogues. For comparative purposes the tungsten anion $[(\eta^3\text{-}C_3H_5)_2W_2(CO)_4Cl_3]^-$ and cation $[(\eta^3\text{-}C_3H_5)W(CO)_2(MeCN)_3]^+$ were synthesised separately and isolated as the Ph_4As^+ and BF_4^- salts respectively. These compounds are discussed first because their ^1H NMR spectra are much simpler than those of the neutral bis-MeCN compounds and as such may be useful in familiarising the reader with the typical ^1H NMR spectra of the η^3-allyl metal species.

EXPERIMENTAL

Details of physical techniques and solvents appear in appendix 3. Details of the yields and analyses (where appropriate) are presented in Table 2.1.

Two methods were employed in the preparation of the compounds $[(\eta^3\text{-}C_3H_4R)M(CO)_2(MeCN)_2X]$[222].

a. Preparation of $[(\eta^3\text{-}C_3H_4R)Mo(CO)_2(MeCN)_2X]$ (R = H, X = Cl or Br; R = Me, X = Cl).

$Mo(CO)_6$ (10.0 mmol, 2.64 g) and excess allyl halide (C_3H_5Cl 5cm^3; C_3H_5Br 4cm^3; C_4H_7Cl 5cm^3;) in acetonitrile (30 cm^3), were refluxed gently under a steady stream of nitrogen gas for 20h (X = Cl) or 6h (X = Br). Evaporation of the solvent to low bulk at room temperature caused precipitation of the analytically pure products which were collected on a sinter and dried *in vacuo*. Yields $>$ 70%.

b. Preparation of $[(\eta^3\text{-}C_3H_5)M(CO)_2(MeCN)_2X]$ (M = Mo, X = I; M = W, X = Cl, Br or I).

A solution of $[(MeCN)_3M(CO)_3]$[252], obtained by refluxing the appropriate hexacarbonyl $M(CO)_6$ (10.0 mmol) in acetonitrile (50 cm^3) (M = Mo, 18h; M = W 150h), was allowed to cool to 60^{o}C and then treated dropwise with a slight excess of allyl halide (2 cm3). The solution was stirred at 60^{o}C until carbon monoxide evolution had ceased. The product in each case was obtained on standing the partially evaporated solution at 0^{o}C, and was collected by filtration and dried *in vacuo*. Yields $>$ 50%. The compounds $[(\eta^3\text{-}C_3H_4R)M(CO)_2(MeCN)_2X]$ were readily soluble in the polar solvents $CHCl_3$, CH_2Cl_2, $(CH_3)_2CO$, CH_3OH, C_2H_5OH and also benzene and toluene. The molybdenum compounds were

found to be slightly more soluble than the tungsten analogues.

Preparation of $[(\eta^3\text{-}C_3H_4R)M(CO)_2(MeCN)_3]BF_4$ (M = Mo or W, R = H; M = Mo, R = Me).

$[(\eta^3\text{-}C_3H_4R)M(CO)_2(MeCN)_2Cl]$ (1.0mmol) was dissolved in acetonitrile (7 cm^3) and $AgBF_4$ (1.0mmol, 0.20g) added. An immediate precipitate of AgCl was observed. After stirring the solution for 20 min at room temperature, the mixture was filtered to remove AgCl and the clear yellow filtrate evaporated to dryness in vacuo. The residue was redissolved in acetonitrile (5 cm^3), the solution filtered, and the filtrate evaporated in vacuo to yield the pure product as an air-sensitive yellow powder. Yields 60%.

The products were soluble in the polar solvents CH_3CN, CH_3OH, $CHCl_3$, CH_2Cl_2 and $(CH_3)_2CO$.

Preparation of $Ph_4As[(\eta^3\text{-}C_3H_5)_2Mo_2(CO)_4Cl_3]$ [257].

Ph_4AsCl (2.4mmol, 1.00g) and $Mo(CO)_6$ (3.0mmol, 0.80g) were refluxed gently in 2-methoxyethyl ether (diglyme) (20 cm^3) until no more carbon monoxide was evolved ($\sim$ 0.25 n). The hot solution was filtered and $Ph_4As[Mo(CO)_5Cl]$ precipitated by the addition of petroleum ether (40-60°C boiling range) to the cooled solution. (Yield - 80%). This complex was isolated, dried in vacuo, then dissolved in tetrahydrofuran (20 cm^3) and stirred with a large excess of C_3H_5Cl (2.5 cm^3) for 12 h at room temperature. The solvent was removed in vacuo and the crude product recrystallised from $CHCl_3$-petroleum ether (40-60°C boiling range). Yield 60%. $Ph_4As[(\eta^3\text{-}C_3H_5)_2Mo_2(CO)_4Cl_3]$ was soluble in most polar solvents such as CH_3CN, $CHCl_3$, $(CH_3)_2CO$ and MeOH and showed no signs of decomposition in air.

The identity and purity of this compound was confirmed by comparison with literature data[257] of the infra-red ν(CO) region; ν(CO) nujol 1926s, 1911s, 1829s, 1802s.

Preparation of $Ph_4As[(\eta^3\text{-}C_3H_5)_2W_2(CO)_4Cl_3]$

A solution of $[(\eta^3\text{-}C_3H_5)_2W_2(CO)_4Cl_2dam]$.toluene, (the preparation of this species is described in Chapter 3), (0.21mmol, 0.25g) in dichloromethane ($10cm^3$) was treated with an equimolar quantity of $Ph_4AsCl.H_2O$ (0.21mmol, 0.09g), and the reaction mixture stirred for 0.5 h at room temperature. The dropwise addition of petroleum ether (60-80°C boiling range) resulted in the precipitation of analytically pure $Ph_4As[(\eta^3\text{-}C_3H_5)_2W_2(CO)_4Cl_3]$ in good yield (74%).

$Ph_4As[(\eta^3\text{-}C_3H_5)_2W_2(CO)_4Cl_3]$ showed similar solubility and stability properties to the molybdenum analogue.

Table 2.1 Yields and Analytical Data

Compound (No.)[a]	Yield (%)	Elemental Analysis found (calc) (%)		
		C	H	N
$[(\eta^3\text{-}C_3H_5)Mo(CO)_2(MeCN)_2Cl]$ (I)	91	34.6	3.6	8.9
		(34.8)	(3.6)	(9.0)
$[(\eta^3\text{-}C_3H_5)Mo(CO)_2(MeCN)_2Br]$ (II)	60	30.6	3.3	7.8
		(30.4)	(3.1)	(7.9)
$[(\eta^3\text{-}C_3H_5)Mo(CO)_2(MeCN)_2I]$ (III)	72	26.6	2.9	6.8
		(26.9)	(2.8)	(7.0)
$[(\eta^3\text{-}2\text{-}MeC_3H_4)Mo(CO)_2(MeCN)_2Cl]$ (IV)	91	37.2	4.2	8.7
		(37.0)	(4.0)	(8.6)
$[(\eta^3\text{-}C_3H_5)W(CO)_2(MeCN)_2Cl]$ (V)	67	27.1	2.8	6.9
		(27.1)	(2.8)	(7.0)
$[(\eta^3\text{-}C_3H_5)W(CO)_2(MeCN)_2Br]$ (VI)	72	24.4	2.6	6.3
		(24.4)	(2.5)	(6.3)
$[(\eta^3\text{-}C_3H_5)W(CO)_2(MeCN)_2I]$ (VII)	55	22.3	2.2	5.9
		(22.1)	(2.2)	(5.7)
$[(\eta^3\text{-}C_3H_5)Mo(CO)_2(MeCN)_3]BF_4$ (VIII)	81	32.2	3.5	9.6
		(32.8)	(3.5)	(10.4)
$[(\eta^3\text{-}2\text{-}MeC_3H_4)Mo(CO)_2(MeCN)_3]BF_4$ (IX)	83	34.1	3.8	9.7
		(34.6)	(3.9)	(10.1)
$[(\eta^3\text{-}C_3H_5)W(CO)_2(MeCN)_3]BF_4$ (X)	65	26.8	2.9	8.6
		(26.9)	(2.9)	(8.6)
$Ph_4As[(\eta^3\text{-}C_3H_5)_2Mo_2(CO)_4Cl_3]$ (XI)	60			
$Ph_4As[(\eta^3\text{-}C_3H_5)_2W_2(CO)_4Cl_3]$ (XII)	74	38.8	2.9	-
		(38.8)	(2.9)	-

[a] - each of the compounds showed signs of decomposition when heated above 50-80°C, consequently accurate melting points were unobtainable.

RESULTS AND DISCUSSION

The Cationic Species $[(\eta^3\text{-}C_3H_4R)M(CO)_2(MeCN)_3]^+$ as their BF_4^- Salts

The method used for the preparation of these compounds was an extension of that used by Brisdon and Cartwright[257] to prepare $[(\eta^3\text{-}C_3H_5)Mo(CO)_2(RCN)_3]PF_6$ (R = Me, Ph), which involved treating a solution of $[(\eta^3\text{-}C_3H_5)Mo(CO)_2(RCN)_2Cl]$ in RCN with KPF_6. The reaction time necessary for the complete abstraction of chloride ions was found to be considerably reduced (from 2 days to 0.33h) when $AgBF_4$ was used in place of KPF_6. The compounds, which were obtained as yellow powders, were easily oxidised in air especially when in solution to metal-oxygen species. [ν (M = O) infrared bands at $\sim$970 cm^{-1} M = Mo; $\sim$955 cm^{-1} M = W[259]]. Prolonged storage of the complexes, even in nitrogen filled ampoules, caused noticeable decomposition and therefore fresh samples were always prepared just prior to their use whether for spectroscopic or experimental purposes.

Selected infra-red data for the compounds (as nujol mulls) are given in Table 2.2. Two infrared ν(CO) absorptions of approximately equal intensity and separated by about 90 cm^{-1}, characteristic of cis-dicarbonyls, and an intense broad, band at about 1040 cm^{-1} attributable to the $\nu_3(T_2)$B-F stretching mode of the tetrahedral anion were clearly evident in each of the spectra. The CN stretching frequency of the co-ordinated nitrile at $\sim$ 2290 cm^{-1} is $\sim$50 cm^{-1} higher than that of free MeCN[ν (CN)MeCN liquid = 2250 cm^{-1} [260,261]] such an increase being characteristic of nitriles bonded through the nitrogen lone pair electrons[262]. Unlike other ligands where electron donation to an electron-deficient centre causes a weakening of the adjacent bond in the ligand, there is an increase in the CN bond

Table 2.2 Selected Infrared Data for the Complexes $[(\eta^3\text{-}C_3H_4R)M(CO)_2(MeCN)_3]BF_4$

Complex (No.)	Nujol Mulls (cm^{-1})[a]			
	ν(CO)		ν(CC)	ν(CN)
	A'	A''	+ $\delta(CH_3)_S$	
$[(\eta^3\text{-}C_3H_5)Mo(CO)_2(MeCN)_3]BF_4$ (VIII)	1948	1860	2318w	2289m
$[(\eta^3\text{-}2\text{-}MeC_3H_4)Mo(CO)_2(MeCN)_3]BF_4$ (IX)	1948	1865	2319w	2294m
$[(\eta^3\text{-}C_3H_5)W(CO)_2(MeCN)_3\ BF_4]$ (X)	1946	1853	2325w	2297m

[a] - All bands intense unless otherwise stated.

strength upon coordination. The reason for this has been the subject of considerable discussion[263-265]. As in the infrared spectra of pure MeCN, and numerous other complexes in which MeCN is present as a ligand[262,263,266-8], a second weaker absorption was observed $\sim$20-40 cm^{-1} higher than ν(CN). This peak is attributable to a combination mode of the symmetric CH_3 deformation and the symmetric C-C stretching of the nitrile[260]. Since the combination is of the same symmetry type as ν(CN), it can steal intensity from this fundamental and become comparatively intense.

$[(\eta^3\text{-}C_3H_5)Mo(CO)_2(MeCN)_3]^+$ has been shown[241] to have a pseudo-octahedral structure with C_s symmetry in the solid state and it is highly likely that both (IX) and (X) possess a similar stereochemistry. Group theory predicts a maximum of three ν(CN) modes (2A' + A'') for

this species, but as shown in Table 2.2 only one absorption is observed. This is quite common for complexes containing ligated MeCN which regardless of their stereochemistry rarely exhibit more than a single ν(CN) band[267].

Solution infrared spectral data[ν(CO) region] were obtained in a variety of solvents [$CHCl_3$, CH_3CN, $(CH_3)_2CO$ and CH_3OH] and are summarised in Table 2.3. The bands observed were broad with half widths of the order of 20-30 cm^{-1}. The reasons for the observation of more than the expected number of ν(CO) absorptions for particular compounds in certain solvents, are discussed in the relevant parts of the following text concerning the solution properties of these compounds.

Solution Behaviour of $[(\eta^3\text{-}C_3H_4R)M(CO)_2(MeCN)_3]BF_4$

Details of the 100 MHz ^1H NMR spectra of these complexes recorded in a variety of solvents [$CDCl_3$, CD_2Cl_2, CD_3CN, $(CD_3)_2CO$ and CD_3OD] are given in Table 2.4. The results of variable temperature ^1H NMR studies of compound (X), are discussed below. As the compounds were particularly prone to decomposition in solution, especially in chlorinated solvents, care was taken to ensure solvent purity and rigorous exclusion of air when preparing samples for spectroscopy. In $CDCl_3$ and CD_2Cl_2, for example, the presence of small quantities of uncoordinated CH_3CN in the ^1H NMR spectra indicated some decomposition (the initial relative intensity of this signal was never in excess of $^1/_{18}$ of the total CH_3CN observed).

Table 2.3: Solution Infrared Spectral Data

[ν(CO) region] for [(η^3-C_3H_4R)$M(CO)_2(MeCN)_3$]BF_4

Complex No.	ν(CO), solution (cm^{-1}) [a]			
	CH_3CN	CH_3OH	$CHCl_3$ [b]	$(CH_3)_2CO$
(VIII)	1968	1946	1962	1937 [c]
	1881	1858	1873	1848
(IX)	1965	1939	1959	1947
				1935
	1882	1846	1872	1848
(X)	1955	1964w [d]	1964	1956
		1931		
	1870	1882w	1877	1874
		1835		

[a] - All bands strong unless otherwise stated.

[b] - In $CHCl_3$ the ν(CO) absorption at highest wavenumber was much broader and more intense than that at lower wavenumber; there was no change in the relative intensities after 10 minutes.

[c] - This band was asymmetric.

[d] - The spectrum recorded immediately showed four ν(CO) bands but the spectrum recorded after 10 minutes exhibited only those bands at 1931s 1835s.

Table 2.4: ^{1}H NMR Data for $[(\eta^{3}\text{-allyl})M(CO)_2(MeCN)_3]BF_4$. Recorded at 30°C

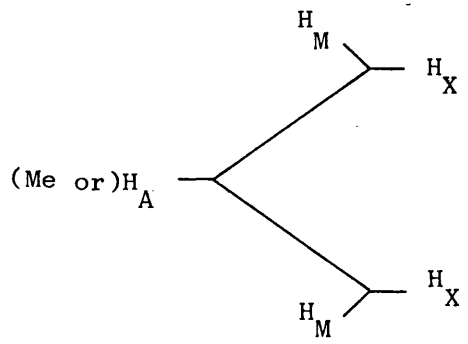

Complex No.	Solvent	δ(p.p.m. rel. to $SiMe_4$, J/Hz)			
		Allyl protons			MeCN
		H_X	H_M	H_A or Me	
VIII	$CDCl_3$	1.39(d J_{AX} 9.9)	3.44(d J_{AM} 7.1)	3.93 (m)	2.41(br.s)
	CD_3CN	1.50(d J_{AX} 10.0)	3.55 (d J_{AM} 6.7)	4.02 (m)	1.98(s)
	$(CD_3)_2CO$	1.43(d J_{AX} 10.8)	3.59(d J_{AM} 6.8)	4.13(m)	2.04(s)
					2.47(br.s)
	CD_3OD	1.19(d J_{AX} 8.8)	3.41(d J_{AM} 7.2)	3.74 (m)	2.04(s)

..../cont'd.

Table 2.4 (cont'd)

Complex No.	Solvent	δ (p.p.m. rel. to $SiMe_4$, J/Hz)			
		Allyl protons			MeCN
		H_X	H_M	H_A or Me	
IX	$CDCl_3$	1.30(s)	3.26(s)	2.17(s)	2.44(br.s)
	CD_3CN	1.37(s)	3.41(s)	2.20(s)	1.98(s)
	$(CD_3)_2CO$[a]	1.36(s)	3.44(s)	2.07(s)	2.56(br.s)
					2.07(s)
	CD_3OD	1.04(s)	3.23(s)	2.05(s)	2.04(s)
X	$CDCl_3$	1.65(d J_{AX} 9.5)	3.24(s)	3.18(m)	2.46(br.s)
	CD_2Cl_2	1.63(d J_{AX} 7.5)	3.27(s)	3.23(m)	2.44(br.s)
	CD_3CN	1.64(d J_{AX} 8.5)	3.33(s)	3.31(m)	1.98(s)
	$(CD_3)_2CO$	1.60(d J_{AX} 7.5)	3.38(s)	3.34(m)	2.04(s)
					2.57(br.s)

[a] - Weak unassigned peaks at 2.26(s), 2.22(s) and 2.12(s)

At all temperatures and regardless of solvent the ^{1}H NMR spectra observed were in accord with the presence of a single species containing a symmetrically bonded η^3-allyl group. For (VIII), the allyl group was characterised by the expected AM_2X_2 spin pattern normally encountered for this entity, but for (X), the H_M resonance appeared not as a doublet, but as a slightly broadened singlet due to the coincidence of the H_M and H_A proton signals (Table 2.4). In $CDCl_3$ at 30°C, the three coordinated MeCN ligands of the cations, gave a single broad resonance at 2.44 p.p.m. In agreement with the findings of Brisdon and Cartwright[257] for (VIII), variable temperature studies on (X), in $CDCl_3$ or CD_2Cl_2, showed that at temperatures below 0°C this signal is resolved into two components centred at 2.63 and 2.38 p.p.m. in $CDCl_3$ and 2.65 and 2.41 p.p.m. in CD_2Cl_2, with intensity ratios of 1:2. These low temperature spectra are in complete accord with the solid state structure of $[(\eta^3\text{-}C_3H_5)M(CO)_2(MeCN)_3]^+$ M = Mo,[241] in which the ligand distribution about the metal centre is basically octahedral and the three MeCN ligands are in a fac arrangement. The single averaged signal found for the three MeCN ligands at 30°C implies that these molecules are stereochemically non-rigid in solution at room temperature.

In CD_3CN, the chemical shifts of the MeCN protons of (VIII) (shown in Figure 2.2) and (IX) occurred in the free nitrile position (1.98 p.p.m.) indicating a facile exchange of the coordinated MeCN with the large excess of solvent. For (X) however, this exchange was considerably slower, and at 30°C a broad resonance at2.35 p.p.m. indicated that the majority of the MeCN was still coordinated to the metal centre. By immediately recording the spectrum of a freshly prepared CD_3CN solution of (X) at -40°C it was possible to observe two

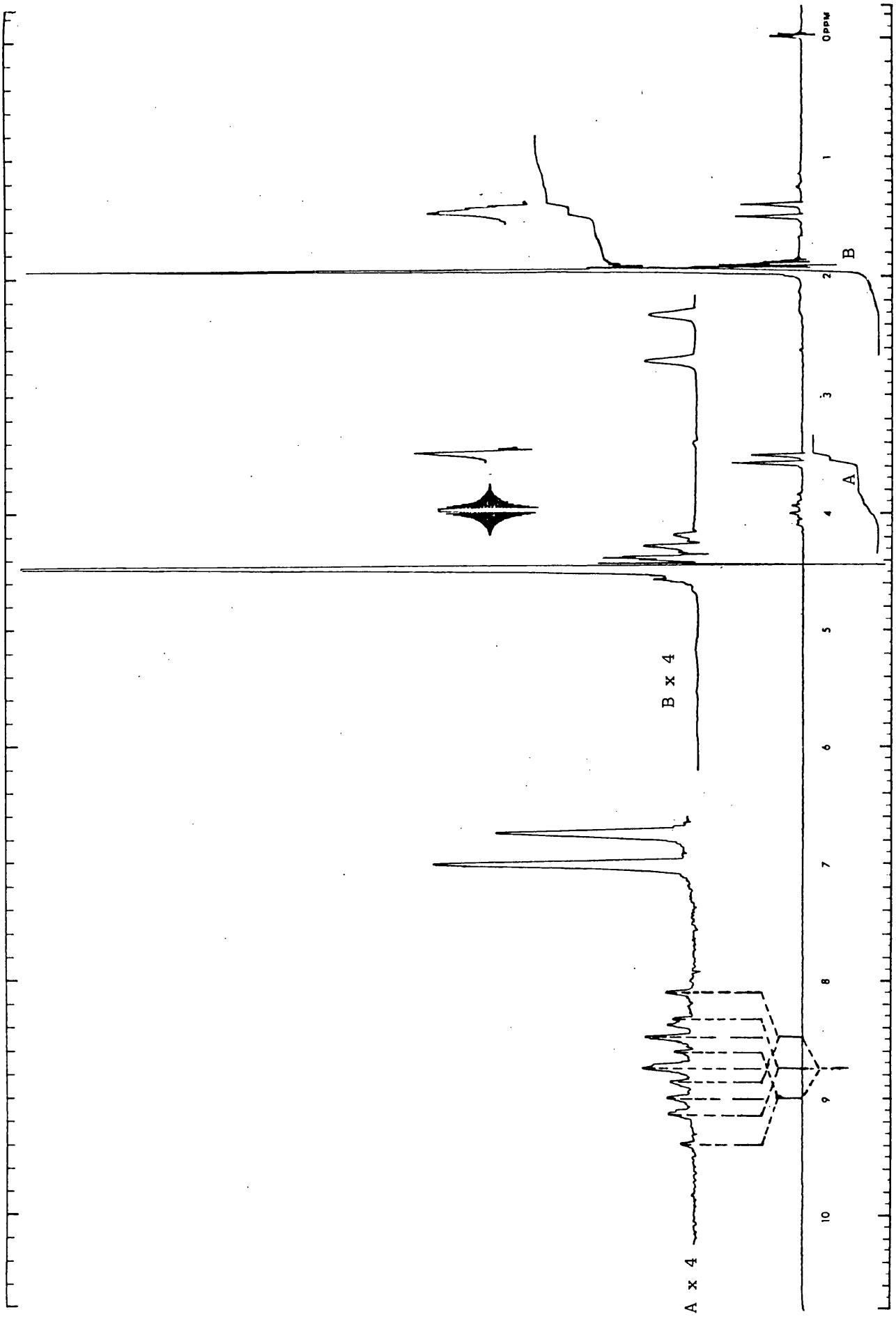

Figure 2.2: ^{1}H NMR spectrum of $[(\eta^{3}\text{-}C_3H_5)Mo(CO)_2(MeCN)_3]BF_4$ in CD_3CN

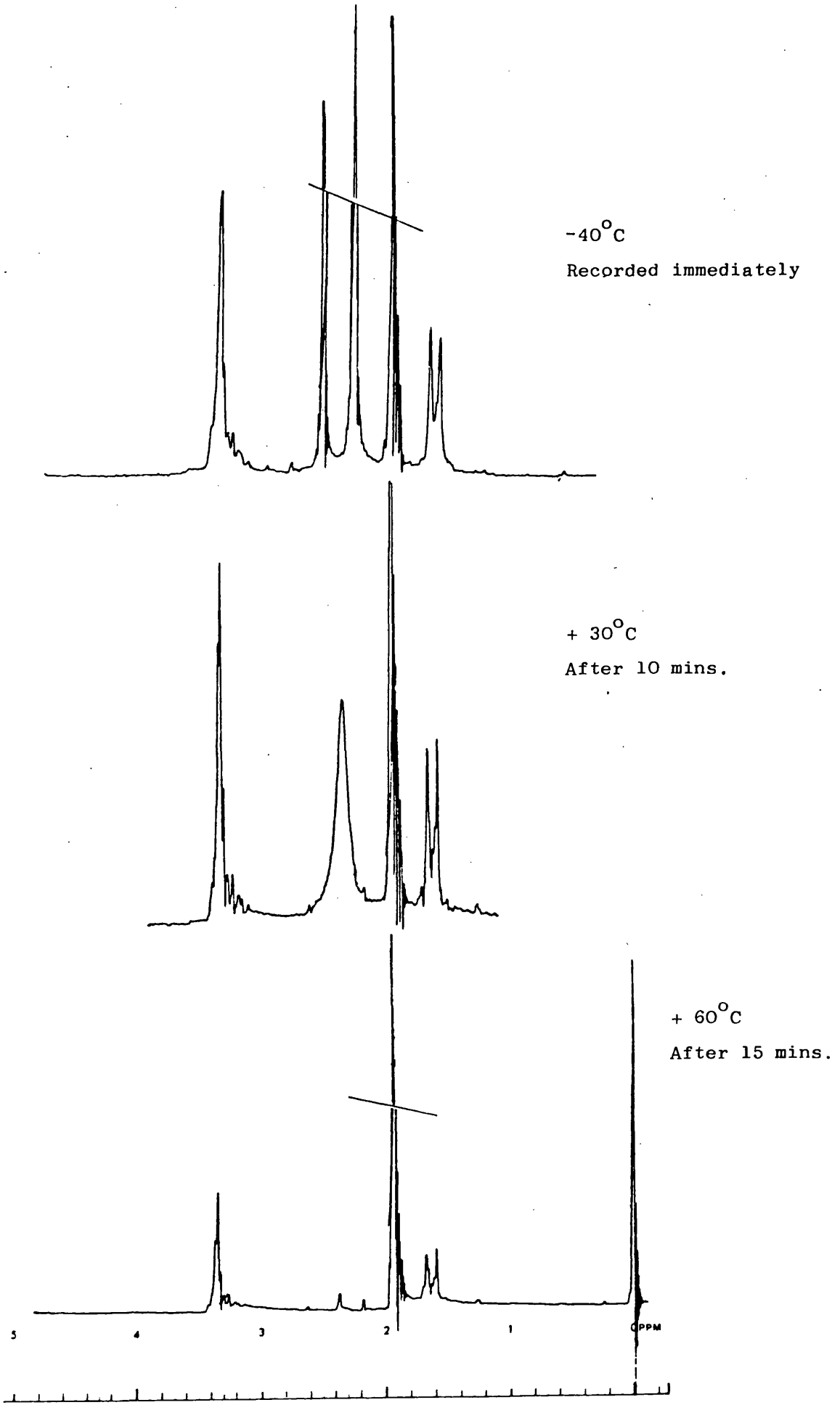

Figure 2.3: Variable Temperature ^{1}H NMR Spectra of $[(\eta^{3}\text{-}C_3H_5)W(CO)_2(MeCN)_3]BF_4$ recorded in CD_3CN

signals for the coordinated MeCN at 2.53 and 2.30 p.p.m. However, the ratio of intensities of these signals was not exactly 1:2 as found in $CDCl_3$ below 0^oC, and in addition a weak band in the free MeCN position was also observed. Warming the solution to room temperature and rescanning after 10 minutes showed that the two nitrile resonances had coalesced into a single broad band at 2.35 p.p.m. indicating that a rapid intramolecular exchange of the MeCN ligands occurs at room temperature. Only on prolonged standing at room temperature or on warming the solution does exchange between the coordinated MeCN and the solvent (CD_3CN) become significant.

An intramolecular rearrangement which is fully consistent with the dynamic NMR spectra is shown below

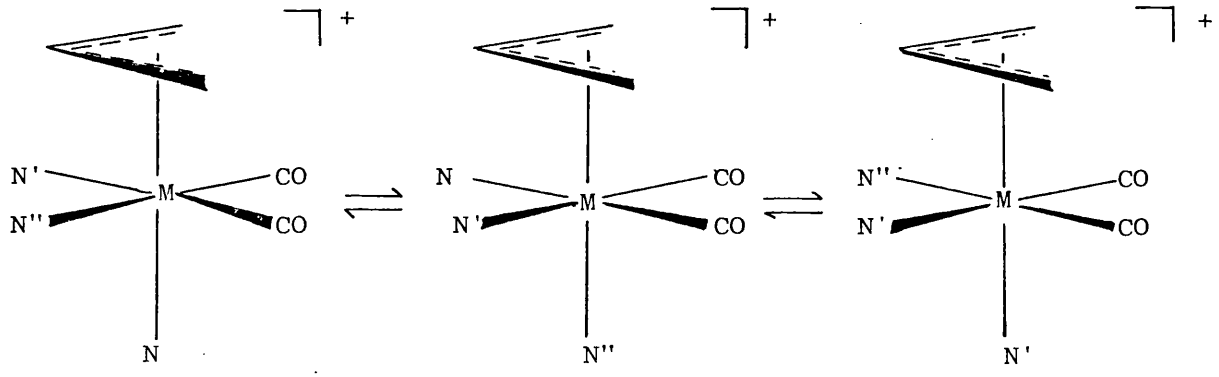

Figure 2.4 An intramolecular rearrangement process for $[(\eta^3\text{-}C_3H_4R)M(CO)_2(MeCN)_3]^+$

This mechanism, which involves a rotation of the triangular face formed by the three nitrogen atoms with respect to the face formed by the allyl and two carbonyl groups has also been suggested to account for the variable temperature NMR spectra observed for related systems [180,229].

At 30°C a broad resonance at ~ 2.5 p.p.m. assignable to coordinated MeCN was observed in the spectrum of each of the cations dissolved in $(CD_3)_2CO$, but the intensity of this signal was invariably less than that expected for three equivalent MeCN ligands. A sharp signal (which was unfortunately partially masked by signals from incompletely deuterated acetone in the solvent) characteristic of free MeCN was also present at 2.04 p.p.m., implying that up to one third of the ligated MeCN had been replaced by the solvent. The infrared spectra of (VIII) and (IX) in $(CH_3)_2CO$ (Table 2.3) also indicate that more than a single carbonyl containing species is present in the solutions. Several attempts to confirm this exchange, by the isolation of a species such as $[(\eta^3\text{-allyl})M(CO)_2(MeCN)_x\{(CH_3)_2CO\}_{3-x}]^+$, by careful removal of the solvent in vacuo, were unsuccessful because extensive decomposition of the complex and polymerisation of the solvent occurred.

In CD_3OD facile exchange of the solvent with the coordinated MeCN of (VIII) and (IX) resulted in the appearance of the signal of the MeCN protons in the free nitrile position (2.04 p.p.m.). The ν(CO) absorptions in the infra-red spectra of (VIII) and (IX) in MeOH (see Table 2.3) are also indicative of this process, for the positions of these bands are at distinctly lower wavenumbers in CH_3OH than in any other solvent. As found in CD_3CN solution, this exchange is much slower for complex (X) and four bands are initially observed in the ν (CO) region of its infrared spectrum (Figure 5a). Those bands at 1964 and 1882 cm^{-1} (both weak) correspond to $[(\eta^3\text{-}C_3H_5)W(CO)_2(MeCN)_3]^+$. The bands at 1931 and 1835 cm^{-1} (both strong) which are much closer to the observed ν(CO) frequencies for

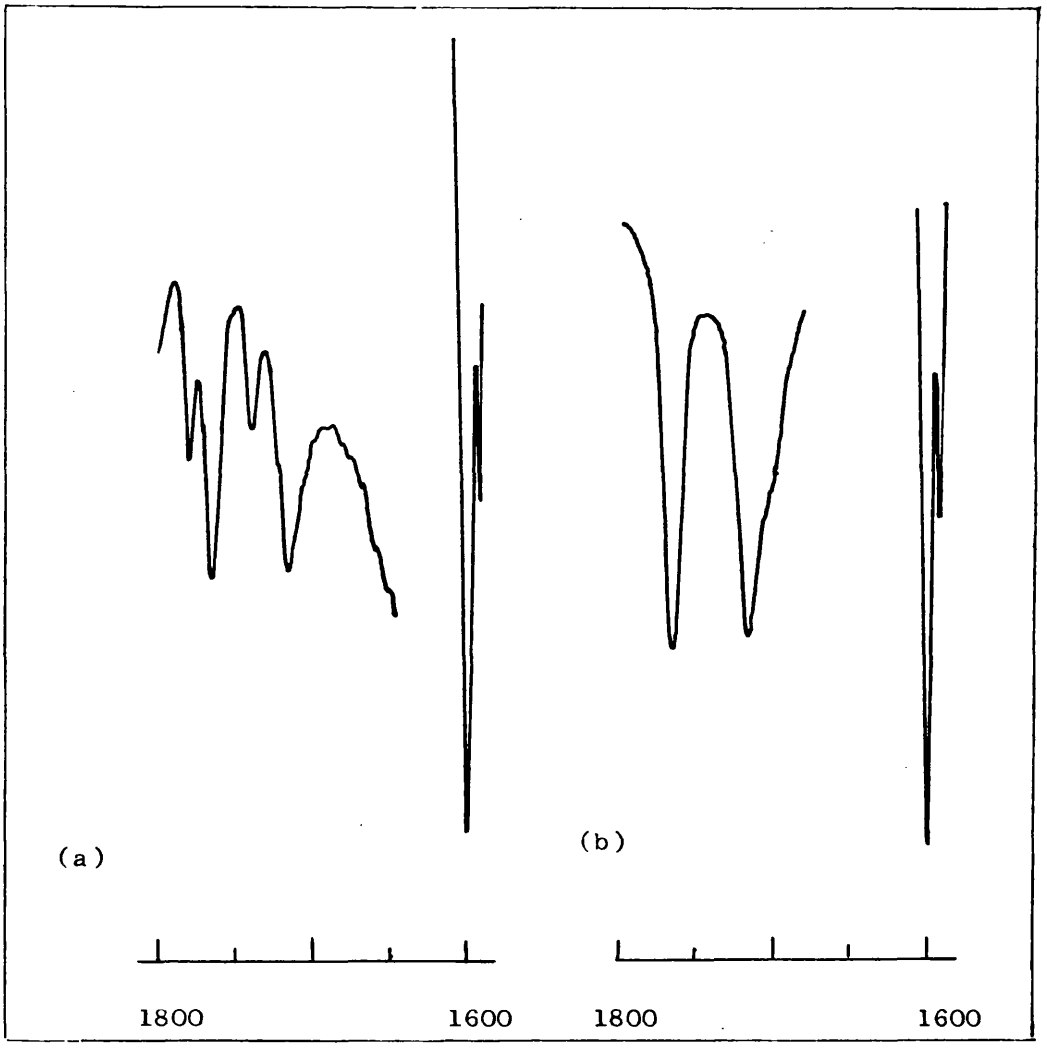

Figure 2.5: Infrared spectra (ν(CO) region) of (X) in CH_3OH solution recorded (a) immediately; (b) after 10 min.

(VIII) and (IX) in CH_3OH, correspond to $[(\eta^3\text{-allyl})M(CO)_2(CH_3OH)_3]^+$. After approximately ten minutes at room temperature only the latter bands were detectable, indicating the complete replacement of MeCN by CH_3OH, for (X).

The Dimeric Anions $[(\eta^3\text{-}C_3H_5)_2M_2(CO)_4Cl_3]^-$ As Their Ph_4As^+ Salts

$Ph_4As[(\eta^3\text{-}C_3H_5)_2Mo_2(CO)_4Cl_3]$ was prepared by literature methods[257], which involved the initial synthesis of the carbonyl halide $[Mo(CO)_5Cl]^-$ and its subsequent reaction with allyl chloride. Although $Et_4N[(\eta^3\text{-}C_3H_5)_2W_2(CO)_4Cl_3]$[75] has also been prepared in this way, the same synthetic procedure using tetraphenylarsonium chloride in place of tetraethylammonium chloride was not successful. The reaction of $Ph_4As[W(CO)_5Cl]$ with allyl chloride was fully investigated, both at room temperature and 40°C. Infrared spectra, run after short reaction times indicated little reaction but longer reaction times (up to 24 h) resulted only in decomposition of the carbonyl halide. However, $Ph_4As[(\eta^3\text{-}C_3H_5)_2W_2(CO)_4Cl_3]$, which was preferred to the Et_4N^+ salt for ^1H NMR studies, was successfully prepared by a rather indirect route which involved the reaction of Ph_4AsCl with $[(\eta^3\text{-}C_3H_5)_2W_2(CO)_4Cl_2dam]$ (this compound being obtained from the reaction of $[(\eta^3\text{-}C_3H_5)W(CO)_2(MeCN)_2Cl]$ with dam as described later in Chapter 3). In this reaction the bridging ditertiary arsine ligand is displaced by a chloride ion.

$$[(\eta^3\text{-}C_3H_5)_2W_2(CO)_4Cl_2dam] + Ph_4AsCl \longrightarrow Ph_4As[(\eta^3\text{-}C_3H_5)_2W_2(CO)_4Cl_3] + dam \qquad (2.3)$$

Selected infrared data for these compounds (solid state) are presented in Table 2.5. The observation of four strong bands in the infrared ν(CO) region is consistent with a confacial bi-octahedral structure for the anions, analogous to that recently reported[241] for $[(\eta^3\text{-}C_3H_5)_2Mo_2(CO)_4Cl_3]^-$.

Table 2.5: Selected Infrared Data (2000-200cm^{-1}) for the Dimeric Anions $[(\eta^3\text{-}C_3H_5)_2M_2(CO)_4Cl_3]^-$ as their Ph_4As^+ Salts. (Nujol Mulls)

Complex				Tentative Assignment
XI	XII	[a] $[Mo_2Cl_9]^{3-}$	$[Et_4N][Re_2(CO)_6(\mu\text{-}Cl)_3]$	
1926 vs	1922 vs			ν(CO)
1911 vs	1905 vs			
1829 vs	1819 vs			
1802 vs	1793 vs			
640 w	640 w		648 s	δ(MCO) + ν(MC)
581 m	572 m		635 s	
503 br m	511 w		510 sh	
	495 w		499 s	
[b] 270 s	272 s	283 - 268	269 s	ν(MCl)$_{bridging}$
[b] 231 s	222 s	252 - 236	251 s	

[a] - The actual position of $\nu(MoCl)_{bridging}$ varies with the counter ion.

[b] - Complex dispersed in a polythene disc.

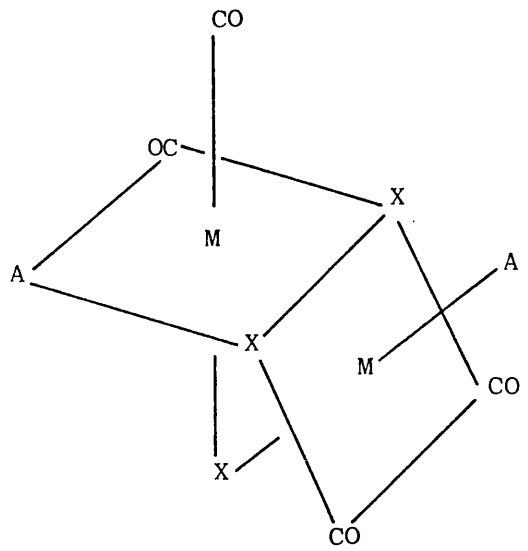

A = Allyl

Figure 2.6: Solid state sterochemistry‡ of $[(\eta^3\text{-}C_3H_5)_2Mo_2(CO)_4Cl_3]^-$

Solution infrared spectra of (XI) and (XII) are presented in Table 2.6. In the majority of solvents only two very broad bands (with half widths in the order of 20 - 30 cm^{-1}) were observed.

‡ This dimeric unit has approximate C_2 symmetry, the C_2 axis running through the unique chlorine atom and the mid-point of the M-M vector.

Table 2.6: Solution Infrared Spectral Data [ν(CO) region] for $Ph_4As[(\eta^3\text{-}C_3H_5)_2M_2(CO)_4Cl_3]$

Complex No.	ν (CO), solution (cm^{-1})[a]			
	CH_3CN	CH_3OH	$CHCl_3$	$(CH_3)_2CO$
(XI)	1937	1946	1938	1947(sh)
	1947			1938
	1862(sh)	1853	1843	1847
	1849			
(XII)	1942	1931	1926	1930
	1847	1832	1829	1839
	1828(sh)			

[a] - All bands strong unless otherwise stated.

The vibrational representations for an isolated $[(\eta^3\text{-}C_3H_5)_2M_2(CO)_4Cl_3]^-$ anion of C_2 symmetry - taking the allyl ligands as point groups - may be derived from a simple group theoretical treatment (outlined in Appendix 2). This serves to illustrate the numerous absorptions which are expected for a molecule with such low symmetry. Unfortunately with the exception of the carbonyl region virtually all the absorptions due to the anions were lost under those of the Ph_4As^+ cation, which dominated the spectra between 1600 and 300 cm^{-1}. Nevertheless three bands for (XI) and four bands for (XII) which are not characteristic of the cation were observed in the 650-490 cm^{-1} region and have been collectively assigned to $\nu(MC) + \delta(MCO)$ modes, which are expected to occur in this region[269-271]. In addition, by careful comparison of the spectra of (XI) and (XII) with those reported for the isoelectronic rhenium anion[272] $Et_4N[Re_2(CO)_6(\mu\text{-}Cl)_3]$, and the trihalo-bridged anion[273], $[Mo_2Cl_9]^{3-}$, it has been possible to make a tentative assignment of two strong bands in the 300-200 cm^{-1} region to $\nu(MX)_{bridging}$ modes.

The ^1H NMR spectrum of (XI) has already been fully described[257]. That of complex (XII) in CD_2Cl_2 and $(CD_3)_2CO$ is completely analogous and is presented in Table 2.7. The two η^3-allyl groups of the anion produced only a single AM_2X_2 resonance pattern with a total intensity of ten hydrogens. This suggests that the species either (i) adopts a more symmetrical stereochemistry in solution than it exhibits in the solid state, or (ii) is stereochemically non-rigid in solution at ambient temperatures. Variable temperature studies for (XI)[257] have been reported to show no significant changes over the temperature range + 55 to -120°C, thus if the anions are stereochemically non-rigid the process involved must have a very low activation energy.

Table 2.7: ^{1}H NMR Data for $Ph_4As[(\eta^3\text{-}C_3H_5)_2W_2(CO)_4Cl_3]$[a]

Solvent	δ(p.p.m. rel. $SiMe_4$, J/Hz)			
	Allyl protons			Ph_4As^+
	H_X	H_M	H_A	
CD_2Cl_2	1.09(d J_{AX} 9.0)	3.19(d J_{AM} 6.5)	2.88(m)	7.79(m)
$(CD_3)_2CO$	1.06(d J_{AX} 9.0)	3.4(d J_{AM} 7.1)	2.84(m)	7.87(s)
CD_3CN	1.10(d J_{AX} 7.5)	3.04(s)	3.04(m)	7.78(m)
	1.30(d J_{AX} 7.5)[b]			

[a] - Determined at 30°C

[b] - Some solvolysis occurred in this solvent producing $[(\eta^3\text{-}C_3H_5)W(CO)_2(CD_3CN)_2Cl]$, but the H_M and H_A resonances of this species are hidden by other resonances.

In CD_3CN, signals for the H_M and H_A protons of the allyl groups were coincident at 3.04 p p.m. and so no J_{AM} coupling was detected. In this solvent two doublets of approximately equal intensity were observed at high fields, one with a chemical shift close to that of the anti protons H_X as found for the anion in other solvents, and the second at 1.30 p.p.m. more characteristic of the anti protons of the allyl entity in the neutral compounds $[(\eta^3\text{-}C_3H_5)W(CO)_2(MeCN)_2Cl]$ (see Table 2.11). Thus this spectrum suggests that a solvolytic process for (XII) occurs in MeCN producing $[(\eta^3\text{-}C_3H_5)W(CO)_2(MeCN)_2Cl]$; [equation (2.4)]

$$Ph_4As[(\eta^3\text{-}C_3H_5)_2W_2(CO)_4Cl_3] \overset{MeCN}{\rightleftharpoons} 2[(\eta^3\text{-}C_3H_5)W(CO)_2(MeCN)_2Cl] + Ph_4AsCl \qquad (2.4)$$

The Neutral Complexes $[(\eta^3\text{-}C_3H_4R)M(CO)_2(MeCN)_2Cl]$ (R = H, M = Mo or W; R = Me, M = Mo)

With the exception of the iodo-complex (III) the molybdenum compounds were very easily prepared by a single step reaction, in which $Mo(CO)_6$ and the allyl halide were heated under reflux in acetonitrile. The relative instability of C_3H_5I as compared with C_3H_5Cl and C_3H_5Br, probably accounts for the failure of this very convenient route for synthesising (III). This method could not be successfully employed for the isolation of the thermally unstable tungsten analogues (V), (VI) and (VII) which presumably decompose during the extended reaction times at elevated temperatures which are necessary for complete formation of the intermediate $[(CH_3CN)_3W(CO)_3]$. However, compounds (III), (V), (VI) and (VII) were easily obtained by an alternative two-step process involving the initial preparation of $[(MeCN)_3M(CO)_3]$[252] (M = Mo or W) and

their subsequent reaction in situ with a slight excess of the appropriate allyl halide at a carefully controlled temperature not exceeding 60°C.

All of the compounds $[(\eta^3\text{-}C_3H_4R)M(CO)_2(MeCN)_2X]$ were isolated as crystalline solids ranging in colour from yellow for the chloro- to deep orange for the iodo-complexes. They could be stored indefinitely in sealed nitrogen-filled ampoules, but decomposed slowly when left standing in air, particularly when in solution in strong sunlight.

Selected infrared data (in nujol mulls) for these compounds are presented in Table 2.8. Two infrared ν(CO) absorptions of approximately equal intensity and separated by about 90cm^{-1} were observed in each case in accord with a cis-arrangement of the two carbonyl ligands. Comparison of the positions of the ν(CO) bands reported in Table 2.8 for the well-known molybdenum compounds with those reported in the literature[243] reveals slight discrepancies (other workers[274] have also noted this). However, since the compounds analyse well for $[(\eta^3\text{-}C_3H_5)Mo(CO)_2(MeCN)_2X]$ (X = Cl, Br, I) the variations in the reported band positions are probably attributable to the improved spectroscopic instrumentation which is now available, and the difficulties experienced in defining the exact maxima of the broad intense bands. Broad ν(CO) bands, with half widths of the order of 20 - 40cm^{-1} were also observed in the solution spectra of these species.

Table 2.8: Selected Infrared Data (4000 - 600cm^{-1}) for the complexes $[(\eta^3\text{-}C_3H_4R)M(CO)_2(MeCN)_2X]$.

Complex (No.)[a]	ν(CO)[b] (cm^{-1}) A'	A''	ν(CC) + $\delta(CH_3)_s$	ν(CN)
$[(\eta^3\text{-}C_3H_5)Mo(CO)_2(MeCN)_2Cl]$ (I)	1943	1853	2315w	2285m
$[(\eta^3\text{-}C_3H_5)Mo(CO)_2(MeCN)_2Br]$ (II)	1940	1851	2311w	2285m
$[(\eta^3\text{-}C_3H_5)Mo(CO)_2(MeCN)_2I]$ (III)	1935	1850	[c]	2275m
$[(\eta^3\text{-}2\text{-}MeC_3H_4)Mo(CO)_2(MeCN)_2Cl]$ (IV)	1945	1847	2325w	2285m
$[(\eta^3\text{-}C_3H_5)W(CO)_2(MeCN)_2Cl]$ (V)	1932	1841	2314w	2283m
$[(\eta^3\text{-}C_3H_5)W(CO)_2(MeCN)_2Br]$ (VI)	1925	1835	2317w	2280m
$[(\eta^3\text{-}C_3H_5)W(CO)_2(MeCN)_2I]$ (VII)	1932	1840	2313w	2283m

[a] - Recorded as Nujol mulls

[b] - All bands are strong.

[c] - not observed.

Peak maxima of the ν(CO) absorptions are approximately 5 - 15cm^{-1} lower than those of the corresponding cations $[(\eta^3\text{-}C_3H_4R)M(CO)_2(MeCN)_3]^+$, reflecting the greater electron density at the metal centre in the neutral species.

Table 2.9: Infrared spectra (400 - 40 cm^{-1}) of the Complexes $[(\eta^3\text{-}C_3H_4R)M(CO)_2(MeCN)_2X]$

Complex (reference number)							Tentative Assignment
Cl (I)	Br (II)	I (III)	Cl (IV)[a]	Cl (V)	Br (VI)	I (VII)	
80brm	86brs	84brs		82brm	87brs	82brs	δ(CMC), δ(CMN) and δ(NMN)
	93brs	94brs			93brs	96brs	
113w	100brs	108brs		107w	100brs	110(sh)	
	128(sh)	125(sh)			127w	125(sh)	
139brm	136brs	135brs		144m	141m	139s	
		168vs				168vs	ν(MI)
178(sh)							
	188vs				183brvs		ν(MBr)
187s				188brm			
200m	214m	208s		208s	217m	212m[b]	ν(MN)
234s	234s	230s		239s	236vs	233s	
	245(sh)						
283brvs			273s	288brvs			ν(MCl)

Ratios ν(MoBr)/ ν(MoCl) = 0.66 ν(WBr)/ ν(WCl) = 0.64 ν(MoI)/ ν(MoCl) = 0.59 ν(WI)/ ν(WCl) = 0.58

a - Recorded as nujol mulls down to 200cm^{-1}.

b - Additional band at 221m alternatively may be due to ν(MN).

Table 2.9 lists the major features observed in the far-infrared spectra (400 - 40cm^{-1}) of the compounds (I) - (III), (V) - (VII). A single, strong halogen-sensitive band was observed in this region and can be confidently assigned to the metal-halogen stretching mode on the basis of the ν(MBr)/ν(MCl) and ν(MI)/ν(MCl) frequency ratios which were calculated to be close to the values of 0.67 and 0.53 respectively, expected from the simple harmonic oscillator approximation[275]. This mass effect is clearly illustrated in Figs. 2.7 and 2.8. The spectrum of (IV) was only recorded to 200cm^{-1} as a nujol mull and a band at 273cm^{-1} has been assigned to ν(MCl) by comparison with the spectrum of (I).

In addition to ν(MX) vibrations, bands due to ν(MN), δ(CMC), δ(CMN), δ(NMN), and modes associated with the η^3-C_3H_5-M unit are also expected in the 400 - 40cm^{-1} region. Metal-ligand deformations (CMC, CMN and NMN) normally occur in approximately the same region[276] and generally below $\sim$150cm^{-1}. No attempt has been made to distinguish between these bands in Table 2.9. Few assignments of ν(MN) modes for transition metal-nitrile complexes have been reported despite the large number of such complexes known. These bands are usually of only medium intensity in the infrared spectrum, and thus often difficult to detect. Moreover values that have been reported[262] vary tremendously from $\sim$100cm^{-1} for trans-$[PdX_2(NCPh)_2]$ (X = Cl, Br)[277] to $\sim$525cm^{-1} for $[M(CO)_3(NCMe)_3]$ (M = Cr, Mo, W)[278]. There is still considerable uncertainty concerning many ν(MN) assignments, but for MeCN adducts of metals, at least, the current opinion is that they occur in the 200 - 300cm^{-1} region[262,279-282]. As shown in Table 2.9 all of the six complexes

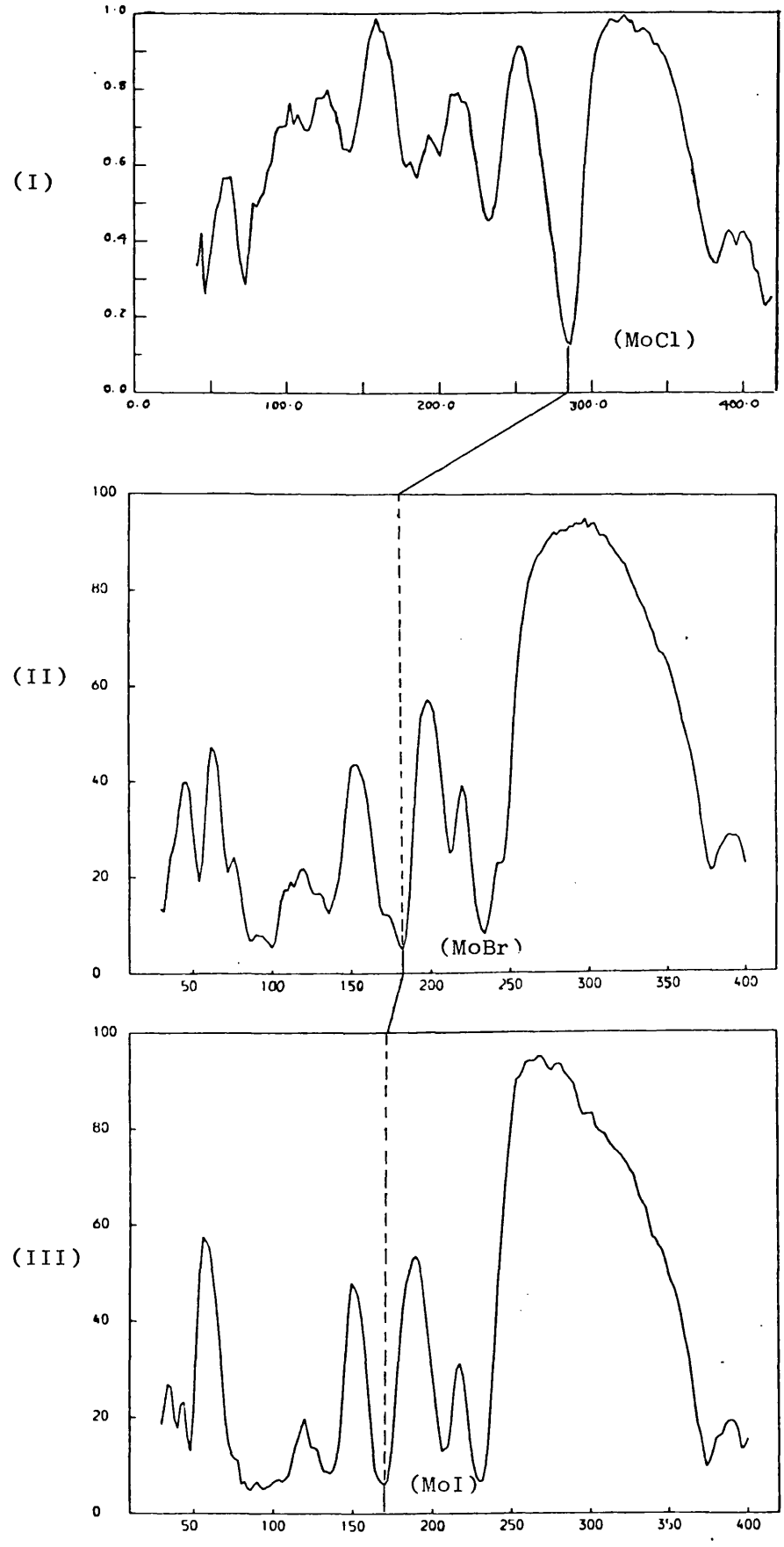

Figure 2.7: Far-infrared Spectra of the Complexes $[(\eta^3\text{-}C_3H_5)Mo(CO)_2(MeCN)_2X]$

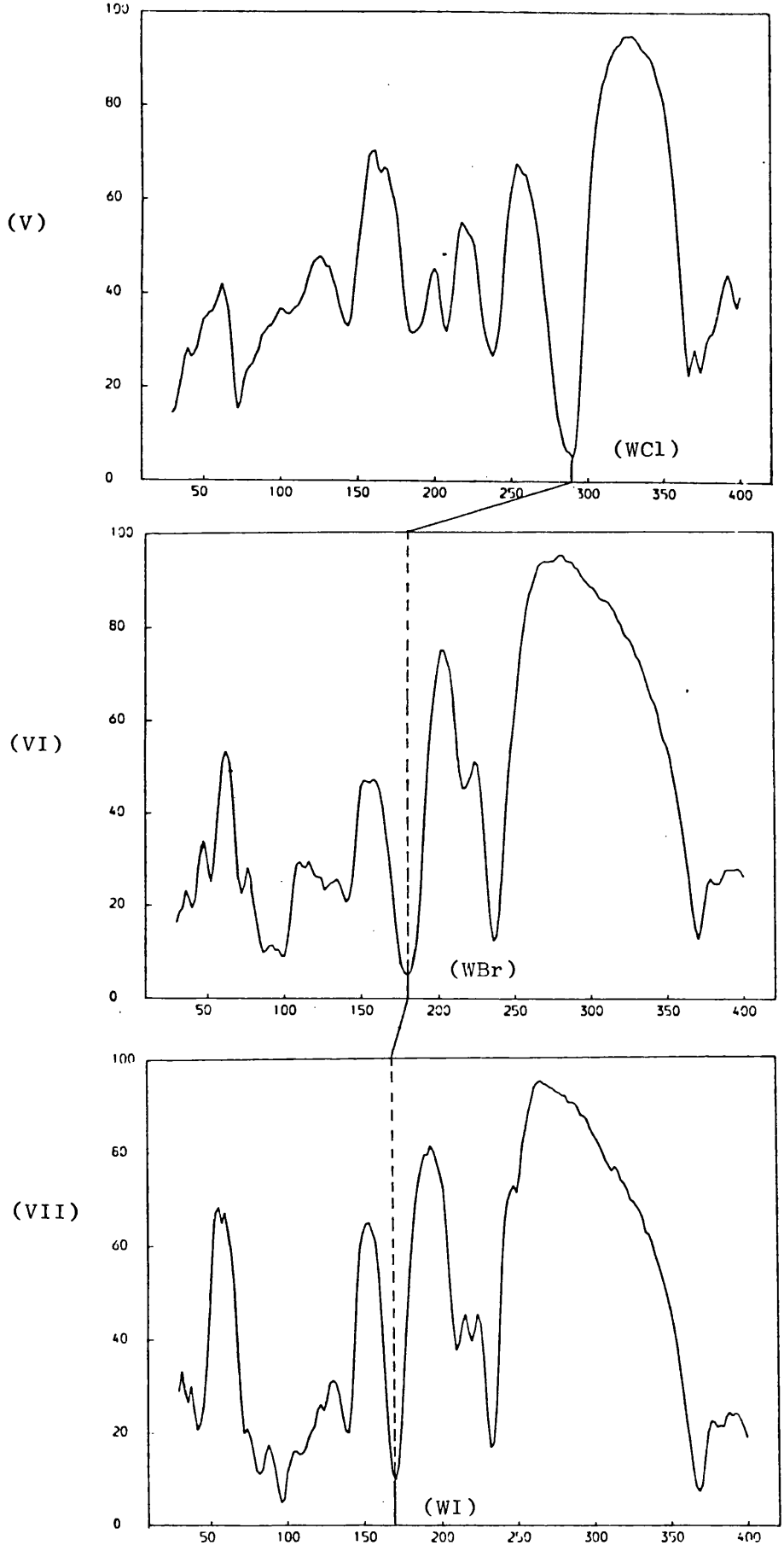

Figure 2.8: Far-infrared Spectra of the Complexes

$[(\eta^3\text{-}C_3H_5)W(CO)_2(MeCN)_2X]$

investigated here exhibit two bands of medium to strong intensity in the region 200 - 240cm^{-1}. Since the frequencies of these bands are too high for deformation modes involving the metal (CMC, XMC, NMC or XMN), and too low for δ(NCC)[267], they have been tentatively assigned by the author as metal-nitrogen stretching modes.

An attempt to further characterise these metal(II) compounds by mass spectrometry proved futile since considerable decomposition occurred in the mass spectrometer. However, the general appearance of the spectra in each case was similar and a number of metal-containing peaks were readily recognised by the characteristic isotope patterns of molybdenum and tungsten. The major metal-containing fragment ions observed in the spectrum of $[(\eta^3\text{-}C_3H_5)W(CO)_2(MeCN)_2Cl]$ (a typical example of the spectra obtained for these compounds) are listed in Table 2.10. In the absence of metastables the exact identity of some fragments is uncertain, and more than one assignment is feasible. Alternative assignments are indicated in the tabulation.

Table 2.10: The Mass Spectrum of $[(\eta^3\text{-}C_3H_5)W(CO)_2(MeCN)_2Cl]$

m/e[a]	Relative Intensity	Possible Assignments
363	9	$[W(CO)_5(C_3H_5)]^+$
350	60	$[W(CO)_6]^+$ or $[MeW(CO)_4(C_3H_5)]^+$
322	9	$[W(CO)_5]^+$ or $[MeW(CO)_3(C_3H_5)]^+$
307	11	$[W(CO)_3(C_3H_5)]^+$
294	44	$[W(CO)_4]^+$ or $[MeW(CO)_2(C_3H_5)]^+$
279	13	$[W(CO)_2(C_3H_5)]^+$
266	100	$[W(CO)_3]^+$ or $[MeW(CO)(C_3H_5)]^+$
251	11	$[W(CO)(C_3H_5)]^+$
238	50	$[W(CO)_2]^+$ or $[MeW(C_3H_5)]^+$
223	18	$[W(C_3H_5)]^+$
210	39	$[W(CO)]^+$
194	23	$[WC]^+$
182	28	$[W]^+$
175	8	$[W(CO)_6]^{2+}$ or $[MeW(CO)_4(C_3H_5)]^{2+}$
161	3	$[W(CO)_5]^{2+}$ or $[MeW(CO)_3(C_3H_5)]^{2+}$
147	12	$[W(CO)_4]^{2+}$ or $[MeW(CO)_2(C_3H_5)]^{2+}$

..../contd.

Table 2.10: contd.

m/e[a]	Relative Intensity	Possible Assignments
119	16	$[W(CO)_2]^{2+}$ or $[MeW(C_3H_5)]^{2+}$
111	7	$[W(C_3H_5)]^{2+}$
105	11	$[W(CO)]^{2+}$

a - ^{182}W-containing ions only.

Metastable supported transition (calculated position in parentheses) $294 \longrightarrow 266$ = 241.0 (240.7)

Solution Behaviour of $[(\eta^3\text{-}C_3H_5)W(CO)_2(MeCN)_2X]$ (X = Cl, Br and I)

None of these compounds were very soluble in CD_3CN and consequently the ^1H NMR spectra obtained in this solvent were of poor quality. Nevertheless there was no indication of more than a single η^3-allyl-containing species for any of the three complexes (V) - (VII), in contrast to the analogous molybdenum chloro- and bromo-complexes[257]. Each of the spectra (Table 2.11) contained a single AM_2X_2 resonance pattern typical of a fluxional or symmetrically bonded $\eta^3\text{-}C_3H_5$ group. A sharp singlet corresponding to free MeCN signified that exchange of ligated MeCN and solvent occurs more readily for these neutral complexes than for the cationic derivative $[(\eta^3\text{-}C_3H_5)W(CO)_2(MeCN)_3]^+$ (see earlier p. 90).

The spectra were essentially unchanged over the temperature range +70 to -40°C although those of (V) and (VI) did suffer a considerable loss of resolution between 28 and 0°C.

In CD_2Cl_2, ^1H NMR studies showed that the chloro-complex (V) ionised in an analogous manner to the corresponding molybdenum complex(I)[257], thus three allyl-containing species were present in solution, two of which were readily identified as $[(\eta^3\text{-}C_3H_5)_2W_2(CO)_4Cl_3]^-$ and $[(\eta^3\text{-}C_3H_5)W(CO)_2(MeCN)_3]^+$ by their chemical shifts and coupling constants (c.f. Table 2.4 and Table 2.7). Two possible equilibria involving the neutral complex may be invoked to account for the presence of these charged entities

viz: $3[(\eta^3\text{-}C_3H_5)W(CO)_2(MeCN)_2Cl] \rightleftharpoons [(\eta^3\text{-}C_3H_5)W(CO)_2(MeCN)_3]^+ + [(\eta^3\text{-}C_3H_5)_2W_2(CO)_4Cl_3]^- + 3MeCN$ (2.5)

or $6[(\eta^3\text{-}C_3H_5)W(CO)_2(MeCN)_2Cl] \rightleftharpoons 4[(\eta^3\text{-}C_3H_5)W(CO)_2(MeCN)_3]^+ + [(\eta^3\text{-}C_3H_5)_2W_2(CO)_4Cl_3]^- + 3Cl^-$ (2.6)

Table 2.11: ^{1}H NMR Data for [(η^3-C_3H_5)$W(CO)_2(MeCN)_2X$] (X = Cl, Br and I)

Complex	Solvent	Temperature (^oC)	δ (p.p.m. rel. to $SiMe_4$ J/Hz) Allyl protons H_X	H_M	H_A	MeCN	Assignments[a] and rel. concn.[b]	
V	CD_3CN	-35	1.32(d J_{AX} 7.7)	3.00(d J_{AM} 6.0)	3.10(m)	1.98(s)	N	
	CD_2Cl_2	-20	1.19(d J_{AX} 9.0)	3.27(d J_{AM} 6.0)	3.02(m)	[c]	A	1.0
			1.48(d J_{AX} 8.5)	~3.1 (m)		2.46(s)	N	1.0
			1.70(d J_{AX} 7.5)	3.30(d J_{AM} 6.0)	3.20(m)	2.45(s)	C	1.0
						2.69(s)		
VI	CD_3CN	-40	1.55(d J_{AX} 8.0)	3.01(d J_{AM} 6.4)	3.12(m)	1.98(s)	N	
	CD_2Cl_2	-50	1.42(d J_{AX} 7.9)	2.98(d J_{AM} 6.5)	3.22(m)	2.36(s)	N	
VII	CD_3CN	-35	1.42(d J_{AX} 7.7)	3.04(d J_{AM} 6.0)	3.22(m)	1.98(s)	N	
	CD_2Cl_2	-20	1.44(d J_{AX} 7.6)	2.94(d J_{AM} 6.0)	3.18(m)	2.33(s)	N	

[a] - N = neutral species, A = anion, C = cation. [b] - Based on the intensities of the signals from the allyl protons.

[c] - Unassigned peak at 2.29 p.p.m.

On the basis of the relative intensities of the allyl proton signals for the charged species (anion : cation = 17:8) plus the observation of free nitrile at 2.00 p.p.m. an equilibrium according to equation (2.5), as suggested for the molybdenum analogue, is favoured for (V), but occurs to a smaller extent, (K, 6 x 10^{-2} mol^2dm^{-2} compared with 6 x $10^2 mol^2 dm^{-2}$ at 27°C for the molybdenum analogue in $CDCl_3$ [257]). Further support for ionisation according to equation (2.5) was obtained by mixing $[(\eta^3\text{-}C_3H_5)W(CO)_2(MeCN)_3]BF_4$ and $Ph_4As[(\eta^3\text{-}C_3H_5)_2W_2(CO)_4Cl_3]$ in a 1:1 mole ratio in CH_3CN at 40°C, this generated a spectrum identical to that of (V) in CH_3CN.

At room temperature the coordinated MeCN groups of the cation gave rise to a single broad resonance at 2.56 p.p.m., this was replaced at low temperatures ($<0^oC$) by two bands, of relative intensities 1:2, at 2.69 p.p.m. and 2.45 p.p.m. as expected (see earlier p. 90). The signal attributable to the coordinated MeCN of the neutral species (at 2.46 p.p.m.) was invariant with temperature (-40°C to +40°C).

The spectra of (VI) and (VII) in CD_2Cl_2 indicated that, apart from slight decomposition, these compounds remain predominantly as the neutral complexes. Well resolved spectra, however, were only obtained at low temperatures ($<0^oC$), broad unresolved signals were observed at room temperature.

Spectra in the more strongly coordinating and polar solvent acetone were more complex, and the results of these studies are presented separately in Table 2.12. For the chloro-complex, at least three allyl-containing species were identified. The most intense signals had chemical shifts indicative of the anion $[(\eta^3\text{-}C_3H_5)_2W_2(CO)_4Cl_3]^-$

Table 2.12. ^{1}H NMR Data for $[(\eta^3\text{-}C_3H_5)W(CO)_2(MeCN)_2X]$ in $(CD_3)_2CO$.

Complex	Temp. (°C)	δ(p.p.m. rel. to $SiMe_4$ J/Hz) Allyl protons H_X	H_M	H_A	MeCN	Assignments[a] and rel. concn.[b]	
V	+50	1.08(d J_{AX} 9.0)	3.18(d J_{AM} 6.5)	2.86(m)	2.04	N(1)	2
		1.36(brd)	3.05(s)	2.96(m)		N(2)	1
		1.68(br)	~3.40br		2.64(brs)	C	1
VI	+50	1.12(d J_{AX} 8.5)	~3.10(m)			A	1
		1.39(d J_{AX} 6.7)	3.08(s)	3.10(m)	2.22(brs)	N(4)	8
		1.68(br)	~3.10(m)		2.64(s)	C	1
	-40	1.24(d J_{AX} 7.5)	2.95(d J_{AM} 6.0)	3.16(m)	2.51(s)	N(2)	3
		1.37(d J_{AX} 8.0)	~3.16(m)		2.51(s), 2.09(s)	N(3)	1
VII	+50	1.44(d J_{AX} 7.7)	3.06(s)	3.14(m)	2.21(s)	N(4)	4
		1.64(d J_{AX} 7.0)	~3.14(m)		2.59(s)	C	1
	-40	1.32(d J_{AX} 8.0)	2.98(d J_{AM} 5.5)	3.2(m)	2.52(s)	N(2)	4
		1.47(brd J_{AX} 7.5)	~3.2(m)		2.52(s), 2.09(s)	N(3)	1

[a] - N(1) = $[(\eta^3\text{-}C_3H_5)W(CO)_2\{(CD_3)_2CO\}_2X]$; N(2) = $[(\eta^3\text{-}C_3H_5)W(CO)_2(MeCN)_2X]$; N(3) = Unknown neutral(?) species possibly $[(\eta^3\text{-}C_3H_5)W(CO)_2(MeCN)X]_2$; N(4) = Averaged high temperature spectrum for interconverting N(2) ⇌ N(3)
A = Anion; C = cation.

[b] - Based on the intensities of the signals from the allyl protons.

(δH_X = 1.08p.p.m.), but these were not accompanied by sufficiently intense signals due to the cationic allyllic protons (δH_X = 1.6p.p.m) and thus it seems doubtful that such an assignment is correct. Since most of the MeCN present gave a signal at the free nitrile position, it is more likely that these allyl resonances are attributable to a neutral species, such as $[(\eta^3\text{-}C_3H_5)W(CO)_2\{(CD_3)_2CO\}_2Cl]$. With the exception of a considerable loss of resolution at low temperatures no changes in this spectrum were observed over the temperature range +50°C to -20°C.

Spectra for (VI) and (VII) in $(CD_3)_2CO$ were similar, but different to that for (V). Well resolved spectra were obtained at +50°C and -40°C but at ambient temperatures only broad featureless bands were observed. At +50°C the spectra were consistent with both complexes remaining as neutral species, although there was some evidence of a low concentration of the cationic allyl[/] species, and for (VI) an indication of $[(\eta^3\text{-}C_3H_5)_2W_2(CO)_4Br_3]^-$ was also found. With the exception of a small signal at ~2.6 p.p.m., corresponding to the coordinated MeCN of the positive ion, the protons of the ligated MeCN produced a single broad resonance at 2.20 p.p.m. By -40°C, however, this band had resolved into two components, one at ~ 2.5p.p.m. and the second very close to the free nitrile position at 2.09p.p.m. In addition, an intense set of η^3-allyl resonances δH_X (VII) 1.32p.p.m. and δH_X (VI) at 1.24p.p.m. were observed, with only weak doublets at 1.45p.p.m. (VII), 1.37p.p.m. (VI) corresponding to the H_X protons of the η^3-allyl species present in greatest concentration at +50°C.

[/] For (VII) this was probably formed by a solvolytic process as suggested for $[(\eta^3\text{-}C_3H_5)Mo(CO)_2(MeCN)I]$[257] in CD_3CN.

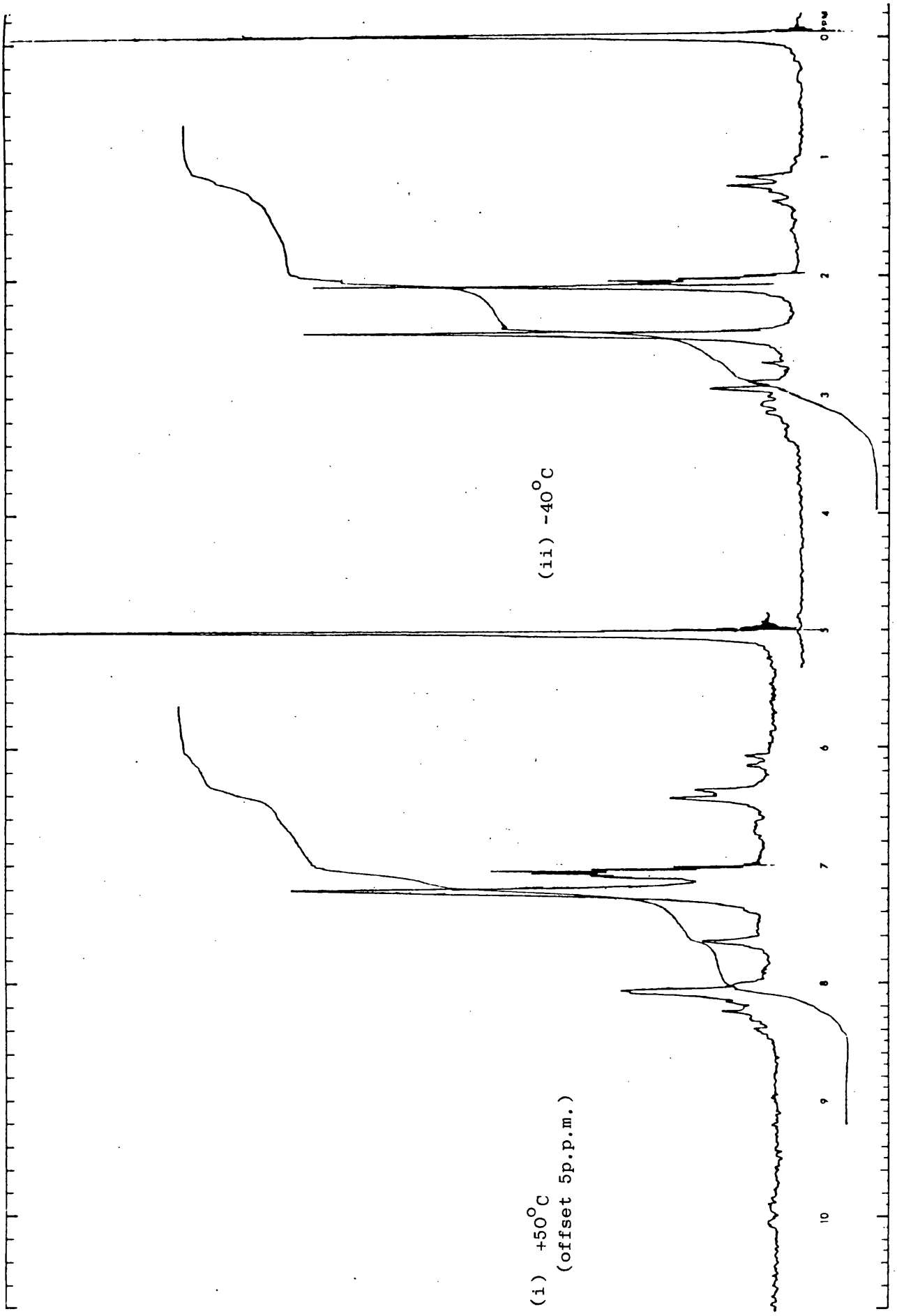

Figure 2.9 ^{1}H NMR Spectra of $[(\eta^{3}\text{-}C_{3}H_{5})W(CO)_{2}(MeCN)_{2}Br]$ in $(CD_{3})_{2}CO$ at (i) +50°C and (ii) -40°C.

These ^{1}H NMR spectra are difficult to explain. The slight ionisation of (VI) and (VII) observed at $+50^{o}C$ is undoubtedly suppressed at low temperatures, but so too is a second equilibrium process involving the neutral species, which results in the observed predominance of an η^{3}-allylic species at $-40^{o}C$ which was not found at $+50^{o}C$. As shown in Figure 2.9 for (VI) there is considerable overlap of the signals observed in the spectra of (VI) and (VII) recorded at $-40^{o}C$, and because of this it is impossible to measure the intensities of specific signals with any degree of accuracy. Nevertheless as far as one can ascertain the signal at ~2.5p.p.m. corresponds to six protons of two MeCN ligands associated with the allylic complex with the anti proton resonance at the highest field those centred at 1.24p.p.m. for (VI) and 1.32p.p.m. for (VII), and for three protons of one MeCN ligand associated with the allylic complex with the anti proton resonance at lower field centred at 1.37p.p.m. (VI) and 1.47p.p.m. (VII) . Presumably the intensity of the free MeCN at 2.09 p.p.m. (which is difficult to measure because of its coincidence with the signal from the incompletely deuterated acetone) corresponds to the missing MeCN. As described earlier the two MeCN resonances (i.e. that at ~ 2.50p.p.m. and 2.09p.p.m.) coalesced on raising the temperature from $-40^{o}C$, and therefore, the variable temperature spectra are not totally consistent with a process of partial MeCN-$(CD_3)_2CO$ exchange which could produce an equilibrium between two neutral allylic species such as that described in equation 2.7.

$$[(\eta^{3}\text{-}C_3H_5)M(CO)_2(MeCN)_2X] \rightleftharpoons^{(CD_3)_2CO} [(\eta^{3}\text{-}C_3H_5)M(CO)_2(MeCN)\{(CD_3)_2CO\}X] \qquad (2.7)$$

For such an exchange process, a signal due to free MeCN would be expected at all temperatures and this is not observed. Neither was a signal due to coordinated $(CH_3)_2CO$ detected when one drop of $(CH_3)_2CO$ was added to the solution and the spectrum recorded at low temperature. However, the variable temperature spectra is indicative of two species co-existing in solution at low temperatures but interconverting at higher temperatures producing an averaged spectrum. The equilibrium implied involves the liberation of MeCN, and could possibly be due to a monomer-dimer type reaction such as that proposed by Dieck[243] (equation 2.8).

$$[(\eta^3\text{-}C_3H_5)M(CO)_2(MeCN)_2X] \rightleftharpoons [(\eta^3\text{-}C_3H_5)M(CO)_2(MeCN)X]_2 + 2MeCN \qquad (2.8)$$

But attempts to suppress the equilibrium by addition of MeCN were unsuccessful and only resulted in complete exchange of coordinated and free MeCN.

Solution Behaviour of $[(\eta^3\text{-}2\text{-}MeC_3H_4)Mo(CO)_2(MeCN)_2Cl]$. (IV)

The ^1H NMR spectra of (IV) in $CDCl_3$ and CD_3CN (Table 2.13) showed that the complex remains unionised in these solvents; three resonances of intensity ratios 2:3:2 were observed for the η^3-2-MeC_3H_4 entity, as expected. Facile MeCN-solvent exchange was indicated in CD_3CN by the position of the MeCN resonance at 1.98p.p.m.

In $(CD_3)_2CO$ solutions two η^3-allyl-containing species were present. The chemical shifts for the major component were identical to those of $[(\eta^3\text{-}2\text{-}MeC_3H_4)Mo(CO)_2(MeCN)_3]^+$ (IX) in $(CD_3)_2CO$ (c.f. Table 2.4). The resonance positions of the η^3-allylic protons

Table 2.13: ^{1}H NMR Data for $[(\eta^{3}\text{-}C_3H_4R)Mo(CO)_2(MeCN)_2Cl]$ Recorded at 26°C

Complex	Solvent	δ(p.p.m. rel. to $SiMe_4$, J/Hz)				Assignment[a] and rel. concn.[b]
		Allyl protons			MeCN	
		H_X	H_M	H_A or Me		
IV	$CDCl_3$	1.00(s)	3.00(s)	2.23(s)	2.08(br s)	N(1)
IV	CD_3CN	1.05(s)	3.02(s)	2.23(s)	1.96(s)	N(1)
IV	$(CD_3)_2CO$	0.96(br s)	2.98(br s)	[c]	2.08(br s)[d] + 2.60(s)	N(1) 1 : C 3
		1.37(s)	3.44(s)	[c]		
IV	CD_3OD	0.87(s)	3.11(s)	2.16(s)	2.07(s)[e]	N(2)
III	CD_3OD	1.04(d J_{AX} 9.5)	3.36(d J_{AM} 6.5)[f]	3.72(m)	2.07(s)	N(2)

[a] - N(1) - $[(\eta^{3}\text{-}C_3H_4R)Mo(CO)_2(MeCN)_2Cl]$; N(2) = $[(\eta^{3}\text{-}C_3H_4R)Mo(CO)_2(MeOH)_2Cl]$; C = cationic species

[b] - Based on the intensities of the signals from the allyl protons.

[c] - Obscured by MeCN resonance.

[d] - Unassigned weak singlets at 2.26 and 2.12p.p.m.

[e] - Very weak signals at 1.05(brs) 2.44(brs) 3.23(brs) possibly due to a little N(1) also present.

[f] - Half of signal obscured by resonances due to solvent impurity; J_{AM} obtained from analysis of H_A resonance pattern.

of the minor component were much closer to those found for (IV) in other solvents. The spectrum is consistent with a simple solvolytic process

$$\text{i.e. } [(\eta^3\text{-allyl})M(CO)_2(MeCN)_2X] + S \rightleftharpoons [(\eta^3\text{-allyl})M(CO)_2(MeCN)_2S]^+ + X^- \quad (2.9)$$

Two signals for MeCN were observed, one at 2.60p.p.m. corresponding to ligated MeCN and the second to free MeCN (2.08p.p.m.). The presence of free MeCN in the $(CD_3)_2CO$ solutions of these complexes is a general feature in these systems, and as has been suggested previously, probably results from partial MeCN-$(CD_3)_2CO$ exchange.

Solution Behaviour of $[(\eta^3\text{-}C_3H_4R)Mo(CO)_2(MeCN)_2Cl]$ in CD_3OD. (R = H, Me).

The ^1H NMR spectra of (I) and (IV) recorded in CD_3OD showed no evidence of any autoionisation. Normal patterns for the η^3-allyl entities were obtained in each instance. Facile exchange of the coordinated MeCN with the solvent was suggested by the resonance position of the MeCN protons, which at 2.07p.p.m. was very close to that of the free nitrile (2.00p.p.m.). This exchange was confirmed for (I) by evaporating a CD_3OD solution to dryness, redissolving the residue in CD_3OD and recording the ^1H NMR spectrum, which was identical to that of (I) in CD_3OD with the exception that no MeCN resonance was detected. Thus, in methanol solutions (I) and (IV) exist predominantly as the methanol and not the acetonitrile adducts.

CONCLUSIONS

Spectral evidence for autoionisation of the tungsten complexes (V) - (VII) according to equation (2.1) was only observed to any appreciable extent for (V) (X = Cl) in CD_2Cl_2. These results and those for the analogous molybdenum complexes suggest that the driving force for this reaction is the formation of the anion $[(\eta^3\text{-allyl})_2M_2(CO)_4X_3]^-$. The magnitude of the equilibrium constants for (I) and (II)[257] parallel the ease of formation of the respective anions, and where the halide in question [iodide in complex(III)] is unable to stabilise an anionic species of this type[223] no autoionisation as described by Equation (2.1) was observed, even though the cationic species $[(\eta^3\text{-allyl})Mo(CO)_2(MeCN)_3]^+$ was easily formed by a simple solvolytic process in MeCN.

In agreement with this postulate, the absence of any autoionisation for (V) in MeCN which was large for (I) can be accounted for in terms of the instability of $[(\eta^3\text{-}C_3H_5)_2W_2(CO)_4Cl_3]^-$ (which undergoes extensive solvolysis to form $[(\eta^3\text{-}C_3H_5)W(CO)_2(MeCN)_2Cl]$) in this solvent. (IV) also failed to ionise according to equation (2.1) although solvolysis occurred in $(CD_3)_2CO$ forming the cationic species $[(\eta^3\text{-2-Me}C_3H_4)Mo(CO)_2(MeCN)_2(CD_3)_2CO]^+$. $[(\eta^3\text{-2-Me}C_3H_4)_2Mo_2(CO)_4Cl_3]^-$ is probably less stable than the corresponding $(\eta^3\text{-}C_3H_5)$ anion by virtue of the strong inductive effect of the methyl substituent on the allyl.

The study of the solution properties of these compounds was complicated by the number of competing reactions such as solvolysis and coordinated MeCN-solvent exchange which occurred in polar solvents. The number and nature of the species present in the solutions of these

compounds is of particular importance when investigating their reactivity. In methanol for example, the ^{1}H NMR spectrum of (I) and (IV) indicated that complete MeCN-MeOH exchange occurred, the complexes existing almost exclusively as $[(\eta^{3}\text{-}C_3H_4R)Mo(CO)_2(MeOH)_2Cl]$. Thus when investigating the reactions of (I) and (IV) in this solvent one is probably concerned with the reactivity of the bis-MeOH adduct and not the bis-MeCN adduct. In solvents where ionisation of the compounds according to equation (2.1) was indicated, an added reagent may react with any of the three species, i.e. neutral, anionic or cationic, which are present. Therefore products of the type (i) $[(\eta^{3}\text{-allyl})M(CO)_2L_2X]$ [162,243,254,247] and (ii) $[M(CO)_2(MeCN)_2L_2]$ [247,249,250,253], which have been isolated from the reactions of the compounds $[(\eta^{3}\text{-}C_3H_4R)M(CO)_2(MeCN)_2X]$ with different nucleophiles L (under ambient conditions) may not simply result from attack occurring at either the metal centre for (i) or the coordinated η^{3}-allyl ligand for (ii) of the <u>neutral</u> species as has been suggested[249], but via much more complex reactions which involve the charged species.

The significance of these findings in relation to the reactivity of the compounds $[(\eta^{3}\text{-}C_3H_4R)M(CO)_2(MeCN)_2Cl]$ with various nucleophiles is discussed in more detail in Chapter 5.

CHAPTER THREE

THE REACTIONS OF SOME DITERTIARY PHOSPHINES AND ARSINES WITH $[(\eta^3\text{-}C_3H_5)W(CO)_2(MeCN)_2X]$, (X = Cl, Br or I).

INTRODUCTION

Prior to the start of this work and as part of a final year undergraduate research project the author had investigated the reactions of a number of ditertiary phosphine and arsine ligands with the molybdenum compounds $[(\eta^3\text{-}C_3H_5)Mo(CO)_2(MeCN)_2X]$ (X = Cl, Br or I)[244]. Under mild conditions molybdenum(II) complexes of stoichiometry $[(\eta^3\text{-}C_3H_5)Mo(CO)_2L_2X]$ [L_2 = bis(diphenylphosphino)methane (dpm), 1,2-bis(diphenylphosphino)ethane (dpe), or 1,2-bis(diphenylarsino)-ethane (dae); X = Cl, Br or I] and $[(\eta^3\text{-}C_3H_5)_2Mo_2(CO)_4X_2L_2]$ [L_2 = bis(diphenylarsino)methane (dam); X = Cl or Br] were isolated. Under more forcing conditions the ditertiary phosphine ligands reacted further to form the molybdenum(0) derivatives *cis*-$[Mo(CO)_2(L_2)_2]$ (L_2 = dpm or dpe).

This chapter describes an extension of that work in which the reactivity of the ditertiary phosphine and arsine ligands (dpm, dpe, dam and dae) towards the tungsten complexes $[(\eta^3\text{-}C_3H_5)W(CO)_2(MeCN)_2X]$ (X = Cl, Br or I) are reported.

EXPERIMENTAL

Details of physical techniques and solvents appear in appendix 3. The methods used for the preparation of the starting materials $[(\eta^3\text{-}C_3H_5)W(CO)_2(MeCN)_2X]$ (X = Cl, Br or I) are described in Chapter 2.

The Reaction of $[(\eta^3\text{-}C_3H_5)W(CO)_2(MeCN)_2Cl]$ with 1,2-Bis(diphenylphosphino)ethane under Forcing Conditions

A solution of $[(\eta^3\text{-}C_3H_5)W(CO)_2(MeCN)_2Cl]$ (1.0 mmol, 0.40g) dissolved in CH_3CN (30 cm^3) was treated with finely divided dpe (2.5 mmol, 1.00g). This resulted in the precipitation of $[(\eta^3\text{-}C_3H_5)W(CO)_2$ (dpe)Cl]. The mixture was heated under reflux for 50 h during which time the initial product gradually redissolved and was replaced by a yellow crystalline deposit. The solution was filtered whilst hot and the crude product recrystallised from $CHCl_3$-light petroleum (60 - 80°C) and identified as cis-$[W(CO)_2(dpe)_2]$.

Changing the solvent to $(CH_3)_2CO$ resulted in the initial precipitate of $[(\eta^3\text{-}C_3H_5)W(CO)_2(dpe)Cl]$ remaining largely unchanged throughout the duration of a two day reflux and it was recovered from the hot reaction medium in 80% yield. An indication that the reduced species cis-$[W(CO)_2(dpe)_2]$ was present in the reaction mixture was obtained from solution infrared studies, but the yield was too low to enable its isolation.

cis-$[W(CO)_2(dpe)_2]$ was found to be insoluble in non-polar solvents such as CCl_4, pentane and petroleum ether and only sparingly soluble in the polar solvents, $CHCl_3$, CH_2Cl_2 and $(CH_3)_2CO$.

The Reaction of $[(\eta^3\text{-}C_3H_5)W(CO)_2(MeCN)_2Cl]$ with Bis(diphenylphosphino)-methane under Forcing Conditions.

$[(\eta^3\text{-}C_3H_5)W(CO)_2(MeCN)_2Cl]$ (1.0 mmol, 0.40 g) in CH_3CN (30 cm^3) was treated with dpm (2.5 mmol, 0.96g) and the solution heated under reflux for 24 h, during which time the initially clear orange solution gradually darkened to a deep red. Two products, one a brown powder and the other flat diamond-shaped yellow crystals were formed under these conditions, and on keeping the filtrate at 0^oC overnight further quantities of both products were deposited.

Since chemical separation was not possible because both products had similar, very low solubilities in common solvents, separation had to be performed by hand. The brown powder (compound XV) has not been fully characterised but the yellow crystals were identified by infrared spectroscopy and analytical data and shown to be cis-$[W(CO)_2(dpm)_2]$.

The Reaction of $[(\eta^3\text{-}C_3H_5)W(CO)_2(MeCN)_2X]$ (X = Cl, Br or I) with 1,2-Bis(diphenylarsino)ethane.

A solution of dae (1.0 mmol, 0.49g) in $(CH_3)_2CO$ (10 cm^3) was added to $[(\eta^3\text{-}C_3H_5)W(CO)_2(MeCN)_2X]$ (1.0 mmol) dissolved in $(CH_3)_2CO$ (15 cm^3). After stirring the reaction mixture at room temperature for 1 h, the precipitated orange crystalline solid was collected by filtration and washed with cold $(CH_3)_2CO$.

The products $[(\eta^3\text{-}C_3H_5)W(CO)_2(dae)X]$ were stable in air and soluble in chlorinated solvents such as $CHCl_3$ and CH_2Cl_2 but insoluble in diethyl ether and petroleum ethers.

The Reaction of $[(\eta^3\text{-}C_3H_5)W(CO)_2(MeCN)_2X]$ (X = Cl or Br) with Bis(diphenylarsino)methane.

The ditertiary arsine dam (1.0 mmol, 0.47 g) was dissolved in warm $(CH_3)_2CO$ (10 cm^3) and treated with $[(\eta^3\text{-}C_3H_5)W(CO)_2(MeCN)_2X]$ (2.0 mmol). The reaction mixture was maintained at 40°C for 0.5 h and the solvent subsequently removed in vacuo at room temperature. The residue was dissolved in boiling toluene (30 cm^3) and the solution filtered. Standing the filtrate at 10°C for 12 h, yielded deep burgundy (X = Cl) or deep purple (X = Br) crystals of $[(\eta^3\text{-}C_3H_5)_2W_2(CO)_4X_2dam]$, toluene.

The compounds $[(\eta^3\text{-}C_3H_5)_2W_2(CO)_4X_2dam]$, toluene were slightly air-sensitive but could be stored indefinitely in sealed nitrogen-filled ampoules. They were soluble in $CHCl_3$, CH_2Cl_2, benzene and toluene, but insoluble in diethyl ether and petroleum ether.

Reactions of $[(\eta^3\text{-}C_3H_5)_2W_2(CO)_4Cl_2(dam)]$, toluene with Other Ligands

(i) With the ditertiary phosphines bis(diphenylphosphino)methane and 1,2-bis(diphenylphosphino)ethane .

A solution of the phosphine (0.42 mmol) dissolved in CH_3CN (10 cm^3) was treated with $[(\eta^3\text{-}C_3H_5)_2W_2(CO)_4Cl_2dam]$, toluene (0.21 mmol, 0.25 g) and the mixture refluxed for 0.8 h. Orange crystals of the known complexes $[(\eta^3\text{-}C_3H_5)W(CO)_2L_2Cl]$ (L_2 = dpe or dpm) were deposited from the clear orange solutions on cooling. Yields 80 - 85%. The

identity and purity of the compounds $[(\eta^3\text{-}C_3H_5)W(CO)_2L_2Cl]$ (L_2 = dpe or dpm) were confirmed by infra-red spectroscopy, particularly a comparison with literature[162] ν(CO) band position.

(ii) With pyridine

Excess pyridine (16 mmol, 1.3 cm^3) was added to $[(\eta^3\text{-}C_3H_5)_2W_2(CO)_4Cl_2(dam)]$, toluene (0.21 mmol, 0.25 g) dissolved in $CHCl_3$ (6 cm^3). The reaction mixture was stirred at room temperature for 0.5 h and then treated with light petroleum (40 - 60°C) to initiate the precipitation of $[(\eta^3\text{-}C_3H_5)W(CO)_2(py)_2Cl]$ as a yellow powder.

This product was soluble in the polar solvents $CHCl_3$, CH_2Cl_2 and $(CH_3)_2CO$.

(iii) With tetraphenylarsoniumchloride

A solution of $[(\eta^3\text{-}C_3H_5)_2W_2(CO)_4Cl_2(dam)]$, toluene (0.21 mmol, 0.25 g) and Ph_4AsCl,H_2O (0.21 mmol, 0.09 g) in CH_2Cl_2 (10 cm^3) was stirred for 0.5 h. The dropwise addition of light petroleum (40 - 60°C) produced a yellow precipitate of $Ph_4As[(\eta^3\text{-}C_3H_5)_2W_2(CO)_4Cl_3]$ in high yield (74%).

Yields, melting points and analyses for the complexes appear in Table 3.1, (except for those of $Ph_4As[(\eta^3\text{-}C_3H_5)_2W_2(CO)_4Cl_3]$ which have previously been listed in Table 2.1).

Table 3.1: Yields, Melting Points and Analytical Data

Complex (No.)	Yield (%)	M.pt. (°C)	Analysis (calcd.) Found (%) C	H
cis-$[W(CO)_2(dpe)_2]$ (XIII)	40	315-320[a]	61.6 (62.6)	4.8 (4.7)
cis-$[W(CO)_2(dpm)_2]$ (XIV)	5	320-325	62.0 (61.9)	4.6 (4.7)
Compound (XV)	[d]	~210[b]	55.3	4.2
$[(\eta^3-C_3H_5)W(CO)_2(dae)Cl]$ (XVI)	35	~200[b]	46.2 (46.4)	3.6 (3.6)
$[(\eta^3-C_3H_5)W(CO)_2(dae)Br]$ (XVII)	39	~205[b]	43.7 (44.0)	3.4 (3.5)
$[(\eta^3-C_3H_5)W(CO)_2(dae)I]$ (XVIII)	40	~205[b]	41.9 (41.6)	3.2 (3.2)
$[(\eta^3-C_3H_5)_2W_2(CO)_4Cl_2(dam)]$, toluene (XIX)	77	~154[b]	41.2 (42.1)	3.4 (3.4)
$[(\eta^3-C_3H_5)_2W_2(CO)_4Br_2(dam)]$, toluene (XX)	64	~130[b]	39.3 (39.2)	3.2 (3.1)
$[(\eta^3-C_3H_5)W(CO)_2(py)_2Cl]$ (XXI)	93	~130[b]	37.4 (38.0)	3.1[c] (2.8)

[a] - Literature value[283] 320-323°C

[b] - Temperature recorded is the decomposition point, melting only occurred at very much higher temperatures.

[c] - Nitrogen analysis: found 5.9%, calculated 5.9%.

[d] - Yield obtained was 0.36 g from 0.40 g $[(\eta^3-C_3H_5)W(CO)_2(MeCN)_2Cl]$

RESULTS AND DISCUSSION

The Reactions of $[(\eta^3\text{-}C_3H_5)W(CO)_2(MeCN)_2Cl]$ with the Ditertiary Phosphines bis(diphenylphosphino)methane and 1,2-bis(diphenylphosphino)ethane.

Brisdon[162] reported that at room temperature the ditertiary phosphines dpe and dpm react with $[(\eta^3\text{-}C_3H_5)W(CO)_2(MeCN)_2X]$ by substitution of MeCN to form the complexes $[(\eta^3\text{-}C_3H_5)W(CO)_2(L_2)X]$ (L_2 = dpe or dpm; X = Cl, Br or I). Under more forcing conditions and in the presence of excess phosphine the reaction has been shown to proceed further with the formation of the reduced W(0) species cis-$[W(CO)_2(L_2)_2]$ (L_2 = dpe or dpm). Both compounds displayed two bands of approximately equal intensity in the ν(CO) region of their infrared spectra at positions which agree well with literature values[283,284] [(XIII): ν (CO)($CHCl_3$) 1850; 1781 cm^{-1}; (XIV): ν (CO)(nujol) 1840; 1780 cm^{-1}]. Neither (XIII) nor (XIV) were particularly soluble in solvents suitable for ^1H NMR spectroscopic studies, however a poorly resolved spectrum was obtained for (XIII) in $CDCl_3$. The methylene protons resonated as a broad multiplet centred at 2.22 p.p.m. and in the aromatic region two resonances were observed, a broad intense multiplet at 7.24 p.p.m. corresponding to 36 protons and a weak triplet at slightly higher fields (6.18 p.p.m.) of intensity 4. Similar ^1H NMR spectra have been recorded for other compounds of type cis-$[M(dpe)_2X_2]$ and according to Ginsberg and Lindsell[285] the presence of the weak triplet is conclusive evidence for the cis geometry of the dpe ligands.

The yields of the cis-dicarbonyl-tungsten (O) products ($\leqslant$ 40%) were comparatively low, whereas in the analogous molybdenum reactions yields of up to 70% were achieved[244]. In addition cis-$[W(CO)_2(dpm)_2]$ could not be prepared without also isolating compound (XV), another carbonyl containing product [ν(CO)(nujol) 1769(m); 1741(m) cm^{-1}] whose exact composition could not be established and may indeed not be a single compound. Attempts to improve the yield of cis-$[W(CO)_2(dpm)_2]$ by varying the reaction time from 2 - 76 h were not successful. After short reaction times neither product had formed in appreciable quantities, whereas extended reaction times only resulted in an increase in the yield of (XV) at the expense of cis-$[W(CO)_2(dpm)_2]$. Reactions carried out in $(CH_3)_2CO$ yielded only compound (XV). Since tungsten (O) species (XIII) and (XIV) are isolated from these high temperature reactions it is evident that the ditertiary phosphines can reduce tungsten(II) in the complex $[(\eta^3\text{-}C_3H_5)W(CO)_2(MeCN)_2Cl]$. However, the high temperatures necessary for the reaction together with the observed intermediacy of the complexes $[(\eta^3\text{-}C_3H_5)W(CO)_2L_2Cl]$ (L_2 = dpe or dpm) indicates that the mode of formation of these compounds is probably unlike that of the W(O) compounds $[W(CO)_2(MeCN)_x(PR_3)_y]$ (R = Ph, x = 2, y = 2; R =n-Bu, x = 1, y = 3) which are prepared under much milder conditions[251], with no evidence of intermediates.

After stepwise displacement of both MeCN ligands in $[(\eta^3\text{-}C_3H_5)W(CO)_2(MeCN)_2Cl]$ by the chelating ditertiary phosphine, reductive elimination of allyl halide occurs at higher temperatures possibly by a similar mechanism to that proposed by Dieck[243]. The

coordinatively unsaturated tungsten(O) species shown in Scheme 3.1 then adds a second chelating phosphine ligand giving the final product.

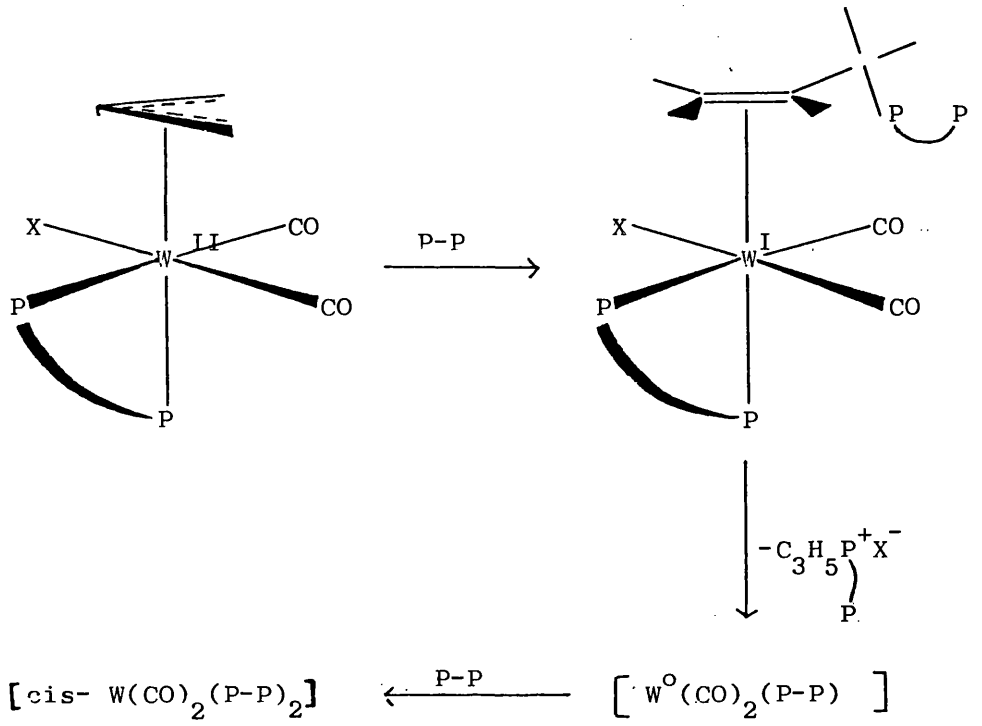

Scheme 3.1

The Reactions of $[(\eta^3\text{-}C_3H_5)W(CO)_2(MeCN)_2X]$ with the Ditertiary Arsines bis(diphenylarsino)methane and 1,2-bis(diphenylarsino)ethane

The complexes $[(\eta^3\text{-}C_3H_5)W(CO)_2(dae)X]$ (XVI-XVIII) were prepared by reaction of $[(\eta^3\text{-}C_3H_5)W(CO)_2(MeCN)_2X]$ (X = Cl, Br and I respectively) with dae in $(CH_3)_2CO$ at room temperature. The same products were obtained in refluxing $(CH_3)_2CO$ or CH_3CN solutions (although in lower yields from the latter solvent). There was no indication of either nucleophilic attack by excess diarsine on the allyl ligand or formation of tungsten(O) complexes. Selected

infrared spectral data for the compounds (XVI - XVIII) are presented in Table 3.2 and are consistent with their formulation as cis-dicarbonyl-products. Between 1600 - 400 cm^{-1} the spectra are dominated by absorptions of the coordinated dae ligands and consequently it has not been possible to assign any bands to vibrations of the allyl or carbonyl fragments in this region. Below 400 cm^{-1} however, a single strong halogen-sensitive band was observed and is assigned to the metal-halogen stretching mode on the basis of the ν(WBr)/ ν(WCl) and ν(WI)/ ν(WCl) frequency ratios[275].

Table 3.2: Selected Infrared Spectral Data for the Complexes $[(\eta^3\text{-}C_3H_5)W(CO)_2(dae)X]$. X = Cl, Br or I.

Complex No. (XVI)	Complex No. (XVII)	Complex No. (XVIII)	Assignment
244br vs	164 br s	132 w	ν(WX) [a]
1935 vs	1940 vs	1940 vs	ν(CO) [b]
1850 vs	1850 vs	1855 vs	ν(CO) [b]

Ratios ν(WBr)/ ν(WCl) = 0.67; ν(WI)/ ν(WCl) = 0.54

[a] Complex dispersed in polythene.

[b] Nujol mulls.

Despite recording the far-infrared spectrum of the ligand dae (which showed bands at 142 w, 192 br m, 242 w, 254 s, 283 vs, 306 vs and 327 vs), assignments of metal-arsenic stretching frequencies for (XVI-XVII) were not possible. Very little information is available regarding ν(M-As) assignments though they are expected to occur below 300 cm^{-1} [270] and to be of only weak intensity in the infrared spectrum. Assignments of ν(M-As) from the Raman Spectra of a few chromium, molybdenum and tungsten compounds[286-288] have been made for bands in the region 146-187 cm^{-1}, but since bands due to metal-ligand deformation modes are also expected in this region such assignments, made without the aid of isotopic shift data, must be viewed with caution.

Mass Spectra:- The most intense peaks in the mass spectra of compounds (XVI-XVIII) were due to the ligand dae and ions associated with its fragmentation[289] the most abundant being $[Ph_2As(CH_2)_2AsPh_2]^+$. For (XVI) and (XVIII) however, metal-containing fragments were present in trace amounts less than 1% relative abundance based on the intensity of $[Ph_2As(CH_2)_2AsPh_2]^+$ but were readily identified by the characteristic isotope pattern of tungsten (see Figure 3.1).

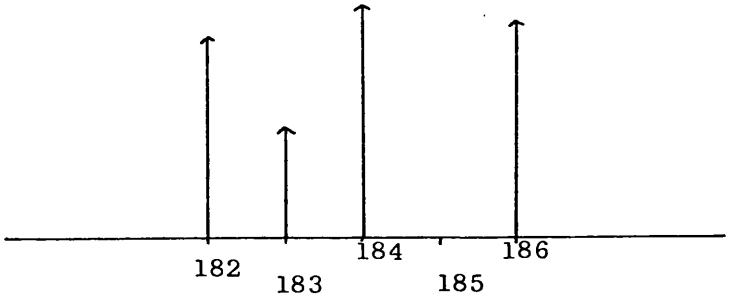

Figure 3.1: The characteristic isotope pattern for tungsten.

The strongest metal-containing ions detected are listed in Table 3.3; their intensities are given relative to a metal-containing base peak of 100 units. That these complexes were not very stable in the spectrometer was indicated by the mass spectrum of the iodo-complex (XVIII) which also showed a strong fragmentation pattern of $[W(CO)_4(dae)]$ in addition to that of $[(\eta^3\text{-}C_3H_5)W(CO)_2(dae)I]$. The bromo-complex (XVII) completely decomposed under the operating conditions used for the other two dae complexes and no metal-containing fragments could be detected.

The molecular ion $[(C_3H_5)W(CO)_2(dae)X]^+$ is observed for both (XVI and XVIII) and consideration of the observed metastable ions indicates that fragmentation proceeds via step-wise elimination of carbonyl ligands followed by loss of allyl.

$$[(C_3H_5)W(CO)_2(dae)X]^+ \xrightarrow{-CO} [(C_3H_5)W(CO)(dae)X]^+$$

$$[(C_3H_5)W(CO)(dae)X]^+ \xrightarrow{-CO} [(C_3H_5)W(dae)X]^+$$

$$[(C_3H_5)W(dae)X]^+ \xrightarrow{-C_3H_5} [W(dae)X]^+$$

Fragmentation of the dae ligand whilst still attached to the metal is a significant feature of the spectra. Loss of halogen from $[W(dae)X]^+$ prior to fragmentation of the attached dae ligand occurs for both (XVI and XVIII), but its retention is clearly favoured for (XVI). [It is difficult to ascertain whether this is also the case for (XVIII), because fragmentation of $[W(CO)_4(dae)]$, which is also observed, will naturally increase the abundance of $[W(dae)]^+$ in the spectrum].

Table 3.3: Tungsten-containing Ions in the Mass Spectra of $[(\eta^3\text{-}C_3H_5)W(CO)_2(dae)X]$. (Based on ^{182}W only).

Ion	X=Cl		X=I	
	m/e	R.I.	m/e	R.I.
$[(C_3H_5)WX(CO)_2(dae)]^+$	800	19	892	31
$[(C_3H_5)WX(CO)(dae)]^+$	772	61	864	76
$[(C_3H_5)WX(dae)]^+$	744	35	836	40
$[(C_3H_3)WX(dae)]^+$	742	54	834	66
$[WX(dae)]^+$	703	35	795	19
$[W(CO)_4(dae)]^+$	-	-	780	51
$[W(CO)_2(dae)]^+$	-	-	724	88
$[WX(Ph_4As_2)]^+$	675	12	-	-
$[WX(Ph_2AsC_2H_4AsPh)]^+$	626	47	-	-
$[WX(Ph_3As_2)]^+$	598	16	690	14
$[W(dae)]^+$	-	-	668	40
$[W(Ph_4As_2)]^+$	-	-	640	66
$[WX(As_2C_{12}H_8)]^+$	519	45	611	23
$[WX(AsC_{12}H_8)]^+$	444	100	536	54
$[W(AsC_{12}H_7)]^+$	408	74	-	-
$[WX(AsC_6H_4)]^+$	368	58	460	56
$[W(AsC_{12}H_8)]^+$	-	-	409	100
Unassigned	558	11	605	28
			575	54
			537	52

Metastables				
	772 → 744	m* = 717.0 (717.0)	864 → 836	m* = 810.0 (808.9)
	703 → 675	m* = 648.0 (648.1)		
	675 → 598	m* 530.0 (529.8)		

The most abundant metal-containing fragments observed are $[WCl(AsC_{12}H_8)]^+$ for (XVI) and $[W(AsC_{12}H_8)]^+$ for (XVIII); these contain an $(AsC_{12}H_8)$ fragment which has been formulated[289] as the stable cyclic ion shown in Figure 3.2. This ion is the second most abundant species in the mass spectrum of uncoordinated dae[289].

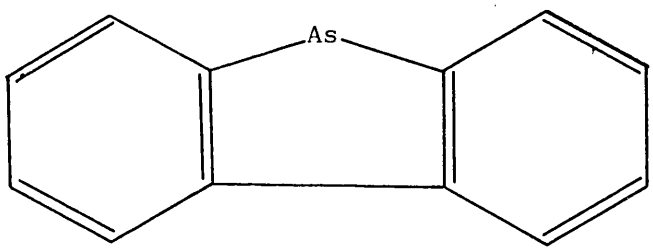

Figure 3.2: Structure of the $AsC_{12}H_8$ fragment.

The ion $[(C_3H_3)W(dae)X]^+$ is of high abundance in both spectra and most probably arises by elimination of the relatively common neutral H_2 fragment[69] ⁄. Similar eliminations have been observed in the mass spectra of several other allyl complexes of transition metals such as $[(\eta^3\text{-}C_3H_5)Rh(\mu\text{-}Cl)]_2$[291], $[(\eta^1\text{-}C_3H_5)Re(CO)_5]$[70] $[(\eta^3\text{-}C_3H_5)W(CO)_2(\eta^5\text{-}C_5H_5)]$ and $[(\eta^1\text{-}C_3H_5)W(CO)_3(\eta^5\text{-}C_5H_5)]$[69], and $[(\eta^3\text{-}C_3H_5)Mo(CO)_2(\eta^5\text{-}C_5H_5)]$[290]. For the last three complexes the most abundant metal-containing ion is in fact $[(C_3H_3)M(C_5H_5)]^+$. The abundance of such ions can be explained by their formulation as η^3-cyclopropenyl-metal species[291].

⁄ Simultaneous loss of 2H and CO, possibly as formaldehyde HCHO[290], is an alternative possibility.

The suggested fragmentation sequences are summarised in Scheme 3.2 (not all of the ions are necessarily observed in both spectra - see Table 3.3).

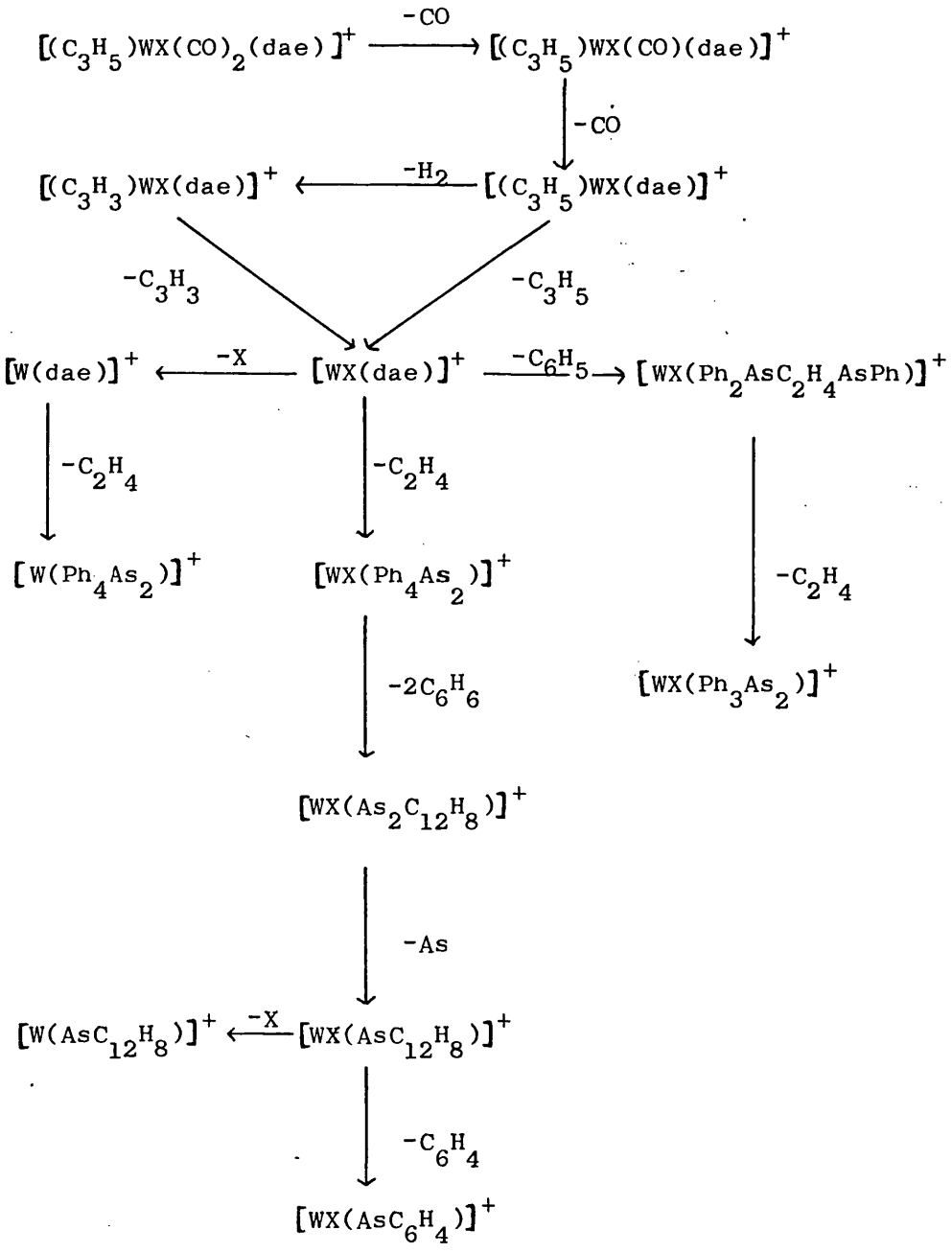
[(C3H5)WX(CO)2(dae)]+
-CO
[(C3H5)WX(CO)(dae)]+
-CO
[(C3H3)WX(dae)]+
-H2
[(C3H5)WX(dae)]+
-C3H3
-C3H5
[W(dae)]+
-X
[WX(dae)]+
-C6H5
[WX(Ph2AsC2H4AsPh)]+
-C2H4
-C2H4
-C2H4
[W(Ph4As2)]+
[WX(Ph4As2)]+
[WX(Ph3As2)]+
-2C6H6
[WX(As2C12H8)]+
-As
[W(AsC12H8)]+
-X
[WX(AsC12H8)]+
-C6H4
[WX(AsC6H4)]+

Scheme 3.2

Table 3.4: ^{1}H NMR Data for the complexes $[(\eta^{3}\text{-}C_3H_5)W(CO)_2(dae)X]$ (X = Cl, Br and I)

Complex	Temp. (°C)	δ*(multiplicity, rel. intensity) Allyl Protons H_X	H_M	H_A	Other Protons $-(CH_2)_2-$	Aromatic
XVI	28[a]	1.88(d, 2H) J_{XA} 8.2	3.28(br s, 2H)	3.38(m, 1H)	2.48[c] (m, 4H)	7.48(m, 20H)
	-125[b]	1.66, 2.02	3.20, 3.44	3.32	2.02, 2.44, 2.62, 3.06	
XVII	28[a]	1.84(d, 2H) J_{XA} 8.3	3.46(br s, 2H)	3.36(m, 1H)	2.56[c](m, 4H)	7.48(m, 20H)
XVIII	28[a]	1.78(d, 2H) J_{XA} 8.5	3.56(br s, 2H)	3.44(m, 1H)	2.55[c](m, 4H)	7.50(m, 20H)
	-125[b]	1.44, 2.03	3.28, 3.64	2.98	1.74, 2.58, 2.56, 3.28	

* - δ in p.p.m. rel. to $SiMe_4$; coupling constants (J) in Hz.

[a] - in $CDCl_3$ solution.

[b] - in $CHCl_2F$ solution, all bands were broad and showed no fine structure.

[c] - centre of an AA'BB' multiplet.

^{1}H NMR Spectra:- Details of the 100 MHz ^{1}H NMR spectra of the complexes (XVI - XVIII) are listed in Table 3.4. At ambient temperatures two sets of resonances, with relative intensities 2:3 were observed for the protons of the allyl ligand. The most intense set comprises signals for the syn protons (H_M) and central protons H_A, the former resonating as a broadened singlet instead of a doublet, as normally observed for symmetrical or fluxional η^3-allyls. Another unusual feature of the spectra is the signal due to the methylene protons of the coordinated dae ligand, which as shown in Figure 3.3, is in the form of an AA'BB' pattern. Theoretically 24 bands are expected for such a spin system and since 20 of these were clearly resolved an analysis of the spectra was undertaken. The proposed assignment of the lines shown in Table 3.5 for (XVI), complies with the general rules governing the transition energies and intensities of an AA'BB' system as formulated by Abraham[292]. The resulting coupling constants which are presented in Table 3.6 are very similar to those reported for $[(\eta^3\text{-}C_3H_5)Mo(CO)_2(dae)Cl]$[171].

Table 3.5 Transition Energies and Intensities for the AA' part of the Methylene Region of $Ph_2As(CH_2)_2AsPh_2$ in Complex (XVI)

Transition	5	9,10	6	4	3	2	1	7	11,12	8
Obs. energy (Hz)[a]	46.5	41.5	35.25	33.0	31.25	29.25	27.0	23.25	20.5	11.75
Obs. intensity[b]	0.19	0.63	0.69	1.08	1.03	0.89	0.95	0.89	1.08	0.58

[a] - Measured from the mid point of the AA'BB' spectrum

[b] - Determined from the peak heights

Table 3.6: Coupling Constants for the Methylene Protons of $Ph_2As(CH_2)_2AsPh_2$ in the Complexes $[(\eta^3\text{-}C_3H_5)W(CO)_2(dae)X]$

Complex	N^a	$(M^2 + L^2)^{\frac{1}{2}}$ a	Calculated Coupling Constants (Hz) J_{AB}	$J_{AB'}$	$J_{AA'} = J_{BB'}$
XVI	-4.3	-21.5	-12.9	8.6	5.9
XVII	-4.9	-21.3	-13.1	8.2	6.7
XVIII	-5.3	-20.8	-13.1	7.8	7.2

a - The separations are based upon the following relationships:

$K = J_{AA'} + J_{BB'}$; $M = J_{AA'} - J_{BB'}$; $\nu_1 - \nu_3 = N$

$L = J_{AB} - J_{AB'}$; $N = J_{AB} + J_{AB'}$; $(M^2 + L^2)^{\frac{1}{2}} = \nu_9 - \nu_{11}$

with the signs of J based upon the observations[293]:

J_{AB} = (-) for geminal protons of disubstituted ethane

$J_{AB'}$ = (+) for vicinal trans protons of disubstituted ethane

$J_{AA'}$ = (+) for vicinal gauche protons of disubstituted ethane

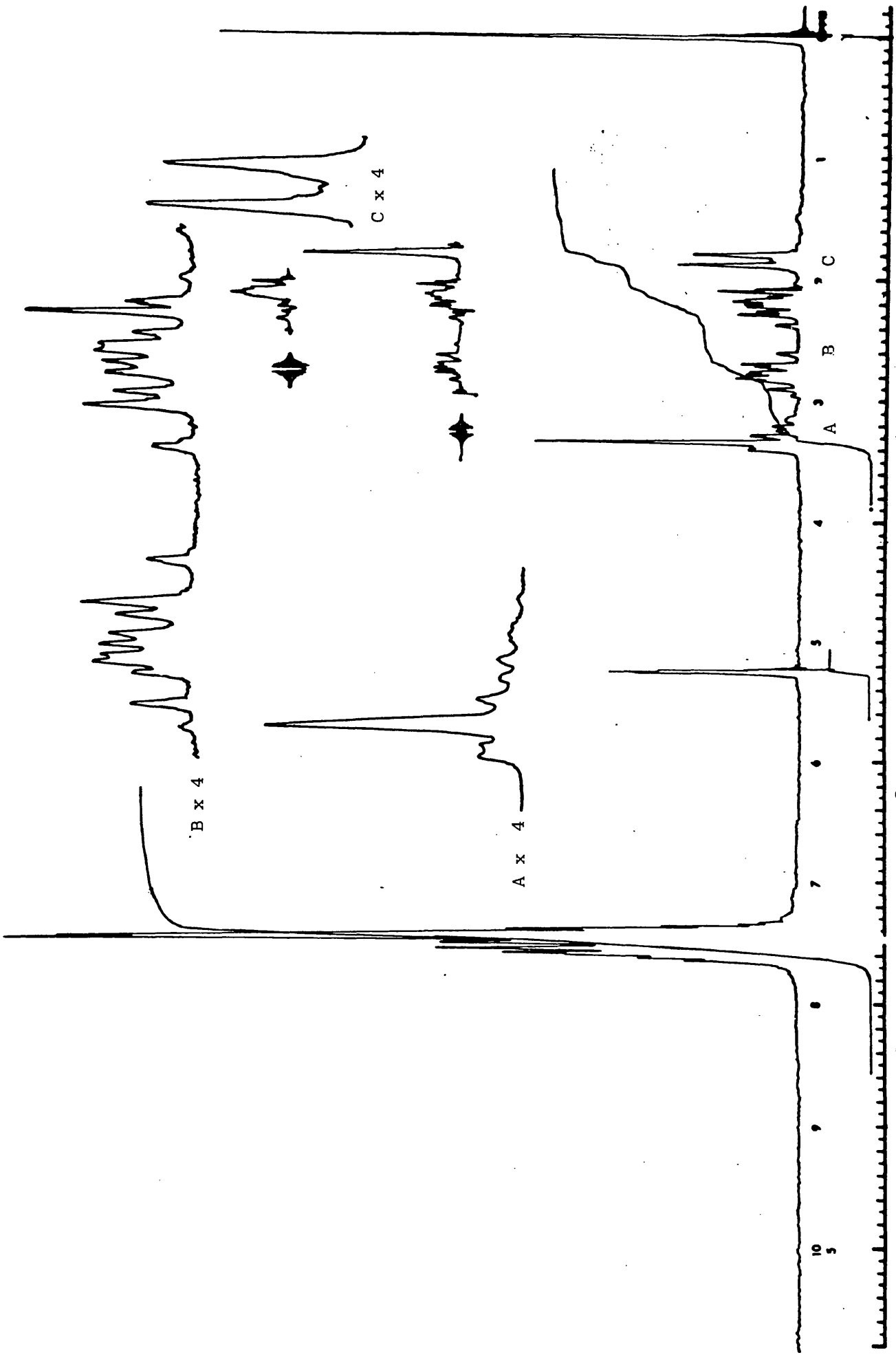

Figure 3.3: ^{1}H NMR Spectrum of $[(\eta^{3}\text{-}C_3H_5)W(CO)_2(dae)Cl]$ in CD_2Cl_2

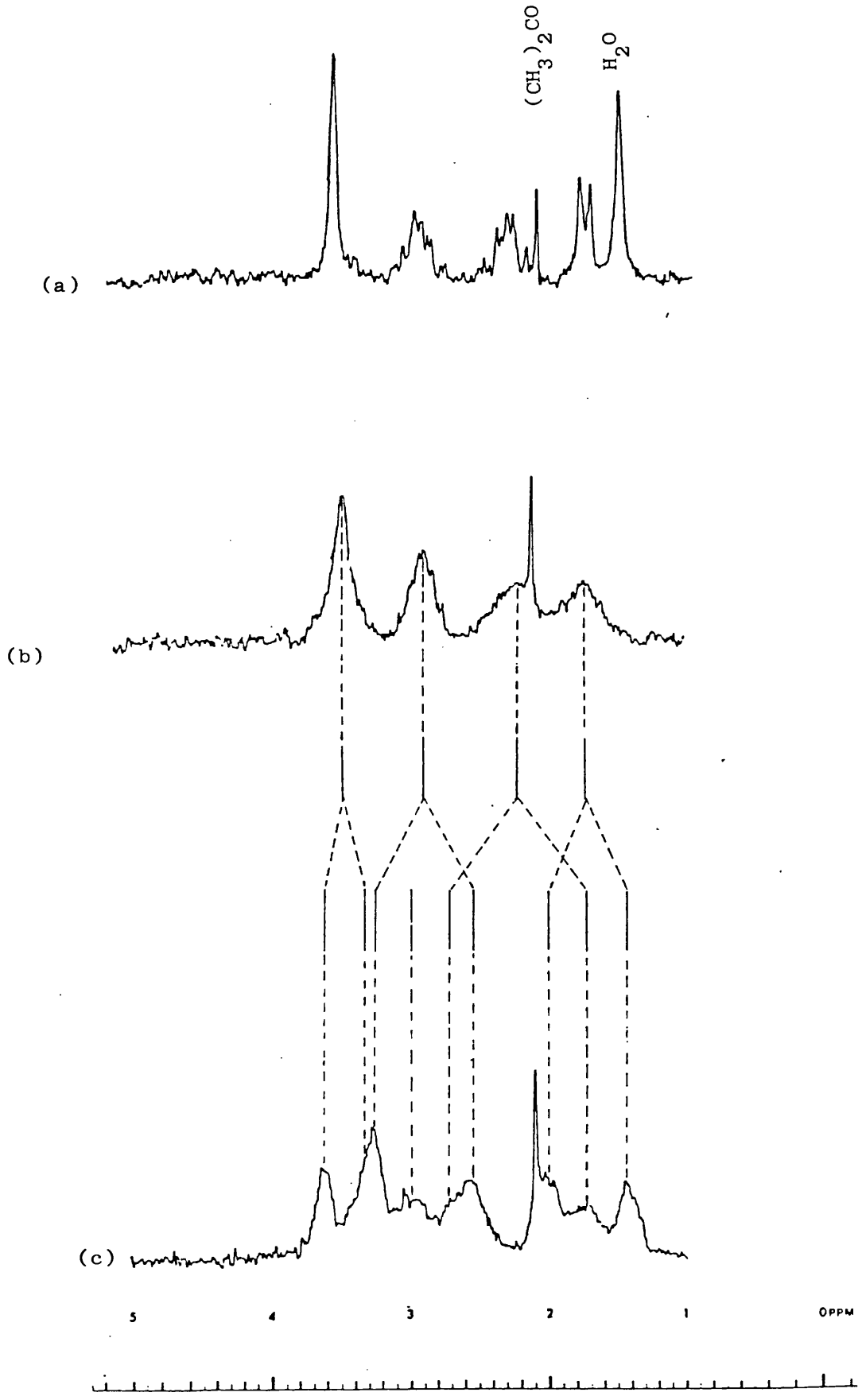

Figure 3.4: ^{1}H NMR Spectra for [(η^3-C_3H_5)W(CO)$_2$(dae)I] recorded at (a) ± 0, (b) -60 and (c) -125°C

^{1}H NMR spectra were recorded for each of the complexes (XVI-XVIII) at various temperatures in the range +70°C - -125°C. Apart from a slight improvement in resolution, the high temperature spectra were unchanged from that observed at room temperature. On lowering the temperature however, the bands lost all fine structure. By -125°C at least seven broad bands could be distinguished for the allyl and methylene protons of complexes (XVI and XVIII) (only very broad overlapping bands were observed for (XVII) even at -125°C). These could be assigned to overlapping ABCDX and ABCD spin patterns of an unsymmetrical allyl system, and inequivalent methylene protons of dae, respectively. (see Figure 3.4). This suggests that the complexes possess a low symmetry instantaneous structure such as that shown below in Figure 3.5.

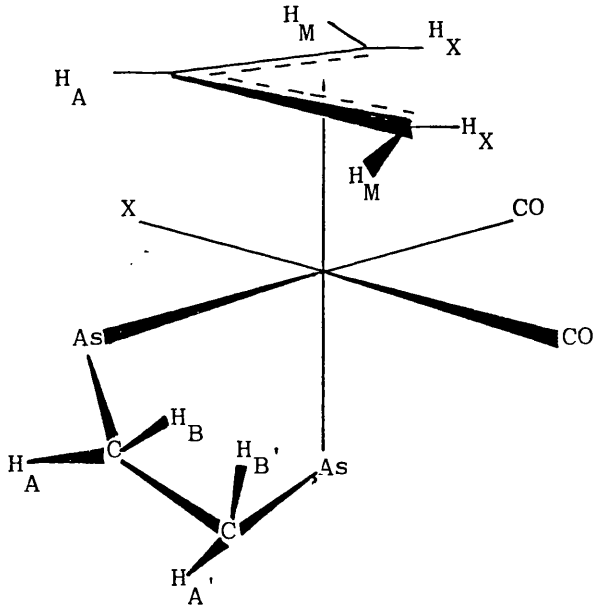

Figure 3.5: A structure for $[(\eta^3\text{-}C_3H_5)W(CO)_2(dae)X]$, lacking a plane of symmetry.

Faller[171] has recently shown that the related complex $[(\eta^3\text{-}C_3H_5)Mo(CO)_2(dpe)Cl]$, which exhibits similar variable temperature ^1H NMR spectral features to those described above, possesses just such a structure in the solid state. He has also proposed that the stereochemical non-rigidity of this species results from a reversible, 120° trigonal twisting motion of the halogen and phosphorus ligands relative to the rest of the complex (see Chapter 1 p.49).

The compounds (XIX) and (XX) isolated from the reactions of dam and $[(\eta^3\text{-}C_3H_5)W(CO)_2(MeCN)_2X]$ (X = Cl or Br) under mild conditions had an allyl to dam ratio of 2:1 and crystallised with a solvent molecule which could not be successfully removed. Recrystallisation of the toluene solvates from acetone simply resulted in the isolation of acetone solvates and heating the solvates in vacuo only led to decomposition. The same products were obtained from reactions employing $[(\eta^3\text{-}C_3H_5)W(CO)_2(MeCN)_2X]$: dam ratios from 1:2 to 2:1. These reactions were carefully monitored by infrared and ^1H NMR spectroscopies but there was no indication that more than one product was formed. Under more forcing conditions in refluxing CH_3CN or $(CH_3)_2CO$, $[(\eta^3\text{-}C_3H_5)_2W_2(CO)_4X_2dam]$ rapidly decomposed, however, there was no evidence to suggest that the decomposition reactions involved attack on the allyl ligand or formation of tungsten (0) species.

Selected infrared and ^1H NMR spectral data for (XIX and XX) are summarised in Tables 3.7 and 3.8 and are consistent with their formulation as binuclear species containing both halogeno- and dam-bridges such as has been suggested and established respectively

for the iso-electronic complexes $[W_2(CO)_4(NO)_2X_2dam]$ (X = Cl, Br or I)[294] and $[Re_2(CO)_6Cl_2dam]$[295].

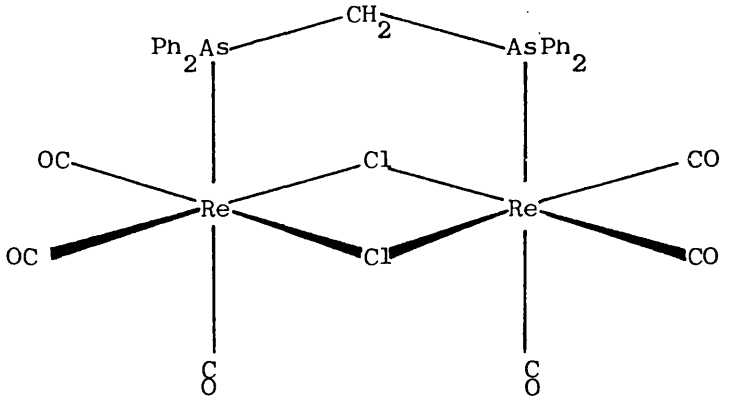

Figure 3.5: The molecular structure of dinuclear $[Re_2(CO)_6Cl_2dam]$

Table 3.7: Selected Infrared Spectral Data for the Complexes $[(\eta^3\text{-}C_3H_5)_2W_2(CO)_4X_2dam]$ (X = Cl or Br)

Complex (No.) (XIX)	Complex (No.) (XX)	Assignment
1935(sh)	1935 br s	ν(C-O)[a]
1926s		
1863m	1863m	
1840vs	1845vs	
270br s	179br s	ν(W-X)[b]
228m	163m	

Ratios ν(WBr)/ ν(WCl) = 179/270 = 0.66 and 163/228 = 0.71

[a] Nujol mulls

[b] Complex dispersed in polythene

Table 3.8: ^{1}H NMR Data for the Complexes $[(\eta^{3}\text{-}C_3H_5)_2W_2(CO)_4X_2dam]^{*}$ (X = Cl or Br)

Complex	Temp. (°C)	δ (multiplicity, rel. intensity)			
		Allyl Protons			
		H_X	H_M	H_A	Other Protons
XIX	28	1.84(d, 2H)		3.46(m + s, 3H)	2.17(s, 3H) $C_6H_5CH_3$
		J_{XA} 8.4			3.23(s, 2H) $-CH_2-$
					7.27(m, 25H) $C_6H_5CH_3$ + dam C_6H_5
XX	28	1.90(d, 2H)	3.70(s, 2H)	3.72(m, 1H)	2.18(s, 3H) $C_6H_5CH_3$
		J_{XA} 8.3			3.58(s, 2H) $-CH_2-$
					7.34(m, 25H) $C_6H_5CH_3$ + dam C_6H_5

* - As the toluene solvates in $CDCl_3$.

As found for the dae complexes $[(\eta^3\text{-}C_3H_5)W(CO)_2(dae)X]$ the room temperature ^1H NMR spectra of (XIX and XX) showed only two sets of resonances, (relative intensities 2:3), for the protons of the allyl ligand. The methylene protons of the coordinated dam ligand resonated as a singlet at a lower field than that observed for free dam [$\delta(CH_2)$ = 2.62 p.p.m.]. According to Colton and co-workers[294,296] the extent of the downfield shift of this signal is dependent on the mode of coordination of the dam ligand and for compounds containing the same halogen, follows the order monodentate < bridging-bidentate < chelating-bidentate. Typical values for tungsten-chloro compounds are $\sim$ 2.9[294], $\sim$3.5[294] and $\sim$ 4.4[297] p.p.m. respectively.

For tungsten-bromo compounds $\delta(CH_2)$ signals at $\sim$3.0 and $\sim$ 3.8 p.p.m. correlate with dam ligands which are monodentate[294] and bridging-bidentate[294] respectively. In the spectra of (XIX) and (XX) the chemical shifts of the methylene protons at 3.23 and 3.58 p.p.m. respectively are consistent with a bridging mode of coordination for the dam ligand. Colton has also proposed that there is a relationship between the chemical shifts of these methylene protons and the type of halogen coordination in a complex. Since it is not always possible to distinguish between bridging and terminal halogens by infrared spectroscopy, such a correlation is of considerable value. Defining a parameter χ as the difference in position of the methylene resonances of chloro- and iodo-derivatives of a series of compounds, Colton has shown for a number of rhenium[296], manganese[298] and tungsten[296] compounds

that χ is small (< 0.3) when the coordinated halogens are terminal, but much larger (~ 0.8) when they are bridging. The magnitude of χ is reported to be independent of the mode of coordination of dam in the complexes. Unfortunately no data are available for the iodo-analogue of $[(\eta^3\text{-}C_3H_5)_2W_2(CO)_4X_2dam]$, —this species could not be prepared using similar reaction conditions to those employed for the chloro and bromo compounds . Nevertheless it is apparent from the difference in the position of the methylene resonances of (XIX) and (XX) that the value of χ for this pair of compounds is large. The indication is, therefore, that the halogens in (XIX) and (XX) are bridging, as would be anticipated for a situation in which each tungsten(II) atom maintains an eighteen electron configuration. The non-formation of an iodo-analogue may well reflect the weaker bridging capacity of this halide.

The molecular symmetry of the binuclear compounds is dependent on the arrangement of the allyl and carbonyl ligands, and the various possibilities are depicted in Table 3.9. Unfortunately it is not possible to dismiss any of these on the basis of the ^1H NMR spectra since variable temperature studies showed the complexes to be stereochemically non-rigid in solution. Although no new bands were observed over the temperature range +30 to -125°C the sharply defined signals observed at room temperature became broad featureless bands by -40°C. The signals sharpened between -50 and -70°C, but below -80°C became broad again.

Table 3.9: Possible Arrangements of the η^3-allyl[a] and Carbonyl Ligands for the Compounds $[(\eta^3\text{-}C_3H_5)_2W_2(CO)_4X_2dam]$

Ligand Arrangement	Pt. Grp	Predicted No. of Bands ν(M-X)	Predicted No. of Bands ν(C-O)
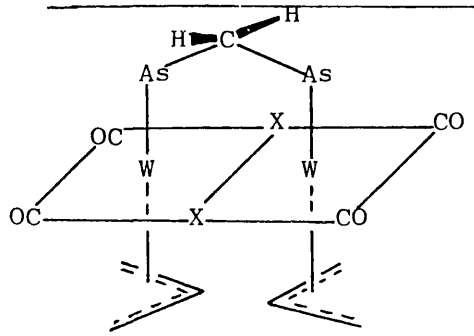	C_{2v}	Infrared Active: $A_1 + B_1 + B_2$ Raman Active: $A_1 + A_2 + B_1 + B_2$	Infrared Active: $A_1 + B_1 + B_2$ Raman Active: $A_1 + A_2 + B_1 + B_2$
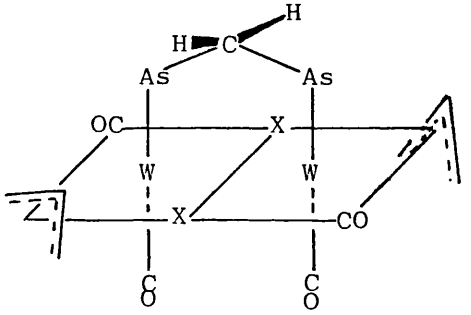	C_2	Infrared & Raman Active: $2A' + 2A''$	Infrared & Raman Active: $2A' + 2A''$
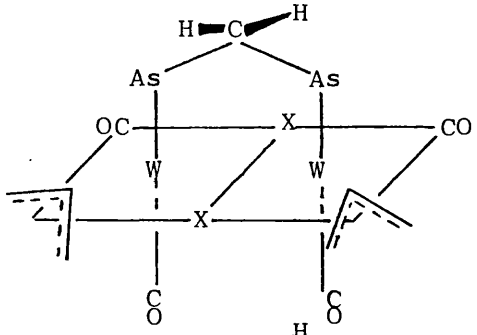	C_s	Infrared & Raman Active: $2A + 2B$	Infrared & Raman Active: $2A + 2B$
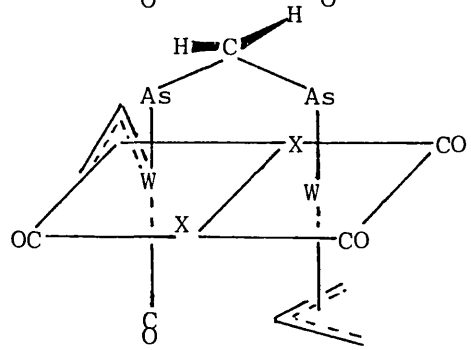	C_1	Infrared & Raman Active: $4A$	Infrared & Raman Active: $4A$

[a] - The allyl groups are depicted lying with their terminal carbon atoms sited above the two cis-carbonyl ligands as generally found for the $[(\eta^3\text{-allyl})M(CO)_2]$ entity (see Introduction p. 69)

Without limiting low temperature spectra it is not possible to draw any conclusions concerning the structure of compounds (XIX) and (XX). The stereochemical non-rigidity of the molecules may be responsible for the apparent equivalence of the two seemingly symmetrical η^3-allyl ligands as well as the observed magnetic equivalence of the two methylene protons of the dam ligand.

The variable temperature ^{1}H NMR studies indicate that at least <u>two</u> dynamic processes occur in these molecules. These could involve a high energy trigonal rotation as proposed to explain the temperature-dependent ^{1}H NMR of $[(\eta^3\text{-}C_3H_5)Mo(CO)_2(pd)py]$[180] and a lower energy trigonal twist as proposed for $[(\eta^3\text{-}C_3H_5)W(CO)_2(dae)X]$, (see earlier). Of course rotation of the η^3-allyl ligand about the tungsten-allyl bond can not be ruled out as a possible mechanism, and the increased broadening of the spectra at very low temperatures could be due to restricted rotation about the arsenic-carbon (aryl) bonds of the bridging diarsine.

Also tabulated in Table 3.9 are the predicted number of ν(M-X) and ν(C-O) bands expected for the various possible isomeric forms of the complexes. From this it is clear that unless the ligand arrangement is as depicted in (i) vibrational studies do not permit an easy distinction between the possible isomeric forms. Nevertheless an infrared study was conducted and the results are summarised in Table 3.7. Nujol mull spectra showed three bands in

the carbonyl stretching region, however, for (XIX) a shoulder on the broad band at highest wavenumber indicated that this band was really composed of two, closely spaced absorptions. Hence the form of the spectra does not allow any of the four possible structures to be ruled out unequivocally, but is consistent with the proposed binuclear formulation. Solution spectra of (XIX) and (XX) recorded in $CHCl_3$ were of poor quality, only two broad bands with half-widths of the order of 30 cm^{-1} were observed. A study of the far-infrared region of the spectra yielded little further information. Due to the large number of ligand bands, it was only possible to identify two halogen-sensitive bands (Table 3.7). These were found at similar frequencies to those of the isoelectronic complexes $[Re_2(CO)_6X_2dam]$[299] and $[(\eta^3\text{-}C_3H_5)_2Mo_2(CO)_4X_2dam]$ (X = Cl, Br)[244]. No absorptions could be confidently assigned as ν(WAs) but three strong bands at ca. 280, 320 and 330 cm^{-1}, in the spectra of both (XIX) and (XX), which are also present in the spectrum of free dam, were assigned to coordinated dam ligand bands.

Chemical Studies.

In order to assess the reactivity of the dam bridged complexes, (XIX) was reacted with other neutral donors. Reaction with pyridine, dpm and dpe resulted in displacement of the diarsine ligand with formation of the mononuclear products $[(\eta^3\text{-}C_3H_5)W(CO)_2L_2Cl]$ (L_2 = dpm, dpe or 2py) in high yields. Spectroscopic data for these products are presented in Table 3.10. The ditertiary phosphine complexes were readily identified by comparison of their

infrared [ν(CO) region] and ^{1}H NMR spectra with literature data[162].

Neither of the ditertiary phosphine ligands was able to simply replace the dam in (XIX) and adopt a bridging mode of coordination. This presumably reflects the stronger chelating character of the ditertiary phosphine ligands[300]. Indeed the inability of one methylene group to easily bridge two large arsenic atoms in chelating dam[301] is most probably responsible for the difference in the nature of the products obtained from reactions of $[(\eta^{3}\text{-}C_3H_5)W(CO)_2(MeCN)_2X]$ (X = Cl, Br) with dam and with the other ditertiary ligands dpe, dpm and dae.

This difference cannot be accounted for in terms of differing M-P and M-As bond strengths[302] (with arsenic being a poorer σ-donor and π-acceptor than P), because dae reacts in an analogous manner to dpe and dpm.

Table 3.10: ^{1}H NMR Data for the Complexes $[(\eta^{3}\text{-}C_3H_5)W(CO)_2L_2Cl]$ (L_2 = dpe, dpm or 2py)*

Complex	δ(multiplicity rel. intensity) Allyl Protons			Other Protons
	H_X	H_M	H_A	
$[(\eta^{3}\text{-}C_3H_5)W(CO)_2(dpe)Cl]$ [a]	1.89(d, 2H)	3.41(qt, 2H)	2.90(m, 1H)	2.46(m, 4H) $-(CH_2)_2-$
	J_{XA} 9.5	J_{MA} 6.0; J_{MP} 3.0		7.50(m, 20H) $-C_6H_5-$
$[(\eta^{3}\text{-}C_3H_5)W(CO)_2(dpm)Cl]$ [a]	1.92(d, 2H)	3.49(qt, 2H)	3.18(m, 1H)	4.56(m, 2H) $-CH_2-$
	J_{XA} 9.0	J_{MA} 6.4; J_{MP} 3.5		7.40(m, 20H) $-C_6H_5-$
$[(\eta^{3}\text{-}C_3H_5)W(CO)_2(py)_2Cl]$ [b]	1.69(br, 2H)	2.59(br, 1H)	2.89(m, 1H)	7.33(dd, 2H) H_2
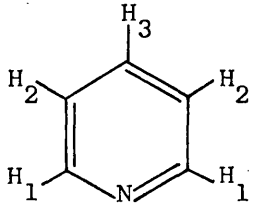		3.71(br, 1H)		7.85(t, 1H) H_3
				J_{23} 8.0
				8.95(d, 2H) H_1
				J_{12} 5.5

* - at 28°C

[a] - in $CDCl_3$

[b] - in CD_2Cl_2

The pyridine complex (XXI) was characterised by analysis, and its solution infrared spectrum showed two strong broad $\nu(CO)$ absorptions of approximately equal intensities at 1923 and 1818 cm^{-1}, consistent with a cis-arrangement of the two carbonyl ligands. The ^{1}H NMR spectrum of (XXI) (at 28°C) showed the ends of the allyl group to be inequivalent. The anti protons (H_X) resonated as a broad band, but two well separated signals (about 1 p.p.m. apart) were observed for the syn protons (H_M). The latter signals showed signs of coalescence at elevated temperatures but a well resolved averaged spectrum was not obtained. Since other workers in our research group[274] are investigating the stereochemical non-rigidity of this and related compounds, further studies were not conducted. Very recently, however, Bevan and Mawby[303] have published their findings on the molybdenum analogue of (XXI) and related compounds containing substituted pyridines. This included a variable temperature ^{1}H and ^{13}C NMR spectral study which showed the inequivalence of the ends of the allyl group, the two carbonyl ligands, and the two pyridine ligands in the limiting low temperature spectra. As the temperature was raised all the pairs of resonances were ultimately replaced by single signals. The most plausible explanation[303] of the observed spectra suggests that these compounds possess a structure without a plane of symmetry, analogous to that of $[(\eta^{3}\text{-}C_3H_5)Mo(CO)_2(dpe)Cl]$ and undergo analogous trigonal twisting motions in solution at ambient temperatures.

The reaction of (XIX) with Ph_4AsCl provided a high yield synthesis of $Ph_4As[(\eta^{3}\text{-}C_3H_5)_2W_2(CO)_4Cl_3]$. In this product the two halogeno-bridges of (XIX) are retained and the bridging dam

ligand is replaced by a third bridging chlorine atom. Spectroscopic data for this compound have already been presented and fully discussed in Chapter 2.

In summary then, it appears that the reactions between the complexes $[(\eta^3\text{-}C_3H_5)W(CO)_2(MeCN)_2X]$ (X = Cl, Br or I) and the ditertiary phosphine ligands dpm and dpe occur in two simple steps; (i) an initial nitrile substitution reaction to give $[(\eta^3\text{-}C_3H_5)W(CO)_2L_2X]$ (L_2 = dpm or dpe) followed by (ii) reductive elimination to form $[W(CO)_2(L_2)_2]$ (L_2 = dpm or dpe). The reactions of the less nucleophilic ditertiary arsines dae and dam resulted in the formation of the tungsten(II) species only i.e. $[(\eta^3\text{-}C_3H_5)W(CO)_2(dae)X]$ (X = Cl, Br or I) and $[(\eta^3\text{-}C_3H_5)_2W_2(CO)_4X_2dam]$ (X = Cl or Br), with no evidence for the formation of tungsten(O) species, even under forcing conditions.

CHAPTER FOUR

THE REACTIONS OF PHOSPHITE LIGANDS WITH $[(\eta^3\text{-}C_3H_4R)M(CO)_2(MeCN)_2X]$

INTRODUCTION

This chapter describes an investigation into the reactivity of a number of phosphite ligands with the compounds $[(\eta^3\text{-}C_3H_4R)M(CO)_2(MeCN)_2X]$ (R = H, M = Mo or W, X = Cl, Br or I; R = Me, M = Mo, X = Cl). A series of complexes $[(\eta^3\text{-}C_3H_4R)M(CO)_2\{P(OR')_3\}_2X]$ have been prepared and found to be stereochemically non-rigid in solution. A detailed examination of their NMR spectra was carried out together with a three-dimensional X-ray crystallographic study of a representative member of the series, namely $[(\eta^3\text{-}C_3H_5)Mo(CO)_2\{P(OMe)_3\}_2Cl]$. This compound has been shown to be of a structural type not previously found for this class of d^4 M(II) compounds.

EXPERIMENTAL

Details of physical techniques and solvents appear in appendix 3. The methods used for the preparation of the starting materials $[(\eta^3\text{-}C_3H_4R)M(CO)_2(MeCN)_2X]$ (R = H, M = Mo or W, X = Cl, Br or I; R = Me, M = Mo, X = Cl) are described in Chapter 1.

The phosphites $P(OMe)_3$, $P(Oi\text{-}Pr)_3$, $P(OEt)_3$ and $P(OPh)_3$ were obtained from commercial sources and were purified before use. $P(OMe)_3$, $P(Oi\text{-}Pr)_3$ and $P(OPh)_3$ were stored over lead-sodium alloy for one week before being fractionally distilled from fresh alloy and then stored over molecular sieves type 4A. The purity of $P(OEt)_3$ was of crucial importance in the reactions described below, and it was found to be imperative to fractionally distil samples of this phosphite at least twice, immediately before use.

Preparation of $[(\eta^3\text{-}C_3H_4R)M(CO)_2\{P(OR')_3\}_2X]$

The complexes $[(\eta^3\text{-}C_3H_4R)M(CO)_2\{P(OR')_3\}_2X]$ (R = H, M = Mo, R' = Me, X = Cl, Br or I; R = H, M = Mo, R' = Et, X = Cl or I; R = H, M = Mo, R' = Pr^i, X = Cl; R = Me, M = Mo, R' = Me, X = Cl; R = H, M = W, R' = Me or Et, X = Cl) were prepared by the direct reaction of $P(OR')_3$ with $[(\eta^3\text{-}C_3H_4R)M(CO)_2(MeCN)_2Cl]$; a typical procedure is given below.

A solution of $[(\eta^3\text{-}C_3H_5)Mo(CO)_2(MeCN)_2Cl]$ (1.0 mmol, 0.31 g) dissolved in $(CH_3)_2CO$ (10 cm^3) was treated with $P(OMe)_3$ (2.0 mmol 0.21 cm^3) at room temperature. After 1h the solution was reduced to low bulk in vacuo. The precipitated product was filtered off,

washed with a little cold $(CH_3)_2CO$ (-20°C), and dried *in vacuo*.

The $P(OEt)_3$ and $P(Oi\text{-}Pr)_3$ complexes crystallised with difficulty and an alternative isolation technique was used. After a reaction time of 1h, the solvent was completely removed and the residue evacuated for 2h. The product was then recrystallised from cold $(CH_3)_2CO$ (-30°C/12h), collected by filtration and washed as above.

The compounds $[(\eta^3\text{-}C_3H_4R)M(CO)_2\{P(OR')_3\}_2X]$ were all obtained as yellow-orange crystals which were soluble in most polar solvents $CHCl_3$, CH_2Cl_2, $(CH_3)_2CO$, benzene, ether .

Preparation of $[(\eta^3\text{-}C_3H_4R)Mo(CO)_2\{P(OMe)_3\}_3]BF_4$

The salt $AgBF_4$ (1mmol, 0.19g) was added to a solution of $[(\eta^3\text{-}C_3H_4R)Mo(CO)_2(MeCN)_2Cl]$ (1mmol) in $(CH_3)_2CO$ (20 cm^3). The mixture was stirred for 10 mins then filtered into a solution of $P(OMe)_3$ (1.5mmol, 0.15 cm^3) in $(CH_3)_2CO$ (5 cm^3). After 0.5h at room temperature, the solution was evaporated at reduced pressure to a volume of *ca*. 6cm^3 and treated dropwise with ether to initiate precipitation of a yellow powder. The product was filtered off and recrystallised from $CHCl_3$-ether, to produce pale yellow crystals.

Details of the yields, elemental analyses and melting points for individual phosphite complexes are presented in Table 4.1.

Structure Determination

A sample of $[(\eta^3\text{-}C_3H_5)Mo(CO)_2\{P(OMe)_3\}_2Cl]$ (XXII), was recrystallised twice from $(CH_3)_2CO$ at -20^oC to provide crystals suitable for an X-ray single crystal structure determination. A crystal with approximate dimensions 0.4 x 0.3 x 0.2mm was mounted with a* parallel to the instrument axis of a General Electric XRD 5 diffractometer which was used to measure diffraction intensities and unit-cell dimensions. The apparatus was equipped with a manual goniostat, scintillation counter, and pulse-height analyser. Zirconium-filtered X-radiation was used. 2,135 independent reflections with $2\theta < 40^o$ were measured using the stationary-crystal-stationary- counter method, a take off angle of 4^o and a counting time of 10s. Of these reflections 1,534 with $I > 3\sigma(I)$ were used in subsequent refinement. Individual backgrounds were taken for those reflections whose counts were seriously affected by the streaking of other orders. For other reflections, backgrounds were taken from plots of background as a function of 2θ. Several standard reflections monitored during the course of the experiment showed no significant changes in intensities. Neither an absorption nor an extinction correction was applied.

Crystal data: $C_{11}H_{23}ClMoO_8P_2$, M = 476.5, Triclinic, a = 13.309(11), b = 10.093(10), c = 8.148(7) Å, α = 114.9(8), β = 93.1(7), γ = 100.6(7)°, U (volume of unit cell) = 965.1 Å^3, D_m ✓ = 1.64g cm^{-3}, Z (number of molecules in the unit cell) = 2, D_c = 1.64g cm^{-3}, F(000) (number of electrons in the unit cell) = 484,

✓ D_m = density of a crystal of $[(\eta^3\text{-}C_3H_5)Mo(CO)_2\{P(OMe)_3\}_2Cl]$ determined by the floatation method using dibromoethane and n-heptane respectively, as the more and less dense liquids.

λ(Mo - K_α) = 0.710 7 Å, μ(Mo - K_α) = 10.0 cm^{-1}, space group $P\bar{1}$ from the successful structure determination.

Solution and Refinement

The positions of the molybdenum atoms were obtained from the Patterson map and the positions of remaining atoms were found by Fourier analysis. The hydrogen-atom positions of the η^3-allyl and methyl group hydrogen-atoms could not be calculated. Although some were observed in a difference Fourier analyses refinement was not successful and they were therefore not included in the final refinement. All the other atoms were given anisotropic thermal parameters and the structure was refined by full-matrix least squares to R = 0.072. The weighting scheme used was $\underline{w}^{\frac{1}{2}} = 1$ for $\underline{F}_o < 40$ and $\underline{w}^{\frac{1}{2}} = 40/\underline{F}_o$ for $\underline{F}_o > 100$.

Calculations were done using SHELX 76[304] at the University of London Computer Centre. Scattering factors and dispersion corrections were taken from reference 305. The final difference-Fourier map showed no unusual features. In the final cycle of refinement all shifts were less than 0.05 σ. The final list of atomic positions is given in Table 4.2 and the bond lengths and angles appear in Table 4.3. A list of the structure factors, together with thermal parameters, are given in Appendix 4.

Table 4.1: Yields, Melting Points and Analytical Data

Compound (No.)	Yield (%)	M.Pt (^{o}C)	Elemental Analysis found (calc.) (%) C	H
$[(\eta^3\text{-}C_3H_5)Mo(CO)_2\{P(OMe)_3\}_2Cl]$ (XXII)	58	76-78	27.5	4.8
			(27.2)	(4.9)
$[(\eta^3\text{-}C_3H_5)Mo(CO)_2\{P(OMe)_3\}_2Br]$ (XXIII)	51	85-88	25.4	4.5
			(25.5)	(4.5)
$[(\eta^3\text{-}C_3H_5)Mo(CO)_2\{P(OMe)_3\}_2I]$ (XXIV)	88	77-79	23.2	4.0
			(23.3)	(4.1)
$[(\eta^3\text{-}2\text{-}MeC_3H_4)Mo(CO)_2\{P(OMe)_3\}_2Cl]$ (XXV)	38	95-97	29.2	5.1
			(29.4)	(5.1)
$[(\eta^3\text{-}C_3H_5)Mo(CO)_2\{P(OEt)_3\}_2Cl]$ (XXVI)	46	38-41	35.1	6.1
			(36.4)	(6.3)
$[(\eta^3\text{-}C_3H_5)Mo(CO)_2\{P(OEt)_3\}_2I]$ (XXVII)	50	46-48	31.4	5.4
			(31.3)	(5.4)
$[(\eta^3\text{-}C_3H_5)Mo(CO)_2\{P(Oi\text{-}Pr)_3\}_2Cl]$ (XXVIII)	54	58-60[a]	42.7	7.3
			(42.8)	(7.4)
$[(\eta^3\text{-}C_3H_5)W(CO)_2\{P(OMe)_3\}_2Cl]$ (XXIX)	57	95-97	23.2	4.1
			(23.4)	(4.1)
$[(\eta^3\text{-}C_3H_5)W(CO)_2\{P(OEt)_3\}_2Cl]$ (XXX)	51	49-52	31.5	5.2
			(31.5)	(5.4)
$[(\eta^3\text{-}C_3H_5)Mo(CO)_2\{P(OMe)_3\}_3]BF_4$ (XXXI)	72	104[b]	25.7	5.0
			(25.8)	(5.0)
$[(\eta^3\text{-}2\text{-}MeC_3H_4)Mo(CO)_2\{P(OMe)_3\}_3]BF_4$ (XXXII)	71	79-82	26.1	5.0
			(27.1)	(5.2)

[a] - melted with decomposition

[b] - decomposition point

RESULTS AND DISCUSSION

Treatment of the molybdenum or tungsten-nitrile starting materials $[(\eta^3\text{-}C_3H_4R)M(CO)_2(MeCN)_2X]$ with the tertiary alkyl phosphites $P(OR')_3$ (R' = Me, Et or i-Pr) yielded a series of substituted complexes $[(\eta^3\text{-}C_3H_4R)M(CO)_2\{P(OR')_3\}_2X]$. Of these, the $P(OMe)_3$ derivatives were by far the most stable and could be stored quite successfully for several months under nitrogen in light protected ampoules. The $P(OEt)_3$ and $P(Oi\text{-}Pr)_3$ compounds were particularly unstable and decomposed rapidly (even at low temperatures under nitrogen in the dark) to form black oils which smelt strongly of phosphite.

The high solubility of the compounds in polar solvents made their isolation from the reaction mixtures extremely difficult (particularly for the $P(OEt)_3$ and $P(Oi\text{-}Pr)_3$ species). Several methods to induce crystallisation were tried. Careful addition of precipitants such as pentane and diethyl ether, produced intractable oils despite prolonged scratching. A common cause of such difficulties is the presence of free phosphite in the reaction mixture, the oily constituency of which inhibits the formation of solids. Attempts to remove such impurities by chromatography using alumina, silica and fluorosil plus a large variety of solvent systems were undertaken but were unsuccessful. Eventually however, it was found that prolonged evacuation of the reaction mixture, so removing all volatile materials, had the desired effect, for after such a work-up recrystallisation of the products from a little cold $(CH_3)_2CO$ (-18^oC) was almost always possible.

The formation of $[(\eta^3\text{-}C_3H_4R)M(CO)_2\{P(OR')_3\}_2X]$ appeared to be virtually instantaneous, this was indicated by the immediate colour, and $\nu(CO)$ changes observed when the reagents were mixed together. No significant difference in the rates of formation of analogous molybdenum and tungsten compounds was noted. The best yields of (XXII-XXX) were obtained using an $(CH_3)_2CO$ reaction medium, (as described in the Experimental section) but the same products were also isolable from reactions in CH_3OH or CH_3CN (yields 20-30%). In contrast to the reactions of $[(\eta^3\text{-}C_3H_5)M(CO)_2(MeCN)_2X]$ with the tertiary phosphines PR_3 (R = n-Bu or Ph) which readily break the metal-allyl linkage to form allylphosphonium salts[249,251], there was no evidence of nucleophilic attack by any of the phosphites on the η^3-allyl ligand, even at elevated temperatures in the presence of excess phosphite.

Several attempts were made to prepare the $P(OPh)_3$ analogues of compounds (XXII-XXX). However, reactions between $[(\eta^3\text{-}C_3H_5)M(CO)_2(MeCN)_2X]$ and $P(OPh)_3$ in mole ratios ranging from 1:2 to 1:10 in a variety of solvents [$CHCl_3$, $(CH_3)_2CO$, CH_3CN], at both ambient and elevated temperatures, gave no indication of the formation of any new cis-dicarbonyl M(II) or M(0) species. After prolonged reaction times extensive decomposition and disproportionation of the nitrile starting materials was observed: in the reactions with $[(\eta^3\text{-}C_3H_5)Mo(CO)_2(MeCN)_2I]$ for example, there was evidence for the formation of $Mo(CO)_6$ [$\nu(CO)$ 1980cm^{-1}] and cis-$[Mo(CO)_4\{P(OPh)_3\}_2]$ [$\nu(CO)$ 2044w, 1962s, 1930s][306]. The non-formation of $P(OPh)_3$ analogues of (XXII-XXX) can be rationalised in terms of the poorer nucleophilicity of this reagent.

The complexes $[(\eta^3\text{-}C_3H_4R)M(CO)_2\{P(OR')_3\}_2X]$ were characterised by their infrared and NMR spectra. During these studies variable temperature multinuclear NMR spectra were obtained which showed the complexes to be fluxional in solution at or above room temperature, but in all instances stereochemically rigid below -40°C. The limiting low temperature NMR spectra were inconsistent with the complexes adopting pseudo-octahedral type geometries as found for all other $[(\eta^3\text{-}C_3H_5)M(CO)_2L_2L']$ complexes. Hence in order to elucidate the molecular configuration of these complexes a crystal structure determination of a representative member, namely $[(\eta^3\text{-}C_3H_5)Mo(CO)_2\{P(OMe)_3\}_2Cl]$ (XXII), was undertaken.

Solid-State Structure of $[(\eta^3\text{-}C_3H_5)Mo(CO)_2\{P(OMe)_3\}_2Cl]$ (XXII)

The molecular structure of the title compound described in this section was determined in collaboration with Dr. M.G.B. Drew at the University of Reading.

The structure of (XXII) consists of discrete molecules of $[(\eta^3\text{-}C_3H_5)Mo(CO)_2\{P(OMe)_3\}_2Cl]$ separated by the usual van der Waals contacts. A diagrammatic view of the structure with the atomic numbering scheme is shown in Figure 4.1. The structure has C_s symmetry within experimental error, with the mirror plane containing the metal atom, both carbonyl groups, the chlorine atom and the central carbon atom of the allyl group. The geometry of (XXII) is best considered in terms of a pentagonal bipyramid with the chlorine atom Cl(1) and a carbonyl carbon atom C(4)

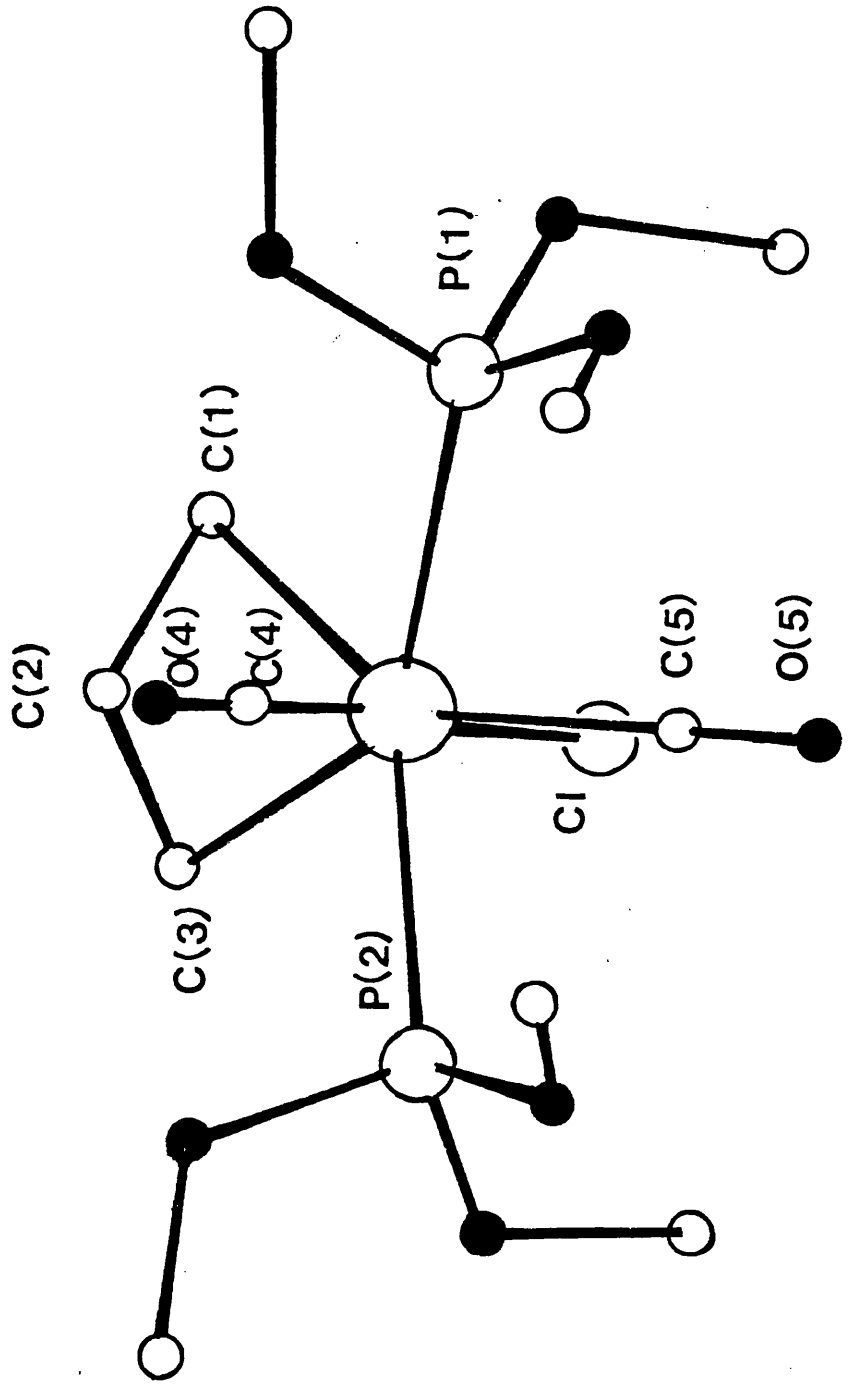

Figure 4.1: The Molecular Structure of $[(\eta^3\text{-}C_3H_5)Mo(CO)_2\{P(OMe)_3\}_2Cl]$.

in axial positions [Cl(1)-Mo-C(4) 178.3(6)°], and the allyl ligand occupying two adjacent sites in the equatorial girdle. Thus the allyl group can be regarded as a bidentate ligand with a small normalised bite[/] of 1.02. The structural type of (XXII) is in fact one of the two low energy alternatives predicted by repulsive energy calculations[307] for complexes of the type [M(bidentate)(unidentate)$_5$] containing bidentates with small normalised bites (below 1.1). The distribution of ligands between equatorial and axial sites of the pentagonal bipyramid however, appears to be inconsistent with molecular orbital predictions for ML_7 complexes[308] which suggest that strong π-acceptors such as carbon monoxide should preferably occupy axial sites and strong π-donors such as chlorine, equatorial sites. Obviously in this instance other effects, such as the σ-properties of the ligands and their steric requirements, are also important in determining the ligand distribution.

The root mean square (r.m.s.) deviation[309] of the coordination sphere of (XXII) from the ideal pentagonal bipyramid is large (0.16Å) indicating severe distortion; however, the deviation from other ideal seven-coordinate polyhedra is considerably larger. The distortions of (XXII) from an ideal pentagonal bipyramid are indicated by the angles subtended by the Mo-Cl(1) bond with Mo-C(5), Mo-C(1) and Mo-C(3) which are 78.0(6), 80.0(6) and 80.5(6)°, and with Mo-P(1) and Mo-P(2) which are 100.8(2)

[/] The "normalised bite", b, of a bidentate ligand is defined as the distance between the donor atoms of the chelate ring divided by the metal-ligand distance.

Table 4.2: Atomic Coordinates ($\times 10^4$) with Estimated Standard Deviations in Parentheses

Atom	X	Y	Z
Mo(1)	7735(1)	7758(2)	5076(2)
Cl(1)	6608(5)	7308(8)	7391(8)
P(1)	7504(4)	10212(6)	5506(8)
P(2)	7583(4)	5165(6)	2912(7)
O(21)	7174(12)	3821(16)	3461(21)
O(22)	8708(11)	4835(17)	2391(20)
O(23)	6845(11)	4488(17)	981(20)
C(21)	6063(20)	3470(32)	3723(42)
C(22)	8795(19)	3308(28)	1026(33)
C(23)	6909(21)	5214(31)	-264(25)
O(11)	8578(11)	11294(16)	5682(21)
O(12)	7040(13)	11218(17)	7264(20)
O(13)	6729(12)	10284(16)	3961(20)
C(11)	8623(21)	12925(29)	6107(37)
C(12)	5986(18)	10733(28)	7592(36)
C(13)	6915(22)	9804(31)	2101(36)
C(1)	8816(18)	9499(27)	7906(30)
C(2)	9312(20)	8348(34)	6946(35)
C(3)	8898(19)	6856(32)	6501(35)
C(4)	8562(18)	8027(21)	3342(30)
O(4)	9095(14)	8195(20)	2283(25)
C(5)	6278(22)	7219(24)	3727(28)
O(5)	5467(15)	6924(20)	3098(26)

Table 4.3: Interatomic Distances (Å) and Angles (°) with Standard Deviations in Parentheses

Mo(1) - Cl(1)	2.606(6)
Mo(1) - P(1)	2.432(6)
Mo(1) - P(2)	2.425(6)
Mo(1) - C(1)	2.403(20)
Mo(1) - C(2)	2.347(24)
Mo(1) - C(3)	2.407(22)
Mo(1) - C(4)	1.914(25)
Mo(1) - C(5)	2.035(27)
P(1) - O(11)	1.589(15)
P(1) - O(12)	1.603(16)
P(1) - O(13)	1.618(16)
P(2) - O(21)	1.632(16)
P(2) - O(22)	1.613(15)
P(2) - O(23)	1.609(15)
O(21) - C(21)	1.504(28)
O(22) - C(22)	1.503(29)
O(23) - C(23)	1.479(28)
O(11) - C(11)	1.521(30)
O(12) - C(12)	1.475(28)
O(13) - C(13)	1.435(31)
C(1) - C(2)	1.403(36)
C(2) - C(3)	1.384(37)
C(4) - O(4)	1.192(26)
C(5) - O(5)	1.099(25)

...../contd.

Table 4.3 (cont'd)

Cl(1) - Mo(1) - P(1)	100.79(21)
Cl(1) - Mo(1) - P(2)	98.71(21)
P(1) - Mo(1) - P(2)	146.12(20)
Cl(1) - Mo(1) - C(1)	80.0(6)
P(1) - Mo(1) - C(1)	75.0(6)
P(2) - Mo(1) - C(1)	135.9(6)
Cl(1) - Mo(1) - C(2)	94.5(6)
P(1) - Mo(1) - C(2)	102.6(7)
P(2) - Mo(1) - C(2)	103.2(7)
C(1) - Mo(1) - C(2)	34.3(8)
Cl(1) - Mo(1) - C(3)	80.5(6)
P(1) - Mo(1) - C(3)	135.4(6)
P(2) - Mo(1) - C(3)	75.1(6)
C(1) - Mo(1) - C(3)	61.2(8)
C(2) - Mo(1) - C(3)	33.8(8)
Cl(1) - Mo(1) - C(4)	178.3(6)
P(1) - Mo(1) - C(4)	80.9(5)
P(2) - Mo(1) - C(4)	79.6(5)
C(1) - Mo(1) - C(4)	100.9(8)
C(2) - Mo(1) - C(4)	85.6(9)
C(3) - Mo(1) - C(4)	98.7(9)
Cl(1) - Mo(1) - C(5)	78.0(6)
P(1) - Mo(1) - C(5)	78.8(6)
P(2) - Mo(1) - C(5)	78.5(6)
C(1) - Mo(1) - C(5)	141.8(9)

...../cont'd.

Table 4.3 (contd)

C(2) - Mo(1) - C(5)	172.5(9)
C(3) - Mo(1) - C(5)	142.7(9)
C(4) - Mo(1) - C(5)	101.9(8)
Mo(1) - P(1) - O(11)	111.1(5)
Mo(1) - P(1) - O(12)	119.8(6)
Mo(1) - P(1) - O(13)	117.7(5)
O(11) - P(1) - O(12)	102.2(8)
O(11) - P(1) - O(13)	106.0(8)
O(12) - P(1) - O(13)	97.9(8)
Mo(1) - P(2) - O(21)	111.5(5)
Mo(1) - P(2) - O(22)	120.7(6)
Mo(1) - P(2) - O(23)	119.3(6)
O(21) - P(2) - O(22)	99.7(8)
O(21) - P(2) - O(23)	105.1(8)
O(22) - P(2) - O(23)	97.7(8)
P(2) - O(21) - C(21)	120.7(13)
P(2) - O(22) - C(22)	119.8(13)
P(2) - O(23) - C(23)	123.2(14)
P(1) - O(11) - C(11)	119.8(13)
P(1) - O(12) - C(12)	122.2(14)
P(1) - O(13) - C(13)	122.4(15)
Mo(1) - C(1) - C(2)	70.7(13)
Mo(1) - C(2) - C(1)	75.0(13)
Mo(1) - C(2) - C(3)	75.4(14)
C(1) - C(2) - C(3)	122.8(25)
Mo(1) - C(3) - C(2)	70.7(13)
Mo(1) - C(4) - O(4)	178.7(18)
Mo(1) - C(5) - O(5)	175.4(20)

and 98.7(2)°. Calculation of the least squares plane through the pentagonal girdle shows a maximum deviation of 0.57Å for an atom from the six-atom plane [plane (1) in Table 4.4]. A major cause of these distortions is the position of the bulky $P(OMe)_3$ ligands with their "propeller" type configurations in the crowded equatorial girdle. This becomes apparent if one considers the proximity of the methoxy groups to other ligands in the complex. Plane (2) in Table 4.4 shows that Mo, P(1), P(2), C(1) and C(3) are almost coplanar - the maximum deviation of any of these atoms from this plane being 0.17Å. However, the atom which completes the pentagonal girdle, C(5), is more than 1Å distant from this plane. The position of C(5) is undoubtedly determined by the positions of the methoxy groups, for if it were to lie in plane (2) it would be involved in impossibly short contacts with O(13) and O(23). By C(5) moving out of this plane much more realistic C(5).....O(n3) distances of 2.96(n = 1) and 2.99Å (n = 2) are obtained.

Table 4.4: Least Squares Planes with Deviations (Å) of Atoms from the Planes.

[Atoms not contributing to the planes are marked with an asterisk]

Plane (1): Mo - 0.05, P(1) - 0.42, P(2) - 0.39, C(1) 0.17 C(3) 0.12, C(5) 0.57, C(2)* - 0.47

Plane (2): Mo - 0.17, P(1) 0.08, P(2) 0.05, C(1) - 0.01, C(3) 0.05, Cl(1)* - 2.67, C(2)* 0.68, C(4)* 1.67, C(5)* - 1.14, O(23)* 0.09, O(13)* 0.09

Plane (3): Mo, C(1), C(3) 0.00, P(1)* 0.36, (P2)* 0.22, C(5)* - 0.80, C(2)* 0.64

Angles between the allyl group C(1), C(2), C(3) and planes 1 and 2 are 68.0 and 78.7° respectively.

The dihedral or allyl tilt angle χ [as defined in Chapter 1 p. 24] is 112° which agrees well with those of other η^3-allyl complexes [see Table 1.1 p. 25].

A study of torsion angles of the type L - Mo - P - O reveals why the orientation of the phosphites is such that O(13) and O(23) lie so close to C(5) and the equatorial girdle. The six C(1) - Mo - P(1) - O(1m) and C(3) - Mo - P(2) - O(2m) angles (m = 1 to 3) are all within 6^{o} of 60, -60 or 180^{o} showing that the P -O bonds are staggered with respect to the allyl group. Such a conformation obviously maximises OMe contacts with the allyl hydrogen atoms (see Figure 4.2). As a consequence the P - O bonds are also staggered with respect to the Mo - C(4) bond, but not to the Mo - Cl(1) or Mo - C(5) bonds. The smallest torsion angles involving these latter two bonds are Cl(1) - Mo - P(n) - O(n2) 15.3, -15.9^{o} for n = 1,2 and C(5) - Mo - P(n) - O(n2) -28.1, 29.1^{o} for n = 1,2. As shown in Figure 4.2, the O(n1) atoms are not involved in close contacts with either Cl(1) or C(5). This is clearly reflected in the Mo - P(n1) - O(n1) angles which are considerably less (by an average of 8.1^{o}) than the Mo - P(n2) - O(n2) and Mo - P(n3) - O(n3) angles.

The distortion in the pentagonal plane results in the axial atoms Cl(1) and C(4) moving out of the perpendicular with respect to the girdle plane (Figure 4.2). The Cl(1) - Mo - C(4) angle at 178.3^{o} is however only slightly reduced from the ideal <u>trans</u> angle of 180^{o}. Cl(1) - Mo - P(n) angles at 100.8(2) and $98.7(2)^{o}$ are larger than the 90^{o} expected for an ideal pentagonal bipyramid, but serve to ensure that the small torsion angles Cl(1) - Mo - P(n) - O(n2) do not lead to short Cl.....O distances. Also instrumental in this is the length of the Mo - Cl(1) bond which at 2.606(6)Å is on average about 0.08Å longer than similar bonds in other molybdenum(II) seven-coordinate systems[309].

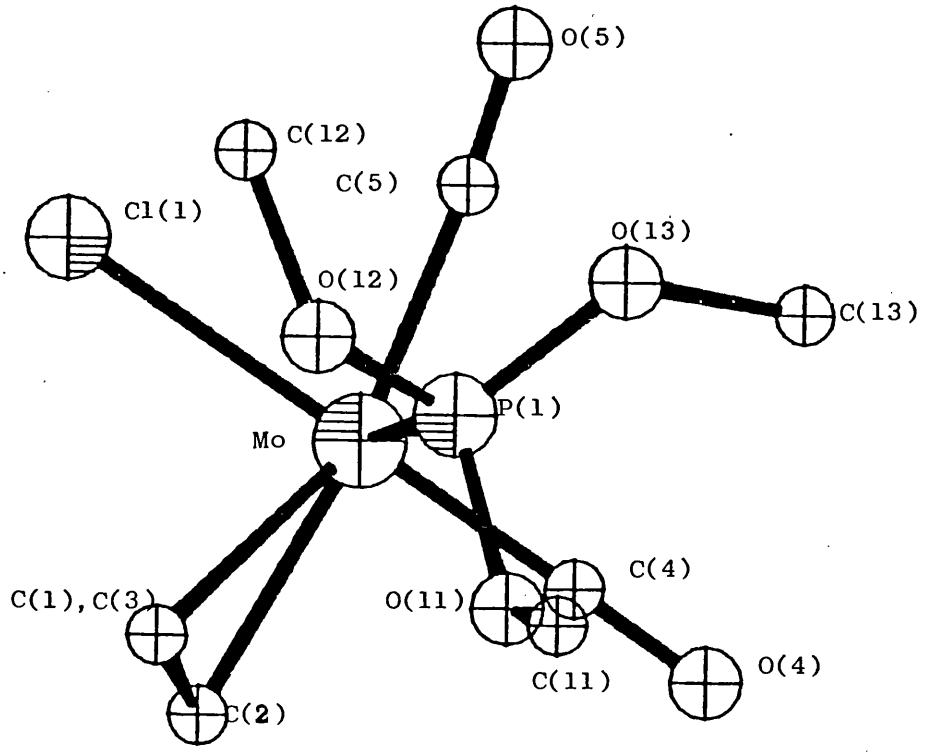

Figure 4.2: Disposition of the trimethylphosphite groups

The figure above shows a projection of (XXII) onto the approximate mirror plane through atoms Mo, Cl(1), C(4), O(4), C(5), O(5) and C(2). In this projection C(1) and C(3) are coincident as are the two trimethylphosphite groups. The disposition of the -OMe groups maximises O.....H_{allyl} contacts.

The carbonyl ligands in (XXII) are essentially linear and the Mo - C(y) - O(y) angles of 178.7(18) and 175.4(20)° for y = 4 and 5 are quite normal for such systems.[310-313] The Mo - C (carbonyl) bond lengths [1.914(25), 2.035(27)] and the C - O (carbonyl) bond lengths [1.192(26), 1.099(25)] are also both within the range of values reported for other molybdenum carbonyl complexes[235,310-313]. However, the difference in the two Mo - C (carbonyl) bond lengths (ca. 0.12Å) with Mo - C(5) > Mo - C(4) is too large to be attributable to the fact that one of the carbonyls [C(4) - O(4)] occupies an axial site whilst the other occupies an equatorial site[309], and must therefore reflect the greater degree of π-bonding between the metal and C(5). The Mo - P (phosphite) bond lengths [2.432(6), 2.425(6)Å] may be compared with similar distances in $[HMo\{P(OCH)_3\}_4(O_2CCF_3)]$[314] [Mo - P average = 2.36Å], $[CpMo(CO)_2\{P(OMe)_3\}I]$ [2.406(9)Å][315] and $[Mo_2(CO)_2\{P(OMe)_3\}(\mu_2\text{-}SBu^t)_3(\eta^7\text{-}C_7H_7)]$ [2.445(2)Å][316].

The Mo - C(allyl) bond lengths [2.403(20), 2.347(24), 2.407(22)Å] and allyl C - C distances [1.403(36), 1.384(37)Å] which characterise the allyl group as a symmetrically bonded trihapto ligand show little deviation from the average values of twenty-one other complexes containing the [Mo(II) - η^3-allyl] entity, (see Table 1.8 p. 70) except that the Mo - C(1) and Mo - C(3) bonds are ca. 0.1Å longer, and the intercarbon angle of the allyl [122.8(25)°] is larger than that normally encountered. These differences are probably due to the allyl ligand in (XXII) attempting to maximise its bonding overlap with the sp^3d^3 hybrid orbitals of the metal.

Crystallographic parameters for (XXII) which define the position and orientation of the allyl group, relative to other substituents, are radically different to those of other compounds of the type $[(\eta^3\text{-allyl})Mo(CO)_2L_2L']$. For instance, in all other structures the plane of the η^3-allyl group is always approximately parallel to a plane containing the metal and four donor atoms. Mainly because of this, the geometry of these formally seven-coordinate molecules, [probably best described in terms of a capped trigonal prism (see Chapter 1 p. 68)], is often considered in terms of a pseudo-octahedron in which the allyl group occupies a single coordination site. A plane through the metal and the two terminal allylic carbon atoms falls close to just one other donor atom, that trans to the allyl group, for example in $[(\eta^3\text{-}C_3H_5)Mo(CO)_2(pd)py]$[180] the trans atom is 0.08Å away from this plane whilst the other four donor atoms are more than 1.45Å distant. By contrast in (XXII), as shown in Table 4.4 (plane 3), both phosphorus atoms are close to the plane of Mo, C(1) and C(3) whilst C(5) is also within 1Å. Thus unlike previous structures it is difficult to describe the geometry of (XXII) in terms of a pseudo-octahedron, nevertheless doing so does serve to illustrate the uniqueness of the ligand arrangement in (XXII) (see Figure 4.3). Details of the earlier structures referred to above have been given previously in Chapter 1 (p. 70) and the striking constancy of the $[(\eta^3\text{-allyl})Mo(CO)_2]$ unit with its fac-octahedral arrangement of the carbonyl and allyl ligands, was also emphasised at that point. It is clear that such an arrangement is absent in (XXII) where the CO - Mo - CO angle is over 100°.

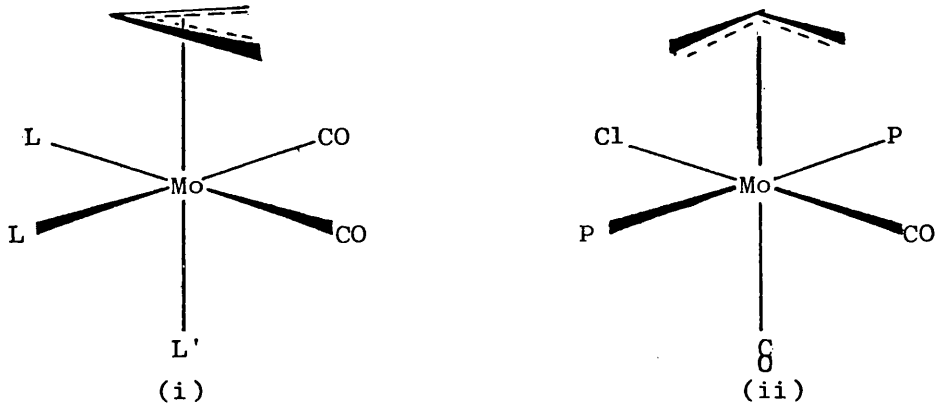

Figure 4.3: Ligand arrangements (i) commonly observed for compounds of the type $[(\eta^3\text{-allyl})Mo(CO)_2L_2L']$ and (ii) found for $[(\eta^3\text{-}C_3H_5)Mo(CO)_2\{P(OMe)_3\}_2Cl]$. (For comparison purposes both structures are presented as pseudo-octahedra).

Exactly why (XXII) should adopt a solid state configuration which is evidently so unique is not easily explained since the arrangement of a set of ligands around a central metal atom is dictated by several factors. Included in these and of considerable importance, is the steric requirements of the ligands involved. It is clear that if (XXII) were to possess the usual pseudo-octahedral geometry, two bulky $P(OMe)_3$ ligands would be forced to occupy cis-positions. It could be argued that such a geometry for (XXII) is not impossible since it is adopted by $[(\eta^3\text{-}C_3H_5)Mo(CO)_2(dpe)Cl]$[171] in which the cone angle of the phosphorus ligand (128^o) is considerably larger than that of $P(OMe)_3$ (107^o)[317]. However, the "cone angle"

concept takes no account of the fact that the two phosphorus donor units in dpe are linked by a common substituent and that consequently steric interactions between the substituents of the two cis-phosphorus donors in $[(\eta^3\text{-}C_3H_5)Mo(CO)_2(dpe)Cl]$ are absent. The presence of a chelating ligand such as dpe must also introduce substantial constraints on the possible structure and stereochemistry of the compound. In this respect it should be noted that with only two exceptions[240,241] all previous structure determinations on this class of complex have been carried out on molecules containing bi- or tri-dentate ligands (see Table 1.8 p. 70) which prevent formation of a structure analogous to (XXII).

The electronic properties of ligands may also influence geometry and stereochemistry. This has already been demonstrated in the fac-octahedral structures where complexes with bidentate ligands possessing appreciable π-acceptor abilities assumed stereochemistries which reduced competition between π-acceptors (see Chapter 1 p. 72). The π-acceptor capacity of $P(OMe)_3$ is considerable[56]. Thus the siting of at least one of these ligands trans to a carbonyl group, as would be inevitable if (XXII) were to adopt a pseudo-octahedral configuration, is probably also instrumental in favouring the pentagonal bipyramidal structure in which any such direct competition between π-acceptors is avoided.

Table 4.5: Selected Infrared Data for the Complexes $[(\eta^3\text{-}C_3H_4R)M(CO)_2\{P(OR')_3\}_2X]$

Complex Number	ν(CO) solid (cm^{-1})[a,b] 2A'	ν(^{13}CO)	$\frac{\nu(^{13}CO)}{\nu(^{12}CO)}$	ν(CO) solution (cm^{-1})[a,c] 2A'	others	$M(CO)_2$ Angle (^{o})[d]	ν(MX)[e] (cm^{-1})
XXII	1984	1942w	0.979	1985	1960m	109	237vs
	1854	1820m,(sh)	0.982	1860			
XXIII	1981	1940w	0.979	1985	1953m	108	151s
	1862	1820m,(sh)	0.977	1955			
XXIV	1979	1940w	0.980	1985	1960m,(sh)	113	102m
	1849	1820m,(sh)	0.984	1960			
XXV	1980	1942w	0.980	1992		110	239vs
	1849	1817w	0.983	1847			
XXVI	1977 }	1938m,(sh)		1985	1960m,(sh)	103	232vs
	1963 }						
	1850 }	1818m,(sh)		1856			
	1840 }						
XXVII	1979br			1983 br,m		110	108m
	1848br			1859 br,m			
XXVIII	1962 }	1930w,(sh)		1967	1936m,(sh)	105	233m
	1946 }						

..../contd.

Table 4.5: (Cont'd)

Complex Number	ν(CO) solid (cm^{-1})[a,b] 2A'	$\nu(^{13}CO)$	$\frac{\nu(^{13}CO)}{\nu(^{12}CO)}$	ν(CO) solution (cm^{-1})[a,c] 2A'	others	$M(CO)_2$ Angle (^{o})[d]	ν(MX)[e] (cm^{-1})
	1859 }			1853			
	1840 }						
XXIX	1966	1925w	0.979	1974	1944m,(sh)	111	239s
	1844	1812m,(sh)	0.983	1848			
XXX	1959br			1967	1942m,(sh)	112	227m
	1852br			1843			

[a] - All bands strong unless otherwise noted.

[b] - Recorded as Nujol mulls.

[c] - Recorded in chloroform solutions

[d] - Calculated from carbonyl band intensity data.

[e] - Recorded on complex dispersed in a polythene disc.

Ratios: For $[(\eta^3\text{-}C_3H_5)Mo(CO)_2\{P(OMe)_3\}_2X]$ ν(MoBr)/ ν(MoCl) = 0.64

ν(MoI)/ ν(MoCl) = 0.51

For $[(\eta^3\text{-}C_3H_5)Mo(CO)_2\{P(OEt)_3\}_2X]$ ν(MoI)/ ν(MoCl) = 0.47

Infrared Spectra

Selected infrared data for the complexes (XXII - XXX) are presented in Table 4.5. As Nujol mulls each of the complexes exhibited the expected two A' carbonyl modes at approximately 1980 and 1850cm^{-1}. In the majority of cases these bands were accompanied by weak bands positioned some 30 - 40cm^{-1} to lower frequency which have been assigned as ^{13}C isotope satellite bands in view of their position and relative intensities. The observed ratios $\nu(^{13}CO)/\nu(^{12}CO)$ fall in the range 0.985 - 0.977 and are very close to the expected value of 0.977[269].

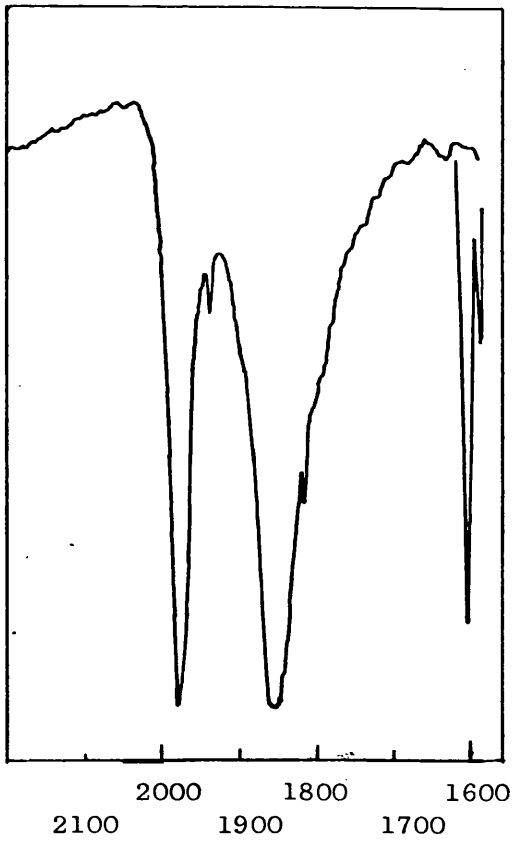

Figure 4.4: The carbonyl region of the solid state infrared spectrum of $[(\eta^3 - C_3H_5)Mo(CO)_2\{P(OMe)_3\}_2Cl]$

For two of the complexes (XXVI and XXVII) the ν(CO) bands were each split into two components. This is presumably caused by solid state or lattice effects, for the splitting was absent in solution spectra.

For each of the complexes the lower frequency asymmetric band was the more intense of the two ν(CO) absorptions. Since the relative intensities of the two bands are dependent upon the angle 2θ between the two carbonyl bonds[318-319] according to the equation $I_a/I_s = \tan^2\theta$, the CO - M - CO angles for (XXII - XXX) appear to be greater than 90^o. Calculated values for these CO - M - CO angles are presented in Table 4.5. For reasons which will become apparent later, these values were determined using carbonyl band intensity data taken from Nujol mull and not solution spectra (which are preferred). Despite this the values for the angles which range between $108 - 113^o$ show reasonable agreement with the solid state CO - M - CO angle (of 102^o) for (XXII).

The solution infrared spectra (Table 4.5) of several of the complexes in CCl_4, $CHCl_3$, CH_2Cl_2 and CH_3NO_2 exhibited an additional band in the ν(CO) region between 1940 - 1960cm^{-1} indicative of the formation of a second isomeric species in solution. The intensity of this band did not increase with time and evaporation of the solutions regenerated the original two band solid-state spectra eliminating decomposition as a possible explanation for the differences between the solid-state and solution spectra. No third

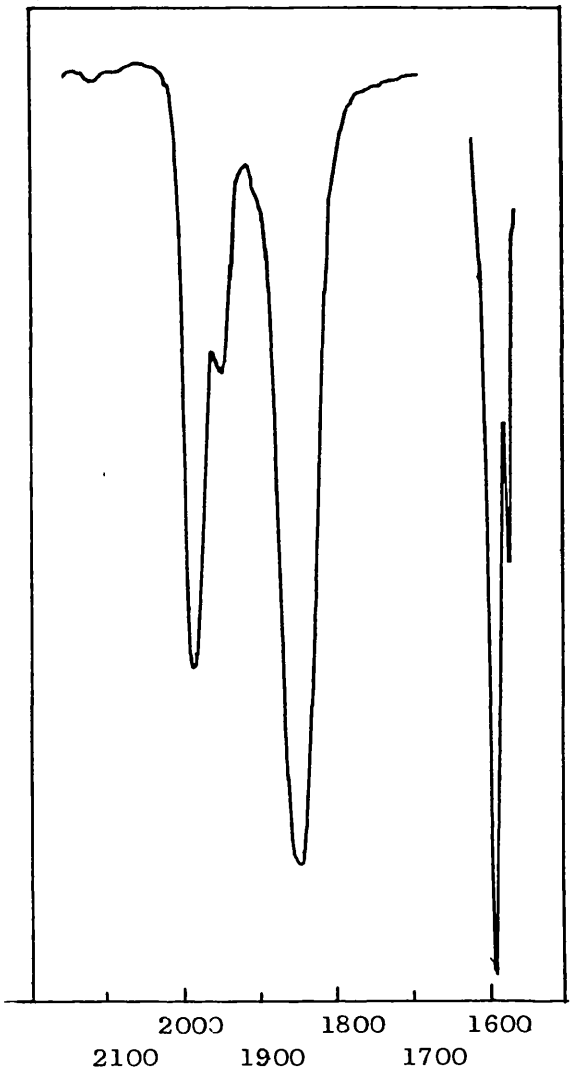

Figure 4.5: Solution ($CHCl_3$) infrared spectrum (carbonyl region) $[(\eta^3 - C_3H_5)Mo(CO)_2\{P(OMe)_3\}_2Cl]$.

ν (CO) absorption was observed in the solution spectrum of (XXV). Neither was it possible to detect any such band in the poorly resolved spectrum of (XXVII). The similarities of the infrared and NMR spectral data (described below) for the complexes (XXII - XXX) indicate that their molecular structures are completely analogous to that of $[(\eta^3 - C_3H_5)Mo(CO)_2\{P(OMe)_3\}_2Cl]$.

NMR Spectra

^{1}H and ^{31}P NMR spectral data for (XXII-XXX) are presented in Table 4.6 and the ^{13}C NMR spectral data for (XXII) and (XXV) are summarised in Table 4.7. The ^{13}C NMR measurements reported in this chapter were kindly made by Dr. M. Murray [School of Chemistry, University of Bristol] and Mr. P. Benyon [J.O.E.L. (U.K.) Ltd.] on solutions prepared by the author some hours in advance, consequently a few weak absorptions observed in the spectra are probably due to decomposition products.

The ^{1}H, ^{31}P and ^{13}C NMR spectra of (XXII) determined below $-40^{o}C$ are in complete accord with the solid state structure. Thus the ^{13}C NMR spectrum recorded at $-90^{o}C$ showed the equivalence of the ends of the allyl group and of the methoxy groups of the phosphite ligands (Table 4.7). Two well separated triplet resonances of approximately equal intensities centred at 233.0 and 225.0 p.p.m. indicated inequivalent carbonyl groups, with both carbonyl carbon atoms strongly coupled to two equivalent phosphorus atoms. In a study of the ^{13}C NMR spectra of complexes of the type $[M(CO)_4(P_2)]$, where M = Mo or W, $P_2 = 2PR_3$ or dpe, Randall *et al*[320] reported that carbonyls *trans* to phosphorus exhibit a ^{31}P - ^{13}C coupling some two to three times larger than *cis*-orientated carbonyls. Reference to Table 4.7 shows the carbonyl carbon at 233.0 p.p.m. exhibits slightly larger coupling to phosphorus than that at 225.0 p.p.m., consequently, in view of the slightly larger P(n) - Mo - C(4) angles [80.9(5), $79.6(5)^{o}$] compared with P(n) - Mo - C(5) angles [78.8(6), $78.5(6)^{o}$] this former resonance is assigned to the axial carbonyl group C(4) - O(4).

Table 4.6: ^{1}H and $^{31}P\{^{1}H\}$ NMR Data for the Complexes $[(\eta^{3} - C_3H_4R)M(CO)_2\{P(OR')_3\}_2X]$

Complex	^{31}P (δ/p.p.m. rel. to H_3PO_4)	^{1}H [δ (multiplicity, rel. intensity)] Allyl Protons H_X	H_M	H_A or Me	Phosphite Protons
XXII	181	3.24(d, 2H)	4.52(dt, 2H)	4.92(m, 1H)	3.85(d, 18H)
		J_{XA} 13.3	J_{MA} 7.9		J_{HP} 11.5
			J_{MP} 3.5		
XXIII	179	3.4(d, 2H)	4.42(dt, 2H)	4.74(m, 1H)	3.80(d, 18H)
		J_{XA} 13.2	J_{MA} 7.8		J_{HP} 11.4
			J_{MP} 3.5		
XXIV	177	*	4.21(dt, 2H)	4.64(m, 1H)	3.79[d, 18H + 2H(H_X)]
			J_{MA} 7.4		J_{HP} 11.0
			J_{MP} 3.5		
XXV	187	3.17(s, 2H)	4.35(d, 2H)	1.81(s, 3H)	3.82(d, 18H)
			J_{MP} 7.0		J_{HP} 11.8
XXVI	176	3.23(d, 2H)	4.40(dt, 2H)	4.85(m, 1H)	1.33(t, 18H) P - $OCH_2\underline{CH}_3$
		J_{XA} 13.5	J_{MA} 7.5		J_{HH} 7.0
			J_{MP} 3.3		4.16(q, 12H) P - $O\underline{CH}_2CH_3$
					J_{HP} 7.0

.....contd.

Table 4.6 (contd.)

Complex	^{31}P (δ /p.p.m. rel. to H_3PO_4)	^{1}H [δ (multiplicity, rel. intensity)] Allyl Protons H_X	H_M	H_A or Me	Phosphite Protons
XXVVII	172	3.77(d, 2H)	*	4.60(m, 1H)	1.30(t, 18H) P - $OCH_2\underline{CH}_3$
		J_{XA} 13.5			J_{HH} 7.0
					4.10[q, 12H + 2H(H_M)] P - $OC\underline{H}_2CH_3$
					J_{HP} 7.0
XXVIII		3.25(d, 2H)	4.30(dt, 2H)	*	1.34(d, 36H) P - $OCH(C\underline{H}_3)_2$
		J_{XA} 13.4	J_{MA} 8.3		J_{HH} 6.3
			J_{MP} 3.2		4.84[m, 6H + 1H(H_A)] P - $OC\underline{H}(CH_3)_2$
					J_{HP} 3.0
XXIX	150	2.88(d, 2H)	4.33(dt, 2H)	4.95(m, 1H)	3.76(d, 18H)
		J_{XA} 13.5	J_{MA} 8.0		J_{HP} 11.8
			J_{MP} 3.7		
XXX		2.87(d, 2H)	4.22(dt, 2H)	4.90(m, 1H)	1.32(t, 18H) P - $OCH_2\underline{CH}_3$
		J_{XA} 13.5	J_{MA} 7.8		J_{HH} 7.2
			J_{MP} 3.5		4.09(q, 12H) P - $OC\underline{H}_2CH_3$

/ Determined at 28°C in $CDCl_3$ solutions. * - Signal hidden by $P(OR')_3$ signal.

Table 4.7: ^{13}C NMR* Data for the Complexes $[(\eta^3\text{-}C_3H_4R)Mo(CO)_2\{P(OMe)_3\}_2L']^{+,o}$

Complex	Temp (°C)	δ +(multiplicity) Allyl C_2	C_1C_3	Me	Carbonyl	Phosphite
XXII[a]	-90	114.4(s)	76.0(s)		233.0(t)	53.6(d)
					J_{CP} 35.9	J_{CP} 4.6
					225.0(t)	
					J_{CP} 27.2	
	0	113.6(s)	75.1(s)		228.4(br)	53.6(br)
	32	112.9(s)	74.7(s)		228.0(t)	53.1(d)
					J_{CP} 29.3	J_{CP} 4.9
XXV[b c]	-30	130.0(s)	75.4(s)	25.1(s)	231.8(t)	53.2(d)
					J_{CP} 35.9	J_{CP} 4.6
					225.4(t)	
					J_{CP} 26.7	
XXXI[d]	-80	103.1(s)	62.1(s)		225.7(dt)	53.4(d)
					J_{CP} 33.3, 19.8	J_{CP} 4.6
					216.4(dt)	54.3(d)
					J_{CP} 58.0, 21.4	J_{CP} 4.6
	32	101.3(s)	61.2(s)		e	54.3(br)

..../contd.

Table 4.7: (Cont'd)

* - Proton decoupled ^{13}C NMR spectra

+ - δ in p.p.m. rel. to $SiMe_4$ in CD_2Cl_2 solutions with 0.5M $Cr(acac)_3$ used as relaxation reagent.

[a] - Weak unassigned peaks at 220.8(br s) and 63.1(br s)

[b] - Weak unassigned peaks at 228.1(br s)

[c] - in $CDCl_3$

[d] - Weak unassigned peaks at 98.1(s) and 57.2(br s). For fuller description of carbonyl region see text

[e] - Signal not resolved from background.

On raising the temperature from -90°C only the resonances for the carbonyl carbons showed any temperature dependency. By 0°C the two carbonyl signals had coalesced into a single broad resonance centred at 228.4 p.p.m. which sharpened into a triplet by room temperature. Thus in the limiting high temperature spectrum the carbonyls are equivalent and coupled equally with both phosphorus atoms. At all temperatures investigated (-90°C to +32°C), only a single resonance was observed for the methylene termini of the allyl group. The allylic carbon atoms failed to show ^{31}P - ^{13}C coupling in common with observations for other complexes[171]. The ^{13}C chemical shifts of the allylic carbons are typical of those observed for η^3-allyl-metal complexes (see Chapter 1 p. 57) but show slight downfield shifts of between 10 - 40 p.p.m. when compared with other Group 6 complexes of a similar type[163,171,180]. The prevalence of strong π-acceptors in (XXII) which presumably encourage the flow of electron density from the allyl to the metal may well be responsible for this apparent deshielding.

The proton-coupled ^{13}C NMR spectrum of (XXII) determined at 32°C showed a clearly resolved quartet of doublets centred at 53.1 p.p.m. for the methoxy carbons of the phosphite ligands. The spin pattern corresponds to the coupling of one phosphorus atom [$^1J(C - P) = 4.6$ Hz] and three equivalent protons. The $^1J(C - H)$ coupling of 147.5 Hz differs little from that observed for the free ligand (144.5 Hz). The central carbon atom C_2 of the allyl resonated as a simple doublet with $^1J(C_2 - H_A) = 161.1$ Hz.

The signal for the terminal carbon atoms of the allyl was not well resolved possibly because of a slight difference in the magnitude of $^{1}J(C_{1,3} - H_M)$ and $^{1}J(C_{1,3} - H_X)$ [other workers have reported $^{1}J(C_{1,3} - H_X) > {}^{1}J(C_{1,3} - H_M)$[147]]. However, the average value for $^{1}J(C_{1,3} - H)$, 161.6 Hz, agrees well with that reported for other η^3 - allyl complexes[141,142,147,196] and is consistent with sp^2 hybridisation for the allylic carbon atoms.

Each of the complexes (XXII - XXX) exhibited similar dynamic ^{1}H NMR spectra. At all temperatures between +70 and -125°C the phosphorus decoupled spectra showed three sets of resonances for the allyl moiety, typical of the AMM'XX' spin system of symmetrical η^3-allyls, together with a singlet for the methoxy protons of the phosphite ligands. As for most other complexes of the Group 6 metals containing coordinated η^3-allyl and phosphorus ligands[171], phosphorus coupling to the <u>anti</u> protons H_X and $H_{X'}$ of the allyl was not observed and only showed as line broadening for the central proton H_A. In the limiting low temperature spectra the <u>syn</u> protons H_M and $H_{M'}$ showed strong coupling to one phosphorus atom (J <u>ca.</u> 7.0 Hz). This is as predicted for the solid state structure in which the two phosphite ligands occupy sites adjacent to the ends of the allyl in the pentagonal girdle and as a consequence are inequivalent with respect to H_M and $H_{M'}$ (see Figure 4.6).

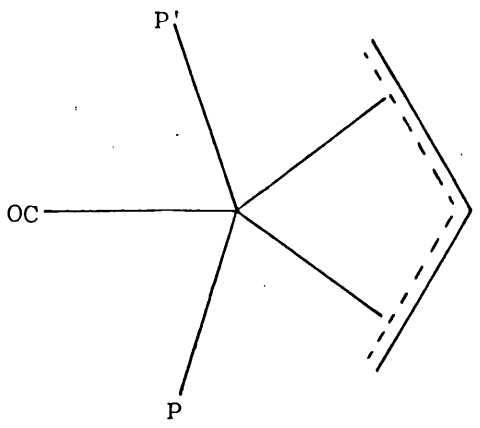

Figure 4.6: The inequivalence of P and P' to H_M and $H_{M'}$ in the solid state structure of $[(\eta^3 - C_3H_5)Mo(CO)_2\{P(OMe)_3\}_2Cl]$.

In view of the work of Shaw et al[159a,b] (see Chapter 1 p.40) the phosphorus atom coupled to each syn proton is most probably that which is approximately trans i.e.

$J(P - H_M) = J(P' - H_{M'}) \gg J(P' - H_M) = J(P - H_{M'}) \sim 0.$

In the limiting high temperature spectra [observed for all but (XXV) by $+32^oC$] both syn protons showed equal coupling to two equivalent phosphorus atoms [$J(P - H) \sim 3.5$ Hz]. Figure 4.7 shows the signal due to the syn protons at several temperatures between $+32^oC$ and -40^oC. In the optimum low temperature spectrum (-40^oC) an $[AX]_2B$ pattern is observed in which two of the four expected lines are coincident. As the temperature increases the three lines observed in the limiting low temperature spectrum persist apparently unchanged whilst two new lines "grow" between them.

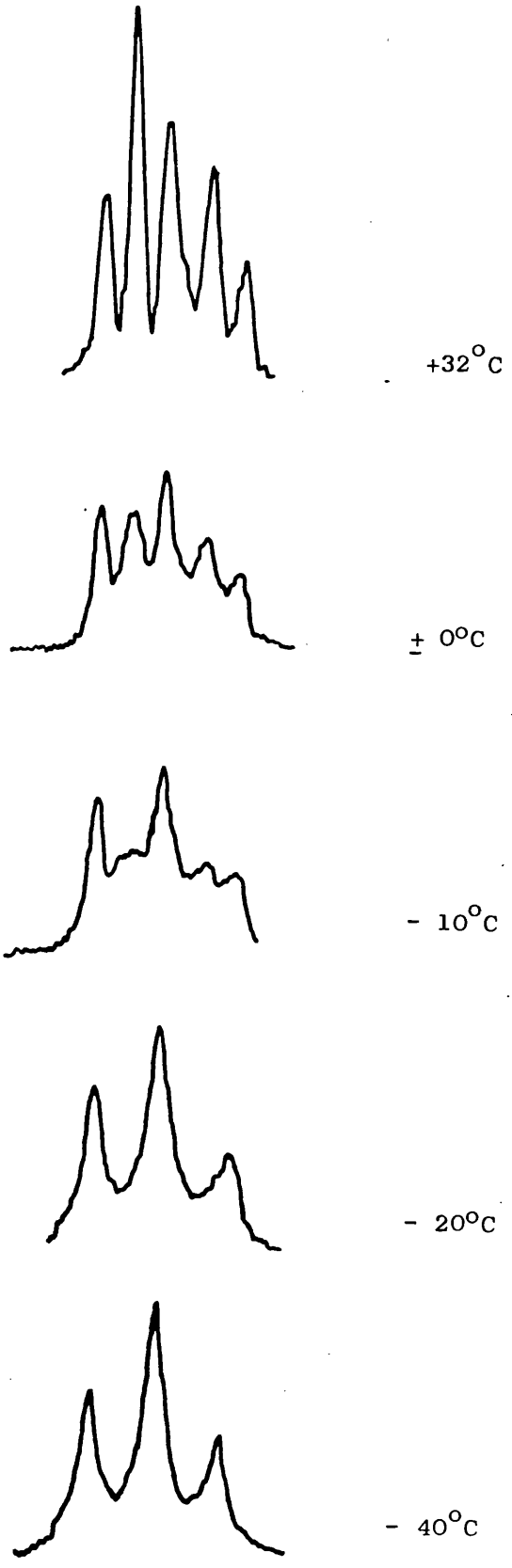

Figure 4.7: The ^{1}H NMR spectrum of the syn protons of $[(\eta^{3}\text{-}C_3H_5)Mo(CO)_2\{P(OMe)_3\}_2Cl]$ at various temperatures between + 32 and - 40°C

By +32°C the optimum high temperature spectrum is obtained and an A_2X_2B spin pattern in which two of the six expected lines are coincident is observed. The intermediate spectra are characteristic of [AA'XX'] B spin systems. The nature of the temperature dependency meant that it was not possible to determine specific coalescence temperatures, only ranges. These are listed in Table 4.8. The 2-methylallyl derivative (XXV) showed similar effects in its ^{1}H NMR but had a higher activation energy (coalescence temperature range +30 to +40°C). Thus this complex is stereochemically rigid on the ^{1}H NMR time scale at room temperature and the limiting high temperature $[AX]_2$ spectrum was not reached until ca. +60°C under which conditions slight decomposition also occurred. The absence of homonuclear coupling effects in (XXV) resulted in simplified spectra which permitted a more detailed study of the intermediary spin patterns. Analyses of the AA'XX' spin systems observed for the syn protons of (XXV) at two temperatures, (54°C and 45°C) were undertaken. The proximity of the composite lines in the pattern made it impossible to determine their positions very accurately, nevertheless the calculated parameters $J_{HP'}$, $J_{HP''}$, $J_{HH'}$ and $J_{PP''}$, given in Table 4.9 were used to calculate theoretical AA'XX' spectra (Figure 4.8) which gave reasonable agreement with the experimentally determined spectra[/]. It must be admitted that the fit of theoretical and experimental spectra is poor, but without use of a computer programme a better simulation is not possible. Figure 4.9 illustrates graphically

/ Relative band widths and intensities were calculated using the relationships tabulated in Ref. 321.

Table 4.8. Coalescence Temperature Ranges for the Complexes $[(\eta^3\text{-}C_3H_4R)M(CO)_2\{P(OR')_3\}_2X]$

Complex	Coalescence Temperature Range for the *syn* protons H_M (^oC)
XXII	-15 to -20
XXIII	-15 to -20
XXIV	-20 to -40
XXV	+30 to +40
XXVI	-15 to -20
XXVII	*
XXVIII	-30 to -40
XXIX	-15 to -20
XXX	-20 to -25

* - Signal hidden by $P(OR')_3$ signal.

Table 4.9: Coupling Constants for the syn Protons of the Allyl in $[(\eta^3\text{-2-MeC}_3\text{H}_4)\text{Mo(CO)}_2\{\text{P(OMe)}_3\}_2\text{Cl}]$

			Calculated Coupling Constants (Hz)			
Temp (^{o}C)	N[a]	$(M^2+L^2)^{\frac{1}{2}}$	J_{HP}	$J_{HP'}$	$J_{PP'}$	$J_{HH'}$
73	6.9	0	$\pm$3.5	$\pm$3.5	0	0
54	6.8	4.0	$\pm$4.9	$\pm$1.9	$\pm_{\pm}$4.4	$\pm\pm$0.4
45	6.9	4.0	$\pm$5.5	$\pm$1.5	$\pm_{\pm}$5.4	$\pm\pm$1.4
28	7.0	0	$\pm$7.0	0	0	0

[a] - The separations are based upon the following relationships:

$K = J_{AA'} + J_{XX'}$; $M = J_{AA'} - J_{XX'}$; $\nu_1 - \nu_3 = N$

$L = J_{AX} - J_{AX'}$; $N = J_{AX} + J_{AX'}$; $(M^2 + L^2)^{\frac{1}{2}} = \nu_9 - \nu_{11}$

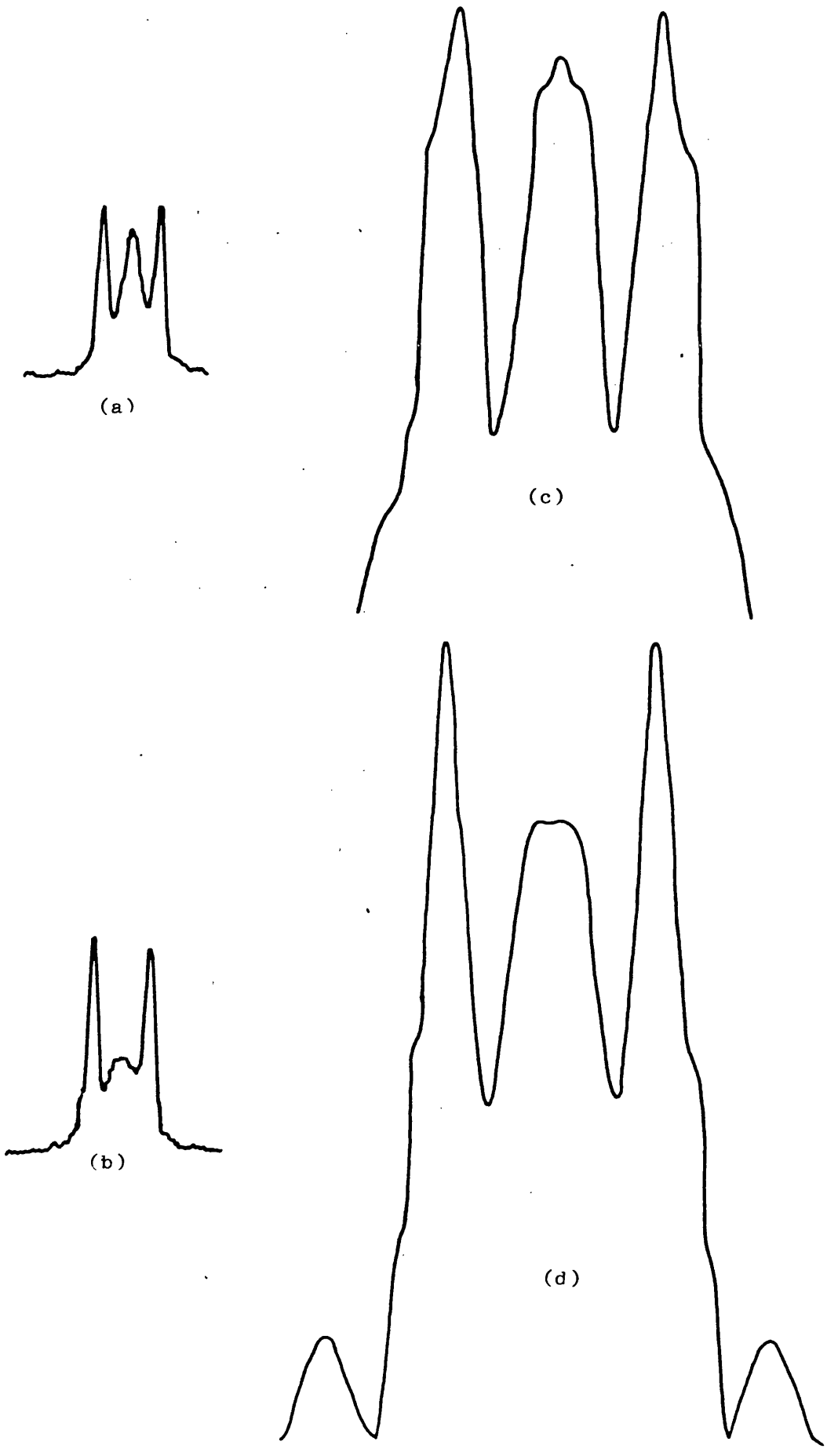

Figure 4.8: The ^{1}H NMR spectra of the syn allylic protons of $[(\eta^{3}\text{-}2\text{-}MeC_3H_4)Mo(CO)_2\{P(OMe)_3\}_2Cl]$ at (a) 54°C and (b) 45°C, and the calculated theoretical spectra at (c) 54°C and (d) 45°C.

(not drawn to scale) how the magnitude of the various coupling parameters alter with change in temperature.

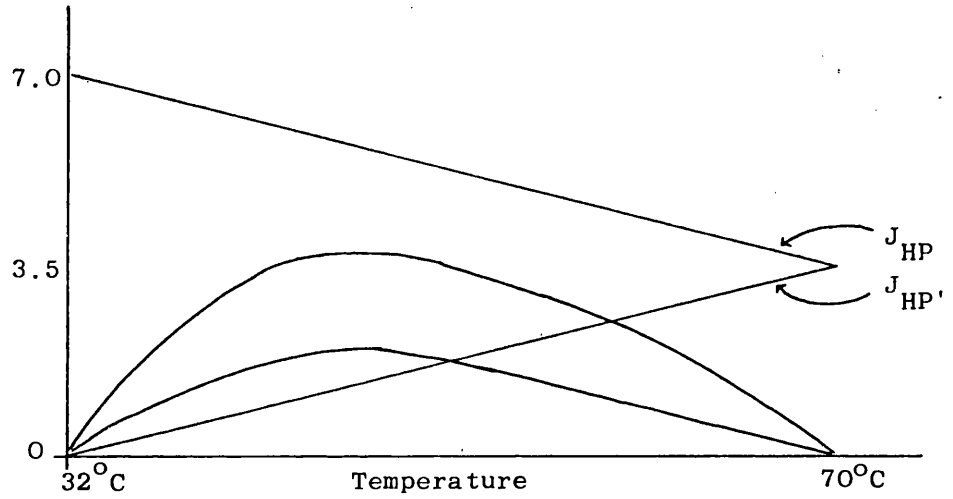

Figure 4.9: Variation of J_{HP}, $J_{HP'}$, $J_{HH'}$ and $J_{PP'}$ with temperature for (XXV)

The $P(OEt)_3$ complexes (XXVI, XXXVII and XXX) showed additional temperature-dependent features in their ^1H NMR spectra. At +32°C the methylene protons of the phosphite ligands resonated as a pseudo-quintet, since $^3J(P - H) \sim {}^3J(H - H)$ caused overlapping of the expected quartet of doublets. Below -40°C an inequivalence of the two protons in each methylene group resulted in two sets of overlapping quintets of equal intensity. [Coalescence temperatures T_c were -20, -10 and -29°C for (XXVI XXVII and XXX) respectively]. For (XXX) and (XXVI) the signal was resolved as a six line multiplet due to coincidence of eight of the ten expected lines, but for (XXVII) all ten lines were clearly resolved. The inequivalence of the methylene protons in the low temperature spectra probably results from restricted rotation about the P - O - C bonds. An estimate of the free

energy of activation $\Delta G^{\neq}_{T_C}$, for this rotation was made using equation 4.1[322]

$$G^{\neq}_{T_C} = RT_C \ln (\pi \Delta \nu \; h/2^{\frac{1}{2}} K_B T_C) \qquad 4.1$$

$G^{\neq}_{T_C}$ = Free energy of activation in J mol^{-1}

T_C = Temperature at coalescence in K

R = Gas constant = 8.314 J K^{-1} mol^{-1}

K_B = Boltzmann constant = 1.38062 x 10^{-23} J K^{-1}

$\Delta \nu$ = Separation of signals undergoing collapse in s^{-1}

h = Planck constant = 6.6260 x 10^{-34} J s

which only strictly applies to a simple two-site exchange with no coupling. The $G^{\neq}_{T_C}$ values for (XXVI, XXVII and XXX) are similar, being 56.2, 57.3 and 53.9 kJ mol^{-1} respectively.

The signals observed for the methyl protons of the phosphite ligands were temperature-invariant. Also the value of $J(H_{methylene} - H_{methyl})$ did not alter indicating that rotation of the methyl group about the C - C bond was unrestricted even at -40°C.

^{31}P NMR spectra for the complexes (XXII - XXX) were determined at several temperatures between +60 and -60°C (+ 60 and - 125°C for XXII) but showed no temperature dependency. The broad band proton-decoupled spectra, which were of distinctly poor quality, consisted of only a single broad band. Coupling of ^{183}W to ^{31}P (usually of the order of 100 Hz - 200 Hz[162,171,323]) was not detected.

The Dynamic Behaviour of the Complexes

$[(\eta^3\text{-}C_3H_4R)M(CO)_2\{P(OR')_3\}_2X]$

Complexes (XXII - XXX) undergo a fast rearrangement on the NMR time scale at room temperature (or just above in the case of XXV). Since the tendency of phosphite ligands to dissociate and re-coordinate is well known, ^1H NMR spectra of (XXII) were recorded at several temperatures in the presence of free $P(OMe)_3$. As far as could be ascertained from this simple experiment intermolecular exchange of the phosphite ligands was not occurring, for two signals corresponding to free and coordinated phosphite were observed at all temperatures. The maintenance of sharp outer lines at all temperatures in the resonance pattern of the allylic syn-protons is also indicative of an intramolecular "mutual" exchange process for the phosphorus ligands with all H - P coupling constants having the same sign[324]. Conductivity measurements on 10^{-3} mol dm^{-3} solutions of (XXII) in CH_3NO_2 were undertaken in order to determine whether ionisation of Cl^- was occurring. The molar conductivity (Λ_M) of the species was found to be 12.63 mhos cm^2 mol^{-1} which lies well outside the range (75-95 mhos cm^2 mol^{-1}) expected for a 1:1 electrolyte[325]. (This low conductivity can be attributed to slight decomposition, since a gradual increase with time was observed with a concomitant change in the colour of the solutions from yellow to green). Since dissociation of the carbonyl or allyl groups in (XXII - XXX) seems unlikely, the rearrangement process occurring is most probably intramolecular.

Stereochemical non-rigidity is commonly encountered for seven-coordinate complexes[308,314,326-8]. Indeed, dynamic NMR, the primary tool for the study of seven-coordinate systems, has revealed no stereochemically rigid ML_7 complex[328]/. With inequivalent or chelating ligands, several examples of quenched exchange are known[314,324,326,329,330], however, with the possible exception of $[TaX(\eta^4\text{-naphthalene})(dmpe)_2]$[329] dmpe = 1,2-bis(dimethylphosphino)ethane and $[MoH(C_2H_4)_2(dpe)_2]BF_4$[330] the mechanisms for ligand exchange are poorly understood[314,324,326,328]. Generally speaking ligand reorganisation may occur by a concerted process, such as that proposed by Faller for the formally seven-coordinate species $[(\eta^3\text{-}C_3H_5)Mo(CO)_2(dpe)X]$[171] or involve a short lived isomeric intermediate. Because there is no regular polyhedron with seven vertices, a variety of isomeric structures are possible (34 in all)[331]. Fortunately, just three high symmetry polyhedra, the pentagonal bipyramid, the capped trigonal prism and the capped octahedron, suffice to describe the established elements of structure observed in seven-coordination. Calculations based on ligand repulsion models[332-335] indicate the energy differences between these three idealised geometries to be minimal and extended Huckel treatments suggest little or no electronic barriers for their interconversion[308].

/ And references therein.

For the complexes (XXII - XXX) equivalence of the carbonyl groups and equivalence of the phosphite ligands is observed in the high temperature limit. The rearrangement process also results in the equivalence of the two phosphite phosphorus nuclei with respect to the allylic syn protons so that in the high temperature spectra each syn proton is coupled to two equivalent phosphorus atoms with coupling constants equal to the average of those observed in the low temperature limit. The actual pathway for the ligand reorganisation is experimentally indeterminate but the observations are clearly inconsistent with a simple rotation of the bidentate (allyl) ligand as proposed for $[TaX(\eta^4\text{-naphthalene})(dmpe)_2]$[329] since this would not result in the carbonyl groups becoming equivalent. Evidence in the infrared spectra of (XXII - XXIV, XXVI - XXX) for a second isomeric species implies a polytopal process involving a short lived intermediate. That there is no indication of any such isomeric species in the infrared spectrum of (XXV) - which is rigid at room temperature - seemingly supports this interpretation.

Only very small bending-stretching modes are necessary to effect interconversions between the various idealised polytopes[308]. However, by virtue of the relatively amorphous potential surface for seven-coordination there may well be several different physical or geometric paths for each type of interconversion which differ little in terms of activation parameters. Simple idealised pathways have, however, been proposed[308,328,336]. Since the theoretical calculations of Dewan et al[307] predict

the most energetically favourable alternative geometry for complexes of the type $[M(unidentate)_5(bidentate)]$ (containing bidentate ligands of small normalised bite) is a capped trigonal prism,in which the bidentate ligand spans the unique edge, an interconversion between pentagonal bipyramid and such a capped trigonal prismatic isomer appears to be the most likely process occurring in complexes (XXII - XXX). However, as demonstrated in Figure 4.10 the idealised geometric pathway[308] interconnecting the two geometries fails to provide a simple one-step route for ligand reorganisation which is compatable with the experimental observations. Indeed the fluxional behaviour of

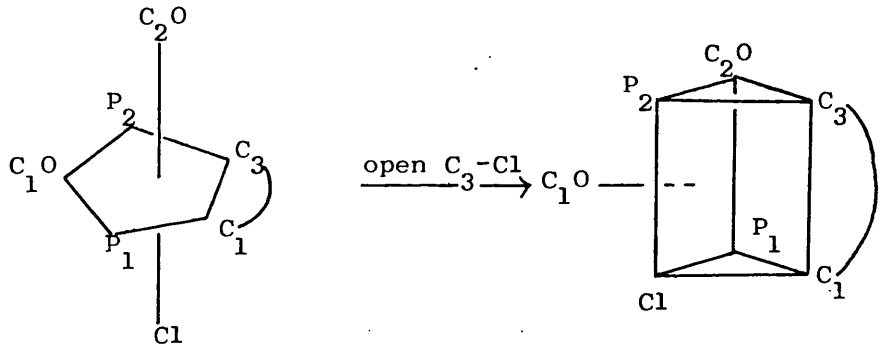

Figure 4.10: Pentagonal bipyramid to capped trigonal prism conversion.

(XXII - XXX) cannot be accounted for by a simple vibrational deformation of the pentagonal bipyramidal reference isomer to any polytopal isomer, for in no instance does this offer a pathway for both carbonyl and phosphorus exchange. A more complex mechanism is therefore implied. One possibility is the two step process shown in Scheme 4.1.

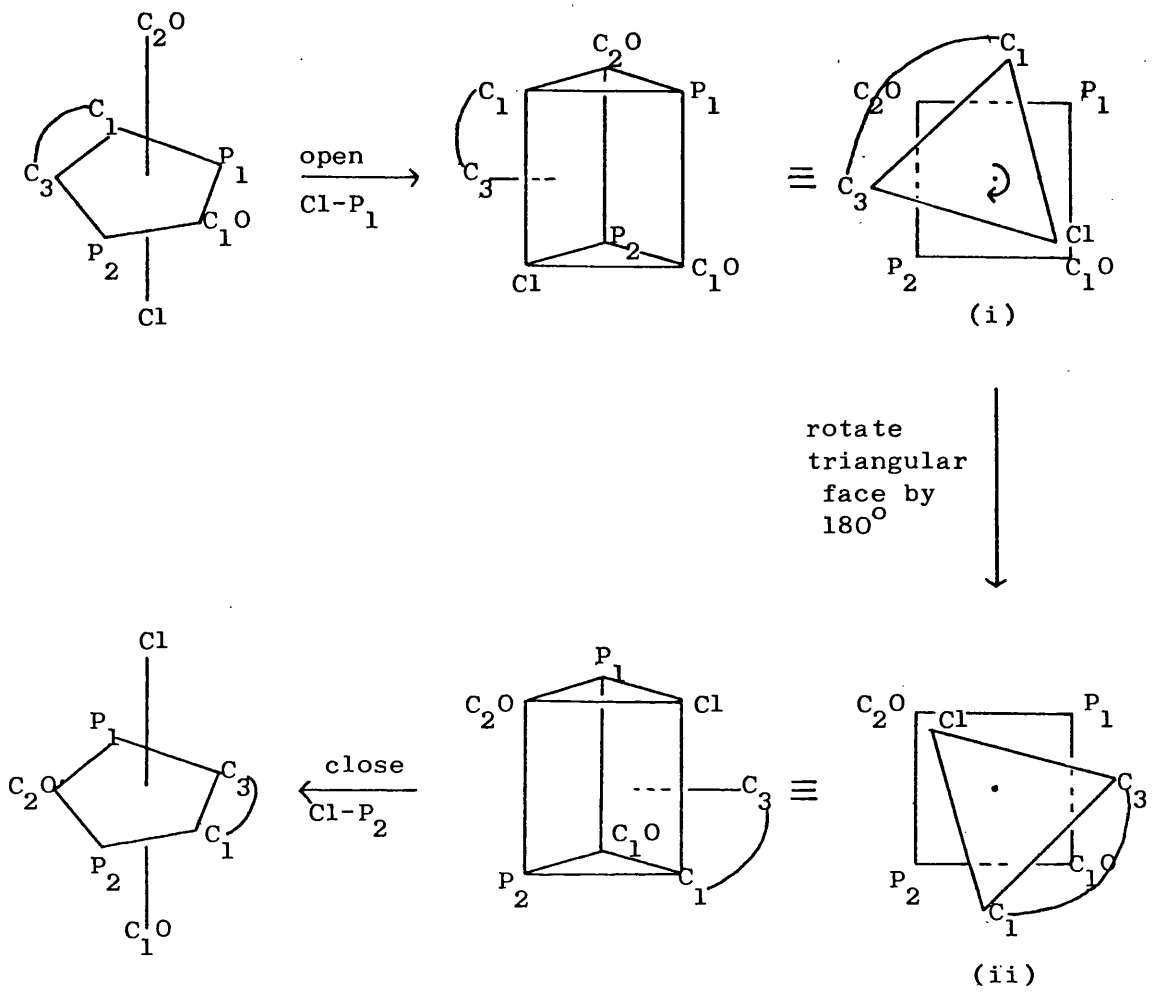

Scheme 4.1

This mechanism involves an interconversion between pentagonal bipyramid and 3:4 (C_s) type structures. This latter geometry is very closely related to the capped trigonal prism, and the interconversion between pentagonal bipyramid and 3:4 geometry is perhaps best envisaged as a slight extension of the simple idealised pathway[308] connecting the pentagonal bipyramid and capped trigonal prismatic geometries, as shown in Figure 4.10. In the 3:4 geometry, (in which, incidentally, the original σ_v mirror plane of the reference isomer is maintained) there are two energetically identical conformations (i) in which the Cl atom is sited above C_1O (ii) in which the Cl atom is sited above C_2O. These two conformations are connected by a simple

concerted rotation of the triangular face formed by the allyl and chlorine ligands. Scheme 4.1 shows that collapse of these two conformations to pentagonal bipyramidal geometries effects simultaneous exchange of both the phosphorus and carbonyl ligands.

The mechanism described above is consistent with all the experimental observations for the neutral complexes $[(\eta^3\text{-allyl})M(CO)_2\{P(OR')_3\}_2X]$. In addition the rearrangement process is anticipated to be slower for the 2-methylallyl than for the allyl complexes, since an increased repulsion between the 2-methyl substituent and the methoxy groups of the phosphite ligands may be expected to raise the activation energy for rotation of the triangular face in the 3:4 type structure.

The Preparation and Characterisation of the Complexes $[(\eta^3\text{-}C_3H_4R)Mo(CO)_2\{P(OMe)_3\}_3]BF_4$, (R = H or Me)

Having observed the somewhat ambiguous temperature-dependent NMR spectra for the neutral complexes $[(\eta^3\text{-}C_3H_4R)M(CO)_2\{P(OR')_3\}_2X]$ the cationic species $[(\eta^3\text{-}C_3H_4R)Mo(CO)_2\{P(OMe)_3\}_3]^+$ were prepared in an attempt to obtain more information about the rearrangement process. In the former complexes no information regarding the participation of the halogen atom in the process could be obtained. Consequently replacement of this ligand with another which could be monitored by NMR seemed an attractive idea. First attempts at the preparation of the complexes $[(\eta^3\text{-}C_3H_4R)Mo(CO)_2\{P(OMe)_3\}_3]BF_4$ were unsuccessful. The method employed was that devised by Hull

and Stiddard[73] who used $NaBF_4$ to abstract the chlorine from $[(\eta^3\text{-allyl})Mo(CO)_2L_2Cl]$ (where M = Mo or W; L_2 = bipy or phen) and replace it with pyridine. Thus, $[(\eta^3\text{-}C_3H_4R)Mo(CO)_2\{P(OMe)_3\}_2Cl]$ $P(OMe)_3$ and $NaBF_4$ were mixed in equimolar quantities in acetone and stirred vigorously at room temperature. The progress of the reaction was monitored by infrared spectroscopy. After three days evidence for the presence of a cationic dicarbonyl species was obtained, but the reaction proved to be so slow that extensive decomposition of both the starting material and product had occurred before it reached completion. At elevated temperatures the starting complex simply decomposed. The $P(OMe)_3$ complexes were eventually prepared using the more soluble $AgBF_4$ in place of $NaBF_4$[163]. This method proved unsuccessful for the analogous $P(OEt)_3$ and $P(Oi\text{-}Pr)_3$ derivatives for although there was clear evidence for cationic dicarbonyl species in the reaction mixtures [ν(CO) 2000 and 1900 cm^{-1}] all attempts to isolate the products failed. Only brown oils which smelt strongly of phosphite could be obtained, even after prolonged pumping in vacuo.

The molar conductivity (Λ_M) of a 10^{-3} mol dm^{-3} solution of (XXXI) in CH_3NO_2 of 92.4 mhos cm^2 mol^{-1} is consistent[325] with its formulation as a 1:1 electrolyte. The infrared spectra of (XXXI and XXXII) showed the two expected bands in the carbonyl region at 2010 and 1923 cm^{-1} for (XXXI) and 2000 and 1917 cm^{-1} for (XXXII). The position of these bands some 10 - 70 cm^{-1} wavenumbers higher than those of the corresponding neutral complexes (XXII and XXV) reflects the reduction of electron

density at the metal centre in the cationic species. The $M(CO)_2$ angles for (XXXI) and (XXXII) (calculated from carbonyl band intensity data) of 114 and 112° respectively are similar to those of the neutral complexes and far too large for the pseudo-octahedral type structure found for other cations of the type $[(\eta^3\text{-}C_3H_5)Mo(CO)_2L_3]^+$ [126,241]. However, in contrast to the neutral complexes there was no evidence in the solution infrared spectra of either (XXXI) or (XXXII) for the presence of isomeric species.

^{1}H NMR Spectra

^{1}H NMR spectral data for the complexes are summarised in Table 4.10. The complexes (XXXI) and (XXXII) exhibited similar dynamic ^{1}H NMR spectra but the barrier to the rearrangement process was much lower for the η^3-allyl, than for the η^3-2-methylallyl complex. For the former, limiting low temperature spectra were not obtained until -30°C whilst the latter was stereochemically rigid at room temperature. In both cases the signal for the syn protons of the allyl was, at all temperatures, completely obscured by that due to the methoxy protons of the phosphite ligands. This made a direct comparison of the temperature dependence of the ^{1}H NMR spectra of these compounds and those of the neutral complexes impossible.

In the limiting low temperature spectra of (XXXI) and (XXXII) two resonances of intensity ratio 1:2 were observed for the phosphite ligands. The anti protons of the allyl ligand

Table 4.10: ^{1}H and ^{31}P NMR Data^{+} for the Complexes $[(\eta^{3}\text{-}C_3H_4R)Mo(CO)_2\{P(OMe)_3\}_3]BF_4$

Complex	Temp (^{o}C)	^{31}P (δ /p.p.m. rel. to H_3PO_4)	δ (multiplicity, rel. intensity)			
			Allyl Protons			Phosphite Protons
			H_X	H_M	H_A	
XXXI	-30		2.96(t, 2H) J_{XA} 12 J_{XP} 12	*	4.98(m, 1H)	3.66(d, ~ 9H) J_{PH} 11.0 3.78 (d, ~18H) J_{PH} 11.2 Total int. 29H [2H(H_M)]
	+28	168	2.81(br d,2H) J_{XA} 12	*	4.98(m, 1H)	3.71[d, 27H + 2H(H_M)] J_{PH} 11.0
XXXII	28	165	3.13(br d,2H) J_{XP} 15.5	*	2.03(br s,1H)	3.13(d,~9H) J_{PH} 10.8 3.81(d,~18H) J_{PH} 11.0 Total int. 29H [2H(H_M)]

+ Determined in $CDCl_3$

showed strong coupling to one phosphorus atom [$^{3}J(P\text{-}H_{X})$ = 12 Hz for (XXXI) and $^{3}J(P\text{-}H_{X})$ = 15.5 Hz for (XXXII)]. Decoupling experiments revealed that there were two ^{31}P decoupling frequencies, the first collapsed the resonance due to the unique phosphite and that due to the anti protons of the allyl showing that both anti protons were infact coupled to the same phosphorus atom. The second collapsed the more intense methoxy signal to a singlet and also resulted in slight sharpening of the signal due to the anti protons. It is not clear whether the two equivalent phosphorus atoms also couple weakly to the anti protons of the allyl or whether the slight sharpening of the latter's signal observed resulted from an off-resonance effect.

The low temperature spectra are consistent with a pentagonal bipyramidal structure for (XXXI and XXXII) such as that which may be derived from the structure of (XXII) by replacement of the halogen by a further $P(OMe)_3$ ligand, [different distortions to those observed in (XXII) are expected for (XXXI and XXXII)].

As the temperature was raised from -30°C, the two phosphite signals in the spectrum of (XXXI) coalesced (T_c = -15°C, $\Delta G^{\neq}$ = 55.8 kJ mol^{-1}) and by +32°C had sharpened into a doublet centred at 3.71 p.p.m. [$^{3}J(P\text{-}H)$ = 11 Hz]. The coordinated phosphite ligands did not exchange with added $P(OMe)_3$ indicating, as observed for the neutral complexes, that a non-dissociative phosphite rearrangement process was occurring. The resonance due to the anti protons of the allyl ligand also showed some temperature dependency. By 30°C

this signal had changed from the A_2BX spin pattern observed in the low temperature limit to a broad doublet [$J(H_A-H_X)$ = 12 Hz] . ^{31}P decoupling resulted in a sharpening of this signal, but neither the number of coupling atoms nor the magnitude of $^3J(P-H_X)$ could be determined. The 2-methylallyl complex (XXXII) showed similar temperature-dependent features to those of (XXXI) but, as for the neutral complexes, the fully dynamic state for this derivative was not reached until higher temperatures (ca. 80°C T_c = 55°C $\Delta G^{\neq}$ = 71.4 kJ mol^{-1}) when decomposition also became significant.

^{13}C NMR Spectra

The ^{13}C NMR spectral data for (XXXI) have been summarised in Table 4.7. The optimum low temperature spectrum recorded at -80°C showed two equivalent and one unique phosphite ligands together with a symmetrically bonded η^3-allyl group, in keeping with the low temperature ^1H NMR results. It was hoped that the carbonyl region of the spectrum would yield further confirmation that the low temperature stereochemistry of (XXXI) was analogous to that of (XXII). Unfortunately these hopes were not fulfilled for, as shown in Figure 4.11, the region of interest was complicated by interference from spurious resonances which made assignments difficult. Nevertheless a clearly defined doublet of triplets was found at 216.4 p.p.m. The coupling pattern of this signal was as expected for the axial carbonyl carbon of the proposed stereochemistry, coupled to two equivalent cis phosphorus atoms [J(P-C) = 21.4 Hz] and one trans phosphorus atom [J(P-C) = 58.0 Hz] . The magnitude of the coupling constants, with the former being almost exactly one

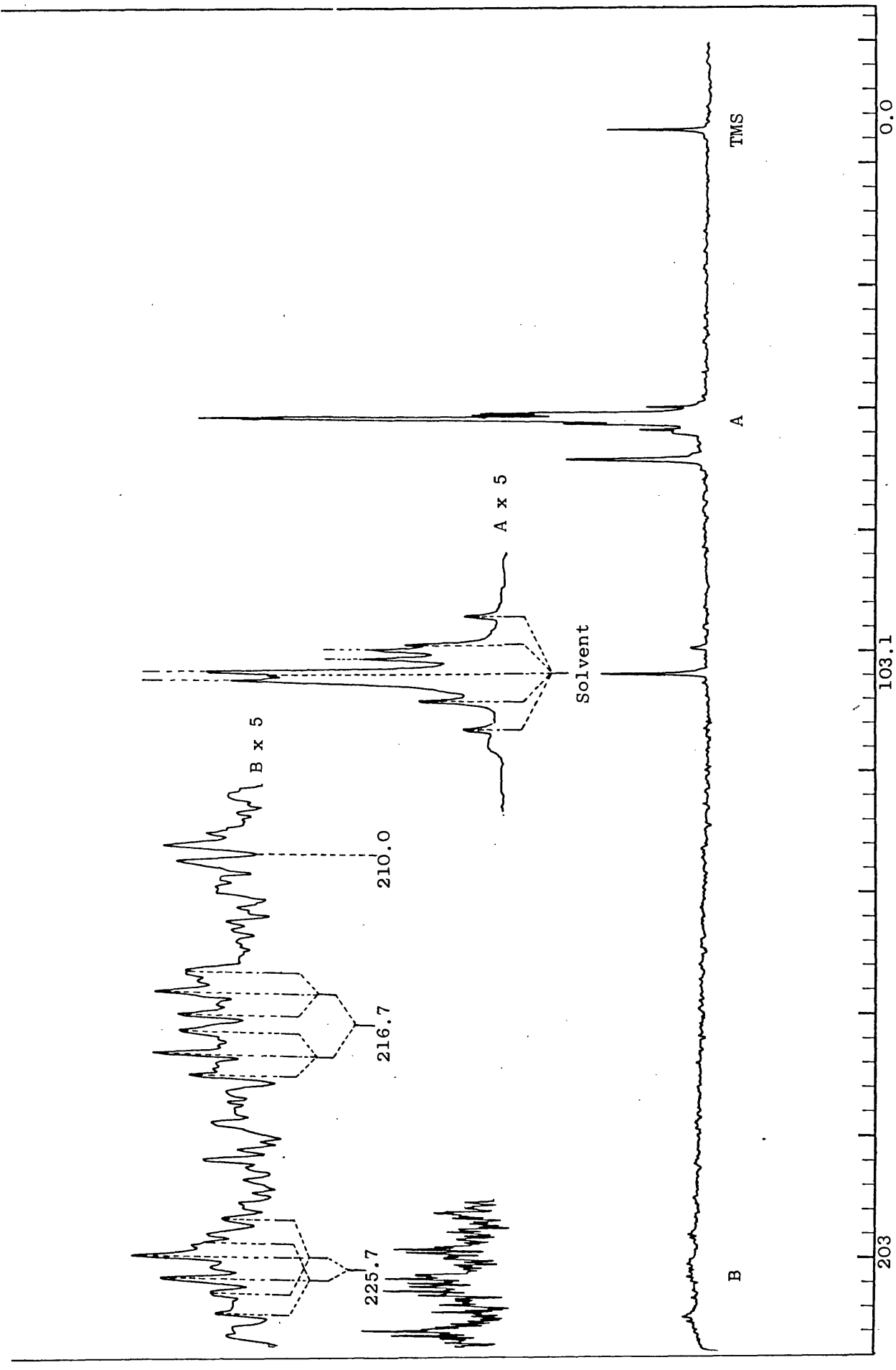

Figure 4.11: The ^{13}C NMR spectrum of $[(\eta^3\text{-}C_3H_5)Mo(CO)_2\{P(OMe)_3\}_3]BF_4$ recorded at -80°C in CD_2Cl_2

third of the latter, agrees well with similar cis and trans P - CO coupling in other phosphorus substituted carbonyl complexes of the Group 6 metals[320]. The position and fine structure of the other carbonyl signal in the spectrum is more uncertain. (see Figure 4.11), and several different assignments are possible, including (i) a quartet centred at 210.0 p.p.m. with all J(P-C) = 15.3 Hz; (ii) a quartet centred at 225.7 p.p.m. with all J(P-C) = 19.8 Hz; (iii) a doublet of triplets also centred at 225.7 p.p.m. in which one phosphorus atom couples with J(P-C) = 19.8 Hz and the other two couple equally with J(P-C) = 33.8 Hz. Randall[320] has demonstrated that the ^{13}C chemical shifts for carbonyl groups are sensitive to both changes in stereochemistry and electronic environment, and that an increase in electron density at the metal centre is reflected by an increase in δ(CO). Thus, since the electron density at the metal in (XXXI) should be less than that in (XXII), a decrease in δ (CO) may be expected for the equatorial carbonyl carbon atom in (XXXI) compared to that in (XXII) (which was assigned at 225.0 p.p.m.). This suggests that the quartet at 210.0 p.p.m. [J(P-C) = 15.3 Hz] is due to the second carbonyl carbon atom. However, if correct, this assignment implies that all three phosphorus atoms in (XXXI) couple equally with the equatorial carbonyl carbon atom which seems somewhat unlikely. Thus, since a more complex spin pattern is anticipated for this carbonyl carbon atom the doublet of triplets centred at 225.7 p.p.m., [$J(P_1\text{-}C)$ = 19.8 Hz, $J(P_2\text{-}C)$ = 33.3 Hz], appears the more probable assignment.

The limiting high temperature spectrum (+32°C) failed to provide any clue as to the true position of the resonance for the second carbonyl carbon because no signals could be detected in this region of the spectrum.

Equivalence of all the phosphite ligands and the equivalence of the ends of the allyl group were observed.

^{31}P NMR spectra The ^{31}P NMR spectrum of both (XXXI) and (XXXII) were of extremely poor quality. Only a single, broad, weak band was observed in each of the spectra regardless of temperature (Table 4.10).

The Dynamic Behaviour of the Complexes

$[(\eta^3\text{-}C_3H_4R)Mo(CO)_2\{P(OMe)_3\}_3]BF_4$

As mentioned earlier, the solution infrared spectrum of (XXXI) did not give any evidence for the presence of a second isomeric species in solution. This, together with the phosphorus coupling to the anti protons in the limiting high temperature ^{1}H NMR spectrum of (XXXI), suggests that the rearrangement processes observed for the neutral and cationic species are not analogous. Indeed only by repeated application of interconversion between the pentagonal bipyramidal and 3:4 type geometries, can interchange of all three phosphite ligands in (XXXI and XXXII) be achieved (see Scheme 4.2). It was not clear from the ^{13}C NMR spectrum of (XXXI) if in fact carbonyl site exchange was also occurring in the rearrangement as observed for (XXII). The phosphorus coupling to the anti protons in the limiting high temperature ^{1}H NMR of the cationic species suggests that the phosphorus atoms occupy sites not occupied or transversed by the phosphorus atoms in the neutral complexes. In view of the large $J(P_{axial}\text{-}H_X)$ coupling observed for (XXXI) and (XXXII) in the limiting low temperature spectra, it seems reasonable to assume that the smaller values of $J(P\text{-}H_X)$ observed in the high temperature spectra arise as a result of the phosphorus ligands occupying

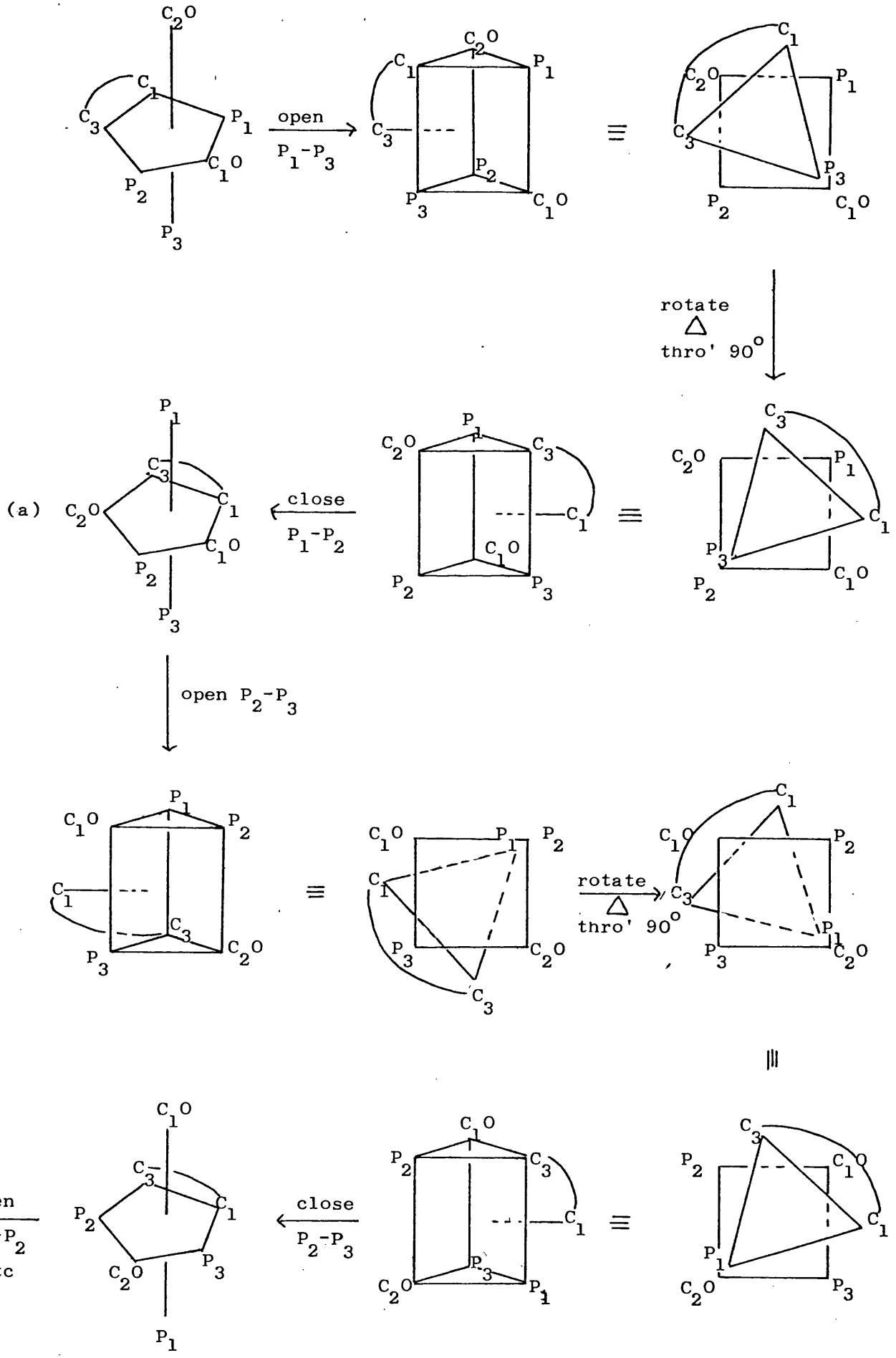
open
P1-P3
rotate
thro' 90°
close
P1-P2
(a)
open P2-P3
rotate
thro' 90°
open
P1-P2
etc
close
P2-P3

Scheme 4.2

axial sites in a short-lived pentagonal bipyramidal structure such as (a) in Scheme 4.2.

At present we are unable to offer any alternative mechanism to that described above to account for the fluxional behaviour of $[(\eta^3\text{-}C_3H_4R)Mo(CO)_2\{P(OMe)_3\}_3]BF_4$. Differences in the variable temperature spectra of these complexes compared to those recorded for their neutral precursors $[(\eta^3\text{-}C_3H_4R)M(CO)_2\{P(OR')_3\}_2X]$ may result from the introduction of a localised charge altering the dynamics of the system. Faller[181] has recently reported completely different dynamic behaviour for closely related neutral and cationic complexes.

Addendum

Late in 1980 whilst this thesis was in preparation a report by Bevan and Mawby[303] briefly mentioned that a crystal structure determination of $[(\eta^3\text{-}C_4H_7)Mo(CO)_2\{PMe_2Ph\}_2Cl]$ had shown that this complex adopts a structure similar to that found by us for $[(\eta^3\text{-}C_3H_5)Mo(CO)_2\{P(OMe)_3\}_2Cl]$ (XXII). The former complex and analogues were reported to exhibit temperature-dependent NMR spectra in which the two phosphorus ligands and the two ends of the η^3-allyl ligand appeared to be equivalent at all temperatures. The rate of rearrangement for the 2-methylallyl analogues was also reported to be slower than for the η^3-allyl complexes. Although, unfortunately, few details were given, the similarities in the behaviour of these complexes and those reported in this Chapter are clear.

The confirmation that other complexes of the type $[(\eta^3\text{-allyl})M(CO)_2L_2X]$, where L = unidentate phosphorus ligand, adopt the same stereochemistry as $[(\eta^3\text{-}C_3H_5)Mo(CO)_2\{P(OMe)_3\}_2Cl]$ suggests that electronic factors (with the phosphine and phosphite ligands being good π-acceptors) are of major importance in determining the stereochemistry of $[(\eta^3\text{-allyl})M(CO)_2]$ containing complexes in combination with three monodentate ligands.

CHAPTER FIVE

THE REACTIONS OF MONOTERTIARY PHOSPHINES AND DIPHENYLPHOSPHINE WITH $[(\eta^3\text{-}C_3H_4R)M(CO)_2(MeCN)_2Cl]$

INTRODUCTION

This chapter describes an investigation of the reactivity of $[(\eta^3\text{-}C_3H_4R)M(CO)_2(MeCN)_2Cl]$ (R = H, M = Mo or W; R = Me, M = Mo) with a variety of monotertiary phosphines, selected on the basis of their differing steric and/or electronic properties. The objective of this work was to extend the range of phosphorus reagents used in reaction with $[(\eta^3\text{-}C_3H_4R)M(CO)_2(MeCN)_2Cl]$ in order to establish if any coherent pattern could be identified which could be used to explain why some reagents, such as PPh_3 and $P(n\text{-}Bu)_3$ [249-251,253] cause reductive elimination of the η^3-allyl entity (via an unknown mechanism) whilst others such as dpe[222], dpm[162], $P(OR)_3$ (R = Me, Et, i-Pr) result in simple MeCN substitution reactions. Some interesting results were obtained when $PMePh_2$ was used, which supplied some mechanistic information on the reductive elimination reactions and this led to an investigation of the reactivity of PPh_3 with the 2-methylallyl complex $[(\eta^3\text{-}2\text{-}MeC_3H_4)Mo(CO)_2(MeCN)_2Cl]$.

EXPERIMENTAL

Details of physical techniques and solvents appear in appendix 3. The methods used for the preparation of the starting materials $[(\eta^3\text{-}C_3H_4R)M(CO)_2(MeCN)_2Cl]$ (R = H, M = Mo or W; R = Me, M = Mo) have been described in Chapter 1. The monotertiary phosphines Pcy_3, $PMePh_2$ and PPh_3, and the secondary phosphine $PHPh_2$, were obtained from commercial sources and used without further purification.

Reaction of $[(\eta^3\text{-}C_3H_5)M(CO)_2(MeCN)_2Cl]$ with Tricyclohexylphosphine

$[(\eta^3\text{-}C_3H_5)M(CO)_2(MeCN)_2Cl]$ (M = Mo or W) (0.5 mmol) in CH_3CN (10 cm^3) was treated with Pcy_3 (1.5 mmol, 0.42 g). The reaction mixture was warmed to ca. 40°C for 20 mins. The pale yellow precipitate which formed was collected by filtration and dried in vacuo. Infrared spectroscopy indicated that the precipitate was a mixture of $[M(CO)_2(Pcy_3)_2(MeCN)_2]$ and trans-$[M(CO)_4(Pcy_3)_2]$ Yields: M = Mo, 0.25 g, M = W, 0.09 g.

Reaction of $[(\eta^3\text{-}C_3H_5)M(CO)_2(MeCN)_2Cl]$ with Diphenylphosphine

Preparation of $[(\eta^3\text{-}C_3H_5)M(CO)_2(PHPh_2)_2Cl]$ (M = Mo or W)

$[(\eta^3\text{-}C_3H_5)M(CO)_2(MeCN)_2Cl]$ (1.0 mmol) dissolved in CH_3OH (15 cm^3) was treated with $PHPh_2$ (2 mmol, 0.35 cm^3) resulting in an immediate colour change from yellow to orange. The reaction mixture was stirred under a flow of nitrogen for 0.5 h and the orange crystals of $[(\eta^3\text{-}C_3H_5)M(CO)_2(PHPh_2)_2Cl]$ so obtained were filtered and recrystallised from $CHCl_3$/petroleum ether (40/60). Yields: M = Mo, 80%; M = W, 78% . Both products were soluble in CH_3CN, $CHCl_3$ and $(CH_3)_2CO$ but insoluble in CH_3OH, diethylether and saturated hydrocarbons.

Preparation of cis-$[M(CO)_2(PHPh_2)_4]$

A solution of $[(\eta^3\text{-}C_3H_5)M(CO)_2(MeCN)_2Cl]$ (1.0 mmol) and $PHPh_2$ (5.0 mmol, 0.88 cm^3) in CH_3OH (20 cm^3) was refluxed gently under nitrogen for 22 h (M = Mo) or 1.5 h (M = W). On cooling the black solution a small amount of brown-yellow powder was obtained. Recrystallisation from $(CH_3)_2CO/CH_3OH$ solution produced pale yellow crystals of analytically pure cis-$[M(CO)_2(PHPh_2)_4]$. Yields: M = Mo, 22%; M = W, 30%.

Reaction of $[(\eta^3\text{-}C_3H_4R)M(CO)_2(MeCN)_2Cl]$ (R = H, M = Mo or W; R = Me, M = Mo) with Methyldiphenylphosphine.

Preparation of $[M(CO)_2(MeCN)(PMePh_2)_3]$

a) From $[(\eta^3\text{-}C_3H_5)Mo(CO)_2(MeCN)_2Cl]$

The addition of $PMePh_2$ (4.0 mmol, 0.72 cm^3) to $[(\eta^3\text{-}C_3H_5)Mo(CO)_2(MeCN)_2Cl]$ (1.0 mmol, 0.31 g) dissolved in CH_3CN or CH_3OH (10 cm^3), caused an immediate colour change from yellow to orange. The mixture was stirred at room temperature for 1 h to give yellow $[Mo(CO)_2(MeCN)(PMePh_2)_3]$, which was collected by filtration, washed with CH_3CN and dried in vacuo. Yield 76%.

b) From $[(\eta^3\text{-}C_3H_5)W(CO)_2(MeCN)_2Cl]$

Treatment of $[(\eta^3\text{-}C_3H_5)W(CO)_2(MeCN)_2Cl]$ (1.0 mmol, 0.4 g) dissolved in CH_3CN (10 cm^3) with $PMePh_2$ (4.0 mmol, 0.72 cm^3) produced an immediate colour change from yellow to orange. After 0.5 h at room temperature a precipitate of $[W(CO)_2(MeCN)(PMePh_2)_3]$ could be obtained by dropwise addition of CH_3OH, or by storing the reaction mixture for 3 days at 10°C when the product crystallised spontaneously. Yield 82%.

The complex $[W(CO)_2(MeCN)(PMePh_2)_3]$ could also be prepared from the same reactants in CH_3OH, but at ambient temperatures the reaction was much slower in this solvent and it was necessary to employ forcing conditions (refluxing CH_3OH for 2 h) in order to achieve a good yield. Yield 62%.

c) From $[(\eta^3\text{-}C_3H_4R)Mo(CO)_2(MeCN)_3]BF_4$ (R = H or Me)

A solution of $[(\eta^3\text{-}C_3H_4R)Mo(CO)_2(MeCN)_3]BF_4$ (1.0 mmol) in CH_3CN or CH_3OH (10 cm^3) was treated with $PMePh_2$ (4.0 mmol, 0.72 cm^3) and the reaction mixture stirred for 0.5 h (R = H) or 1 h (R = Me). Yellow $[Mo(CO)_2(MeCN)(PMePh_2)_3]$ was filtered from the solution, washed with CH_3CN and dried *in vacuo*. Yields: R = H, 80%; R = Me, 60%.

d) From $Ph_4As[(\eta^3\text{-}C_3H_5)_2Mo_2(CO)_4Cl_3]$

A solution of $Ph_4As[(\eta^3\text{-}C_3H_5)_2Mo_2(CO)_4Cl_3]$ (0.33 mmol, 0.29 g) in CH_3CN (5 cm^3) was stirred for 1 h with $PMePh_2$ (2.64 mmol, 0.49 cm^3). The product $[Mo(CO)_2(MeCN)(PMePh_2)_3]$ which precipitated from the solution was collected by filtration, washed with CH_3CN, and dried *in vacuo*. Yield 45%.

e) From $[(\eta^3\text{-}C_3H_5)M(CO)_2(PMePh_2)_2Cl]$

(For the preparation of $[(\eta^3\text{-}C_3H_4R)M(CO)_2(PMePh_2)_2Cl]$ (R = H, M = Mo or W; R = Me, M = Mo) see below).

i) In CH_3CN

Addition of $PMePh_2$ (1 mmol, 0.18 cm^3) to a suspension of $[(\eta^3\text{-}C_3H_5)M(CO)_2(PMePh_2)_2Cl]$ (0.5 mmol) in CH_3CN (10 cm^3) produced an orange colouration in the previously colourless CH_3CN. The mixture was stirred with complete exclusion of air for 12 h (M = Mo) or 3 days (M = W) and the precipitate of $[M(CO)_2(MeCN)(PMePh_2)_3]$ collected by filtration, washed with CH_3CN, and dried *in vacuo*. At no time during the reaction period did the reaction mixture become a homogeneous solution. A yellow deposit of unreacted $[(\eta^3\text{-}C_3H_5)M(CO)_2(PMePh_2)_2Cl]$ was slowly replaced by solid $[M(CO)_2(MeCN)(PMePh_2)_3]$. Yields: M = Mo, 79%; M = W, 63%.

ii) In CH_3OH

For these reactions $[(\eta^3\text{-}C_3H_5)M(CO)_2(PMePh_2)_2Cl]$ was generated *in situ* by treating $[(\eta^3\text{-}C_3H_5)M(CO)_2(MeCN)_2Cl]$ (0.5 mmol) in CH_3OH (10 cm^3) with two equivalents of $PMePh_2$ (1.0 mmol, 0.18 cm^3). The precipitate obtained at this stage was identified as $[(\eta^3\text{-}C_3H_5)M(CO)_2(PMePh_2)_2Cl]$ (M = Mo or W) by infrared spectroscopy. After approximately 15 mins. the formation of $[(\eta^3\text{-}C_3H_5)M(CO)_2(PMePh_2)_2Cl]$ was assumed complete and the reaction mixture was treated with excess $PMePh_2$ (1 mmol, 0.18 cm^3). The phosphine formed an immiscible layer at the bottom of the reaction flask, and the precipitate of $[(\eta^3\text{-}C_3H_5)M(CO)_2(PMePh_2)_2Cl]$ slowly coagulated in the oily phosphine layer. For M = Mo, vigorous stirring of the reaction mixture for 1 h followed by scratching with a glass rod initiated precipitation of analytically pure $[Mo(CO)_2(MeCN)(PMePh_2)_3]$ in good yield. Reaction of $[(\eta^3\text{-}C_3H_5)W(CO)_2(PMePh_2)_2Cl]$ with $PMePh_2$ proved to be slower and it was necessary to boil the solution for 2 h in order to achieve reduction to yield analytically pure $[W(CO)_2(MeCN)(MePPh_2)_3]$. Yields: M = Mo, 76%; M = W, 52%.

The compounds $[M(CO)_2(MeCN)(PMePh_2)_3]$ were soluble in $CHCl_3$, CH_2Cl_2, $(CH_3)_2CO$ but insoluble in CH_3OH and saturated hydrocarbons. The tungsten derivative was also readily soluble in CH_3CN.

Preparation of $[(\eta^3\text{-}C_3H_4R)M(CO)_2(PMePh_2)_2Cl]$ (R = H, M = Mo or W; R = Me, M = Mo).

Dropwise addition of $PMePh_2$ (2.0 mmol, 0.36 cm^3) to a stirred solution of $[(\eta^3\text{-}C_3H_4R)M(CO)_2(MeCN)_2Cl]$ (1.0 mmol) in CH_3OH (20 cm^3) gave an orange precipitate which after 0.5 h at room temperature was filtered, washed with CH_3OH, and dried *in vacuo*. The products were

readily soluble in $CHCl_3$, CH_2Cl_2 and $(CH_3)_2CO$ and very slightly soluble in CH_3OH and CH_3CN. Yields: R = H, M = Mo, 64%; R = H, M = W, 83%; R = Me, M = Mo, 77%.

Preparation of $[PMePh_2(\sigma\text{-}C_3H_5)][(\eta^3\text{-}C_3H_5)M(CO)_2(PMePh_2)Cl_2]$ (M = Mo or W).

Addition of $PMePh_2$ (2.4 mmol, 0.44 cm^3) to $[(\eta^3\text{-}C_3H_5)M(CO)_2(MeCN)_2Cl]$ (1.0 mmol) dissolved in CH_3CN (10 cm^3) produced a deposit of $[M(CO)_2(MeCN)(PMePh_2)_3]$ which was filtered off after 1 h (M = Mo) or 3 days at 10°C (M = W). The filtrate was concentrated to ca. 6 cm^3 by evaporation at room temperature and treated dropwise with diethylether (ca. 1 cm^3). Storage of this solution at -10°C for 3 days (M = Mo) or 7 days (M = W) produced large crystals of analytically pure $[PMePh_2(\sigma\text{-}C_3H_5)][(\eta^3\text{-}C_3H_5)M(CO)_2(PMePh_2)Cl_2]$. These compounds were soluble in polar solvents but extremely sensitive to oxygen. Yields: M = Mo or W, 19%.

Preparation of mer-$[M(CO)_3(PMePh_2)_3]$. (M = Mo or W)

A solution of cis-mer-$[M(CO)_2(MeCN)(PMePh_2)_3]$ in CH_2Cl_2 (at room temperature) was outgassed and then saturated with carbon monoxide for ½ h. Addition of n-pentane to the brown solution produced a yellow precipitate of mer-$[M(CO)_3(PMePh_2)_3]$ which was recrystallised from $CHCl_3/CH_3OH$ at -10°C. Yield ca. 40%.

The yields of mer-$[M(CO)_3(PMePh_2)_3]$ obtained were greatly increased (M = Mo, 82%; M = W, 55%) when CH_3OH was used as solvent. However, the relative insolubilities of the starting material and products in this solvent necessitated much longer reaction times

at ambient temperatures (M = Mo, 2 days; M = W, 2 weeks). While a reaction time of only 5 h was required to prepare mer-$[Mo(CO)_3(PMePh_2)_3]$ (in quantitative yield) from cis-mer-$[Mo(CO)_2(MeCN)(PMePh_2)_3]$ in refluxing CH_3OH (with a carbon monoxide bubbler), the tungsten analogue could not be prepared in a similar manner.

Preparation of fac-$[M(CO)_3(PMePh_2)_3]$

(i) From cis-mer-$[M(CO)_2(MeCN)(PMePh_2)_3]$

Refluxing cis-mer-$[M(CO)_2(MeCN)(PMePh_2)_3]$ in CH_3CN (M = Mo or W) or CH_3OH (M = W) under an atmosphere of carbon monoxide for 3 h gave an insoluble off-white powder which was filtered off and recrystallised from $CHCl_3/CH_3OH$ at -10^oC to produce pure white crystals of fac-$[M(CO)_3(PMePh_2)_3]$. (Yield: M = W, ca. 60%; M = Mo, 47%).

(ii) From mer-$[Mo(CO)_3(PMePh_2)_3]$

Refluxing mer-$[Mo(CO)_3(PMePh_2)_3]$ in CH_3CN for 3 h produced insoluble fac-$[Mo(CO)_3(PMePh_2)_3]$ which was recrystallised from $CHCl_3/CH_3OH$. Yield 60%.

Reaction of $[(\eta^3\text{-}2\text{-}MeC_3H_4)Mo(CO)_2(MeCN)_2Cl]$ with Triphenylphosphine.

Preparation of $[Mo(CO)_2(MeCN)_2(PPh_3)_2]$

A solution of $[(\eta^3\text{-}2\text{-}MeC_3H_4)Mo(CO)_2(MeCN)_2Cl]$ (0.5 mmol, 0.16g) in CH_3CN (10 cm^3) was treated with 3 equivalents of PPh_3 (1.5 mmol, 0.39 g). The reaction mixture was thoroughly saturated with nitrogen and the vessel tightly sealed. After stirring for 4 days at room temperature the yellow precipitate was collected by filtration and

characterised by analysis and infrared spectroscopy.

Yield 37%. ν(CO) (nujol mull) 1809 shp s; 1738 shp s; ν(CN) 2263w. Literature[253] ν(CO) 1807s 1740s; ν(CN) 2265w. Analytical data Found: C, 66.0; H, 4.8; N, 3.8%. Calcd. for $MoC_{42}H_{36}N_2O_2P_2$: C, 66.5; H, 4.8; N, 3.7%.

Preparation of $[(\eta^3\text{-}2\text{-}MeC_3H_4)Mo(CO)_2(MeCN)(PPh_3)Cl].MeCN$

Triphenylphosphine (1 mmol, 0.26 g) in CH_3CN (20 cm^3) was warmed to effect solution. When the solution had cooled to room temperature $[(\eta^3\text{-}2\text{-}MeC_3H_4)Mo(CO)_2(MeCN)_2Cl]$ (1 mmol 0.32 g) was added. The reaction mixture was stirred at room temperature for ca. 0.5 h, during which time it gradually darkened in colour to a brownish-orange. Scratching the sides of the container initiated precipitation of a flocculent yellow precipitate which was collected by filtration and recrystallised from a large volume of CH_3CN to give fine yellow needle-like crystals on cooling to -18^oC. Yield 62%. The product was soluble in CH_3OH and chlorinated organic solvents but insoluble in saturated hydrocarbons and diethylether.

Details of elemental analyses and melting points where appropriate for the characterisation of new or previously only poorly characterised compounds are presented in Table 5.1.

Table 5.1: Melting Points and Analytical Data

Compound (No.)	M.Pt (°C)	Elemental Analysis found (calc.)(%) C	H
$[(\eta^3\text{-}C_3H_5)Mo(CO)_2(PHPh_2)_2Cl]$ (XXXIII)	98[a]	57.9 (58.0)	4.5 (4.5)
$[(\eta^3\text{-}C_3H_5)W(CO)_2(PHPh_2)_2Cl]$ (XXXIV)	119[a]	50.8 (50.6)	3.9 (4.0)
cis-$[Mo(CO)_2(PHPh_2)_4]$ (XXXV)	149-151	66.6 (67.0)	5.1 (5.0)
cis-$[W(CO)_2(PHPh_2)_4]$ (XXXVI)	161[b]	59.9 (61.0)	4.5 (4.5)
$[Mo(CO)_2(MeCN)(PMePh_2)_3]$ (XXXVII)[c]	75	64.2 (65.1)	5.3 (5.3)
$[W(CO)_2(MeCN)(PMePh_2)_3]$ (XXXVIII)[d]	100[a]	58.7 (58.6)	4.8 (4.8)
$[(\eta^3\text{-}C_3H_5)Mo(CO)_2(PMePh_2)_2Cl]$ (XXXIX)	91-95	58.7 (59.2)	5.2 (5.0)
$[(\eta^3\text{-}C_3H_5)W(CO)_2(PMePh_2)_2Cl]$ (XXXX)	115-117	51.7 (51.9)	4.4 (4.4)
$[(\eta^3\text{-}2\text{-}MeC_3H_4)Mo(CO)_2(PMePh_2)_2Cl]$ (XXXXI)	109-110	59.7 (59.8)	5.2 (5.0)
$[PMePh_2(\sigma\text{-}C_3H_5)][(\eta^3\text{-}C_3H_5)Mo(CO)_2(PMePh_2)Cl_2]$ (XXXXII)[e]	127-129	57.2 (57.9)	5.1 (5.1)
$[PMePh_2(\sigma\text{-}C_3H_5)][(\eta^3\text{-}C_3H_5)W(CO)_2(PMePh_2)Cl_2]$ (XXXXIII)	115[a]	51.0 (51.4)	4.6 (4.6)
mer-$[Mo(CO)_3(PMePh_2)_3]$ (XXXXIV)		63.8 (64.6)	4.9 (5.0)
mer-$[W(CO)_3(PMePh_2)_3]$ (XXXXV)		57.1 (58.1)	4.7 (4.3)
fac-$[Mo(CO)_3(PMePh_2)_3]$ (XXXXVI)		66.8 (64.6)	5.2 (5.0)
fac- $[W(CO)_3(PMePh_2)_3]$ (XXXXVII)		57.3 (58.1)	4.7 (4.5)
$[(\eta^3\text{-}2\text{-}MeC_3H_4)Mo(CO)_2(MeCN)(PPh_3)Cl].MeCN$ (XXXXVIII)[f]	76-79	57.32 (57.30)	4.7 (4.81)

...../cont'd

[a] - decomposed [b] - melts with decomposition

[c] - also analysed for nitrogen N 1.7 (1.8) %

[d] - also analysed for nitrogen N 1.7 (1.6)%

[e] - also analysed for chlorine Cl 9.9 (10.1)%

[f] - also analysed for nitrogen and chlorine; N 4.82 (4.92), Cl 6.28 (6.04)%.

RESULTS AND DISCUSSION

Reaction of $[(\eta^3\text{-}C_3H_5)M(CO)_2(MeCN)_2Cl]$ with Tricyclohexylphosphine

Tricyclohexylphosphine reacted with $[(\eta^3\text{-}C_3H_5)M(CO)_2(MeCN)_2Cl]$ (M = Mo or W) under mild conditions to form the reduced cis-dicarbonyl compounds $[M(CO)_2(MeCN)_2(Pcy_3)_2]$. The marked instability of these compounds was indicated by their rapid decomposition in solution to trans-$[M(CO)_4(Pcy_3)_2]$[337] and as a consequence analytically pure samples could not be obtained. However, similarities in the positions of the ν(CO) and ν(CN) stretching frequencies for the compounds, (Table 5.2) and the data reported for the PPh_3 derivatives $[M(CO)_2(MeCN)_2(PPh_3)_2]$ [M = Mo[253], ν(CO) 1807s 1740s, ν(CN) 2265w; M = W[251], ν(CO) 1803s, 1733s, ν(CN) 2260w] supports their formulation as $[M(CO)_2(MeCN)_2(Pcy_3)_2]$. The reaction between Pcy_3 and $[(\eta^3\text{-}C_3H_5)M(CO)_2(MeCN)_2Cl]$ was conducted at both high (+80°C) and low (-18°C) temperatures, but in neither instance was there any evidence for the formation of an intermediate such as $[(\eta^3\text{-}C_3H_5)M(CO)_2(Pcy_3)_2Cl]$, prior to the formation of the reduced product.

Table 5.2: Selected Infrared Data* for the Compounds $[M(CO)_2(Pcy_3)_2(MeCN)_2]$ and trans-$[M(CO)_4(Pcy_3)_2]$

Compound	ν(CO)		ν(CN)
$[Mo(CO)_2(MeCN)_2(Pcy_3)_2]$	1787s	1713s	2230w
$[W(CO)_2(MeCN)_2(Pcy_3)_2]$	1784s	1719s	2230w
trans-$[Mo(CO)_4(Pcy_3)_2]$[a]	1920w	1867s	
trans-$[W(CO)_4(Pcy_3)_2]$[b]	1912w	1865s	

* - As nujol mulls. [a] - Literature data for trans-$[Mo(CO)_4(Pcy_3)_2]$[337] ν(CO)(KBr); 2000vw 1922w 1860vs. [b] - Literature data for trans-$[W(CO)_4(Pcy_3)_2]$[337] ν(CO)(KBr); 1917(sh) 1856vs.

Despite several attempts, utilizing a variety of conditions, no reaction between PCl_3 and $[(\eta^3\text{-}C_3H_5)M(CO)_2(MeCN)_2Cl]$ (M = Mo or W) could be detected. This was not surprising since $P(OPh)_3$ which is also a poor nucleophile was similarly found to be unreactive towards $[(\eta^3\text{-}C_3H_5)M(CO)_2(MeCN)_2Cl]$ (see Chapter 4).

Reaction of $[(\eta^3\text{-}C_3H_5)M(CO)_2(MeCN)_2Cl]$ (M = Mo or W) with Diphenylphosphine.

Diphenylphosphine reacted with $[(\eta^3\text{-}C_3H_5)M(CO)_2(MeCN)Cl]$ (M = Mo or W) in an analogous manner to the ditertiary phosphines dpm and dpe. Under ambient conditions in CH_3OH, virtually quantitative yields of the orange crystalline compounds $[(\eta^3\text{-}C_3H_5)M(CO)_2(PHPh_2)_2Cl]$ were obtained. The same products, although in considerably reduced yields (ca. 45%) could also be isolated when using CH_3CN as solvent. Under more forcing conditions (in CH_3OH), and in the presence of excess phosphine, reduction occurred to give cis-$[M(CO)_2(PHPh_2)_4]$ (M = Mo or W). Somewhat surprisingly reaction times of 22h were necessary to prepare cis-$[Mo(CO)_2(PHPh_2)_4]$ whilst the tungsten analogues could be isolated in similar yield after only 1.5 h.

Table 5.3: Selected Infrared Data for $[(\eta^3\text{-}C_3H_5)M(CO)_2(PHPh_2)_2Cl]$ and cis-$[M(CO)_2(PHPh_2)_4]$, (M = Mo or W)

Complex Number	ν(CO) (cm^{-1})[a] 2A'	$M(CO)_2$ Angle (°)[b]	ν(MX) (cm^{-1})[c]	ν(PH) (cm^{-1})[c]
XXXIII	1952s 1855s	85	234s	2337br w
XXXIV	1940s 1845s	80	245s	2340br w
XXXV	1871s 1806s	90	-	2295w 2260w
XXXVI	1864s 1802s	91	-	2280br w

[a] - in $CHCl_3$

[b] - Calculated from carbonyl band intensity data

[c] - Recorded on Nujol mulls.

Table 5.4: ^{1}H NMR Data for the Compounds $[(\eta^{3}\text{-}C_3H_5)M(CO)_2(PHPh_2)_2Cl]$ (M = Mo or W).

Complex	Temp. (°C)	δ(multiplicity, rel. intensity) Allyl Protons H_X	H_M	H_A	Other Protons
XXXIII	29[a]	1.80(dd, 2H) J_{XA} 10.0 J_{XP} 2.0	3.49 (dt, 2H) J_{MA} 7.3 J_{MP} 2.8	3.71 (m, 1H)	5.88 (m[b], 2H) $\underline{P}HPh_2$ 7.72 (m, 20H) $P\underline{HPh_2}$
	-125[c]	1.43 2.09	3.46 3.17	3.29	4.09}[d] 3.79} $\underline{P}HPh_2$
XXXIV	29[a]	1.91 (dd, 2H) J_{XA} 9.0 J_{XP} 2.0	3.35 (dt, 2H) J_{MA} 5.5 J_{MP} 3.0	3.04 (m, 1H)	6.24 (m[e], 2H) $\underline{P}HPh_2$ 7.42 (m, 20H) $P\underline{HPh_2}$
	-125[c]	1.60 2.10	3.00 3.26	2.78	4.28 v br[f]

[a] - In $CDCl_3$; [b] - Centre of an XAA'X' spectrum in which J(AX) = 345 Hz and J(AX') = 15 Hz; [c] - In $CHCl_2F$; [d] - Splitting of high field part of XAA'X' spectrum observed at 29°C; [e] - Centre of an XAA'X spectrum in which J(AX) = 352 Hz and J(AX') = 6 Hz; [f] - High field part of XAA'X' spectrum observed at room temperature.

Characterisation of the Products obtained from the Reaction of $[(\eta^3\text{-}C_3H_5)M(CO)_2(MeCN)_2Cl]$ (M = Mo or W) with Diphenylphosphine

Selected infrared spectral data for the compounds $[(\eta^3\text{-}C_3H_5)M(CO)_2(PHPh_2)_2Cl]$ and cis-$[M(CO)_2(PHPh_2)_4]$ (M = Mo or W) are presented in Table 5.3. ^{1}H NMR spectral data for the former compounds are summarised in Table 5.4.

(i) $[(\eta^3\text{-}C_3H_5)M(CO)_2(PHPh_2)_2Cl]$ (M = Mo or W)

These complexes have been reported previously[254] in the proceedings of a conference but details of their preparation and characterisation have yet to appear in the primary literature. The infrared spectra of (XXXIII) and (XXXIV) consisted of two bands of approximately equal intensity in the carbonyl region, typical of cis-dicarbonyls. Intensity measurements were used to estimate $M(CO)_2$ bond angles, the values of which, at 85° and 80° [for (XXXIII) and (XXXIV) respectively] are some 15-20° smaller than those determined for the analogous $P(OMe)_3$ derivatives (XXII - XXX), but similar to those reported for other compounds of the type $[(\eta^3\text{-allyl})M(CO)_2L_2X]$ (see Table 1.8) which adopt pseudo-octahedral geometries in the solid state.

Both (XXXIII) and (XXXIV) exhibit dynamic ^{1}H NMR spectra. The phosphorus-decoupled spectra at room temperature showed three sets of resonances for the allyl moiety, typical of the AMM'XX' spin system of symmetrical or fluxional allyls. In the phosphorus-coupled spectra the syn protons showed equal coupling to two phosphorus nuclei, [$J(P\text{-}H_M)$ ca. 3 Hz] with the anti protons coupled to just one phosphorus nucleus [$J(P\text{-}H_X)$ ca. 2 Hz]. As mentioned in Chapter 1,

coupling of phosphorus to the anti allylic protons [H_X] of a Group VI metal-allyl compound is rarely observed and in this instance it is difficult to explain why the anti protons should couple strongly with only one phosphorus, whilst the syn protons couple equally with two. The resonance pattern observed for the P-H protons of the equivalent $PHPh_2$ ligands was easily identified as the X part of an XAA'X' (X = H; A = P) spin system and is characteristic of the type which corresponds to "intermediate" phosphorus-phosphorus coupling. Harris[338] has developed the theory of nuclear spin systems of the $X_nAA'X_n'$ type (with the X nuclei magnetically equivalent) and has shown that a simple 1:2:1 triplet will be observed in the X spectrum when $|J(A-A')| \gg |J(A-X) - J(A-X')|$ i.e. when the A nuclei are strongly (or so-called "virtually") coupled. His equations also indicate that when $|J(A-A')|$ is small a 1:1 doublet should be observed. When $|J(A-A')|$ is intermediate however, several X absorption resonances lying between a 1:1 doublet of separation $|J(A-X) + J(A-X')|$ would be expected. For (XXXIII) and (XXXIV) the ^1H NMR spectrum of the P-H protons consisted of four lines with spacings N and L (see Figure 5.1) and evaluation of both $|J(A-X)| = |^1J(P-H)|$ and $|J(A-X')| = |^3J(P-H)|$ was possible (see Table 5.4).

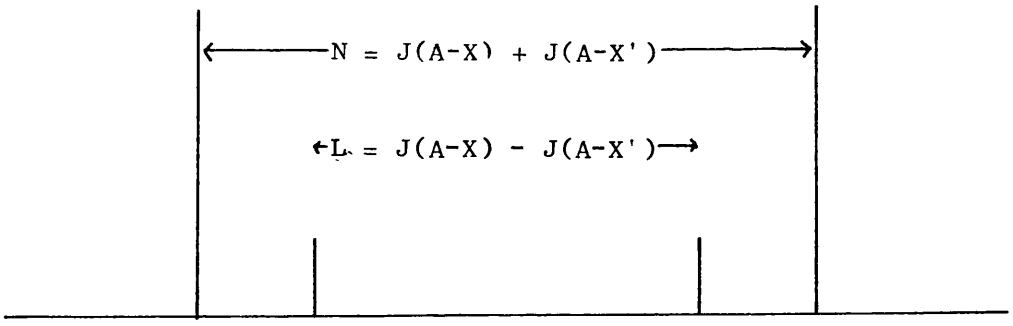

Figure 5.1: Diagrammatic representation of the X part of an XAA'X' spin system.

The limiting low temperature spectra for (XXXIII) and (XXXIV) obtained below -120°C showed the inequivalence of the two ends of the allyl moiety. Thus at -125°C the spectrum of the molybdenum complex (XXXIII), showed five resonances of equal intensity in the allyl region centred at 1.43 and 2.09 p.p.m. (H_X); 3.46 and 3.17 p.p.m. (H_M) and 3.29 p.p.m. (H_A). Inequivalence of the $PHPh_2$ ligands was also indicated by the splitting of the high field part of the XAA'X' signal (observed at room temperature), into two components (at 3.79 and 4.09 p.p.m.). The low field part of the XAA'X' resonance was obscured by signals due to the solvent $CHCl_2F$.

The variable temperature ^1H NMR spectra of (XXXIII) and (XXXIV) are analogous to that reported for the related compound $[(\eta^3\text{-}C_3H_5)Mo(CO)_2(dpe)Cl]$[171] and this implies that their dynamic behaviour involves a similar rearrangement process[171]. The optimum low temperature spectra suggest that the complexes adopt low symmetry pseudo-octahedral geometries in solution at low temperatures, and thus it seems reasonable to assume that the solid-state structures of (XXXIII) and (XXXIV) are analogous to that of $[(\eta^3\text{-}C_3H_5)Mo(CO)_2(dpe)Cl]$[171] and unlike those of $[(\eta^3\text{-}C_3H_5)Mo(CO)_2\{P(OMe)_3\}_2Cl]$ and $[(\eta^3\text{-}2\text{-}MeC_3H_4)Mo(CO)_2(PPhMe_2)_2Cl]$.[303] This is somewhat surprising when one considers the similarity of the electronic and steric requirements[317] of $PHPh_2$, $P(OMe)_3$ and $PMePh_2$.

(ii) cis-$[M(CO)_2(PHPh_2)_4]$ (M = Mo or W).

Relatively few compounds of the type cis-$[M(CO)_2(P)_4]$ (where M = Cr, Mo or W and P = monodentate phosphorus ligand) are known[339-342]. The reduced products cis-$[M(CO)_2(PHPh_2)_4]$ (M = Mo or W) reported here provide new examples. The infrared spectra of (XXXV) and (XXXVI) (see Table 5.3) agree with their formulation as cis-dicarbonyl compounds, for (XXXV) two ν(P-H) stretching bands were clearly resolved, however, only a single broad band was observed in this region for (XXXVI). The ^1H NMR spectra of $CDCl_3$ solutions of the compounds were disappointing for they showed only a broad resonance (7.5-7.1 p.p.m.) for the aromatic protons of the $PHPh_2$ ligands — no signals for the P-H protons could be detected. Complex resonance patterns were anticipated for the latter protons because of their coupling to phosphorus nuclei involved in "virtual" and "intermediate" coupling (strong phosphorus-phosphorus coupling of phosphines occupying trans positions giving rise to virtually coupled systems is frequently encountered[343-345]). Failure to observe the resonances may be associated with the small intensities of the constituent lines of these patterns.

✓ The species claimed[342] to be cis-$[Mo(CO)_2(PPh_3)_4]$ has ν(CO) bands at 1940 and 1840 cm^{-1}. These frequencies are so different to those of cis-$[Mo(CO)_2(PHPh_2)_4]$ (1871 and 1806 cm^{-1}) and other dicarbonylmolybdenum(0) complexes[339-341] as to raise doubts as to whether the complex has in fact been correctly formulated.

Reactions of $[(\eta^3\text{-}C_3H_4R)M(CO)_2(MeCN)_2Cl]$ (R = H, M = Mo or W; R = Me, M = Mo) with Methyldiphenylphosphine

From the results thus far described it appears that the reactivity of phosphorus ligands with $[(\eta^3\text{-}C_3H_5)M(CO)_2(MeCN)_2Cl]$ could, perhaps, be correlated with their size. Thus phosphorus donors with small cone angles[317] (see Table 5.5) such as $P(OMe)_3$, $P(OEt)_3$, dpm, dpe, $PHPh_2$ and $P(Oi\text{-}Pr)_3$ react with $[(\eta^3\text{-}C_3H_5)M(CO)_2(MeCN)_2Cl]$, under ambient conditions, to give the M(II) compounds $[(\eta^3\text{-}C_3H_5)M(CO)_2L_2Cl]$ whereas donors with greater steric requirements e.g. $P(n\text{-}Bu)_3$, PPh_3 and Pcy_3 effect reduction to yield the Mo(0) compounds $[M(CO)_2(MeCN)L_2L']$ (L' = L or MeCN). There is no doubt however, that electronic factors are also important in determining the reactivity of the phosphorus ligands. This has been demonstrated by our observations that weakly nucleophilic PR_3 reagents (where R is a particularly electronegative substituent such as -Cl or -OPh), fail to attack $[(\eta^3\text{-}C_3H_5)M(CO)_2(MeCN)_2Cl]$ at all. Although it is extremely difficult to gauge the electronic properties of a set of reagents, since many different contributary factors may be involved[346], an estimate of σ-donor or nucleophilicity may be obtained by considering pK_a[347]≠ values; however, since this parameter is actually a measure of basicity its use in this way should be viewed with caution. Tolman[317] and others[348] are of the opinion that phosphorus ligands can be ranked in an electronic series based on the ν(CO) stretching frequencies of uncrowded mono-substituted metal carbonyl compounds such as $Ni(CO)_3L$ (where L = phosphorus ligand). Whilst this has been found to be a reasonable guide, both the σ-donor

≠ $pK_b = pK_w - pK_a$ where pK_a is for the conjugate acid BH^+ of the base B.

and π-acceptor capabilities of individual ligands are involved, and thus this approach should not be viewed as a comparative measure of one or the other. Having pointed out these shortcomings, we feel reasonably confident in describing the phosphorus ligands PPh_3 and $P(n\text{-}Bu)_3$ which cause reduction of $[(\eta^3\text{-}C_3H_5)M(CO)_2(MeCN)_2Cl]$ under ambient conditions, as the most nucleophilic of the reagents which have been investigated to this point.

With these trends and correlations in mind it seemed appropriate to select for further study, a phosphine ligand with steric and electronic requirements intermediary between those which give adduct formation and those which cause reduction. The choice was based on the electronic parameters and cone angles for phosphorus ligands compiled by Tolman[317]. $PMePh_2$ and PMe_2Ph appeared to be the most suitable candidates, for both had smaller cone angles than PPh_3, and PMe_2Ph also had a smaller cone angle than $P(n\text{-}Bu)_3$, but were less electronegative (see Table 5.5). The former, $PMePh_2$ was eventually selected for the investigations in view of its greater availability.

Treatment of $[(\eta^3\text{-}C_3H_5)M(CO)_2(MeCN)_2Cl]$ (M = Mo or W) in CH_3OH with two equivalents of $PMePh_2$ under ambient conditions yielded the substituted complexes $[(\eta^3\text{-}C_3H_5)M(CO)_2(PMePh_2)_2Cl]$. Addition of an excess of the phosphine (two equivalents) and a prolonged reaction time (1 h at room temperature M = Mo; 2 h at 60°C for M = W) resulted in the formation of the reduced products <u>cis-mer-</u> $[M(CO)_2(MeCN)(PMePh_2)_3]$. The reduced products

Table 5.5: Electronic Parameters and Cone Angles for Phosphorus Ligands*

Phosphorus Ligand	Electronic Parameter (cm^{-1})	Cone Angle (^{o})
$P(OMe)_3$	2070.5	104
$P(OEt)_3$	2076.3	109
dpm	a	121
PMe_2Ph	2065.3	122
PCl_3	2097.0	124
dpe	a	125
$PHPh_2$	2073.3	128
$P(OPh)_3$	2085.3	128
$P(Oi\text{-}Pr)_3$	2075.9	130
$P(n\text{-}Bu)_3$	2060.3	132
$PMePh_2$	2067.0	136
PPh_3	2068.9	145

* - Values as reported in ref. 317

a - not reported.

(XXXVII) and (XXXVIII) could also be obtained, and in similar yield, when CH_3CN was used as solvent; however, the neutral bis-$PMePh_2$ derivatives, (XXXIX) and (XXXX), did not appear to be important intermediates in the reduction process in this solvent. The solubility of (XXXIX) and (XXXX) in CH_3CN is so low that if they were formed in any significant quantities their precipitation would, undoubtedly, have occurred. In addition the preformed adducts, (XXXIX) and (XXXX), were observed to react much more slowly with CH_3CN solutions of $PMePh_2$ (M = Mo T = 12 h; M = W T = 3 days), to form the reduced products, than the corresponding starting materials, $[(\eta^3\text{-}C_3H_5)M(CO)_2(MeCN)_2Cl]$ (M = Mo T = 1 h; M = W T = 0.5 h). When CH_3CN solutions of $[(\eta^3\text{-}C_3H_5)M(CO)_2(MeCN)_2Cl]$ were treated with less than four equivalents of $PMePh_2$, the cis-mer-$[M(CO)_2(MeCN)(PMePh_2)_3]$ complexes were still obtained, (although in reduced yields). Under these conditions it was also possible to isolate the new unreduced compounds, $[PMePh_2(\sigma\text{-}C_3H_5)][(\eta^3\text{-}C_3H_5)M(CO)_2(PMePh_2)Cl_2]$ M = Mo (XXXXII) and M = W (XXXXIII) from the reaction mixtures. The crystal structure of $NEt_4[(\eta^3\text{-}C_3H_5)W(CO)_2(PPh_3)Cl_2]$, containing a very similar anion, has been determined recently[240]. Interestingly, the authors[349] of this work have reported that this compound, together with $[W(CO)_2(MeCN)_2(PPh_3)_2]$, is formed by the reaction of $[(\eta^3\text{-}C_3H_5)_2W_2(CO)_4Cl_3]^-$ with PPh_3 in CH_3CN. Since the analogous tri-halo-bridged anion $[(\eta^3\text{-}C_3H_5)_2Mo_2(CO)_4Cl_3]^-$ is present in CH_3CN but not CH_3OH solutions of $[(\eta^3\text{-}C_3H_5)Mo(CO)_2(MeCN)_2Cl]$ ✓ it seems likely that $[(\eta^3\text{-}C_3H_5)Mo(CO)_2(PMePh_2)Cl_2]$ and at least some of the reduced

✓ See Chapter 2

product cis-mer-$[Mo(CO)_2(MeCN)(PMePh_2)_3]$, obtained from the reaction of $[(\eta^3\text{-}C_3H_5)Mo(CO)_2(MeCN)_2Cl]$ and $PMePh_2$ in CH_3CN, results from the reaction of the phosphine with $[(\eta^3\text{-}C_3H_5)_2Mo_2(CO)_4Cl_3]^-$. Indeed, the treatment of CH_3CN solutions of $[(\eta^3\text{-}C_3H_5)_2Mo_2(CO)_4Cl_3]^-$ with excess $PMePh_2$ confirmed that cis-mer-$[Mo(CO)_2(MeCN)(PMePh_2)_3]$ was produced, although $[(\eta^3\text{-}C_3H_5)Mo(CO)_2(PMePh_2)Cl_2]^-$ could not be isolated from the same reaction mixture. Further studies revealed that exposure of $[(\eta^3\text{-}C_3H_5)Mo(CO)_2(PMePh_2)Cl_2]^-$ in CH_3CN to excess $PMePh_2$ also led to the formation of the reduced products.

Acetonitrile solutions of $[(\eta^3\text{-}C_3H_5)Mo(CO)_2(MeCN)_2Cl]$ also contained significant concentrations of the cation $[(\eta^3\text{-}C_3H_5)Mo(CO)_2(MeCN)_3]^+$. For purely electronic reasons[350] one would anticipate that this cation would be much more susceptible to nucleophilic attack than either the anion, $[(\eta^3\text{-}C_3H_5)_2Mo_2(CO)_4Cl_3]^-$, or the neutral complex $[(\eta^3\text{-}C_3H_5)Mo(CO)_2(MeCN)_2Cl]$. For this reason the reactivity of $PMePh_2$ with $[(\eta^3\text{-}C_3H_5)Mo(CO)_2(MeCN)_3]BF_4$ was investigated. As predicted, a rapid reaction occurred and cis-mer-$[Mo(CO)_2(MeCN)(PMePh_2)_3]$ was obtained in very good yield. Despite employing a variety of reaction conditions no intermediate, for example a metal-stabilised C-phosphonium complex similar to that proposed by McCleverty et al[351] or a phosphine-substituted Mo(II) derivative, could be isolated from the reaction. Hence no distinction between the two most probable modes of reaction (i.e. direct addition to the allyl ligand or initial attack at the metal centre with displacement of a MeCN ligand) was possible.

The experimental observations described above suggest that the reduced product cis-mer-$[Mo(CO)_2(MeCN)(PMePh_2)_3]$ is formed by either of two routes which are solvent-dependent according to Scheme 5.1. For the tungsten compound a similar reaction scheme is proposed despite our inability to detect any appreciable ionisation of $[(\eta^3\text{-}C_3H_5)W(CO)_2(MeCN)_2Cl]$ in CH_3CN; as pointed out in Chapter 1 this is probably due to the pronounced tendency of $[(\eta^3\text{-}C_3H_5)_2W_2(CO)_4Cl_3]^-$ to be solvolysed to $[(\eta^3\text{-}C_3H_5)W(CO)_2(MeCN)_2Cl]$ in excess CH_3CN. The isolation of $[PMePh_2(\sigma\text{-}C_3H_5)][(\eta^3\text{-}C_3H_5)W(CO)_2(PMePh_2)Cl_2]$ from reaction mixtures of $[(\eta^3\text{-}C_3H_5)W(CO)_2(MeCN)_2Cl]$ and $PMePh_2$ in CH_3CN, suggests that $[(\eta^3\text{-}C_3H_5)_2W_2(CO)_4Cl_3]^-$ is present, albeit only transiently, in these solutions.

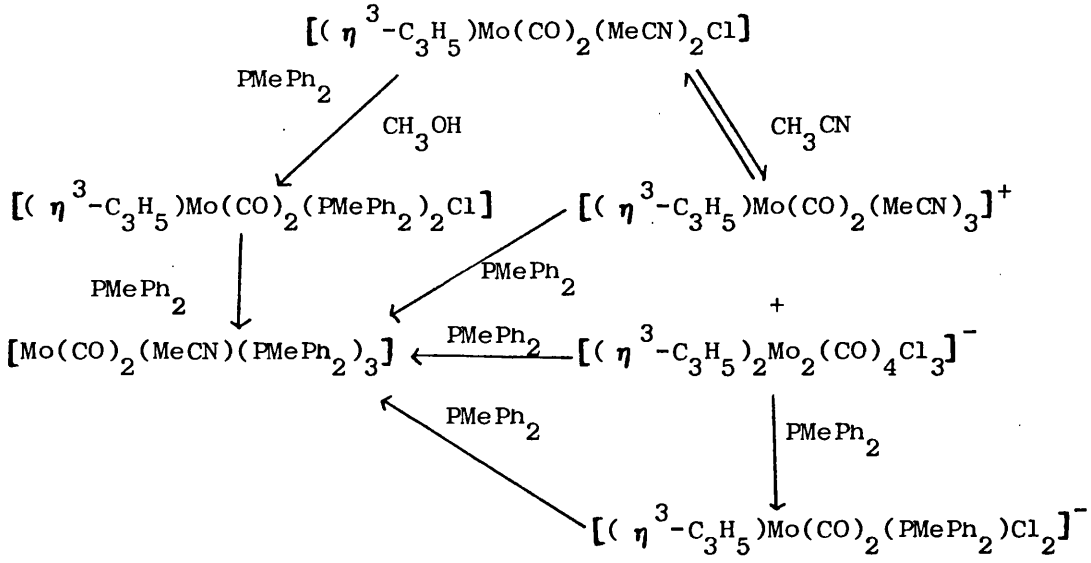

Scheme 5.1

The 2-methylallyl complex $[(\eta^3\text{-2-Me}C_3H_4)Mo(CO)_2(MeCN)_2Cl]$ which does not ionise in CH_3CN or CH_3OH, reacts with $PMePh_2$ in either of these solvents to form the substituted complex $[(\eta^3\text{-2-Me}C_3H_4)Mo(CO)_2(PMePh_2)_2Cl]$ (XXXXI) in similar yield. Reduction of this species with $PMePh_2$ was, however, so much slower than for the corresponding allyl complexes (XXXIX) and (XXXX), that it was only possible to isolate samples of cis-mer-$[Mo(CO)_2(MeCN)(PMePh_2)_3]$ which were contaminated with either the unreduced 2-methylallyl complex, or with mer-$[Mo(CO)_3(PMePh_2)_3]$ (which, as is discussed later, arises as a decomposition product of cis-mer-$[Mo(CO)_2(MeCN)(PMePh_2)_3]$). Extended reaction times, under ambient conditions, in CH_3CN gave only mer-$[Mo(CO)_3(PMePh_2)_3]$ but the use of more forcing conditions produced mixtures of mer- and fac-$[Mo(CO)_3(PMePh_2)_3]$, together with other carbonyl-containing decomposition products.

The difference in the rates of reduction of (XXXXI) and (XXXIX), and (XXXX) probably reflects the inductive effect of the methyl substituent on the allyl ligand. It is, however, also plausible that attack by the phosphine on the 2-methylallyl derivative may be sterically hindered by the methyl substituent. This protective capacity of the methyl substituent did not, however, extend to the cationic species $[(\eta^3\text{-2-Me}C_3H_4)Mo(CO)_2(MeCN)_3]^+$ which was readily reduced by $PMePh_2$ in CH_3CN and CH_3OH to form cis-mer-$[Mo(CO)_2(MeCN)(PMePh_2)_3]$ in good yield.

Whilst the work described in this section was being conducted some other co-workers, Mawby *et al*[352] were also engaged on an investigation of the reactivity of the molybdenum compounds $[(\eta^3\text{-}C_3H_4R)Mo(CO)_2(MeCN)_2Cl]$ (R = H or Me) with $PMePh_2$ and PMe_2Ph. From their experimental observations they suggested that, regardless of solvent, reaction of both phosphines occurs in two steps - initial substitution to form $[(\eta^3\text{-}C_3H_4R)Mo(CO)_2L_2Cl]$ (L = $PMePh_2$ or PMe_2Ph) followed by subsequent reduction to give $[Mo(CO)_2(PMe_2Ph)_4]$ or $[Mo(CO)_2(MeCN)(PMePh_2)_3]$. Although neither of the unsubstituted allyl compounds $[(\eta^3\text{-}C_3H_5)Mo(CO)_2L_2Cl]$, was actually isolated from the reaction mixtures their intermediate formation in the reduction process was implied by a comparison of the solution infrared spectra of the reaction mixtures with those of the isolated 2-methylallyl derivatives $[(\eta^3\text{-}2\text{-}MeC_3H_4)Mo(CO)_2(L)_2Cl]$, (L = $PMePh_2$ or PMe_2Ph). Careful comparison by us of the solution infrared spectrum of $[(\eta^3\text{-}C_3H_5)Mo(CO)_2(PMePh_2)_2Cl]$ in CH_3CN with that of the reaction mixture of $[(\eta^3\text{-}C_3H_5)Mo(CO)_2(MeCN)_2Cl]$ and $PMePh_2$ in CH_3CN, did disclose certain coincidences in the carbonyl region but since the bands were very broad, and the ν(CO) band positions for $[(\eta^3\text{-}C_3H_5)M(CO)_2(PMePh_2)_2Cl]$ (M = Mo ν(CO)CH_3CN 1932s, 1840s) and $[PMePh_2(\sigma\text{-}C_3H_5)][(\eta^3\text{-}C_3H_5)M(CO)_2(PMePh_2)Cl]$ (M = Mo ν(CO)CH_3CN 1936 br s, 1845 br s) are very similar, we could not determine with any confidence whether or not the substituted species were in fact present in these reaction mixtures. However, on the basis of the differences in the rate of reaction of $[(\eta^3\text{-}C_3H_5)Mo(CO)_2(PMePh_2)_2Cl]$ and $[(\eta^3\text{-}C_3H_5)Mo(CO)_2(MeCN)_2Cl]$ with $PMePh_2$ in CH_3CN we consider that the reduction of $[(\eta^3\text{-}C_3H_5)Mo(CO)_2(MeCN)_2Cl]$ by $PMePh_2$ in this solvent does not involve the neutral substituted derivatives as suggested by the other workers[352].

Physical data for $[(\eta^3\text{-}2\text{-}MeC_3H_4)Mo(CO)_2(PMePh_2)_2]$ and $[Mo(CO)_2(MeCN)(PMePh_2)_2]$ reported by Mawby *et al*[352] agree well with those presented below for these compounds.

Characterisation and Properties of the Products obtained from the Reaction of $[(\eta^3\text{-}C_3H_4R)M(CO)_2(MeCN)_2Cl]$ (R = H, M = Mo or W; R = Me, M = Mo) with Methyldiphenylphosphine.

(i) $[(\eta^3\text{-}C_3H_4R)M(CO)_2(PMePh_2)_2Cl]$ (R = H, M = Mo or W; R = Me, M = Mo)

Infrared and ^1H NMR spectral data for (XXXIX), (XXXX) and (XXXXI) are presented in Table 5.6. The solution infrared spectra of the compounds contained two bands of approximately equal intensity at *ca*. 1930 and 1830 cm^{-1}, as expected for *cis*-dicarbonyl species. Regardless of solvent ($(CH_3)_2CO$, $CHCl_3$, CH_2Cl_2 or CH_3CN) the bands were notably broad and appreciable changes in the spectra were observed with time. The solid-state spectra, recorded as nujol mulls, showed an additional sharp weak band in the carbonyl region at *ca*. 1960 cm^{-1}. Rather surprisingly, storage of the compounds *in vacuo* resulted in a reduction of the intensity of this band but conventional methods of purification such as column chromatography and fractional recrystallisation failed to produce a similar effect, thus it seems unlikely that this band is due to an impurity in the samples. This deduction was supported by analytical and ^1H NMR spectral data which were in each case as expected for the compounds $[(\eta^3\text{-}C_3H_4R)M(CO)_2(PMePh_2)_2Cl]$.

The ^{31}P-decoupled ^1H NMR spectra of (XXXIX), (XXXX) and (XXXXI) were typical of symmetrical or fluxional η^3-allyl systems. For the 2-methylallyl derivative (XXXXI), the spectrum was invariant with

temperature over the range +70 to -120°C. Both the syn and the anti protons of the allyl showed strong coupling with only a single phosphorus nucleus. In contrast the unsubstituted allyl compounds exhibited dynamic ^{1}H NMR spectra. At room temperature both the syn and anti allylic protons were strongly coupled to two equivalent phosphorus nuclei with the respective coupling constants being approximately half those observed for the 2-methylallyl compound. As the temperature was lowered from +28°C considerable broadening of the allylic proton signals was observed; at ~ 0°C the resonance due to the central proton H_A could not be detected but on decreasing the temperature further it reappeared as a poorly resolved multiplet shifted some 0.7 p.p.m. to low field. Below -20°C the signal due to the anti protons H_X was completely lost under the methyl signal of the equivalent phosphine ligands and so its fine structure at low temperatures could not be seen. The resonance due to the allyl syn protons H_M remained clearly visible at all temperatures but it too suffered loss of fine structure as the temperature was decreased from 28°C. By -40°C, however, it had sharpened again into an overlapping doublet of doublets indicating that each of the syn protons were now only coupled with a single phosphorus nucleus. Between -80 and -120°C further broadening of all the signals occurred but no other changes were detected.

Table 5.6: ^{1}H NMR and Selected Infrared Spectral Data* for the Compounds $[(\eta^3\text{-}C_3H_4R)M(CO)_2(PMePh_2)_2Cl]$

Complex(No)	Infrared (cm^{-1})[a]			^{1}H NMR: δ(multiplicity, rel. intensity).			
				Allyl Protons			Other Protons
	ν(MCl)[b]	ν(CO)	$M(CO)_2$ Angle[c]	H_X	H_M	H_A (or 2-Me)	
(XXXIX)	247	1937 1835	88	2.66(dt, 2H) J_{XA} 12.8 J_{XP} 2.5	3.44(dt, 2H) J_{MA} 7.7 J_{MP} 4.9	4.82(m, 1H)	2.22(d, 6H) $PC\underline{H}_3Ph_2$ J_{HP} 8.3 7.48(m, 20H) $PCH_3\underline{Ph}_2$
(XXXX)	248	1926 1822	87	2.45(dt, 2H) J_{XA} 12.0 J_{XP} 3.1	3.33(dt, 2H) J_{MA} 7.8 J_{MP} 4.8	4.52(m, 1H)	2.27(d, 6H) $PC\underline{H}_3Ph_2$ J_{HP} 8.8 7.50(m, 20H) $PCH_3\underline{Ph}_2$
(XXXXI)	246	1936 1819	90	2.73(d, 2H) J_{XP} 5.0	3.44(d, 2H) J_{MP} 9.5	1.78(s, 3H)	2.30(d, 6H) $PC\underline{H}_3Ph_2$ J_{HP} 8.0 7.53(m, 20H) $PCH_3\underline{Ph}_2$

* - In $CDCl_3$ or $CHCl_3$ at room temperature unless otherwise stated.

[a] - All bands strong

[b] - Recorded on Nujol mulls

[c] - Calculated from carbonyl band intensity data.

The marked similarities in the variable temperature ^{1}H NMR data for (XXXIX) and (XXXX) with those recorded for the related bis-phosphite derivatives suggest that the dynamic behaviour, instantaneous low-temperature stereochemistry, and solid state structures for each of these compounds are identical. Also, as found for $[(\eta^3\text{-}2\text{-}MeC_3H_4)Mo(CO)_2\{P(OMe)_3\}_2Cl]$, the 2-methylallyl derivative, (XXXXI), was stereochemically rigid in solution at room temperature. Rather surprisingly, the $M(CO)_2$ angles for the $PMePh_2$ compounds, calculated from carbonyl band intensity data were smaller than those calculated for the bis-phosphite compounds. The values (see Table 5.6) of between 85-91° are in line with those reported for compounds such as $[(\eta^3\text{-}C_3H_5)Mo(CO)_2(dpe)Cl]$[171] which adopt the more usual pseudo-octahedral geometry. However, the limiting low-temperature ^{1}H NMR spectra of (XXXIX), (XXXX) and (XXXXI) are clearly inconsistent with these molecules adopting a stereochemistry such as that possessed by $[(\eta^3\text{-}C_3H_5)Mo(CO)_2(dpe)Cl]$[171], (and, also indicated for $[(\eta^3\text{-}C_3H_5)M(CO)_2(PHPh_2)_2Cl]$ - see earlier), since inequivalence of the termini of the allylic ligand was not observed even at -120°C. It seems likely, therefore, that the ligand arrangements in (XXXIX), (XXXX) and (XXXXI) are similar to that of $[(\eta^3\text{-}C_3H_5)Mo(CO)_2\{P(OMe)_3\}_2Cl]$ and that the structures of these compounds differ significantly only in terms of their $M(CO)_2$ angles.

(ii) $[PMePh_2(\sigma\text{-}C_3H_5)][(\eta^3\text{-}C_3H_5)M(CO)_2(PMePh_2)Cl_2]$ (M = Mo or W)

These compounds were only moderately stable, and could not be stored for any length of time even under nitrogen at -10°C. Their extreme sensitivity in solution resulted in either the loss, or else severe broadening of the two ν(CO) bands present in their solid-state

spectra (see Table 5.7). Oxygen-free CH_3CN proved to be the most suitable solvent system for the compounds and ^1H NMR spectra were successfully recorded in this solvent. No assignments could be made for the tungsten analogue because of extensive decomposition, but the molybdenum complex proved slightly more stable in solution and a reasonably complete assignment of the spectrum was possible. (Table 5.7). The spectrum - reproduced in Figure 5.2 - showed the presence of coordinated $PMePh_2$, a $[PMePh_2(\sigma\text{-}C_3H_5)]^+$ cation, and a symmetrically bonded η^3-allylic species. This, in conjunction with infrared spectral data (which indicated the presence of two mutually cis-carbonyl groups), and analytical data (see Table 5.1), implies that the compound be best formulated as $[PMePh_2(\sigma\text{-}C_3H_5)]^+ [(\eta^3\text{-}C_3H_5)Mo(CO)_2(PMePh_2)Cl_2]^-$. As the ^1H NMR spectra were, at best, poorly resolved no ^{31}P coupling to the syn allylic protons could be measured.

Rather surprisingly, ^1H NMR spectral data for $Et_4N[(\eta^3\text{-}C_3H_5)W(CO)_2(PPh_3)Cl_2]$ [240] were not reported in the publication concerning its preparation and structure so to enable us to compare assignments for this compound and those made by us for $[PMePh_2(\sigma\text{-}C_3H_5)][(\eta^3\text{-}C_3H_5)Mo(CO)_2(PMePh_2)Cl_2]$. The former was prepared by reaction of $Et_4N[W(CO)_5Cl]$ with C_3H_5Cl and PPh_3 in benzene-CH_3CN solution[240]. On recording the ^1H NMR spectrum it was discovered that the signals due to the allylic protons were obscured by those of the Et_4N^+ cation, however, their approximate positions were deduced, H_X occurred between ca. 1.4 and 1.1 p.p.m. and H_M and H_A between ca. 3.4 and 3.1 p.p.m. The positions of

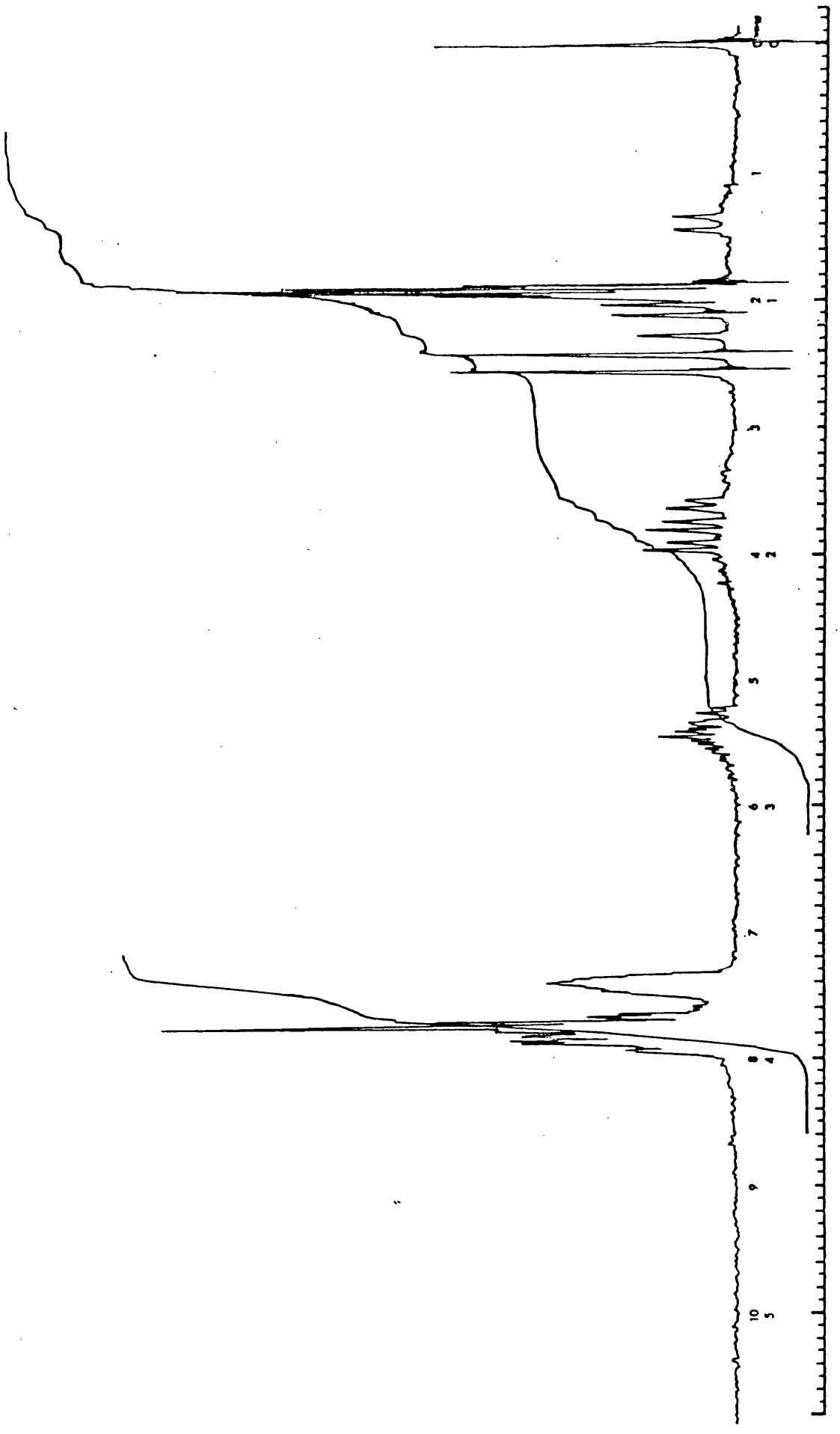

Figure52: ^{1}H NMR Spectrum of $[PMePh_2-(\sigma-C_3H_5)_2][(\eta^3-C_3H_5)Mo(CO)_2(PMePh_2)Cl_2]$(XXXXII) in CD_3CN

Table 5.7: ^{1}H NMR and Selected Infrared Spectral Data for the Compounds $[PMePh_2(\sigma\text{-}C_3H_5)][(\eta^3\text{-}C_3H_5)M(CO)_2(PMePh_2)Cl_2]$ (M = Mo or W)

Complex (No.)	Infrared (cm^{-1})[a] ν(MCl)[b]	ν(CO)[c]	ν(CO)[b]	^{1}H NMR[d]: δ(multiplicity, rel. intensity) Allyl Protons H_X	H_M	H_A	Other Protons
XXXXII	246 223	1936 1845	1910 1812	1.39(d, 2H) J_{XA} 10.0	3.59(d, 2H) J_{MA} 7.0	3.84(m, ~1H)	2.47(d, 3H) $[P\underline{Me}Ph_2(\sigma\text{-}C_3H_5)]^+$ J_{HP} 13.7 3.84(dd, ~2H) $[P\text{-}\underline{CH_2}CH{=}CH_2(MePh_2)]$ J_{HH} 6.3; J_{HP} 16.3 5.44(m, 3H) $[P\text{-}CH_2\underline{CH}{=}\underline{CH_2}(MePh_2)]^+$ 7.50(m) aromatic protons[e] Unassigned:- 2.46(br s, 1H) 2.1(br s, 2H) 2.02(br s, 2H)
XXXXIII	267(sh) 252 232	1930 1834	1903 1802	[f]			3.85(dd, 2H) $[P\text{-}\underline{CH_2}CH{=}CH_2(MePh_2)]^+$ J_{HH} 6.8; J 15.9 5.43(m, 3H) $[PCH_2\underline{CH}{=}\underline{CH_2}(MePh_2)]^+$ 7.61(m) aromatic protons

[a] - All bands strong unless otherwise stated. [b] - Recorded on Nujol mulls. [c] - Recorded in CH_3CN solution at room temperature. [d] - Recorded in CD_3CN. [e] - $P\underline{Me}Ph_2$ signal hidden under solvent. [f] - Decomposition far too extensive to permit confident assignments.

these resonances show reasonable agreement with those assigned to the corresponding protons of (XXXXII). Attempts to prepare the analogous $[Ph_4P]^+$ and $[Ph_4As]^+$ salts of $[(\eta^3\text{-}C_3H_5)W(CO)_2(PPh_3)Cl_2]^-$ were unsuccessful, as were those made to effect the preparation of the molybdenum analogues. Neither was it possible to isolate any species using other phosphine ligands.

(iii) $[M(CO)_2(MeCN)(PMePh_2)_3]$.

Despite slight decomposition in solution the stereochemistry of the reduced products (XXXVII) and (XXXVIII) was readily determined by spectroscopy. The infrared spectra (Nujol mulls) of the compounds showed a weak band at 2255 cm^{-1} M = Mo; 2250 cm^{-1} M = W, attributable to ν (C ≡ N) of the MeCN ligand, and two strong bands [at 1837s 1758s, M = Mo; 1829s 1752s, M = W] in the carbonyl region which indicated the presence of mutually cis-carbonyl groups. Only two cis-dicarbonyl isomers were possible with the three phosphine ligands occupying fac or mer positions. ^1H NMR spectra (CD_2Cl_2), recorded as soon after the preparation of the solutions as was possible, were only consistent with the mer-arrangement. Both the molybdenum and tungsten complexes exhibited two signals in the methyl region of their spectra arising from coordinated $PMePh_2$. The downfield band, (relative intensity 6), [M = Mo, δ = 1.75 (t), $|J^1(P\text{-}H) + J^2(P\text{-}H)|$ = 4.8 Hz; M = W, δ = 1.86 (t), $|J^1(P\text{-}H) + J^3(P\text{-}H)|$ = 5.6 Hz] was observed as an approximate triplet, as a result of intermediate[338] coupling of the two trans phosphorus atoms. This phenomenon has been observed previously for other mer-phosphine complexes[353]. The

upfield signal, (relative intensity 3), was a doublet [M = Mo, δ = 1.40 (d) J(P-H) = 3.5 Hz; M = W, δ = 1.50 (d), J(P-H) = 5.0 Hz] and so assigned to the methyl group of the unique phosphine ligand occupying a site mutually cis to the other two phosphines. Consequently the phosphorus atom is not participating in any strongly coupled system. Each spectrum also exhibited a resonance in this region attributable to coordinated MeCN, [M = Mo, δ = 1.40 (s); M = W, δ = 1.38 (s)]. For the tungsten compound (XXXVIII) this signal was broad but sharpened considerably on ^{31}P decoupling.

As mentioned above the compounds mer-$[M(CO)_2(MeCN)(PMePh_2)_3]$ slowly decompose in solution. Decomposition of the molybdenum compound (XXXVII) occurred faster than for the tungsten analogue and could easily be monitored by infrared spectroscopy. A freshly prepared CH_2Cl_2 solution of (XXXVII) initially displayed two infrared ν(CO) bands, but on standing these bands gradually broadened and decreased in intensity whilst a number of new bands developed in the 2000-1800 cm^{-1} region. The most intense of these occurred at 1846 cm^{-1}, the characteristic frequency of the strong B_1 mode of mer-$[Mo(CO)_3(PMePh_2)_3]$[354]. Indeed analytically pure samples of this complex were subsequently isolated from the solutions on addition of n-pentane (yields $<$ 10%).

Very recently, the decomposition of cis-$[Mo(CO)_2(PMe_2Ph)_4]$ to mer-$[Mo(CO)_3(PMePh_2)_3]$ has been reported[352]. It was suggested that

the decomposition proceeds via initial dissociation of a phosphine ligand sited trans to a carbonyl group to produce the stereochemically rigid five-coordinate intermediate $[Mo(CO)_2(PMe_2Ph)_3]$, which then partly decomposes liberating CO which reacts with more $[Mo(CO)_2(PMe_2Ph)_3]$ to generate mer-$[Mo(CO)_3(PMe_2Ph)_3]$. The decomposition of $[M(CO)_2(MeCN)(PMePh_2)_3]$, reported here may occur by a similar mechanism, probably involving loss of MeCN as a first step.

The yields of mer-$[M(CO)_3(PMePh_2)_3]$ (M = Mo or W) and their rate of formation from $[M(CO)_2(MeCN)(PMePh_2)_3]$, were greatly improved by the use of solvents saturated with carbon monoxide. Virtually quantitative yields were obtained when CH_3OH was used as solvent but the times necessary for complete reaction were long (2 days M = Mo; 2 weeks M = W) because of the insolubility of both the starting materials and products in this solvent. Refluxing $[M(CO)_2(MeCN)(PMePh_2)_3]$ in CH_3OH, whilst purging the solution with carbon monoxide, effectively reduced the reaction time necessary for quantitative formation of mer-$[Mo(CO)_3(PMePh_2)_3]$ (5 h at 60°C) but for $[W(CO)_2(MeCN)(PMePh_2)_3]$ the use of such forcing conditions (2 h at 60°C) resulted in the formation of the fac rather than the mer isomer of $[W(CO)_3(PMePh_2)_3]$. Mer to fac isomerisation of $[Mo(CO)_3(PMePh_2)_3]$ in refluxing CH_3OH was found to be very slow. Even after several days only a very small conversion to the fac isomer had occurred and other carbonyl-containing decomposition products [predominantly cis-$[Mo(CO)_4(PMePh_2)_2]$(ν(CO) 2028m, 1931m, 1906vs)[354]] were also obtained. When CH_3CN was used as solvent

a good yield of fac-$[Mo(CO)_3(PMePh_2)_3]$ resulted after only 5 h. Similarly, treatment of $[Mo(CO)_2(MeCN)(PMePh_2)_3]$ with carbon monoxide in refluxing CH_3CN gave only fac-$[Mo(CO)_3(PMePh_2)_3]$. These results suggest that both fac isomers (M = Mo or W) are thermodynamically more stable than the corresponding mer isomers. This is in agreement with electronic considerations as the facial arrangement allows π-bonding to occur between each of the three carbonyl groups and three separate metal d_π - orbitals, whereas for the mer isomers, two of the carbonyl ligands are in direct competition for the same d_π -electron density. The observation that mer $\rightarrow$ fac isomerisation of $[W(CO)_3(PMePh_2)_3]$ occurred in boiling CH_3OH (b.pt. 60°C) while the corresponding conversion for the molybdenum complex could only be achieved in boiling CH_3CN (b.pt. 80°C) may simply reflect a higher activation energy for the isomerisation of the molybdenum analogue. As there was insufficient time to extend the range of solvents examined or determine whether an inter- or intra-molecular rearrangement was occurring in these systems, no further speculation is justified other than to note that in at least one other instance the solvent has been critical in mer- or fac-isomer formation in molybdenum carbonyl chemistry[355].

Characterisation of mer- and fac-$[M(CO)_3(PMePh_2)_3]$ (M = Mo or W).

Although none of the tricarbonyl compounds described in this section are novel - mer- and fac$[Mo(CO)_3(PMePh_2)_3]$ have been reported in ref. 354 and mer- and fac-$[W(CO)_3(PMePh_2)_3]$ in ref. 356 - their spectroscopic characterisation appears to have been somewhat neglected. No ^1H NMR data have been reported for any of these complexes and in some

instances even infrared ν(CO) band positions have not been listed. Consequently both ^{1}H NMR and vibrational data were obtained for all four compounds.

^{1}H NMR

The two isomers *mer*- and *fac*-$[M(CO)_3(PMePh_2)_3]$ (M = Mo or W) were easily distinguished by their ^{1}H NMR spectra. The methyl resonance of the *fac*-isomers consisted of a single broad peak (M = Mo, 1.72 p.p.m.; M = W, 1.80 p.p.m.) which sharpened considerably on ^{31}P-decoupling. Similar ^{1}H NMR spectra have been reported for the analogous compounds *fac*-$[M(CO)_3(PMe_2Ph)_3]$ (M = Mo or W)[353] and probably result from the coupling of the methyl protons to phosphorus nuclei involved in complex coupling with each other[353]. The complexes *mer*-$[M(CO)_3(PMePh_2)_3]$, (M = Mo or W), showed two methyl resonances of relative intensities 2:1 in their ^{1}H NMR spectra. The most intense of these at 1.76 p.p.m. $[J^1(P-H) + J^3(P-H) = 5.1$ Hz] (M = Mo) and 1.96 p.p.m. $[J^1(P-H) + J^3(P-H) = 5.1$ Hz)] (M = W) consisted of a broad central peak with two partially resolved side bands characteristic of intermediate phosphorus-phosphorus coupling of the mutually *trans* phosphorus nuclei, and a well defined 1:1 doublet [M = Mo, δ = 1.40, J_{PH} = 4.7 Hz; M = W, δ = 1.62, J_{PH} 5.2 Hz] due to the unique $PMePh_2$ ligand (sited *trans* to a carbonyl group).

Vibrational Spectra

The large number of bands in the vibrational spectra of *mer*- and *fac*-$[M(CO)_3(PMePh_2)_3]$ associated with the internal vibrations of the phosphine ligands, made complete assignments impossible.

However, those regions of the spectra where absorptions due to the $[M(CO)_3]$ fragment should appear were reasonably clear of phosphine bands, so assignments of ν(CO) and tentative assignments of some ν(MC) and δ(MCO) modes were possible.

The spectral features observed in the ν(CO), ν(MC) and δ(MCO) regions corresponded closely with those predicted for an $M(CO)_3$ unit under the constraints of either C_{2v} (in mer-$[M(CO)_3L_3]$) or C_{3v} (in fac-$[M(CO)_3L_3]$) symmetries. For the most part individual bands in the infrared and Raman spectra occurred at coincident frequencies (within experimental error) indicating that factor group[357] couplings were negligible. However, some intense Raman bands e.g. ν(MC) modes may not be detected in the infrared spectra due to their predictably low intensity, and the reverse situation can also occur in some circumstances e.g. δ(MCO) modes. The splitting of some of the degenerate E modes observed in the solid-state spectra of fac-$[M(CO)_3(PMePh_2)_3]$ can be accounted for in terms of site-symmetry effects.

Table 5.8: Vibrations of an $[M(CO)_3]$ Unit[a] in C_{2v} and C_{3v} Symmetries

Vibrational Mode	C_{2v} Symmetry Species[b]	C_{3v} Symmetry Species[c]
ν(CO)	$2A_1 + B_2$	$A_1 + E$
ν(MC)	$2A_1 + B_2$	$A_1 + E$
δ(MCO)	$A_1 + A_2 + 2B_1 + 2B_2$	$A_1 + A_2 + 2E$

[a] - For derivation see Appendix 2
[b] - All bands infrared- and Raman-active, except A_2 which is only Raman-active.
[c] - All bands infrared- and Raman-active except A_2 which is totally inactive.

The number of vibrations predicted for an $[M(CO)_3]$ unit under the constraints of C_{2v} in mer-$[M(CO)_3(PMePh_2)_3]$ and C_{3v} in fac-$[M(CO)_3(PMePh_2)_3]$ symmetries have been deduced from group theoretical treatments (see Appendix 2) and are summarised in Table 5.8. The vibrational spectra of solid mer- and fac-$[M(CO)_3(PMePh_2)_3]$ (M = Mo or W) in the relevant regions are presented in Tables 5.9 and 5.10. Decomposition of solutions of the compounds on irradiation by He/Ne laser meant that Raman polarisation measurements could not be carried out. The ν(CO) modes were therefore assigned by analogy with other tricarbonyl species.

A total of three ν(CO) vibrations ($2A_1 + B_1$) which are all infrared and Raman active are expected for mer-$[M(CO)_3L_3]$ species. The assignment of the ν(CO) bands of mer-$[M(CO)_3(PMePh_2)_3]$

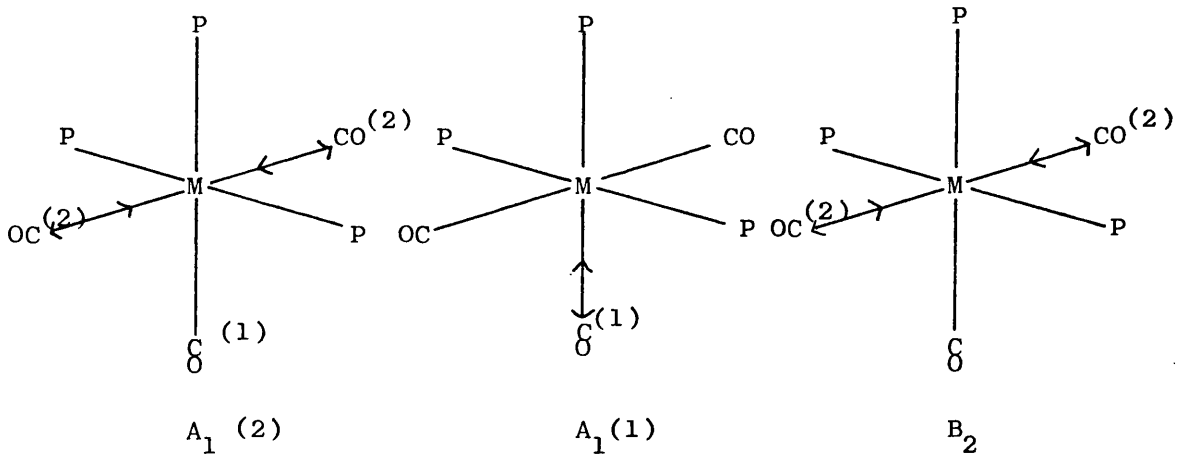

Figure 5.3: Normal ν(CO) modes of $[M(CO)_3L_3]$ in C_{2v} symmetry

Table 5.9: Vibrational Spectra of Solid[≠] *mer*- and *fac*-$[M(CO)_3(PMePh_2)_3]$ in the Carbonyl Region

Complex		Assignment *mer*-$[M(CO)_3(PMePh_2)_3]$			*fac*-$[M(CO)_3(PMePh_2)_3]$		
		$A_1^{(2)}$	$A_1^{(1)}$	B_2	A_1	E^a	
XXXXIV	i.r	1959 w	1853 s(sh)	1845 br vs			
	R	1958 s	1850 m	1844 m			
XXXXV	i.r	1952 w	1845 s(sh)	1834 br vs			
	R	1952 s	1845 m	1834 w			
XXXXVI	i.r				1926 s	1832 brs	1804 s(sh)
	R				1927 w	1831 m	1808 m
XXXXVII	i.r				1919 s	1823 brs	1797 brs
	R				1919 w	1826 m	1801 m

≠ - Infrared spectra data from Nujol mulls

a - Split by solid state effects.

(Table 5.9) are in agreement with those reported for other mer-$[M(CO)_3L_3]$ systems in that the frequencies decrease in the order $A_1^{(2)} > A_1^{(1)} > B_1$. In CH_2Cl_2 solution only two infrared bands at 1959(w) and 1846(br vs) for M = Mo and 1949(w) and 1839(br vs) for M = W were clearly resolved for each complex. George and Seibold[354] previously reported two weak (at 1960 and 1940 cm^{-1}) and one very strong (at 1845 cm^{-1}) bands for mer-$[Mo(CO)_3(PMePh_2)_3]$ in CH_2Cl_2; however, one weak and two strong absorptions are expected for complexes of this type[358], and since in a number of other examples the two strong bands have been found to overlap[359,360] it seems likely that an impurity is responsible for the weak band at 1940 cm^{-1} observed by these workers. In the past such results have caused considerable confusion over the correct assignments of ν(CO) bands for mer-tricarbonyls[361,362].

In agreement with group theory predictions the fac-tricarbonyl complexes fac-$[M(CO)_3(PMePh_2)_3]$ had two intense absorptions in the ν(CO) region of their solution ($CHCl_3$) infrared spectra at 1920(shp s) and 1819(br s) for M = Mo and 1931 (shp s) 1838 (br s) for M = W. By analogy with other fac-tricarbonyl species of C_{3v} symmetry[353,360,363-365] the less intense of the two bands observed at higher frequency is assigned to the A_1 mode and the other to the E mode. The latter band showed considerable splitting in the solid state (Table 5.9).

Table 5.10: Solid State Vibrational Spectra between 700-300 cm^{-1} for the Complexes[≠] mer- and fac-$[M(CO)_3(PMePh_2)_3]$ (M = Mo or W) and for $PMePh_2$ (liquid)

Complex		δ(MCO)				ν(MC)			Ligand Bands						
XXXXIV	i.r	610s	589 s	573 s		454 s	440 m	421 s	695 s	681 s	620 w	506 s	482 s	404 s	350 w [a]
	R		587 w		462 s		[b]	425 s		682 m	616 w	499 w	480 w	399 m	343 m [c]
XXXXV	i.r	606 s	584 m	564 w		457 m	443 *w	427 m	696 s	680 m	618 m	504 s	482 m	407 s	345 w [d]
	R		584 w		471 s		448 s	417 w		683 w	618 w	510 w		402 w	344 w [e]
$MePPh_2$	i.r.								695 s	675 s	618 w	507 s	480 s	420 s	323 w [f]
	R									672 s	616 w			423 w	323 w
XXXXVI	i.r.	630 m	594 m	527 s		479 m		450 w	692 s	680 *m	618 *w	511 s	470 *m	404 s	358 w
	R		590 w	523 w		486 s		448 s		677 s	613 m	512 w		400 s	349 w
XXXXVII	i.r.	621 m	591 m	529 s		487 *m			692 s	680 *s	615 *m	511 s	470 s	405 s	360 m [g]
	R	620 *w	589 w	528 w		495 s	484 s	466 s		682 s	616 m	516 w		404 s	355 w [h]

≠ - Infrared spectra recorded on Nujol mulls * - shoulder

[a] - Additional unassigned bands at 623 w; 538 vw; 340 *w. [b] - May be under a strong broad band at 462 cm^{-1}

[c] - Additional unassigned bands at 534 w; 512 w. [d] - Unassigned band at 454 vw. [e] - Unassigned band at 545 w. [f] - Broad shoulder 398 w. [g] - Unassigned band at 490 vw. [h] - Unassigned bands at 657 w; 418 w.

The δ(MCO) and ν(MC) region

The δ(MCO) and ν(MC) vibrations are expected to lie in the 700 - 300 cm^{-1} region[271,276,366,367] and the former generally, but not invariably, appear at higher frequencies. One of the problems in assigning such vibrations is that extensive mixing of modes of the same symmetry will occur owing to the small frequency differences between δ(MCO) and ν(MC) fundamentals[368]. Because of this, some authors prefer not to distinguish between the two types of vibration, but collectively assign bands in the 700 - 300 cm^{-1} region to δ(MCO) + ν(MC)[369]. However, it is true that ν(MC) modes in neutral Group VI species are rarely found above 500 cm^{-1}[70,276,367,370] and when both infrared and Raman spectra have been recorded differentiation between the two types of vibration may be attempted by comparing the relative intensity of the bands in the two spectra - δ(MCO) bands are normally much more intense in the infrared than Raman, the reverse being true for ν(MC) bands. The major difficulty in assigning bands to δ(MCO) and ν(MC) vibrations in the case of *mer*- and *fac*-$[M(CO)_3(PMePh_2)_3]$ is the presence of phosphine ligand bands in the 700 - 300 cm^{-1} region. Comparisons of the spectra with that of free methyldiphenylphosphine (Table 5.10) was of some assistance in this respect, but frequency shifts on coordination complicated ligand band assignments.

For the *mer*-tricarbonyl complexes (C_{2v} symmetry) the total number of modes expected in this region (see Table 5.10) is nine (eight infrared-active), but only seven bands were observed. Of these, three bands between 610 - 560 cm^{-1} were very intense in the infrared but had only weak or non-detectable Raman counterparts

and so are assigned to δ(MCO) vibrations. An intense band in the Raman spectra of both (XXXXIV) and (XXXXV) found at ca. 465 cm^{-1} which fails to correlate convincingly with any infrared-active band is also assigned as a δ(MCO) mode. It is conceivable that this band is associated with the A_2 δ(MCO) mode which is only Raman-active. The other three bands observed between 460 - 415 cm^{-1} are tentatively assigned to ν(MC) modes. The weak infrared band at 440 cm^{-1} observed in the spectrum of mer-$[Mo(CO)_3(PMePh_2)_3]$ which did not appear in the Raman spectrum is assigned to ν(MC) by comparison with assignments made for the tungsten analogue.

For the fac-tricarbonyl complexes (XXXXVI) and (XXXXVII) of C_{3v} symmetry, group theory (Table 5.8) predicts two ν(MC) $[A_1 + E]$ and three δ(MCO) $[A_1 + 2E]$ modes. Three bands of medium to strong intensity were observed in the infrared spectra of both compounds between 630 - 520 cm^{-1} and these are assigned to δ(MCO) modes. In the Raman spectrum of fac-$[Mo(CO)_3(PMePh_2)_3]$ two intense absorptions at 486 and 448 cm^{-1} have been assigned as ν(MC) vibrations. In the corresponding region of the Raman spectrum of fac-$[W(CO)_3(PMePh_2)_3]$ (XXXXVII) three strong bands were observed, and two of these, at 495 and 484 cm^{-1}, have been attributed to the split E ν(MC) mode. The corresponding region of the infrared spectrum was complicated by phosphine bands. Only a weak shoulder at ca. 488 cm^{-1} in both the solid and solution ($CHCl_3$) infrared spectra of fac-$[W(CO)_3(PMePh_2)_3]$ could be correlated with these two intense Raman bands. The third intense Raman band at 466 cm^{-1} for fac-$[W(CO)_3(PMePh_2)_3]$ can therefore be assigned to the A_1 ν(MC) mode.

The frequencies of the proposed δ(MCO) and ν(MC) bands of fac-$[M(CO)_3(PMePh_2)_3]$ are in close agreement with those reported for fac-$[Mo(CO)_3(PPh_3)_3]$[271].

Comparison of the positions of the δ(MCO) and ν(MC) bands for the molybdenum and tungsten compounds reveals that individual bands suffer little mass effect on changing from molybdenum to tungsten. Indeed in most instances vibrations for the tungsten compounds are observed at slightly higher frequencies than those of the corresponding molybdenum compounds. Similar trends have been observed by other workers[366,367].

Reactions of $[(\eta^3\text{-}2\text{-}MeC_3H_4)Mo(CO)_2(MeCN)_2Cl]$ with Triphenylphosphine

Triphenylphosphine has been reported to react with $[(\eta^3\text{-}C_3H_5)M(CO)_2(MeCN)_2Cl]$ (M = Mo or W) under ambient conditions in CH_3CN or CH_3OH to produce by reduction cis-trans-$[M(CO)_2(PPh_3)_2(MeCN)_2]$ M = Mo[253], M = W[251]. For M = Mo the reaction has also been investigated at low (-18°C)[255] and high (80°C)[243] temperatures in attempts to detect the formation of intermediates or other products in the reduction process. However in neither investigation was any other intermediate, apart from the by-product $[PPh_3(\sigma\text{-}C_3H_5)][(\eta^3\text{-}C_3H_5)_2Mo_2(CO)_4Cl_3]$, isolated from the reaction mixtures. During the course of this work several attempts were made to isolate PPh_3 analogues of the compounds $[PMePh_2(\sigma\text{-}C_3H_5)][(\eta^3\text{-}C_3H_5)M(CO)_2(PMePh_2)Cl_2]$ (M = Mo or W) from equimolar reaction mixtures of $[(\eta^3\text{-}C_3H_5)M(CO)_2(MeCN)_2Cl]$ and PPh_3 in CH_3CN but these were met with little success, thus no analogies between the modes

of reaction of PPh_3 and $PMePh_2$ could be established. However, since it had been established by us that the reaction of $PMePh_2$ with $[(\eta^3\text{-}2\text{-}MeC_3H_4)Mo(CO)_2(MeCN)_2Cl]$ was not only independent of solvent but was also much slower than with the corresponding unsubstituted allyl derivative, it seems reasonable therefore that if any intermediate, such as $[(\eta^3\text{-allyl})Mo(CO)_2(PPh_3)_2Cl]$, was formed during the reduction process it was much more likely to be identified in the reactions with the 2-methylallyl than the allyl compound. Thus the reaction of PPh_3 with $[(\eta^3\text{-}2\text{-}MeC_3H_4)Mo(CO)_2(MeCN)_2Cl]$ in various solvent systems was investigated. As expected PPh_3 reacted much more slowly with $[(\eta^3\text{-}2\text{-}MeC_3H_4)Mo(CO)_2(MeCN)_2Cl]$ than with $[(\eta^3\text{-}C_3H_5)Mo(CO)_2(MeCN)_2Cl]$: after 4 days at room temperature reactions in CH_3CN or CH_3OH yielded the reduced products $[Mo(CO)_2(MeCN)_2(PPh_3)_2]$, although from the latter solvent only samples contaminated with decomposition products [tentatively identified by infrared spectroscopy as fac-$[Mo(CO)_3(PPh_3)_3]$ and cis-$[Mo(CO)_4(PPh_3)_2]$[306] could be obtained. After only very short reaction times in CH_3CN (0.5 h) scratching the sides of the reaction vessel initiated precipitation of a yellow flocculent precipitate which on the basis of analytical and spectroscopic evidence was formulated as $[(\eta^3\text{-}2\text{-}MeC_3H_4)Mo(CO)_2(MeCN)(PPh_3)Cl].MeCN$. Varying the mole ratios of $[(\eta^3\text{-}2\text{-}MeC_3H_4)Mo(CO)_2(MeCN)_2Cl]$ to PPh_3 from 1:1 to 1:3 had no effect on the reaction, the same product was isolated in similar yields from each. Thus it seems likely that the reduction of $[(\eta^3\text{-}2\text{-}MeC_3H_4)Mo(CO)_2(MeCN)_2Cl]$ by PPh_3 proceeds via initial attack by PPh_3 at the metal centre so displacing a MeCN ligand. Although different reaction conditions were employed no

bis-triphenylphosphine adduct was isolated prior to formation of the Mo(0) compound $[Mo(CO)_2(MeCN)_2(PPh_3)_2]$. So, for the 2-methylallyl complex (IV), which does not undergo autoionisation in solution, there is quite definite evidence that adduct formation precedes reduction - whether subsequent direct attack on the allyl ligand [(A) in Scheme 5.2] or replacement of the second MeCN ligand (B) follows, is, however, uncertain.

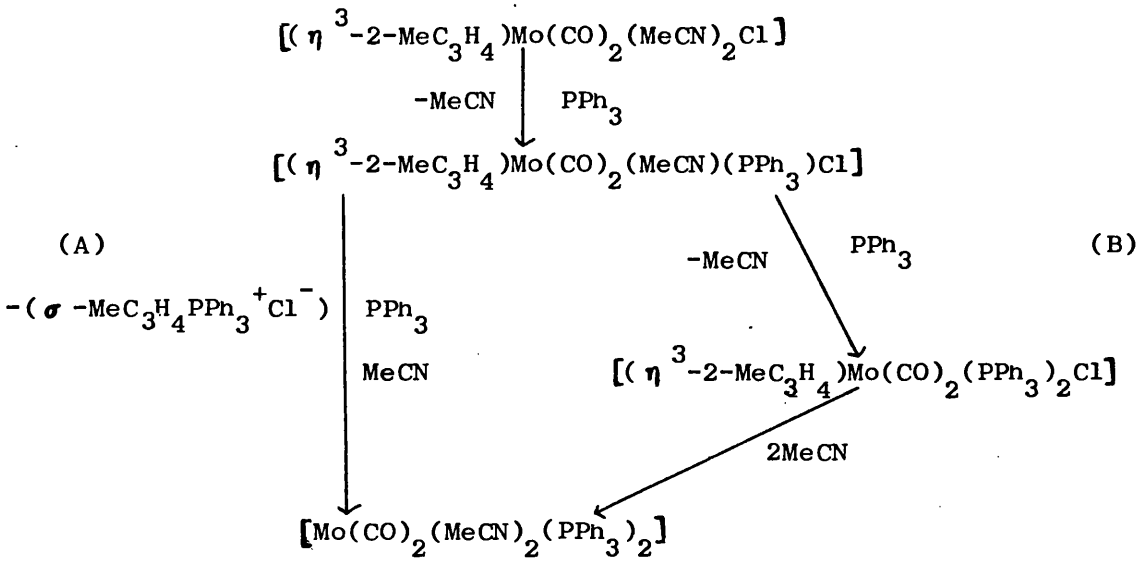

Scheme 5.2

Characterisation of the Compound $[(\eta^3\text{-}2\text{-}MeC_3H_4)Mo(CO)_2(MeCN)(PPh_3)Cl]$. MeCN

Conductivity measurements on (10^{-3}M) solutions of (XXXVIII) in CH_3NO_2 or $(CH_3)_2CO$ showed that it behaved essentially as a non-electrolyte[325] [$\Lambda_M CH_3NO_2$ 20.7; $\Lambda_M (CH_3)_2CO$ 20.3 mhos cm^2 $mole^{-1}$].

Therefore the incoming PPh_3 ligand has not displaced the chloride ion from the original starting material to give a cation. This was confirmed by the position of the two ν(CO) bands in the infrared spectrum which, at 1927 (shp s) and 1836 (shp s) cm^{-1} (nujol mulls), were characteristic of an uncharged Mo(II) cis-dicarbonyl species. The observation of three sharp but weak absorptions in the ν(CN) region of the spectrum ν(CN)(nujol mulls) 2310, 2280, 2260 cm^{-1} implied that the compound contained two MeCN molecules in different chemical environments (possibly one ligated and one solvated). The remainder of the infrared spectrum was dominated by bands due to the PPh_3 ligand and so was of little diagnostic value, however a single intense absorption in the far infrared region at 243 cm^{-1} was assigned to ν(Mo-Cl).

^{1}H NMR Spectrum

The ^{1}H NMR spectrum of (XXXXVIII) proved to be temperature-dependent, and the dynamics of the system were also solvent-dependent. In some solvents, e.g. CD_3OD, spectra recorded at low temperatures (see Figure 5.4) were so complex and poorly resolved that no confident interpretation can be offered. At +60°C in CD_3OD, however, an averaged spectrum was obtained which showed the presence of a symmetrical or fluxional η^3-2-MeC_3H_4 ligand[δ,0.95 (s 2H) H_X; 3.15 (s, 2H) H_M; 2.15 (s 3H) Me], a single PPh_3 [δ , 7.5 (m 15H)] ligand and two equivalent MeCN ligands [δ, 2.01 (s 6H)] . The allylic protons, somewhat surprisingly, showed no detectable coupling with phosphorus.

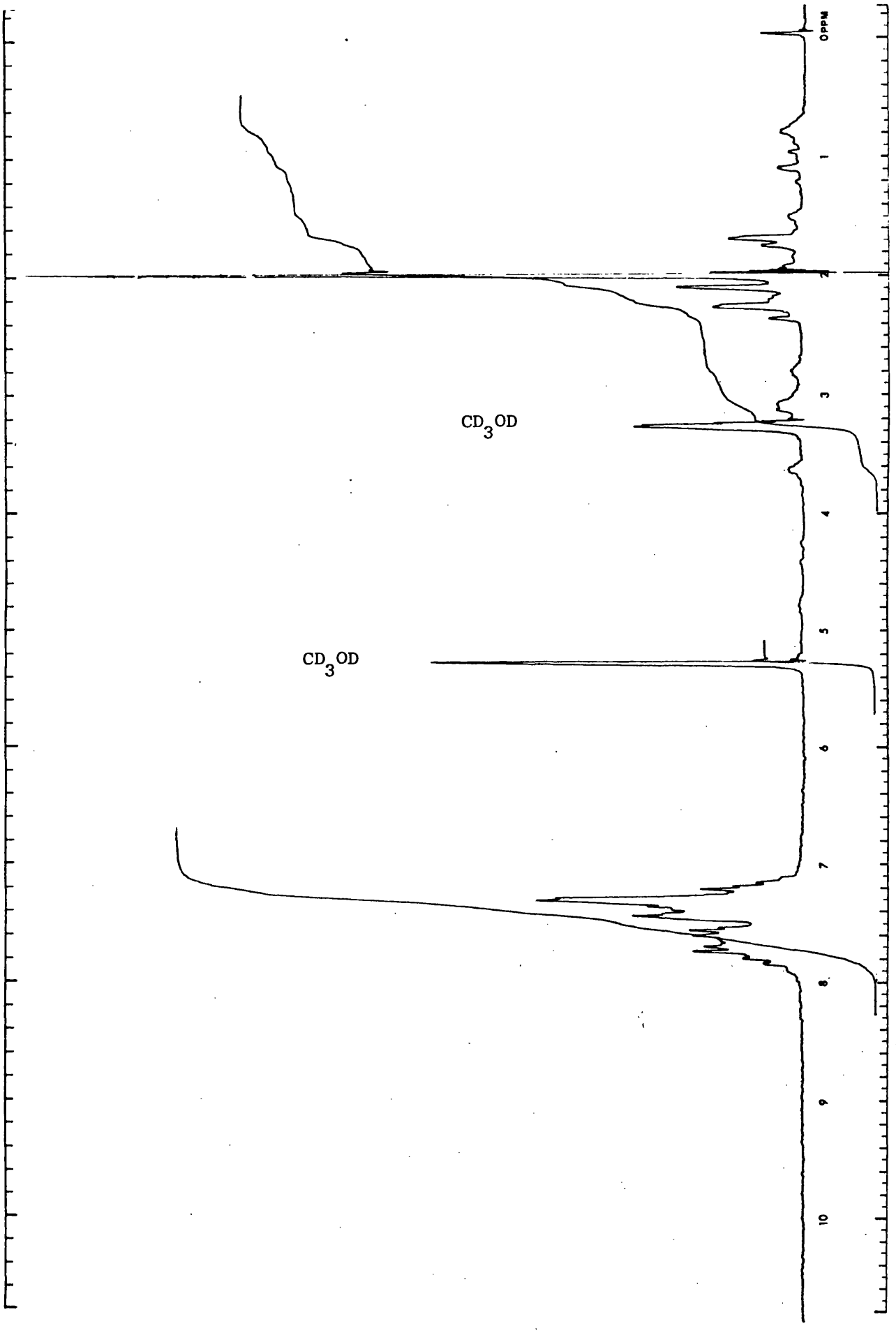

Figure 5.4: The ^{1}H NMR spectrum of (XXXXVIII) in CD_3OD at $-20^{o}C$

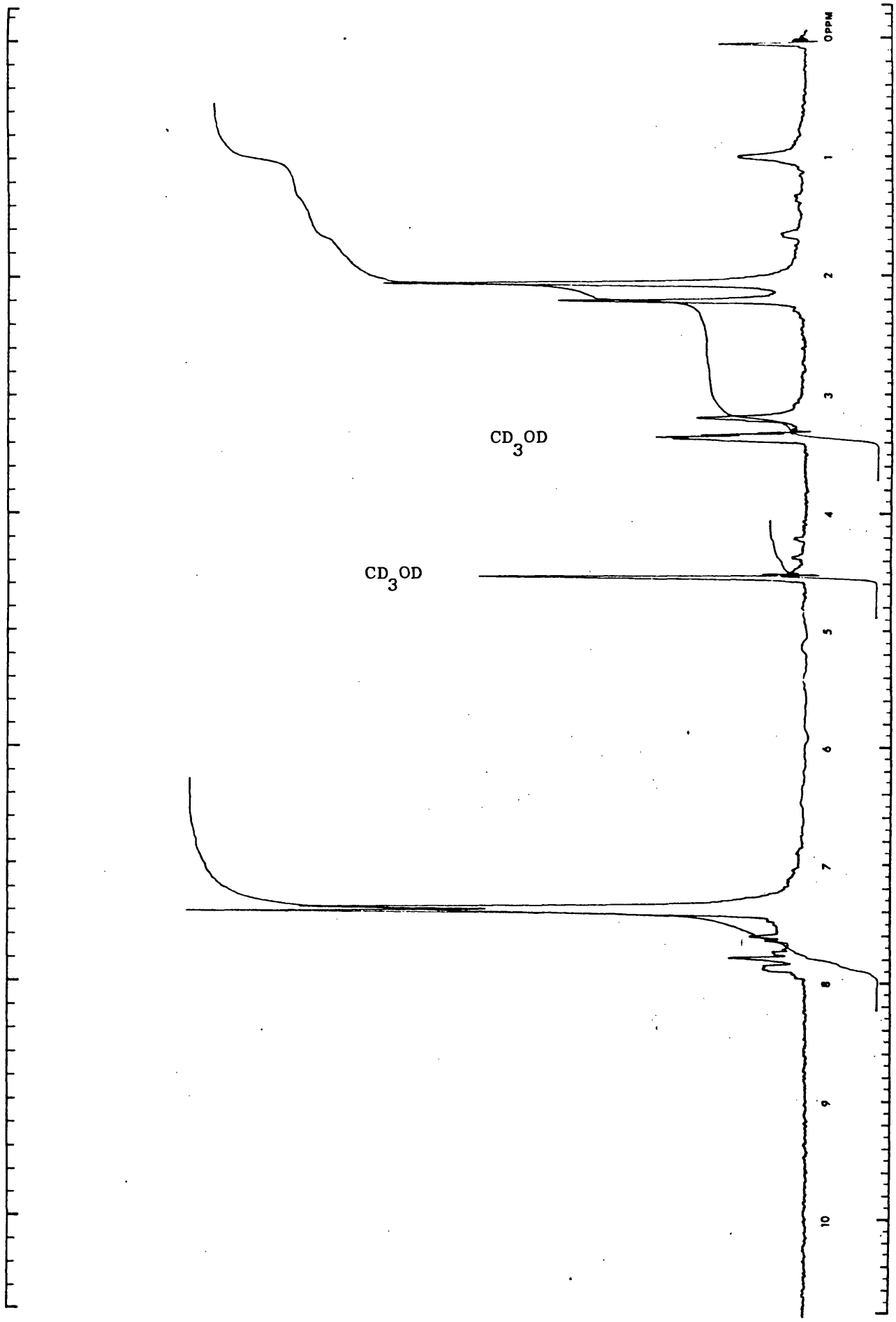

Figure 5.5: The ^{1}H NMR Spectrum of (XXXXVIII) in CD_3OD at 60°C

This may result from the dynamics of the species shifting the phosphorus ligand rapidly between sites where phosphorus-allylic proton couplings are very small. The physical data for (XXXXVIII) suggests that the compound is best formulated as an 18-electron pseudo-octahedral Mo(II) species which crystallises with a solvated molecule of MeCN. In solution at ambient temperatures the molecule is dynamic and fast exchange between free and coordinated MeCN or even replacement of MeCN by CD_3OD, accounts for the NMR equivalence of the nitrile groups which is observed.

APPENDIX 1

Application of the Hückel Molecular Orbital Method to the η^3-Allyl Entity

After construction of the basic σ-bonded framework of the η^3-allyl group, linear combinations of the $2p_z$ orbitals of each of the three carbon atoms form delocalised π molecular orbitals:

$$\psi_{C\text{-}C(\pi)} = c_1\phi_1 + c_2\phi_2 + c_3\phi_3 \qquad (1)$$

Values of ψ which satisfy the wave equation (2)

$$\hat{H}\psi = E\psi \qquad (2)$$

and conform to the normal boundary conditions describe the molecular orbitals, and thus the allowed distribution of the m electrons under consideration. The ground state configuration of the set of electrons must correspond to the most stable distribution possible, and must be describable by some function ψ_o with energy E_o. Any other ψ must represent a less probable electronic arrangement and must correspond to a higher energy. This argument leads to the Variation Principle which states: "Given any approximate wavefunction ψ_j satisfying the boundary condition of the problem, the expectation energy E_j calculated from this function will always be higher than the true ground state energy E_o"

i.e. $\hat{H}\psi = E\psi$

by multiplying both sides by ψ and integrating over volume $\delta\tau$ gives

$$E = \frac{\int \psi \hat{H} \psi}{\int \psi^2} \, \delta\tau > E_o \qquad (3)$$

The best approximation to E_o is obtained by minimising E with respect to ψ thus approaching E_o and ψ_o as closely as possible under the present Linear Combination of Atomic Orbitals - Molecular Orbital treatment. Thus substituting the approximate wavefunction

expression (equation (1)) for Ψ in equation (3) for E gives

$$E = \frac{\int (c_1\phi_1 + c_2\phi_2 + c_3\phi_3)\,\hat{H}\,(c_1\phi_1 + c_2\phi_2 + c_3\phi_3)\,\delta\tau}{\int (c_1\phi_1 + c_2\phi_2 + c_3\phi_3)(c_1\phi_1 + c_2\phi_2 + c_3\phi_3)\,\delta\tau}$$

$$= \frac{\begin{aligned}&\int (c_1\phi_1\,\hat{H}\,c_1\phi_1 + c_1\phi_1\,\hat{H}\,c_2\phi_2 + c_1\phi_1\,\hat{H}\,c_3\phi_3 + c_2\phi_2\,\hat{H}\,c_1\phi_1 \\ &+ c_2\phi_2\,\hat{H}\,c_2\phi_2 + c_2\phi_2\,\hat{H}\,c_3\phi_3 + c_3\phi_3\,\hat{H}\,c_1\phi_1 + c_3\phi_3\,\hat{H}\,c_2\phi_2 \\ &+ c_3\phi_3\,\hat{H}\,c_3\phi_3)\,\delta\tau\end{aligned}}{\begin{aligned}&\int (c_1\phi_1 c_1\phi_1 + c_1\phi_1 c_2\phi_2 + c_1\phi_1 c_3\phi_3 + c_2\phi_2 c_1\phi_1 + c_2\phi_2 c_2\phi_2 + \\ &c_2\phi_2 c_3\phi_3 + c_3\phi_3 c_1\phi_1 + c_3\phi_3 c_2\phi_2 + c_3\phi_3 c_3\phi_3)\,\delta\tau\end{aligned}}$$

$$= \frac{\begin{aligned}&c_1^2 \int \phi_1\,\hat{H}\,\phi_1\,\delta\tau + c_1c_2 \int \phi_1\,\hat{H}\,\phi_2\,\delta\tau + c_1c_3 \int \phi_1\,\hat{H}\,\phi_3\,\delta\tau \\ &+ c_2c_1 \int \phi_2\,H\,\phi_1\,\delta\tau + c_2c_3 \int \phi_2\,H\,\phi_3\,\delta\tau + c_2^2 \int \phi_2\,\hat{H}\,\phi_2\,\delta\tau \\ &+ c_3c_1 \int \phi_3\,\hat{H}\,\phi_1\,\delta\tau + c_3c_2 \int \phi_3\,\hat{H}\,\phi_2\,\delta\tau + c_3^2 \int \phi_3\,\hat{H}\,\phi_3\,\delta\tau\end{aligned}}{\begin{aligned}&c_1^2 \int \phi_1\phi_1\,\delta\tau + c_1c_2 \int \phi_1\phi_2\,\delta\tau + c_1c_3 \int \phi_1\phi_3\,\delta\tau + c_2c_1 \int \phi_2\phi_1\,\delta\tau \\ &+ c_2^2 \int \phi_2\phi_2\,\delta\tau + c_2c_3 \int \phi_2\phi_3\,\delta\tau + c_3c_1 \int \phi_3\phi_1\,\delta\tau \\ &+ c_3c_2 \int \phi_3\phi_2\,\delta\tau + c_3^2 \int \phi_3\phi_3\,\delta\tau\end{aligned}}$$

In order to simplify the equation we make the following assumptions

(i) Let $H_{rr} = \int \phi_r\,\hat{H}\,\phi_r\,\delta\tau$

where H_{rr}, the coulomb integral, represents the approximate energy of an electron in a carbon $2p_z$ atomic orbital.

(ii) Let $H_{rs} = \int \phi_r\,\hat{H}\,\phi_s\,\delta\tau$

where H_{rs}, the resonance integral, represents the energy of interaction of two atomic orbitals or the energy of an electron between two carbon atoms.

(iii) Let $S_{rs} = \int \phi_r\phi_s\,\delta\tau$

where S_{rs}, the overlap integral, gives a measure of the extent of

overlap of two atomic orbitals. For normalised atomic orbitals

$\int \phi_r \phi_s \, \delta\tau = 1.$

Substituting in the equation for E above gives:

$$E = \frac{\begin{array}{l} c_1^2 H_{11} + c_1 c_2 H_{12} + c_1 c_3 H_{13} + c_2 c_1 H_{21} + c_2 c_3 H_{23} \\ + c_2 c_3 H_{23} + c_2^2 H_{22} + c_3 c_1 H_{31} + c_3 c_2 H_{32} + c_3^2 H_{33} \end{array}}{\begin{array}{l} c_1^2 S_{11} + c_1 c_2 S_{12} + c_1 c_3 S_{13} + c_2 c_1 S_{21} + c_2^2 S_{22} \\ + c_2 c_3 S_{23} + c_3 c_1 S_{31} + c_3 c_2 S_{32} + c_3^2 S_{33} \end{array}} \qquad (4)$$

In order to evaluate the minimum value of E we set $\frac{\delta E}{\delta c} = 0$ but first to simplify the calculations the following mathematically valid rearrangement is carried out,

Let $E = \frac{N}{D}$ where N = numerator and D = denominator;

differentiating E with respect to c_1 gives

$$\frac{\partial E}{\partial c_1} = \left(\frac{\partial N}{\partial c_1}\right) \Big/ D - N \left(\frac{\partial D}{\partial c_1}\right) \Big/ D^2$$

$$= \frac{1}{D}\left[\frac{\partial N}{\partial c_1} - \frac{N}{D}\left(\frac{\partial D}{\partial c_1}\right)\right]$$

$$= \frac{1}{D}\left[\frac{\partial N}{\partial c_1} - E\left(\frac{\partial D}{\partial c_1}\right)\right]$$

For the minimum value of E with respect to c_1 we set $\frac{\partial E}{\partial c_1} = 0$

$\therefore$ if $\frac{1}{D} \neq 0$ then $\left[\left(\frac{\partial N}{\partial c_1}\right) - E\left(\frac{\partial D}{\partial c_1}\right)\right] = 0 \qquad (5)$

Thus for equation (4)

Differentiating N with respect to c_1 gives:

$$\frac{\partial N}{\partial c_1} = 2c_1 H_{11} + c_2 H_{12} + c_3 H_{13} + c_2 H_{21} + c_3 H_{31}$$

Differentiating D with respect to c_1 gives:

$$\frac{\partial D}{\partial c_1} = 2c_1 S_{11} + c_2 S_{12} + c_3 S_{13} + c_2 S_{21} + c_3 S_{31}$$

Substituting for N and D in equation (5) gives:

$$2c_1H_{11} + c_2H_{12} + c_3H_{13} + c_2H_{21} + c_3H_{31} - E(2c_1S_{11} + c_2S_{12} + c_3S_{13} + c_2S_{21} + c_3S_{31}) = 0 \qquad (6)$$

Since H_{rr} equals the approximate energy of an electron in a carbon $2p_z$ atomic orbital and since we are concerned with a π-lattice that consists entirely of carbon atoms, we may assume that all such integrals are equal i.e. $H_{11} = H_{22} = H_{33} = \alpha$ (α is a negative term because the electrons are attracted to the nuclei).

H_{rs} is clearly dependent on the distance between the two atomic orbitals and hence it is reasonable to assume that when r and s are not bonded in the classical representation of the structure, $H_{rs} = 0$. For bonded atoms r and s, H_{rs} is finite, but if all the bond distances are equal and the atomic orbitals share the same nodal plane, the various H_{rs} values will be of comparable magnitude, and we therefore assume all H_{rs} values for bonded atoms r and s to be equal to β (β is also negative since it also represents an energy of attraction).

The overlap integral, S_{rs} as we have stated previously, equals $\int \phi_r \phi_s \delta\tau$ which according to the normalization condition is unity. S_{rs} for atoms r and s separated by large distances is vanishingly small i.e. $S_{rs} = S_{sr} = 0$, with the orbitals assumed to be orthogonal with no overlap. This is, of course, a gross over-simplification since we think of π-bonds being formed by the overlap of atomic orbitals. Nevertheless it can be shown mathematically to be less drastic than it first appears[131] and valid in this approximate calculation.

$\therefore$ Putting $H_{12} = H_{21}$

$H_{13} = H_{31}$

and $S_{12} = S_{13} = S_{21} = S_{31}$ in equation (6) gives

$$2c_1H_{11} + 2c_2H_{12} - E(2c_1S_{11} + 2c_2S_{12} + 2c_3S_{12}) = 0$$

dividing by 2 and collecting the terms gives

$$c_{11}(H_{11} - S_{11}E) + c_2(H_{12} - S_{12}E) + c_3(- S_{12}E) = 0 \qquad (7)$$

Similarly minimising E with respect to c_2 and with respect to c_3 gives respectively;

$$c_1(H_{12} - S_{12}E) + c_2(H_{22} - S_{22}E) + c_3(H_{12} - S_{12}E) = 0 \qquad (8)$$

and $$c_1(- S_{12}E) + c_2(H_{12} - S_{12}E) + c_3(H_{33} - S_{33}E) = 0 \qquad (9)$$

Putting $S_{12} = S_{21} = S_{13} = S_{23} = S_{32} = S_{31} = 0$

and $S_{11} = S_{22} = S_{33} = 1$ in equations (7), (8) and (9) gives respectively (10), (11) and (12)

$$c_1(H_{11} - E) + c_2H_{12} + 0 = 0 \qquad (10)$$

$$c_1H_{12} + c_2(H_{22}-E) + c_3H_{12} = 0 \qquad (11)$$

$$0 + c_2H_{12} + c_3(H_{33}-E) = 0 \qquad (12)$$

Putting $H_{11} = H_{22} = H_{33} = \alpha$ and $H_{12} = H_{21} = \beta$ gives

$$(\alpha - E) + \beta + 0 = 0 \qquad (10)$$

$$\beta + (\alpha - E) + \beta = 0 \qquad (11)$$

$$0 + \beta + (\alpha - E) = 0 \qquad (12)$$

or as a 3rd order determinant:

$$c_1c_2c_3 \begin{vmatrix} \alpha - E & \beta & 0 \\ \beta & \alpha - E & \beta \\ 0 & \beta & \alpha - E \end{vmatrix} = 0$$

Dividing by β and putting $\frac{\alpha - E}{\beta} = x$ gives

$$c_1c_2c_3 \begin{vmatrix} x & 1 & 0 \\ 1 & x & 1 \\ 0 & 1 & x \end{vmatrix} = 0$$

According to the normal expansion of a 3rd order determinant as shown below

$$\begin{vmatrix} a_1 & b_1 & c_1 \\ a_2 & b_2 & c_2 \\ a_3 & b_3 & c_3 \end{vmatrix} = \begin{matrix} a_1b_2c_3 + b_1c_2a_3 + c_1a_2b_3 \\ - a_3b_2c_1 - b_3c_2a_1 - c_3a_2b_1 \end{matrix}$$

The secular polynomial for the allyl entity is

$$x^3 + 2x = 0$$

Solutions for this are $x = 0$ and $x = \pm \sqrt{2}$

Since $x = \frac{\alpha - E}{\beta}$ when $x = 0 \quad E = \alpha$

$x = +\sqrt{2} \quad E = \alpha - 2\beta$

$x = -\sqrt{2} \quad E = \alpha + 2\beta$

This produces three permissible energy levels for the π-electrons of the allyl entity. The number of electrons to be fed into these levels depends on whether one is considering the allyl cation (two electrons), the allyl radical (three electrons) or the allyl anion (four electrons). However, the bonding energy for each is the same at $2\sqrt{2}\beta$

ψ_1, ψ_2 and ψ_3 represent the wavefunctions describing each of the three molecular orbitals of the delocalised π-system for the allyl entity. The contribution of each of the three carbon $2p_z$ atomic orbitals (designated by the coefficients

c_1, c_2 and c_3), in each of these molecular orbitals can be evaluated by the solution of the secular equations for each value of x.

The secular determinant established earlier was:

$$c_1 c_2 c_3 \begin{vmatrix} x & 1 & 0 \\ 1 & x & 1 \\ 0 & 1 & x \end{vmatrix} = 0$$

The three secular equations are:

$$c_1 x + c_2 = 0 \qquad (13)$$

$$c_1 + c_2 x + c_3 = 0 \qquad (14)$$

$$c_2 + c_3 x = 0 \qquad (15)$$

Solution of these three equations together with the use of the normalisation condition:

$$c_1^2 + c_2^2 + c_3^2 = 1 \qquad (16)$$

for each value of x produces a set of values of c_1, c_2 and c_3 which describe the contributions of each carbon atom 1, 2 and 3 to the three molecular orbitals ψ_1, ψ_2 and ψ_3.

For ψ_1, substituting $x = -\sqrt{2}$ in equations (13), (14) and (15) gives

$$\sqrt{2}\, c_1 = c_2$$

$$\sqrt{2}\, c_3 = c_2$$

$$\therefore \quad c_1 = c_3$$

Substituting $c_1 = c_3$, $c_2 = \sqrt{2}\, c_1$ in (16) gives

$$c_1^2 + (\sqrt{2}\, c_1)^2 + (-c_1)^2 = 1$$

$$\therefore \quad c_1 = \frac{1}{2}$$

$$\therefore \quad c_1 = \frac{1}{2}; \quad c_3 = \frac{1}{2}; \quad c_2 = \frac{1}{\sqrt{2}}$$

Thus $\psi_1 = \frac{1}{2}\phi_1 + \frac{1}{\sqrt{2}}\phi_2 + \frac{1}{\sqrt{2}}\phi_3$

Similarly using values of x = O gives ψ_2:

$$\psi_2 = \frac{1}{\sqrt{2}}\phi_1 - \frac{1}{\sqrt{2}}\phi_3$$

and x = 2 gives

$$\psi_3 = \frac{1}{2}\phi_1 - \frac{1}{\sqrt{2}}\phi_2 + \frac{1}{2}\phi_3$$

Hence the wavefunctions and energies of the three molecular π-orbitals of the allyl entity are as follows:

$$\psi_1 = \frac{1}{2}\phi_1 + \frac{1}{\sqrt{2}}\phi_2 + \frac{1}{2}\phi_3 \qquad E = \alpha + \sqrt{2}\beta$$

$$\psi_2 = \frac{1}{\sqrt{2}}\phi_1 - \frac{1}{\sqrt{2}}\phi_3 \qquad E = \alpha$$

$$\psi_3 = \frac{1}{2}\phi_1 - \frac{1}{\sqrt{2}}\phi_2 + \frac{1}{2}\phi_3 \qquad E = \alpha - \sqrt{2}\beta$$

ψ_1 is essentially bonding, ψ_2 essentially non-bonding and ψ_3 essentially anti-bonding.

APPENDIX 2

GROUP THEORETICAL TREATMENT OF SELECTED MOLECULES AND SYSTEMS

1. The η^3 - Allyl - Metal system: C_s Symmetry

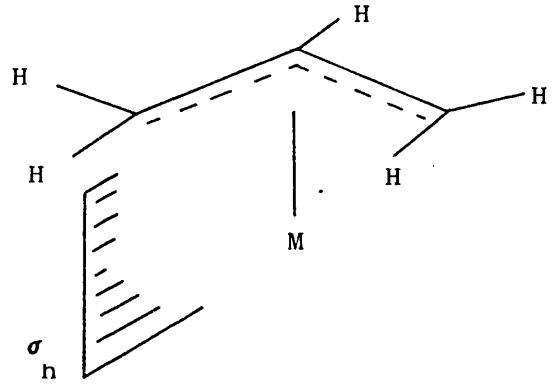

Figure 2A.1: The η^3-allyl-metal system with σ_h plane

A total representation for the molecular motions of the isolated [(η^3-allyl)-M] entity (Figure 2A.1) may be obtained using a set of 27 vectors (3 Cartesian coordinate vectors x, y and z for each of the N atoms where N = 9). Those atoms which are displaced under the operation of a certain symmetry element, R, contribute zero to its character, χ(R).

C_s	E	σ_h
Γ_{3N}	27	3

The total representation Γ_{3N} includes translational (Γ_{trans}) and rotational (Γ_{rot}) descriptions which must be subtracted to give the vibrational representation:-

C_s	E	σ_h
Γ_{3N}	27	3
Γ_{trans}	3	1
Γ_{rot}	3	-1
Γ_{vib}	21	3

This is a reducible representation which gives the following irreducible representations.

$\Gamma_{vib} = 12A' + 9A''$ (all modes are infrared and Raman active)

A description of the stretching vibrations may be derived by using the vectors generated by the linear distortion of the interatomic bonds (Figure 2A.2) as follows:

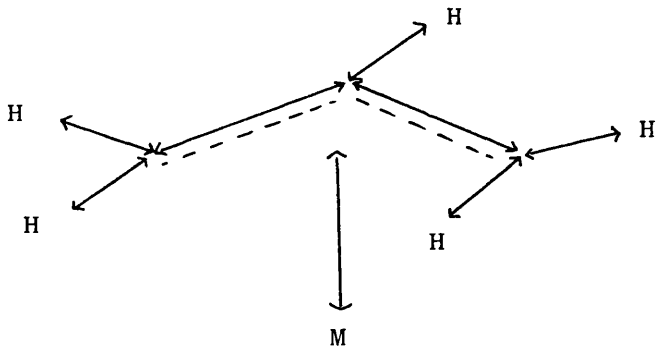

Figure 2A.2: Linear distortion vectors for the η^3-allyl-M system

C_s	E	σ_h
$\Gamma_{\nu(CCC)}$	2	0
$\Gamma_{\nu(CH)}$	1	1
$\Gamma_{\nu(CH_2)}$	4	0
$\Gamma_{\nu(M\text{-allyl})}$	1	1

These representations reduce to give:-

$$\Gamma_{\nu(CCC)} = A' + A'' \quad (1)$$

$$\Gamma_{\nu(CH)} = A' \quad (2)$$

$$\Gamma_{\nu(CH_2)} = 2A' + 2A'' \quad (3)$$

$$\Gamma_{\nu(M\text{-allyl})} = A' \quad (4)$$

The in plane deformations of the allyl are described by the vectors illustrated in Figure 2A.3 (some redundancies are inevitable because all the angles cannot be deformed independently.

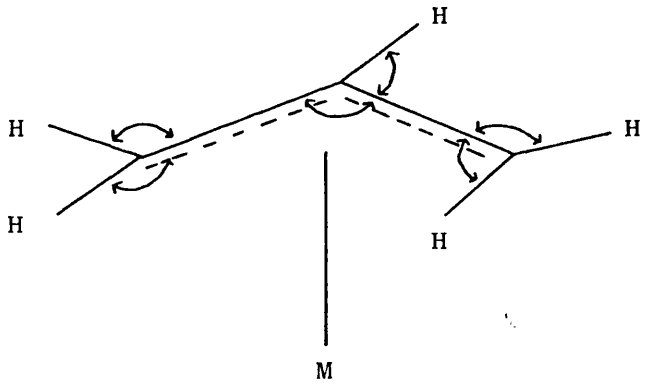

Figure 2A.3: A representation for deformations occurring in the plane of the η^3-allyl ligand.

C_s	E	σ_h
$\Gamma_{(\text{in plane def})}$	6	0

Thus $\Gamma_{(\text{in plane def})} = 3A' + 3A''$

Approximate descriptions of these modes are:-

δ (CH)	A"	(5)
δ (CCC)	A'	(6)
δ (CH_2)	A' + A"	(7)
ρ_r (CH_2)	A' + A"	(8)

The out-of-plane (i.e. out of the plane of the allyl group) deformations are best considered in two sets, those involving either (i) the carbon-hydrogen bonds ($\Gamma_{(i)}$) or (ii) the carbon-carbon skeleton $\Gamma_{(ii)}$.

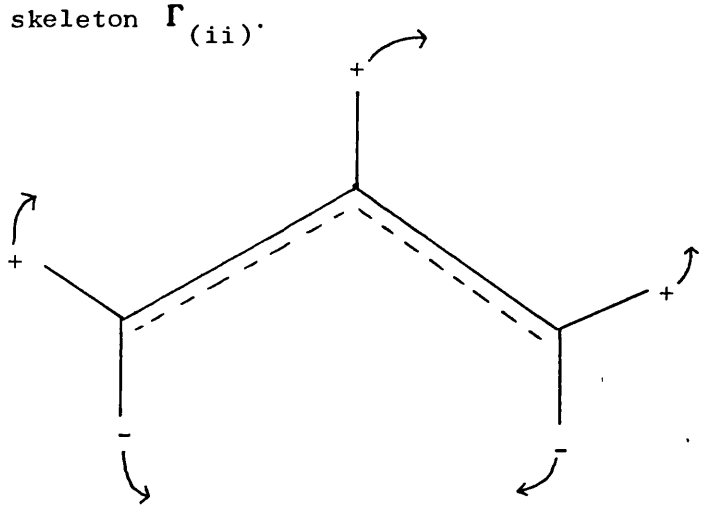

Figure 2A.4: A representation for the out-of-plane carbon-hydrogen bond deformations

C_s	E	σ_h
$\Gamma_{(i)}$	5	1

Thus $\Gamma_{(i)}$ = 3A' + 2A"

Approximate descriptions of these modes are

$\rho_t(CH_2)$	A' + A"	(9)
$\rho_w(CH_2)$	A' + A"	(10)
π (CH)	A'	(11)

If the vibrations accounted for in representations (1) - (11) are subtracted from the total Γ_{vib} then the remainder (A' + A") gives the skeletal modes associated with the $\eta^3 - C_3H_5 - M$ unit. These are depicted in Figure 2A.5 and are best described as symmetry tilts.

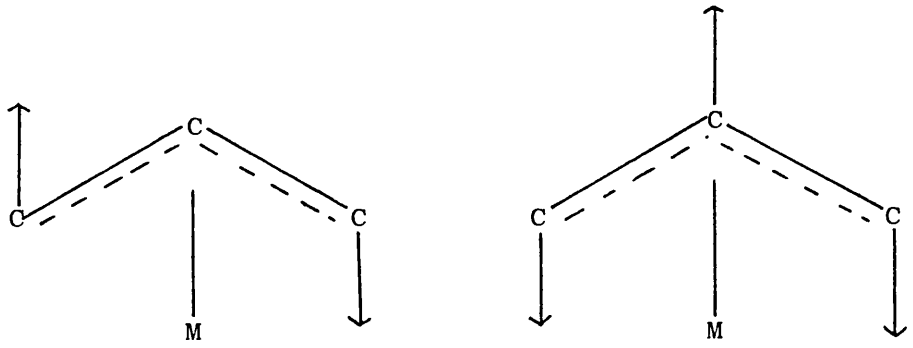

Figure 2A.5: The Symmetry tilt skeletal modes of the η^3-C_3H_5-M unit.

2. The Anion $[(\eta^3\text{-}C_3H_5)_2M_2(CO)_4Cl_3]^-$: C_2 Symmetry

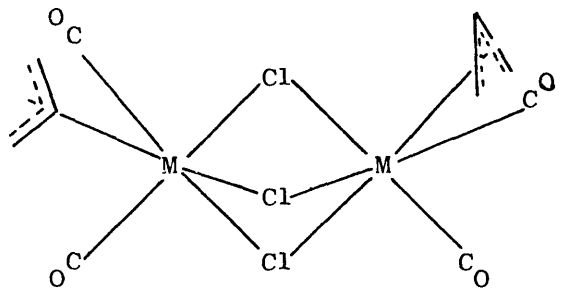

Figure 2A.6: The anion $[(\eta^3\text{-}C_3H_5)_2M_2(CO)_4Cl_3]^-$ with C_2 symmetry

An overall vibrational representation of the anion $[(\eta^3\text{-}C_3H_5)_2M_2(CO)_4Cl_3]^-$ may be derived as described in the preceding section by considering the effect of the C_2 symmetry operators on the three Cartesian coordinates associated with each of the 15 atoms (to simplify the treatment both allyl groups are considered as point groups) thus:-

C_2	E	C_2
Γ_{3N}	45	-1
Γ_{trans}	3	-1
Γ_{rot}	3	-1
Γ_{vib}	39	+1

Reduction of Γ_{vib} gives·

Γ_{vib} = 20A + 19B, all modes being infrared and Raman active.

A description of the stretching vibrations may be derived by using the vectors generated by linear distortion of the relevant interatomic bonds (Figure 2A.7) as follows:

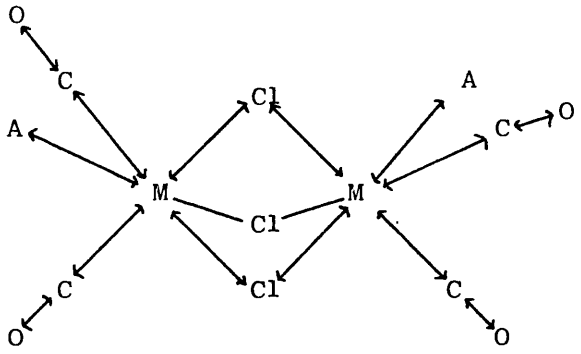

Figure 2A.7: Linear distortion vectors for the C_2 Anion

C_2	E	C_2
$\Gamma_{\nu(CO)}$	4	0
$\Gamma_{\nu(MC)}$	4	0
$\Gamma_{\nu(MA)}$	2	0
$\Gamma_{\nu(MCl)}$	6	0

These representations reduce to:

$$\Gamma_{\nu(CO)} = 2A + 2B \quad (1)$$

$$\Gamma_{\nu(MC)} = 2A + 2B \quad (2)$$

$$\Gamma_{\nu(MA)} = A + B \quad (3)$$

$$\Gamma_{\nu(MCl)} = 3A + 3B \quad (4)$$

For the δ(MCO) bending modes it is necessary to define two orthogonal angular distortion vectors for each MCO group (Figure 2A.8)

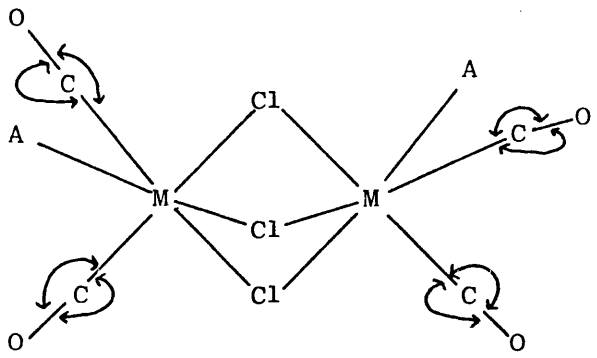

Figure 2A.8: Angular distortion vectors for the C_2 anion

C_2	E	C_2
δ(MCO)	8	0

δ(MCO) reduces as follows

$$\delta(MCO) = 4A + 4B \qquad (5)$$

Independent descriptions for the skeletal deformations δ(AMC), δ(AMCl), δ(CMC), δ(CMCl) and δ(ClMCl) are difficult to ascertain. However, an approximate representation of the δ(ClMCl) vibrations may be distinguished by considering the $[M_2(\mu\text{-}Cl)_3]$ unit under C_2-symmetry in isolation (Figure 2A.9)

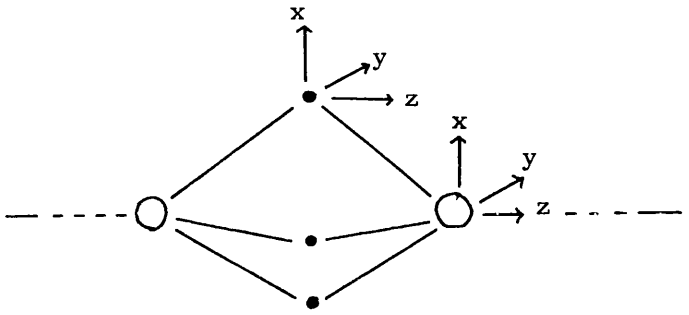

Figure 2A.9: The $[M_2(\mu\text{-Cl})_3]$ unit

The vibrational representation for this unit follows the same reasoning as for the complete molecule:

C_2	E	C_2
Γ_{tot}	15	-1
Γ_{rot}	3	-1
Γ_{trans}	3	-1
Γ_{vib}	9	+1

Thus $\Gamma_{vib} = 5A + 4B$ (6)

This description includes the $\Gamma_{\nu(MCl)}$ representation already derived and so its subtraction gives

$\Gamma_{\delta(ClMCl)} = 2A + B$

If the vibrations accounted for in representations (1) - (6) are subtracted from the total Γ_{vib} then the remainder gives the skeletal vibrations δ(AMC), δ(AMCl), δ(CMC) and δ(CMCl):-

$$\Gamma_{\delta(AMC)} + \Gamma_{\delta(AMCl)} + \Gamma_{\delta(CMC)} + \Gamma_{\delta(CMCl)} = 6A + 6B$$

3. The Tricarbonyl Complexes Mer- and Fac-$[M(CO)_3P_3]$

a) Mer-Tricarbonyls: C_{2v} Symmetry

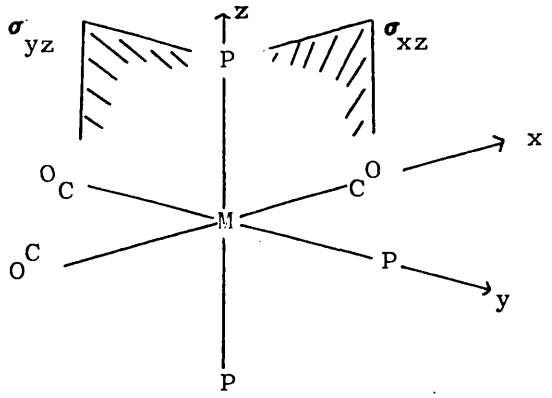

Figure 2A.10: The $[M(CO)_3P_3]$ unit with C_{2v} symmetry

The total representation for the mer-$[M(CO)_3P_3]$ unit is:-

C_{2v}	E	C_2	$\sigma_v(xz)$	$\sigma'_v(yz)$
Γ_{3N}	30	-4	8	6
Γ_{rot}	3	-1	-1	-1
Γ_{trans}	3	-1	1	1
Γ_{vib}	24	-2	8	6

On reduction:- $\Gamma_{vib} = 9A_1 + 2A_2 + 7B_1 + 6B_2$

A_1, B_1 and B_2 modes are infrared and Raman active, the A_2 mode is Raman active only.

The vectors generated by the linear distortion of the CO, MC and MP bonds give rise to the following descriptions for ν(CO),

ν(MC) and ν(MP):-

C_{2v}	E	C_2	$\sigma_v(xz)$	$\sigma'_v(yz)$
$\Gamma_{\nu(tot)}$	9	3	5	5
$\Gamma_{\nu(CO)}$	3	1	1	3
$\Gamma_{\nu(MC)*}$	3	1	1	3
$\Gamma_{\nu(MP)}$	3	1	3	1

These representations reduce to give:-

$$\Gamma_{\nu(CO)} = 2A_1 + B_2 \qquad (1)$$

$$\Gamma_{\nu(MC)} = 2A_1 + B_2 \qquad (2)$$

$$\Gamma_{\nu(MP)} = 2A_1 + B_1 \qquad (3)$$

The δ(MCO) vibrations may be described by pairs of orthogonal angular distortion vectors as shown in Figure 2A.11.

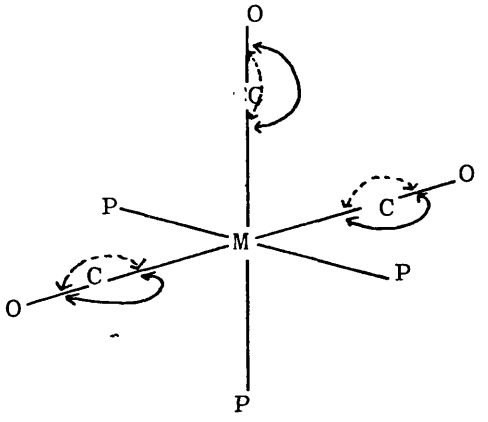

Figure 2A.11: Vectors for the δ(MCO) vibrations

* Making the assumption that C $\sim$ CO

Thus the reducible representation for the MCO deformations is given by:

C_{2v}	E	C_2	$\sigma_v(xz)$	$\sigma'_v(yz)$
$\Gamma_{\delta(MCO)}$	6	-2	0	0

Thus $\Gamma_{\delta(MCO)} = A_1 + A_2 + 2B_1 + 2B_2$

Figure 2A.12 shows the two vectors for the δ(CMC) deformations:-

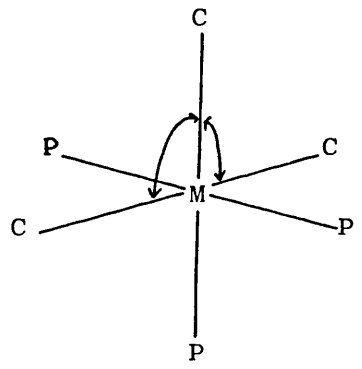

Figure 2A.12: Vectors for the δ(CMC) vibrations

These vectors give rise to the reducible representation:-

C_{2v}	E	C_2	$\sigma_v(xz)$	$\sigma'_v(yz)$
$\Gamma_{\delta(CMC)}$	2	0	2	0

Thus $\Gamma_{\delta(CMC)} = A_1 + B_1$ (4)

Similarly

$$\Gamma_{\delta(PMP)} = A_1 + B_2 \quad (5)$$

Subtraction of the vibrations accounted for in representations (1) - (5) from the total Γ_{vib} gives the skeletal vibration δ(CMP):-

$$\Gamma_{\delta(CMP)} = A_2 + 3B_1 + B_2$$

b) Fac-Tricarbonyls: C_{3v} Symmetry

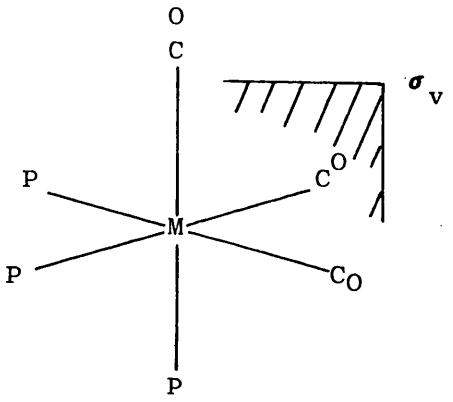

Figure 2A.13: The $[M(CO)_3P_3]$ unit with C_{3v} symmetry

The total representation for the fac-$[M(CO)_3P_3]$ unit is:-

C_{3v}	E	$2C_3$	$3\sigma_v$
Γ_{3N}	30	0	4
Γ_{rot}	3	0	-1
Γ_{trans}	3	0	1
Γ_{vib}	24	0	4

On reduction:- $\Gamma_{vib} = 6A_1 + 2A_2 + 8E$

A_1 and E modes are infrared and Raman active, the A_2 mode is inactive.

The vectors generated by the linear distortions of the CO, MC and MP bonds and the angular distortions of the M - C - O, C - M - C and P - M - P bonds give rise to the following descriptions for the ν(CO), ν(MC), ν(MP), δ(MCO), δ(CMC) and δ(PMP) vibrations:-

C_{3v}	E	$2C_3$	$3\sigma_v$
$\Gamma_{\nu(CO)}$	3	0	1
$\Gamma_{\nu(MC)}$	3	0	1
$\Gamma_{\nu(MP)}$	3	0	1
$\Gamma_{\delta(MCO)}$	6	0	0
$\Gamma_{\delta(CMC)}$	3	0	1
$\Gamma_{\delta(PMP)}$	3	0	1

These representations reduce to give:-

$\Gamma_{\nu(CO)} = A_1 + E$

$\Gamma_{\nu(MC)} = A_1 + E$

$\Gamma_{\nu(MP)} = A_1 + E$

$\Gamma_{\delta(MCO)} = A_1 + A_2 + 2E$

$\Gamma_{\delta(CMC)} = A_1 + E$

$\Gamma_{\delta(PMP)} = A_1 + E$

Subtraction of the above representations from Γ_{vib} gives δ(CMP):-

$\Gamma_{\delta(CMP)} = A_2 + E$

APPENDIX 3

Solvents, Reagents, Physical Methods and Instrumentation.

General

The preparation of the complexes described were carried out under an atmosphere of dry nitrogen gas at room temperature unless otherwise stated. Standard Quickfit glassware was dried at 110°C for several hours prior to assembly and thoroughly purged with dry nitrogen gas before use. All reactions involving carbonyls were monitored by infrared spectroscopy.

Solvents

All standard Laboratory Reagent grade solvents were dried over molecular sieves or sodium wire as appropriate and deoxygenated before use. Nitromethane for conductance measurements required further purification. It was refluxed over P_2O_5 and then fractionated, the fraction boiling between 99-100°C (P = 750 mm Hg) being collected. Finally to remove traces of P_2O_5, the CH_3NO_2 was distilled from 3A molecular sieves in a closed nitrogen filled system. In this way the conductance of the solvent could be reduced to 1×10^{-7} mhos but strict exclusion of moisture was necessary to maintain this figure.

Reagents

Unless otherwise stated Analar and Standard Laboratory Reagents were used as received without further purification.

Infrared Spectroscopy

Infrared spectra in the 4000 - 200 cm^{-1} region were obtained on a Hilger-Watts Infrascan H 1200 or on Perkin-Elmer 735 and 597 spectrophotometers. Samples were prepared as Nujol mulls held between CsI plates or as solutions in a Beckmann-RIIC FS 125 0.1 mm KBr cell. A polystyrene film was used for calibration. Far-infrared spectra (400 - 40 cm^{-1}) of samples dispersed in pressed polythene discs were recorded using a Beckmann-RIIC FS 720 interferometer. Fourier transforms of the interferograms were computed on an ICL 4-50 computer by means of a Fortran IV programme.

Raman Spectroscopy

Raman spectra of solid samples held in capillary tubes were measured using a Spex 1401 spectrometer in conjunction with a Spectra-Physics 125 He-Ne laser having an output of ca. 50 mW at 632.8 nm, a cooled (-15°C) photomultiplier and photon-counting detection. The spectra were calibrated by means of several lines in the neon gas emission spectrum and from known indene peaks.

Mass Spectroscopy

Mass spectra were obtained on an AEI MS 12 spectrometer using direct insertion probes or an all glass heated inlet system (AGHIS). A source temperature of 220°C was normally used to volatilize the sample, and ionisation energies of 70 eV and ca. 12 eV were generally employed. For high molecular weight samples calibration with perfluorokerosene (PFK) was sometimes necessary .

NMR Spectroscopy

^{1}H NMR spectra were measured on a JEOL PS 100 spectrometer, together with the associated variable temperature controller. Tetramethylsilane (TMS) was used as internal reference. Samples were dissolved under nitrogen to give 5 - 10% solutions held in 4 mm silica tubes. The spectrograde solvents CD_2Cl_2, $CDCl_3$, CD_3CN and CD_3OD were used as received apart from drying over molecular sieves.

^{31}P NMR spectra were measured on a JEOL PS 100 spectrometer and calibrated against the resonance of H_3PO_4 (external reference).

^{13}C NMR spectra were recorded on JEOL PTF-100 by Mr. P. Benyon at JEOL (UK) Ltd., and FX-90 by Dr. M. Murray, University of Bristol spectrometers on solutions containing ca. 20% of sample using TMS as internal reference.

Conductivity

Conductivity measurements were determined at 25°C using a Wayne-Kerr Autobalance bridge and a dip-type cell with platinum electrodes. A cell constant of 1.56 cm^{-1} was determined by measuring the conductance of aqueous 0.1 M KCl (Λ_M = 128.96 mhos cm^2 mol^{-1}).

Analysis

Carbon, hydrogen, nitrogen and chloride analyses were determined by Dr. F.B. Strauss at the microanalytical laboratories, Oxford.

Melting Points.

Melting points were recorded on an Electrothermal apparatus.

APPENDIX 4

Calculated and Observed Structure Factors and Thermal Parameters

H	K	L	FO	FC	H	K	L	FO	FC	H	K	L	FO	FC	H	K	L	FO	FC	H	K	L	FO	FC
2	0	0	200	-248	7	2	0	86	78	-9	5	0	25	32	-1	8	0	51	-48	-6	-5	1	98	89
5	0	0	38	-45	8	2	0	14	16	-8	5	0	26	-27	0	8	0	12	22	-4	-5	1	131	-123
6	0	0	67	-62	9	2	0	29	-30	-7	5	0	50	-57	1	8	0	37	38	-3	-5	1	28	-27
7	0	0	29	-29	10	2	0	9	-10	-6	5	0	5	-6	2	8	0	11	-15	-2	-5	1	79	78
8	0	0	63	58	-12	3	0	35	35	-5	5	0	45	36	0	-9	1	68	-25	-1	-5	1	25	27
9	0	0	84	80	-11	3	0	36	37	-4	5	0	40	38	2	-9	1	38	36	0	-5	1	43	-45
10	0	0	38	-33	-10	3	0	38	-40	-3	5	0	46	-51	3	-9	1	36	31	1	-5	1	41	-37
11	0	0	63	-62	-9	3	0	30	-31	-2	5	0	51	-45	4	-9	1	46	-41	2	-5	1	54	49
-12	1	0	17	-17	-8	3	0	38	41	-1	5	0	79	77	5	-9	1	48	-41	3	-5	1	68	67
-11	1	0	19	-16	-7	3	0	36	40	0	5	0	11	14	-4	-8	1	9	10	4	-5	1	15	-17
-10	1	0	45	44	-6	3	0	6	-9	1	5	0	41	-41	-3	-8	1	47	51	5	-5	1	103	-109
-9	1	0	13	13	-5	3	0	33	-36	3	5	0	30	28	-1	-8	1	53	-57	6	-5	1	22	20
-8	1	0	118	-106	-4	3	0	35	-33	4	5	0	66	64	0	-8	1	12	-19	7	-5	1	66	71
-7	1	0	28	-27	-3	3	0	95	102	5	5	0	6	9	1	-8	1	54	53	9	-5	1	37	-38
-6	1	0	71	68	-2	3	0	88	82	6	5	0	41	-45	2	-8	1	27	38	10	-5	1	19	-23
-5	1	0	65	65	-1	3	0	219	-233	7	5	0	9	-10	3	-8	1	49	-45	11	-5	1	27	27
-4	1	0	18	-22	0	3	0	22	-25	8	5	0	23	24	5	-8	1	41	39	-9	-4	1	35	-41
-3	1	0	35	-32	1	3	0	89	100	-11	6	0	24	27	6	-8	1	38	37	-7	-4	1	65	63
-2	1	0	8	9	3	3	0	17	-16	-10	6	0	17	22	7	-8	1	43	-43	-6	-4	1	27	27
-1	1	0	121	137	4	3	0	33	-34	-9	6	0	20	-17	8	-8	1	42	-44	-5	-4	1	87	-91
0	1	0	19	21	5	3	0	8	6	-7	6	0	22	21	-6	-7	1	18	-27	-4	-4	1	57	-58
1	1	0	89	-105	6	3	0	49	47	-5	6	0	34	-32	-4	-7	1	23	25	-3	-4	1	84	85
2	1	0	25	-25	7	3	0	5	9	-4	6	0	42	-38	-1	-7	1	8	8	-2	-4	1	33	35
3	1	0	41	33	8	3	0	47	-43	-2	6	0	70	66	2	-7	1	45	-43	-1	-4	1	64	-68
4	1	0	27	30	10	3	0	33	32	-1	6	0	49	44	3	-7	1	37	-32	1	-4	1	124	124
6	1	0	86	-81	-12	4	0	48	52	0	6	0	8	12	5	-7	1	54	47	2	-4	1	94	94
7	1	0	10	8	-11	4	0	32	-31	1	6	0	13	-11	6	-7	1	20	19	3	-4	1	52	-53
8	1	0	107	94	-10	4	0	51	-60	2	6	0	36	-36	7	-7	1	34	-31	4	-4	1	115	-115
9	1	0	23	-20	-9	4	0	51	60	4	6	0	15	15	8	-7	1	17	-22	6	-4	1	73	73
10	1	0	40	-42	-8	4	0	50	58	5	6	0	20	-21	9	-7	1	19	18	7	-4	1	22	21
-12	2	0	11	14	-7	4	0	14	-18	6	6	0	13	-15	10	-7	1	28	29	8	-4	1	34	-38
-11	2	0	25	26	-6	4	0	69	-77	7	6	0	22	23	-7	-6	1	11	-13	10	-4	1	48	55
-10	2	0	7	5	-5	4	0	19	-17	-9	7	0	38	-37	-6	-6	1	10	10	11	-4	1	23	20
-8	2	0	9	-12	-4	4	0	90	92	-7	7	0	33	33	-5	-6	1	19	29	-11	-3	1	20	-23
-7	2	0	49	52	-3	4	0	42	44	-5	7	0	41	-38	-3	-6	1	40	-41	-9	-3	1	12	13
-6	2	0	28	22	-2	4	0	135	-152	-3	7	0	61	53	-2	-6	1	11	11	-8	-3	1	28	29
-5	2	0	50	-44	-1	4	0	75	-74	-2	7	0	50	45	-1	-6	1	14	-11	-6	-3	1	41	-43
-4	2	0	25	27	0	4	0	120	123	-1	7	0	33	-30	0	-6	1	27	28	-5	-3	1	23	-28
-3	2	0	53	55	1	4	0	52	54	0	7	0	28	-29	2	-6	1	82	-77	-4	-3	1	36	32
-2	2	0	44	38	2	4	0	61	-61	2	7	0	25	22	3	-6	1	15	13	-3	-3	1	19	-21
-1	2	0	13	6	3	4	0	49	-49	4	7	0	32	-33	4	-6	1	78	76	-2	-3	1	71	62
0	2	0	52	-56	4	4	0	26	28	5	7	0	21	-23	6	-6	1	48	-49	-1	-3	1	17	-21
1	2	0	52	-42	5	4	0	76	69	-7	8	0	22	21	8	-6	1	19	19	0	-3	1	27	-24
2	2	0	61	-65	6	4	0	7	6	-6	8	0	28	-34	9	-6	1	18	18	1	-3	1	145	158
3	2	0	54	52	7	4	0	90	-85	-5	8	0	44	-40	10	-6	1	11	-9	2	-3	1	36	-28
4	2	0	6	3	8	4	0	18	18	-4	8	0	53	52	11	-6	1	26	-26	3	-3	1	160	-152
5	2	0	70	-66	9	4	0	56	57	-3	8	0	76	66	-9	-5	1	10	11	4	-3	1	24	-25
6	2	0	13	-9	-10	5	0	29	31	-2	8	0	62	-52	-8	-5	1	41	-48	5	-3	1	61	73

H	K	L	FO	FC	H	K	L	FO	FC	H	K	L	FO	FC	H	K	L	FO	FC	H	K	L	FO	FC
6	-3	1	25	24	9	-1	1	41	-34	11	1	1	27	26	-4	4	1	50	-55	2	7	1	46	-42
8	-3	1	15	-17	10	-1	1	37	-40	-12	2	1	9	-9	-2	4	1	67	67	3	7	1	17	16
9	-3	1	7	6	11	-1	1	13	11	-9	2	1	30	30	-1	4	1	16	16	-4	8	1	23	-28
10	-3	1	23	26	-11	0	1	37	36	-8	2	1	42	37	0	4	1	74	-71	-3	8	1	46	-40
12	-3	1	48	-54	-10	0	1	33	35	-7	2	1	17	-20	1	4	1	56	-67	-2	8	1	32	35
-11	-2	1	9	-10	-9	0	1	53	-54	-6	2	1	49	-43	2	4	1	76	70	-1	8	1	49	44
-10	-2	1	19	-21	-8	0	1	57	-59	-4	2	1	42	-37	3	4	1	67	63	0	8	1	27	-23
-9	-2	1	34	32	-7	0	1	65	66	-3	2	1	65	67	4	4	1	31	-30	-2	-9	2	39	-46
-7	-2	1	81	-78	-6	0	1	107	97	-2	2	1	59	-61	5	4	1	36	-40	0	-9	2	40	55
-6	-2	1	12	15	-5	0	1	104	-102	-1	2	1	60	-59	6	4	1	12	12	1	-9	2	23	20
-5	-2	1	113	118	-4	0	1	63	-62	0	2	1	126	152	7	4	1	53	49	2	-9	2	56	-43
-4	-2	1	18	-17	-3	0	1	84	78	1	2	1	72	68	8	4	1	12	-12	3	-9	2	23	-18
-3	-2	1	39	-42	-2	0	1	131	138	2	2	1	114	-98	9	4	1	36	-39	4	-9	2	45	41
-2	-2	1	15	-7	-1	0	1	42	-47	3	2	1	75	-73	-11	5	1	10	10	5	-9	2	21	19
-1	-2	1	63	-67	0	0	1	169	-207	4	2	1	15	18	-10	5	1	15	-13	6	-9	2	51	-51
0	-2	1	32	33	1	0	1	12	13	5	2	1	17	18	-9	5	1	22	-24	-5	-8	2	35	34
1	-2	1	86	85	2	0	1	132	133	6	2	1	27	23	-7	5	1	15	17	-3	-8	2	50	-50
2	-2	1	25	-28	3	0	1	42	43	7	2	1	19	-19	-4	5	1	42	-36	-1	-8	2	55	61
3	-2	1	79	-76	4	0	1	103	-95	8	2	1	21	-23	-3	5	1	15	14	0	-8	2	11	8
4	-2	1	114	111	5	0	1	27	-30	9	2	1	39	33	-2	5	1	50	63	1	-8	2	58	-53
5	-2	1	13	13	6	0	1	49	47	10	2	1	42	44	-1	5	1	47	-47	6	-8	2	47	-48
6	-2	1	51	-48	7	0	1	38	37	-12	3	1	28	-29	0	5	1	66	-58	7	-8	2	9	10
7	-2	1	44	-44	8	0	1	55	-52	-11	3	1	50	-47	1	5	1	31	34	8	-8	2	59	56
8	-2	1	19	-18	9	0	1	36	-34	-10	3	1	52	47	2	5	1	42	48	-6	-7	2	10	9
9	-2	1	76	71	10	0	1	32	29	-9	3	1	65	76	3	5	1	13	-11	-5	-7	2	16	16
10	-2	1	21	20	11	0	1	45	40	-8	3	1	44	-48	4	5	1	22	-21	-4	-7	2	25	-20
11	-2	1	63	-56	12	0	1	9	-9	-7	3	1	102	-109	5	5	1	14	-12	-3	-7	2	30	-29
12	-2	1	24	-21	-11	1	1	12	13	-6	3	1	37	34	7	5	1	25	24	-2	-7	2	14	17
-12	-1	1	37	-39	-10	1	1	27	-22	-5	3	1	80	83	-10	6	1	32	-33	-1	-7	2	26	28
-11	-1	1	19	9	-9	1	1	19	-17	-4	3	1	29	-23	-9	6	1	9	9	0	-7	2	8	-11
-10	-1	1	63	63	-8	1	1	83	79	-3	3	1	100	-94	-8	6	1	27	26	1	-7	2	21	-20
-9	-1	1	32	33	-7	1	1	14	14	-2	3	1	46	37	-4	6	1	32	29	2	-7	2	7	7
-8	-1	1	64	-64	-6	1	1	111	-101	-1	3	1	135	139	-2	6	1	34	-32	3	-7	2	19	20
-7	-1	1	82	-92	-5	1	1	9	2	1	3	1	95	-101	-1	6	1	41	-36	5	-7	2	66	-68
-6	-1	1	63	60	-4	1	1	23	21	2	3	1	90	-87	1	6	1	56	53	6	-7	2	29	-27
-5	-1	1	100	103	-3	1	1	23	-19	3	3	1	47	44	2	6	1	13	19	7	-7	2	71	68
-4	-1	1	91	-96	-2	1	1	75	78	4	3	1	51	52	3	6	1	21	-23	8	-7	2	46	51
-3	-1	1	44	-45	0	1	1	71	-84	6	3	1	43	-40	4	6	1	28	-29	9	-7	2	32	-33
-2	-1	1	92	88	1	1	1	5	5	7	3	1	28	27	5	6	1	16	19	10	-7	2	28	-27
-1	-1	1	167	197	2	1	1	90	86	8	3	1	53	47	6	6	1	22	20	-8	-6	2	22	22
0	-1	1	70	-77	3	1	1	100	-97	9	3	1	14	-13	-7	7	1	66	-57	-7	-6	2	30	29
1	-1	1	164	-189	4	1	1	38	-35	10	3	1	44	-42	-5	7	1	67	52	-5	-6	2	31	-31
3	-1	1	115	116	5	1	1	49	43	-12	4	1	28	-28	-4	7	1	51	46	-3	-6	2	42	46
4	-1	1	29	29	6	1	1	54	50	-10	4	1	41	44	-3	7	1	47	-46	-2	-6	2	20	22
5	-1	1	85	-88	7	1	1	30	30	-9	4	1	49	-51	-2	7	1	38	-34	-1	-6	2	57	-52
6	-1	1	31	-30	8	1	1	78	-68	-8	4	1	70	-77	-1	7	1	43	37	0	-6	2	82	-79
7	-1	1	50	48	9	1	1	36	-34	-7	4	1	50	54	0	7	1	32	31	1	-6	2	40	34
8	-1	1	49	48	10	1	1	49	40	-6	4	1	92	85	1	7	1	33	-36	2	-6	2	70	65

H	K	L	FO	FC	H	K	L	FO	FC	H	K	L	FO	FC	H	K	L	FO	FC	H	K	L	FO	FC
-3	-8	3	23	32	-6	-5	3	69	71	5	-3	3	33	30	9	-1	3	8	-11	-2	2	3	77	-76
-2	-8	3	22	25	-5	-5	3	10	6	6	-3	3	80	83	-12	0	3	9	-8	-1	2	3	26	29
-1	-8	3	21	-22	-4	-5	3	47	-47	7	-3	3	70	-65	-11	0	3	23	22	0	2	3	40	38
0	-8	3	37	-41	-3	-5	3	11	-11	8	-3	3	73	-73	-9	0	3	13	-10	1	2	3	10	10
1	-8	3	17	18	-2	-5	3	57	64	9	-3	3	40	43	-8	0	3	24	-24	2	2	3	51	-47
2	-8	3	20	18	-1	-5	3	38	36	10	-3	3	61	69	-6	0	3	37	32	3	2	3	23	-22
3	-8	3	10	-7	0	-5	3	95	-95	11	-3	3	10	-12	-5	0	3	12	8	4	2	3	46	44
4	-8	3	27	-26	1	-5	3	31	-31	-11	-2	3	56	-48	-4	0	3	118	-116	5	2	3	41	37
5	-8	3	10	11	2	-5	3	41	41	-10	-2	3	36	34	-2	0	3	157	156	6	2	3	40	-32
6	-8	3	64	59	3	-5	3	40	38	-9	-2	3	69	73	-1	0	3	22	-24	7	2	3	25	-22
7	-8	3	11	8	4	-5	3	29	-25	-7	-2	3	73	-85	0	0	3	29	-19	-10	3	3	27	27
8	-8	3	64	-59	5	-5	3	48	-45	-6	-2	3	19	-23	1	0	3	37	-39	-9	3	3	20	19
-7	-7	3	21	-25	7	-5	3	54	54	-5	-2	3	70	62	2	0	3	23	-20	-7	3	3	22	-30
-6	-7	3	7	-11	9	-5	3	40	-40	-4	-2	3	90	85	3	0	3	83	71	-6	3	3	24	17
-5	-7	3	9	-11	-9	-4	3	18	-25	-3	-2	3	45	-40	5	0	3	89	-92	-5	3	3	92	91
-3	-7	3	36	41	-8	-4	3	25	22	-2	-2	3	105	-104	6	0	3	37	38	-4	3	3	19	-22
-2	-7	3	18	-16	-7	-4	3	17	17	-1	-2	3	78	69	7	0	3	75	78	-3	3	3	113	-124
-1	-7	3	61	-60	-6	-4	3	9	13	0	-2	3	30	32	8	0	3	22	-19	-2	3	3	23	21
0	-7	3	50	52	-4	-4	3	55	-55	1	-2	3	70	-67	9	0	3	64	-64	-1	3	3	37	42
1	-7	3	64	59	-3	-4	3	6	-6	2	-2	3	59	-68	-12	1	3	32	32	3	3	3	22	18
2	-7	3	33	-25	-2	-4	3	108	113	3	-2	3	41	40	-10	1	3	49	-51	4	3	3	36	33
3	-7	3	56	-55	-1	-4	3	19	-19	4	-2	3	67	75	-8	1	3	13	15	5	3	3	32	-30
5	-7	3	55	53	0	-4	3	97	-94	5	-2	3	34	34	-7	1	3	29	30	6	3	3	45	-42
6	-7	3	19	14	1	-4	3	20	-16	6	-2	3	51	-49	-6	1	3	30	28	-7	4	3	39	-40
7	-7	3	56	-55	2	-4	3	73	77	7	-2	3	36	-38	-5	1	3	57	-52	-6	4	3	29	39
8	-7	3	37	-38	3	-4	3	17	16	8	-2	3	39	39	-4	1	3	35	-32	-5	4	3	48	49
9	-7	3	57	57	4	-4	3	84	-88	9	-2	3	7	9	-3	1	3	92	90	-4	4	3	59	-55
10	-7	3	26	27	5	-4	3	28	-29	10	-2	3	11	-12	-2	1	3	34	28	-3	4	3	38	-36
-8	-6	3	29	-29	6	-4	3	73	73	11	-2	3	16	-20	-1	1	3	55	-61	-2	4	3	44	34
-7	-6	3	50	-44	7	-4	3	54	57	-11	-1	3	9	10	0	1	3	61	-61	-1	4	3	37	42
-5	-6	3	47	54	8	-4	3	66	-63	-10	-1	3	59	58	1	1	3	56	55	0	4	3	20	-17
-4	-6	3	9	-11	9	-4	3	39	-35	-9	-1	3	13	-12	2	1	3	54	60	1	4	3	52	-48
-3	-6	3	57	-59	10	-4	3	19	22	-8	-1	3	47	-63	3	1	3	45	-43	3	4	3	65	60
-2	-6	3	22	-26	11	-4	3	28	31	-7	-1	3	29	-23	4	1	3	88	-81	5	4	3	73	-65
-1	-6	3	113	115	-10	-3	3	38	-36	-6	-1	3	54	52	5	1	3	34	35	-9	5	3	35	-36
0	-6	3	60	59	-8	-3	3	31	30	-5	-1	3	61	56	6	1	3	88	87	-7	5	3	32	32
1	-6	3	103	-103	-7	-3	3	25	23	-4	-1	3	34	-35	7	1	3	23	-26	-5	5	3	29	-33
2	-6	3	13	-11	-6	-3	3	25	-24	-3	-1	3	124	-120	8	1	3	46	-47	-4	5	3	18	-22
3	-6	3	33	27	-5	-3	3	14	-18	-2	-1	3	78	67	9	1	3	12	-12	-3	5	3	16	17
4	-6	3	9	-9	-4	-3	3	20	18	-1	-1	3	78	73	-11	2	3	63	-60	0	5	3	35	-40
5	-6	3	13	-10	-3	-3	3	97	96	0	-1	3	84	-69	-10	2	3	23	-24	1	5	3	11	12
6	-6	3	27	-20	-2	-3	3	70	-77	1	-1	3	47	-50	-9	2	3	58	69	2	5	3	69	65
8	-6	3	53	53	-1	-3	3	143	-155	2	-1	3	41	39	-8	2	3	43	48	4	5	3	63	-56
9	-6	3	14	11	0	-3	3	70	69	3	-1	3	98	91	-7	2	3	59	-56	-6	6	3	50	-50
10	-6	3	41	-41	1	-3	3	31	29	4	-1	3	14	15	-6	2	3	43	-45	-4	6	3	53	52
-9	-5	3	35	-38	2	-3	3	37	35	5	-1	3	52	-55	-5	2	3	35	35	-3	6	3	10	6
-8	-5	3	66	-57	3	-3	3	6	5	6	-1	3	42	-43	-4	2	3	85	83	-2	6	3	34	-30
-7	-5	3	24	27	4	-3	3	67	-69	7	-1	3	34	32	-3	2	3	41	-47	-1	6	3	9	-13

H	K	L	FO	FC	H	K	L	FO	FC	H	K	L	FO	FC	H	K	L	FO	FC	H	K	L	FO	FC
0	6	3	19	20	5	-6	4	30	23	-4	-3	4	31	-30	8	-1	4	42	-44	1	2	4	22	22
1	6	3	15	19	7	-6	4	13	-12	-3	-3	4	51	-50	-11	0	4	24	-20	3	2	4	10	-10
-2	-9	4	23	-26	8	-6	4	23	-24	-2	-3	4	33	31	-10	0	4	28	-27	4	2	4	13	-17
-1	-9	4	17	-17	9	-6	4	11	-12	-1	-3	4	43	44	-9	0	4	15	15	5	2	4	18	-17
0	-9	4	26	30	10	-6	4	16	12	1	-3	4	85	-90	-8	0	4	23	19	7	2	4	29	25
1	-9	4	23	22	-9	-5	4	6	8	2	-3	4	9	11	-7	0	4	19	-16	-9	3	4	21	-21
2	-9	4	39	-43	-8	-5	4	38	35	3	-3	4	66	66	-6	0	4	46	-39	-8	3	4	11	10
3	-9	4	24	-22	-7	-5	4	29	-29	4	-3	4	43	42	-5	0	4	8	-9	-7	3	4	31	28
4	-9	4	45	40	-6	-5	4	41	-42	6	-3	4	28	-28	-4	0	4	109	101	-5	3	4	40	-44
5	-9	4	20	21	-5	-5	4	24	18	7	-3	4	30	33	-3	0	4	24	25	-3	3	4	43	42
-5	-8	4	18	26	-4	-5	4	23	24	8	-3	4	25	28	-2	0	4	108	-96	-2	3	4	24	25
-3	-8	4	26	-32	-3	-5	4	61	58	9	-3	4	32	-34	-1	0	4	41	-42	-1	3	4	38	-46
-2	-8	4	40	-43	-2	-5	4	6	-6	10	-3	4	55	-57	0	0	4	100	89	0	3	4	55	-54
-1	-8	4	31	31	-1	-5	4	75	-73	-11	-2	4	36	41	1	0	4	55	58	1	3	4	29	27
0	-8	4	55	55	0	-5	4	6	5	-10	-2	4	11	-15	2	0	4	56	-54	2	3	4	45	41
1	-8	4	14	-16	1	-5	4	79	73	-9	-2	4	67	-66	3	0	4	51	-53	3	3	4	6	-7
2	-8	4	51	-52	2	-5	4	36	-32	-8	-2	4	55	50	4	0	4	23	22	4	3	4	36	-34
3	-8	4	24	21	3	-5	4	102	-91	-7	-2	4	100	94	5	0	4	63	60	5	3	4	23	17
4	-8	4	59	60	4	-5	4	50	45	-6	-2	4	39	-41	6	0	4	35	-41	-8	4	4	26	30
5	-8	4	24	-23	5	-5	4	41	42	-5	-2	4	57	-55	7	0	4	71	-73	-5	4	4	53	-52
6	-8	4	55	-51	7	-5	4	33	-30	-4	-2	4	46	-41	8	0	4	16	14	-4	4	4	34	38
8	-8	4	52	50	8	-5	4	33	-31	-3	-2	4	10	-9	9	0	4	72	74	-3	4	4	48	44
-6	-7	4	36	35	10	-5	4	38	41	0	-2	4	52	-48	-11	1	4	10	-7	-2	4	4	28	-30
-5	-7	4	16	-14	-10	-4	4	18	-16	1	-2	4	30	33	-10	1	4	57	53	-1	4	4	38	-41
-4	-7	4	31	-32	-9	-4	4	27	21	2	-2	4	99	105	-8	1	4	66	-61	0	4	4	38	35
-3	-7	4	7	6	-8	-4	4	34	37	3	-2	4	45	-48	-6	1	4	15	15	1	4	4	46	46
-2	-7	4	37	39	-7	-4	4	27	-30	4	-2	4	37	-41	-5	1	4	55	49	2	4	4	19	-16
-1	-7	4	18	19	-6	-4	4	25	-27	5	-2	4	15	17	-4	1	4	29	32	3	4	4	56	-51
0	-7	4	46	-44	-5	-4	4	38	38	6	-2	4	17	17	-3	1	4	53	-57	-5	5	4	35	31
1	-7	4	39	-36	-4	-4	4	48	51	9	-2	4	26	-26	-2	1	4	21	-22	-4	5	4	8	10
2	-7	4	28	25	-3	-4	4	31	-31	-11	-1	4	17	16	-1	1	4	71	67	-3	5	4	48	-46
3	-7	4	70	66	-2	-4	4	102	-105	-10	-1	4	29	-28	0	1	4	15	15	-2	5	4	11	-15
4	-7	4	7	-8	-1	-4	4	33	31	-9	-1	4	42	-39	1	1	4	99	-89	-1	5	4	36	39
5	-7	4	52	-52	0	-4	4	102	102	-8	-1	4	54	48	3	1	4	40	41	-2	-9	5	51	51
6	-7	4	9	-6	2	-4	4	105	-101	-7	-1	4	37	35	4	1	4	18	22	-1	-9	5	12	10
7	-7	4	41	38	3	-4	4	22	-23	-6	-1	4	58	-52	5	1	4	17	-18	0	-9	5	42	-42
9	-7	4	44	-42	4	-4	4	59	57	-5	-1	4	41	-36	6	1	4	45	-42	1	-9	5	25	-24
-8	-6	4	20	20	5	-4	4	38	39	-4	-1	4	22	15	8	1	4	46	44	2	-9	5	24	25
-7	-6	4	49	48	6	-4	4	59	-54	-3	-1	4	66	63	-10	2	4	24	25	3	-9	5	41	38
-6	-6	4	38	-40	7	-4	4	41	-42	-2	-1	4	37	-38	-9	2	4	57	-50	4	-9	5	24	-19
-5	-6	4	60	-60	8	-4	4	64	61	-1	-1	4	78	-75	-8	2	4	8	-11	-3	-8	5	35	38
-4	-6	4	58	52	9	-4	4	73	64	0	-1	4	28	29	-7	2	4	84	72	-2	-8	5	15	14
-3	-6	4	50	54	10	-4	4	26	-33	1	-1	4	85	94	-6	2	4	23	22	-1	-8	5	31	-32
-1	-6	4	57	-55	-10	-3	4	41	37	2	-1	4	27	29	-5	2	4	44	-42	0	-8	5	27	-26
0	-6	4	29	-29	-8	-3	4	61	-60	3	-1	4	24	-23	-3	2	4	15	18	2	-8	5	57	54
1	-6	4	51	48	-7	-3	4	8	7	4	-1	4	37	-41	-2	2	4	51	51	3	-8	5	18	-15
2	-6	4	26	25	-6	-3	4	77	75	6	-1	4	23	23	-1	2	4	14	-15	4	-8	5	87	-82
3	-6	4	45	-40	-5	-3	4	8	10	7	-1	4	23	-25	0	2	4	35	-32	5	-8	5	27	25

H	K	L	FO	FC	H	K	L	FO	FC	H	K	L	FO	FC	H	K	L	FO	FC	H	K	L	FO	FC
6	-8	5	75	68	-6	-4	5	42	43	-1	-1	5	72	68	3	2	5	15	-14	-1	-5	6	48	-48
7	-8	5	18	-17	-5	-4	5	63	-68	0	-1	5	45	41	-7	3	5	26	-41	0	-5	6	44	47
-6	-7	5	18	-22	-4	-4	5	26	-26	1	-1	5	106	-100	-5	3	5	45	42	1	-5	6	89	88
-5	-7	5	10	13	-3	-4	5	57	59	2	-1	5	54	-55	-4	3	5	18	22	2	-5	6	20	-21
-4	-7	5	35	36	-2	-4	5	16	15	3	-1	5	55	64	-3	3	5	26	-23	3	-5	6	68	-79
-3	-7	5	19	-23	-1	-4	5	22	-22	4	-1	5	38	42	-2	3	5	47	-52	5	-5	6	73	78
-2	-7	5	49	-49	0	-4	5	59	-59	5	-1	5	43	-44	-1	3	5	37	40	7	-5	6	52	-58
-1	-7	5	6	8	1	-4	5	5	3	6	-1	5	19	-18	0	3	5	59	64	-7	-4	6	20	-20
0	-7	5	30	28	2	-4	5	104	112	7	-1	5	22	22	1	3	5	53	-51	-6	-4	6	35	-28
1	-7	5	25	19	3	-4	5	25	23	8	-1	5	39	40	2	3	5	58	-52	-5	-4	6	31	33
2	-7	5	26	-25	4	-4	5	76	-81	-10	0	5	24	21	3	3	5	38	34	-4	-4	6	30	30
3	-7	5	43	-39	5	-4	5	29	-28	-9	0	5	24	-25	-3	4	5	19	-18	-3	-4	6	55	-58
4	-7	5	16	17	6	-4	5	57	52	-8	0	5	18	-17	-2	4	5	25	29	-2	-4	6	12	-14
5	-7	5	32	29	8	-4	5	33	-32	-7	0	5	39	37	-1	4	5	26	30	-1	-4	6	41	41
7	-7	5	11	-13	9	-4	5	37	-32	-6	0	5	45	45	-3	-8	6	20	-28	0	-4	6	33	33
-7	-6	5	17	-18	-9	-3	5	19	14	-5	0	5	24	-27	-2	-8	6	6	-7	2	-4	6	34	-33
-6	-6	5	27	22	-8	-3	5	30	30	-4	0	5	71	-62	-1	-8	6	27	29	3	-4	6	13	-14
-5	-6	5	40	40	-7	-3	5	24	-27	-2	0	5	30	30	1	-8	6	27	-26	4	-4	6	36	41
-4	-6	5	10	-8	-6	-3	5	40	-37	-1	0	5	48	52	2	-8	6	27	-26	5	-4	6	16	16
-3	-6	5	62	-64	-4	-3	5	48	51	0	0	5	67	-63	3	-8	6	22	20	6	-4	6	38	-44
-2	-6	5	19	-24	-3	-3	5	25	25	1	0	5	54	-52	4	-8	6	44	43	7	-4	6	31	-25
-1	-6	5	36	33	-2	-3	5	32	-33	2	0	5	86	85	5	-8	6	7	-7	-8	-3	6	11	-9
0	-6	5	8	8	-1	-3	5	22	-19	3	0	5	41	43	-4	-7	6	23	-35	-6	-3	6	9	12
2	-6	5	17	-14	1	-3	5	56	56	4	0	5	52	-62	-2	-7	6	37	44	-5	-3	6	12	9
3	-6	5	29	28	3	-3	5	39	-45	5	0	5	37	-34	-1	-7	6	22	-24	-4	-3	6	51	-52
4	-6	5	27	26	5	-3	5	21	17	6	0	5	24	27	0	-7	6	30	-28	-2	-3	6	57	53
5	-6	5	10	-11	8	-3	5	23	-25	7	0	5	41	40	1	-7	6	12	10	0	-3	6	30	21
6	-6	5	25	-23	-9	-2	5	32	29	-8	1	5	41	37	2	-7	6	13	10	2	-3	6	53	-57
7	-6	5	10	-10	-8	-2	5	13	10	-7	1	5	12	14	4	-7	6	18	18	4	-3	6	26	28
-8	-5	5	36	-35	-7	-2	5	49	-44	-6	1	5	55	-52	5	-7	6	27	-21	5	-3	6	31	-38
-7	-5	5	31	-28	-6	-2	5	8	-8	-5	1	5	38	-41	6	-7	6	25	-26	6	-3	6	12	-17
-6	-5	5	39	42	-5	-2	5	51	51	-4	1	5	26	28	-5	-6	6	27	-27	7	-3	6	21	23
-5	-5	5	8	12	-4	-2	5	31	28	-3	1	5	23	26	-4	-6	6	19	-21	-8	-2	6	33	-32
-4	-5	5	62	-60	-3	-2	5	34	-38	-1	1	5	20	-17	-3	-6	6	50	49	-7	-2	6	22	20
-3	-5	5	39	-37	-2	-2	5	18	-20	1	1	5	31	27	-2	-6	6	21	22	-6	-2	6	57	57
-2	-5	5	47	46	0	-2	5	52	47	3	1	5	20	-21	-1	-6	6	40	-41	-5	-2	6	35	-35
-1	-5	5	46	47	2	-2	5	53	-54	4	1	5	16	-16	0	-6	6	23	-22	-4	-2	6	45	-42
0	-5	5	14	16	4	-2	5	22	25	6	1	5	17	17	1	-6	6	4	4	-3	-2	6	47	48
1	-5	5	80	-78	6	-2	5	10	-15	-8	2	5	21	20	2	-6	6	33	33	-2	-2	6	37	37
2	-5	5	24	-20	7	-2	5	16	-11	-7	2	5	32	-28	3	-6	6	21	13	-1	-2	6	22	-20
3	-5	5	99	103	-10	-1	5	21	20	-6	2	5	18	-19	4	-6	6	51	-50	0	-2	6	54	-51
5	-5	5	96	-88	-9	-1	5	71	65	-5	2	5	26	26	6	-6	6	62	59	1	-2	6	5	-7
7	-5	5	59	60	-8	-1	5	31	-28	-4	2	5	17	17	-7	-5	6	26	26	2	-2	6	34	36
8	-5	5	21	18	-7	-1	5	61	-58	-2	2	5	22	-27	-6	-5	6	33	-33	3	-2	6	19	20
9	-5	5	37	-32	-6	-1	5	51	49	-1	2	5	25	-21	-5	-5	6	53	-53	4	-2	6	39	-46
-9	-4	5	31	-31	-5	-1	5	48	45	0	2	5	46	46	-4	-5	6	36	38	5	-2	6	22	-24
-8	-4	5	43	-43	-4	-1	5	50	-49	1	2	5	26	24	-3	-5	6	40	39	6	-2	6	30	31
-7	-4	5	55	54	-3	-1	5	42	-39	2	2	5	22	-24	-2	-5	6	54	-53	-8	-1	6	24	24

H	K	L	FO	FC	H	K	L	FO	FC	H	K	L	FO	FC	H	K	L	FO	FC	H	K	L	FO	FC
-6	-1	6	15	-12	-1	0	6	12	-14	0	-7	7	22	22	2	-5	7	38	41	-6	-2	7	55	-58
-5	-1	6	62	-57	0	0	6	18	13	1	-7	7	25	25	3	-5	7	22	26	-5	-2	7	17	15
-4	-1	6	27	27	1	0	6	33	31	2	-7	7	7	-8	4	-5	7	9	-9	-4	-2	7	71	57
-3	-1	6	50	53	2	0	6	33	-33	3	-7	7	24	-23	5	-5	7	29	-36	-3	-2	7	30	-31
-2	-1	6	20	-17	3	0	6	41	-37	-4	-6	7	33	34	-2	-4	7	20	19	-2	-2	7	57	-55
-1	-1	6	88	-78	4	0	6	42	43	-3	-6	7	34	-31	0	-4	7	33	-31	-1	-2	7	49	49
0	-1	6	19	-17	5	0	6	31	31	-2	-6	7	28	-29	1	-4	7	13	-13	0	-2	7	57	55
1	-1	6	84	81	-7	1	6	28	-31	-1	-6	7	46	50	2	-4	7	19	18	1	-2	7	32	-31
2	-1	6	30	31	-5	1	6	14	16	0	-6	7	38	37	3	-4	7	19	21	2	-2	7	36	-37
3	-1	6	65	-69	-4	1	6	41	-41	1	-6	7	51	-50	4	-4	7	23	-27	-5	-1	7	40	36
4	-1	6	27	-25	-2	1	6	18	21	2	-6	7	39	-39	5	-4	7	17	-22	-4	-1	7	15	-13
5	-1	6	47	48	-1	1	6	11	12	3	-6	7	12	13	-6	-3	7	15	-11	-3	-1	7	45	-44
6	-1	6	21	23	0	1	6	10	13	4	-6	7	34	37	-5	-3	7	21	-21	-2	-1	7	22	18
-8	0	6	15	13	2	1	6	30	-32	-5	-5	7	44	41	-4	-3	7	13	10	-1	-1	7	51	49
-7	0	6	22	-21	-2	2	6	28	32	-4	-5	7	37	-35	-3	-3	7	27	24	1	-1	7	36	-35
-6	0	6	39	-40	-1	2	6	23	23	-3	-5	7	45	-45	-1	-3	7	37	-37	2	-1	7	17	-17
-5	0	6	55	33	0	2	6	36	-37	-2	-5	7	43	42	1	-3	7	23	23	-4	0	7	8	-7
-4	0	6	40	35	1	2	6	37	-35	-1	-5	7	41	42	2	-3	7	13	14	-2	0	7	21	23
-3	0	6	19	-20	-2	-7	7	12	-14	0	-5	7	54	-55	3	-3	7	17	-18	0	0	7	20	-21
-2	0	6	14	-15	-1	-7	7	12	-12	1	-5	7	38	-38	4	-3	7	18	-19					

ANISOTROPIC AND ISOTROPIC THERMAL PARAMETERS

ANISOTROPIC IN THE FORM EXP(-2*PI*PI*(U11*(ASTAR*H)**2 +....
...U23*BSTAR*CSTAR*K*L + ...))

ISOTROPIC EXP(-8*PI*PI*U*(SIN(THETA)/LAMBDA)**2)

ALL VALUES *1000

ATOM	U11(OR U)	U22	U33	U23	U13	U12
MO(1)	34(2)	37(2)	30(2)	13(2)	-1(2)	10(2)
CL(1)	62(4)	86(5)	46(4)	36(4)	11(3)	14(4)
P(1)	39(4)	43(4)	32(4)	14(3)	0(3)	11(3)
P(2)	35(4)	41(4)	34(4)	13(3)	-1(3)	9(3)
O(21)	44(9)	54(10)	42(9)	16(8)	7(7)	9(8)
O(22)	61(10)	48(10)	53(10)	32(8)	13(8)	15(8)
O(23)	57(10)	47(10)	42(9)	11(8)	-8(8)	11(8)
C(21)	63(17)	53(16)	53(16)	11(14)	9(14)	20(14)
C(22)	61(18)	75(19)	98(22)	48(17)	31(16)	32(15)
C(23)	80(20)	79(21)	59(17)	46(16)	2(15)	4(16)
O(11)	36(9)	45(10)	65(11)	24(8)	10(8)	19(7)
O(12)	74(12)	45(10)	45(10)	12(8)	19(8)	26(9)
O(13)	72(11)	38(9)	47(10)	14(8)	13(9)	22(8)
C(11)	79(18)	58(18)	67(18)	23(15)	1(15)	19(15)
C(12)	37(15)	60(16)	76(18)	28(14)	6(13)	14(12)
C(13)	78(19)	72(19)	56(18)	24(15)	-2(14)	19(15)
C(1)	55(15)	54(16)	31(13)	9(12)	-28(12)	-10(13)
C(2)	68(17)	81(22)	46(15)	32(15)	-6(13)	26(16)
C(3)	55(16)	77(20)	60(17)	32(15)	-16(13)	26(15)
C(4)	54(15)	22(12)	34(13)	12(10)	4(12)	7(10)
O(4)	73(12)	69(13)	62(12)	35(10)	13(11)	5(10)
C(5)	54(18)	32(13)	21(12)	-7(10)	-14(13)	2(12)
O(5)	45(11)	71(13)	72(13)	29(10)	-13(10)	-5(10)

REFERENCES

1. G. Wilke, B. Bogdanovic, P. Hardt, P. Heirnbach, W. Kiren, M. Kroner, W. Oberkirch, K. Tanaka, E. Steinruke, D. Walter, and H. Zimmermann, Angew. Chem. Int. Ed., Engl., 1966, 5, 151.

2. G. Wilke, Angew. Chem. Int. Ed., Engl., 1963, 2, 105.

3. G.N. Schrauzer, (Ed.) "Transition Metals in Homogeneous Catalysis", Marcel Dekker, Inc., New York, 1971.

4. R. Baker and M.G. Kelley, J.C.S. Chem. Comm., 1980, 307.

5. L.S. Stuhl, Diss. Abstr., Int. B, 1978, 39, 1759.

6. F. Dewans and D. Morel, J. Mol. Catal., 1978, 3, 403.

7. R. Baker, Chem. Rev., 1973, 73, 487.

8. H. Heirnbach, P.W. Jolly and G. Wilke, Advan. Organometal. Chem., 1970, 8, 29.

9. C.E.H. Bawn, D.G.T. Cooper and A.M. North, Polymer. 1966, 7, 113.

10. M.I. Lobach, B.D. Babitskii and V.A. Kormer Russ. Chem. Rev., 1967, 36, 476.

11. M.B.H. Studiengesellschaft Kohle, Neth. Appl. P 6,409,179.

12. N.W. Obsenchalova, V. Sh. Feldblyum and N.M. Paschenko, J. Org. Chem. (U.S.S R.), 1968, 4, 982.

13. J.J. Rooney and G. Webb, J. Catalysis, 1964, 3, 488.

14. M.A. Schroeder and M.S. Wrighton, J. Amer. Chem. Soc., 1976, 98, 551.

15. J. Müller, W. Holzinger and H. Menig, Angew. Chem. Int. Ed., Engl. 1976, 15, 702.

16. E.O. Sherman and M. Olson, J. Organometal. Chem., 1979, 172, C13.

17. R. Huttel and J. Krantzer, Chem. Ber., 1964, 97, 1438.

18. H.J. Clase, A.J. Cleland and M.J. Newlands, J. Organometal. Chem., 1975, 93, 231.

19. S. Siegel and G. Perot, J.C.S. Chem. Comm., 1978, 114.

20. J. Tsuji, K. Kiji, S. Imamura and M. Morikawa, J. Amer. Chem. Soc., 1964, 86, 4350.

21. M. Dubini, G.P. Chiusoli and F. Montino, Tetrahedron Letters, 1963, 1591.

22. L.S. Stuhl and E.L. Muetterties, Inorg. Chem., 1978, 17, 2148.

23. L.S. Stuhl, M. Rakowski, F.J. Hirsekorn, J.R. Bleeke, A.E.Stevens and E.L. Muetterties, J. Amer. Chem. Soc., 1978, 100, 2405.

24. H. Pasternak, T. Glowiak and F. Pruchnik, Inorg. Chim. Acta, 1976, 19, 11.

25. M. Botrill and M. Green, J. Organometal. Chem., 1976, 111, C6.

26. G. Strukul and G. Carturan, Inorg. Chim Acta., 1979, 35, 99.

27. K. Sato, S. Inone, S. Ota and Y. Fujita, J. Org. Chem., 1972, 37, 462.

28. R. Baker, R.C. Cookson and J.R. Winson, J.C.S. Chem. Comm., 1974, 515.

29. D.E. Korte, L.S. Hegedus and R.K. Wirth, J. Org. Chem., 1977, 42, 1329.

30. S.F.A. Kettle and R. Mason, J. Organometal. Chem., 1966, 5, 573.

31. P.W.N.M. Van Leeuwen and A.P. Praat, J. Organometal. Chem., 1970, 21, 501.

32. I.H. Hilliere and R.M. Canadine, Disc. Farad. Soc., 1969, 47, 27.

33. L.A. Fedorov, Russ. Chem. Rev., 1970, 39, 655.

34. IUPAC Nomenclature of Inorganic Chemistry, Definition Rules 1970, Pure Appl. Chem. 1971, 28, 1.

35. M.G.B. Drew and L.S. Pu, Acta Crystallogr., 1977, B33, 1207.

36. H.L. Clarke and N.J. Fitzpatrick, J. Organometal. Chem., 1972, 40, 379.

37. G. Raper and W.S. McDonald, J.C.S. Dalton Trans., 1972, 265.

38. T. Aoki, A. Furusaki, Y. Tomiie, K. Ono and K. Tanaka, Bull. Chem. Soc. Japan, 1969, 42, 545.

39. A. Keasey, P.M. Bailey and P.M. Maitlis, J.C.S. Chem. Comm. 1977, 178.

40. J. Smidt and W. Hafner, Angew. Chem., 1959, 71, 284.

41. R.F. Heck and D.S. Breslow, J. Amer. Chem. Soc., 1960, 82, 750.

42. A.E. Smith, Inorg. Chem., 1972, 11, 2306.

43. A.E. Smith, Acta Crystallogr., 1965, 18, 331.

44. H.L. Clarke, J. Organometal. Chem., 1974, 80, 155.

45. K. Oda, N. Yasuoka, T. Ueki, N. Kasai, M. Kakudo, Y. Tezuka, T. Ogura and S. Kawaguchi, J.C.S. Chem. Comm., 1968, 989.

46. M.R. Churchill and T.A. O'Brien, Inorg. Chem., 1967, 6, 1386.

47. H. Alper and H.-N. Paik, J. Organometal. Chem., 1976, 121, 225.

48. R. Victor, V. Usieli and S. Sarel, J. Organometal. Chem., 1977, 129, 387.

49. F.A. Cotton and M.D. LaPrade, J. Amer. Chem. Soc., 1968, 90, 5418.

50. M.R. Churchill and J. Wormald, J.C.S. Chem. Comm., 1968, 1597.

51. N.W. Alcock and J.A. Conneely, Acta Crystallogr., 1977, B33, 141.

52. D.L. Weaver and R.M. Tuggle, J. Amer. Chem. Soc., 1969, 91, 6506.

53. D.A. Clement, J.F. Nixon and B. Wilkins, J. Organometal. Chem., 1972, 37, C43.

54. M.J. Bennett, J.L. Pratt, K.A. Simpson, L.K.K. Li Shing Man and J. Takats, J. Amer. Chem. Soc., 1976, 98, 4810.

55. E.G. Bryan, B.F.G. Johnson and J. Lewis, J. Organometal. Chem., 1976, 122, 249.

56. C.A. McAuliffe and W. Levason, "Phosphine, Arsine and Stibine Complexes of the Transition Elements", Elsevier, London 1979.

57. N. Yoshimura, S. -I. Murahashi and I. Moritani, J. Organometal. Chem., 1973, 52, C58.

58. T. Inglis, M. Kilner and T. Reynoldson, J.C.S. Chem. Comm., 1972, 774.

59. L.J. Guggenberger, A.R. Kane and E.L. Muetterties, J. Amer. Chem. Soc., 1972, 94, 5665.

60. C.A. Ghilardi, S. Midollini, A. Orlandini and L. Sacconi, Inorg. Chem., 1980, 19, 301.

61. G. Huttner, G. Mohr and A. Frank, Angew. Chem. Int. Ed., Engl., 1976, 15, 682.

62. W.W. Pritchard, U.S. Patent 2 600 571 June 17, 1952.

63. H.B. Jonassen, R.I. Stearns, J. Kenttämaa, D.W. Moore and A.G. Whittaker, J. Amer. Chem. Soc., 1958, 80, 2586.

64. P. Chini and S. Martinego, Inorg. Chem., 1967, 6, 837.

65. E.O. Fischer and G. Burger, Z. Naturforsch., 1961, 16B, 77.

66. M. Wada and T. Wakabayashi, J. Organometal. Chem., 1975, 96, 301.

67. P.J. Candlin, A.H. Mawby, H. Thomas, Ger. Patent 2 313 947.

68. E.W. Abel and S. Moorhouse, Angew. Chem. Int. Ed., Engl., 1971, 10, 339.

69. R.B. King and M. Ishaq, Inorg. Chim. Acta, 1970, 4, 258.

70. B.J. Brisdon, D.A. Edwards and J.W. White, J. Organometal. Chem., 1979, 175, 113.

71. R.F. Heck and C.R. Boss, J. Amer. Chem. Soc., 1964, 86, 2580.

72. H.C. Volger and K. Vrieze, J. Organometal. Chem., 1967, 9, 527.

73. C.G. Hull and M.H.B. Stiddard, J. Organometal. Chem., 1967, 9, 519.

74. A.J. Deeming and B.L. Shaw, J. Chem. Soc. A, 1971, 376.

75. H.D. Murdoch, J. Organometal. Chem., 1965, 4, 119.

76. J.E. Ellis and R.A. Faltynek, J. Organometal. Chem., 1975, 93, 205.

77. B.J. Brisdon and G.F. Griffin, J. Organometal. Chem., 1974, 76, C47.

78. I.P. Beletskaya, G.A. Artamkina and O.A. Reutov, Russ. Chem. Rev 1976, 45, 330.

79. J.K. Stille and K.S.Y. Lau, Accounts Chem. Res., 1977, 10, 434.

80. K.S.Y. Lau, R.W. Fries and J.K. Stille, J. Amer. Chem. Soc., 1974, 96, 4983.

81. P.K. Wong, K.S.Y. Lau and J.K. Stille, J. Amer. Chem. Soc., 1974, 96, 5956.

82. R.G. Pearson, Fortschr. Chem. Forsch., 1973, 4, 76.

83. J.S. Bradley, D.G. Connor, D. Dolphin, J.A. Labinger and J.A. Osborn, J. Amer. Chem. Soc., 1972, 94, 4043.

84. J.A. Labinger, A.V. Kramer and J.A. Osborn, J. Amer. Chem. Soc., 1973, 95, 7908.

85. J.A. Osborn, Y. Ishii and M. Tsutsui, (Eds.) "Organotransition Metal Chemistry" Plenum Publishing Corp., New York 1975.

86. J.A. Kaduk, A.T. Poulos and J.A. Ibers, J. Organometal. Chem., 1977, 127, 245.

87. R. Hüttel and H. Dietl, Chem. Ber., 1965, 98, 1753.

88. E.O. Fischer and H. Werner, Chem. Ber., 1962, 95, 695.

89. G.E. Coates, M.L.H. Green and K. Wade, "Organometallic Compounds" Methuen, London 1968.

90. J. Kwiatek and J.K. Seyler, J. Organometal. Chem., 1965, 3, 421.

91. C.A. Reilly and H. Thyret, J. Amer. Chem. Soc., 1967, 89, 5144.

92. M. Green and R.I. Hancock, J. Chem. Soc. A, 1968, 109.

93. R.F. Heck, J. Amer. Chem. Soc., 1963, 85, 3381.

94. S.D. Robinson and B.L. Shaw, J. Chem. Soc. A, 1968, 4806.

95. G.F. Emerson and R. Petit, J. Amer. Chem. Soc., 1962, 84, 4591.

96. L.A. Oro, Inorg. Chim. Acta, 1977, 21, L6.

97. R.W. Fish, W.P. Giering, D. Marten and M. Rosenblum, J. Organometal. Chem., 1976, 105, 101.

98. W.R. McClelland, H.H. Hoehn, H.N. Cripps, E.L. Muetterties and B.W. Howk, J. Amer. Chem. Soc., 1961, 83, 1601.

99. N.M. Boag, M. Green, J.L. Spencer and F.G.A. Stone, J. Organometal. Chem., 1977, 127, C51.

100. M.A. Bennett, R.N. Johnson, G.B. Robertson, I.B. Tomkins and P.O. Whimp, J. Amer. Chem. Soc., 1976, 98, 3514.

101. A.N. Nesmeyanov, G.G. Aleksandrov, N.G. Bokii, I.B. Zlotina, Yu. T. Struchkov and N.E. Kolobova, J. Organometal. Chem., 1976, 111, C9.

102. R.G. Schultz, Tetrahedron Letters, 1964, 301.

103. A. Borrini and G. Ingrosso, J. Organometal. Chem., 1977, 132, 275.

104. E.V. Dehmlow, Angew. Chem. Int. Ed., Engl., 1974, 13, 170.

105. H. Alper, H. des Abbayes and D. des Roches, J. Organometal. Chem., 1976, 121, C31.

106. W. Hieber, J. Sedlmeier and W. Abeck, Chem. Ber., 1953, 86, 700.

107. D.H. Gibson, Wen-Liang Hsu and Da-Sheng Lin, J. Organometal. Chem., 1979, 172, C7.

108. D.J. Darensbourg and J.A. Froelich, J. Amer. Chem. Soc., 1978, 100, 338.

109. J.L. Cihonski and R.A. Levenson, Inorg. Chim. Acta, 1976, 18, 215.

110. T.E. Baush and W.P. Giering, J. Organometal. Chem., 1976, 114, 165.

111. R.D. Rieke, A.V. Kavaliunas and L.D. Rhyne, J. Amer. Chem. Soc., 1979, 101, 246.

112. M.J. Piper and P.L. Timms, J.C.S. Chem. Comm., 1972, 50.

113. K. Ehrlich and G.F. Emerson, J. Amer. Chem. Soc., 1972, 94, 2464.

114. B. Kanellokopulos, D. Nothe, K. Weidenhammer, H. Wienand and M.L. Ziegler, Angew. Chem. Int. Ed., Engl., 1977, 16, 261.

115. M.I. Bruce, M.Z. Iqbal and F.G.A. Stone, J. Organometal. Chem., 1969, 20, 161.

116. A. Efraty, J. Organometal. Chem., 1973, 57, 1.

117. A.N. Nesmeyanov, S.P. Gubin and A.Z. Rubezhov, J. Organometal. Chem., 1969, 16, 163.

118. W.S. Trahanowsky and R.A. Hall, J. Amer. Chem. Soc., 1977, 99, 4850.

119. J.M. Rowe, Proc. Chem. Soc., 1962, 66.

120. V.F. Sevdik and M.A. Porai-Koshits, Zh. Strukt. Khim., 1965, 3, 472.

121. W.E. Oberhansli and L.F. Dahl, J. Organometal. Chem., 1965, 3, 43.

122. A.E. Smith, Preprints Amer. Chem. Soc. Meeting, New York, 1969, Paper XIV-17.

123. T.J. Greenhough, P. Legzdins, D.T. Martin and J. Trotter, Inorg. Chem., 1979, 18, 3268.

124. P.R.H. Alderman, P.G. Owston and J.M. Rowe, Acta Crystallogr., 1960, 13, 149.

125. M.R. Churchill and R. Mason, Nature (London),1964, 204, 777.

126. R.H. Fenn and A.J. Graham, J. Organometal. Chem., 1972, 37, 137.

127. C.F. Putnik, J.J. Welter, G.D. Stucky, M.J. D'Aniello, B.A. Sosinsky, J.F. Kirner and E.L. Muetterties, J. Amer. Chem. Soc.,1978, 100, 4107.

128. M.R. Churchill and T.A. O'Brien, J.C.S. Chem. Comm,, 1968, 246.

129. T.G. Hewitt, J.J. De Boer and K. Anzenhofer, Acta Crystallogr. 1970, B26, 1244.

130. R.B. Helmholdt, F. Jellinek, H.A. Martin and A. Vos, Rec. Trav. Chim. Pays-Bas, 1967, 86, 1263.

131. A. Streitwieser Jr., "Molecular Orbital Theory for Organic Chemists", Wiley, New York 1961.

132. M.L.H. Green and P.L.I. Nagy, Adv. Organometal. Chem., 1964, 2, 325.

133. R. Mason and A.G. Wheeler, J. Chem. Soc. A, 1968, 2549.

134. G.R. Davies, R.H.B. Mais, S. O'Brien and P.G. Owston, J.C.S. Chem. Comm., 1967, 1151.

135. R. Mason and A.G. Wheeler, J. Chem. Soc. A, 1968, 2543.

136. M.K. Minasyan, S.P. Gubin and Yu. T. Struchkov, Zh. Strukt. Khim., 1967, 8, 1108.

137. A.D. Broadbent and G.E. Pringle, J. Inorg. Nucl. Chem., 1971, 33, 2009.

138. K. Vrieze, C. MacLean, P. Crosse and C.W. Hilbers, Rec. Trav. Chim. Pays-Bas, 1966, 85, 1077.

139. M.-M. Rohmer, J. Demuynck and A. Veillard, Theoret. Chim. Acta, 1974, 36, 93.

140. D.A. Brown and A. Owens, Inorg. Chim. Acta, 1971, 5, 675.

141. A. Oudeman and T.S. Sorensen, J. Organometal. Chem., 1978, 156, 259.

142. D.H. Gibson and T.S. Ong, J. Organometal. Chem., 1978, 155, 221

143. G.A. Olah and H. Mayr, J. Amer. Chem. Soc., 1976, 98, 7333.

144. J. Chatt and L.A. Duncanson, J. Chem. Soc., 1953, 2939.

145. J.C. Bailar, H.J. Emeleus, R.S. Nyholm and A.F. Trotman-Dickenson (Eds.), "Comprehensive Inorganic Chemistry" Vol. 4, Pergamon Press, Oxford, 1973.

146. H.S. Gutowsky, M. Karplus and D.M. Grant, J. Chem. Phys., 1959, 31, 1278.

147. B.E. Mann, R. Pietropaolo and B.L. Shaw, J.C.S. Dalton Trans., 1973, 2390.

148. D.W. Moore, H.B. Jonassen, T.B. Joyner and A.J. Bertrand, Chem. and Ind., 1960, 1304.

149. B.E. Mann, B.L. Shaw and G. Shaw, J. Chem. Soc. A, 1971, 3536.

150. M.H. Chisholm and H.C. Clark, Inorg. Chem., 1973, 12, 991.

151. H.C. Clark and C.R. Jablouski, Inorg. Chem., 1975, 14, 1518.

152. S. Numata, R. Okawara and H. Kurosawa, Inorg. Chem., 1977, 16, 1737.

153. T.G. Appleton, H.C. Clark and L.E. Manzer, Co-ord. Chem. Rev., 1973, 10, 335.

154. J. Powell and B.L. Shaw, J. Chem. Soc. A, 1968, 583.

155. J.K. Becconsall and S.O'Brien, J.C.S. Chem. Comm., 1966, 720.

156. A. Davison, J.A. McCleverty and G. Wilkinson, J. Chem. Soc., 1963, 1133.

157. J.W. Akitt, "NMR and Chemistry", Chapman and Hall, London 1973.

158. M.L.H. Green, L. Pratt and G. Wilkinson, J. Chem. Soc., 1958, 3916.

159a. J. Chatt, B.L. Shaw and A.E. Field, J. Chem. Soc., 1964, 3466.

159b. J. Chatt, N.P. Johnson and B.L. Shaw, J. Chem. Soc., 1964, 1625.

160. J. Collin, Cl.Charrier, M.J. Pouet, P. Cadiot and J.L. Roustan, J. Organometal. Chem., 1979, 168, 321.

161. U. Franke and E. Weiss, J. Organometal. Chem., 1979, 172, 341.

162. B.J. Brisdon, J. Organometal. Chem., 1977, 125, 225.

163. P. Powell, J. Organometal. Chem., 1977, 129, 175.

164. B.J. Brisdon, D.A. Edwards and J.W. White, J.C.S. Dalton Trans., 1980, 2129.

165. M.W. Schoonover and R. Eisenburg, J. Amer. Chem. Soc., 1977, 99, 8371.

166. H.L. Clarke and N.J. Fitzpatrick, J. Organometal. Chem., 1974, 66, 119.

167. J.F. Nixon, B. Wilkins and D.A. Clements, J.C.S. Dalton Trans.,1974, 1993.

168. T.H. Tulip and J.A. Ibers, J. Amer. Chem. Soc., 1979, 101, 4201.

169. M. Oslinger and J. Powell, Can. J. Chem., 1973, 51, 274.

170. U. Franke and E. Weiss, J. Organometal. Chem., 1979, 168, 311.

171. J.W. Faller, D.A. Haitko, R.D. Adams and D.F. Chodosh, J. Amer. Chem. Soc., 1979, 101, 865.

172. D.V. Rinze and U. Mueller, Chem. Ber., 1979, 112, 1973.

173. D.J. Smith and J.D. Oliver, Inorg. Chem., 1978, 17, 2585.

174. J.K. Becconsall, B.E. Job and S. O'Brien, J.C.S. Chem. Comm., 1966, 302.

175. J.K. Becconsall, B.E. Job and S. O'Brien, J. Chem. Soc. A, 1967, 423.

176. L.M. Jackman and F.A. Cotton, (Eds.) 'Dynamic Nuclear Magnetic Resonance Spectroscopy', Academic Press, New York, 1975.

177. J.K. Krieger, J.M. Deutch and G.M. Whitesides, Inorg. Chem., 1973, 12, 1535.

178. K. Vrieze and H.C. Volger, J. Organometal. Chem., 1967, 9, 537.

179. P.W.N.M. Van Leeuwen and A.P. Praat, J.C.S. Chem. Comm., 1970, 365.

180. B.J. Brisdon and A.A. Woolf, J.C.S. Dalton Trans., 1978, 291.

181. J.W. Faller and D.A. Haitko, J. Organometal. Chem., 1978, 149, C19.

182. M. Cooke, R.J. Goodfellow and M. Green., J. Chem. Soc. A., 1971, 16.

183. C.K. Brown, W. Mowat, G. Yagupsky and G. Wilkinson, J. Chem. Soc. A., 1971, 850.

184. A.N. Nesmeyanov, Yu. A. Utynyuk, I.I. Kritskaya and G.A. Schembelor, J. Organometal. Chem., 1968, 14, 395.

185. M. Kh. Minasyan, Yu. T. Struchkov, I.I. Kritskaya, and R.L. Avoyan, Zh. Strukt. Khim., 1966, 7, 903.

186. A. Davison and W.C. Rode, Inorg. Chem., 1967, 6, 2124.

187. F.A. Cotton, Accounts Chem. Res., 1968, 1, 257.

188. E.L. Muetterties, Inorg. Chem., 1965, 4, 769.

189. D.L. Tibbetts and T.L. Brown, J. Amer. Chem. Soc., 1970, 92, 3031.

190. K. Vrieze, P . Crossee, A.P. Praat and C.W. Hilbers, J. Organometal. Chem., 1968, 11, 353.

191. A. Zwijnenburg, H.O. Van Oven, C.J. Groeneboom and H.J. De Liefde Meijer, J. Organometal. Chem., 1975, 94, 23.

192. U. Franke and E. Weiss, J. Organometal. Chem., 1978, 153, 39.

193. A.N. Nesmeyanov, L. Fedorov, N.P. Avakyan, P.V. Petrovskii, E.I. Fedin, E.V. Arshavskaya and I.I. Kritskaya, J. Organometal. Chem., 1975, 101, 121.

194. P. Powell and L.J. Russell, J. Organometal. Chem., 1977, 129, 415.

195. D.E.Axelson and C.E.Holloway, J.C.S. Chem. Comm., 1973, 455.

196. L.A. Churlyaeva, M.I. Lobach, G.P. Kondratenkov and V.A. Kormer, J. Organometal. Chem., 1972, 39, C23.

197. D.M. Grant and E.G. Paul, J. Amer. Chem. Soc., 1964, 86, 2984.

198. P.A. Dobosh, D.G. Gresham, C.P. Lillya and E.S. Magyer, Inorg. Chem., 1976, 15, 2311.

199. E. Farnell, E.W. Randall and E. Rosenburg, J.C.S. Chem. Comm., 1971, 1078.

200. B.E. Mann, J.C.S. Chem. Comm., 1971, 976.

201. H.C. Clarke and J.E.H. Ward, Can. J. Chem., 1974, 52, 570.

202. J.W. Emsley, J. Feeney and L.H. Sutcliffe, "High Resolution Nuclear Magnetic Resonance Spectroscopy' Vol. 2, Pergamon Press, 1968.

203. G. Davidson, Organometal. Chem. Rev. Sec. A, 1972, 8, 303.

204. H.P. Fritz, Chem. Ber., 1961, 94, 1217.

205. K. Shobatake and K. Nakamoto, J. Amer. Chem. Soc., 1970, 92, 3339.

206. D. Adams and A. Squire, J. Chem. Soc. A, 1970, 1808.

207. G. Davidson and D.C. Andrews, J.C.S. Dalton Trans., 1972, 126.

208. G. Davidson and D.C. Andrews, J.C.S. Dalton Trans., 1972, 1381.

209. G. Davidson and D.C. Andrews, J. Organometal. Chem., 1973, 55, 383.

210. G. Paliani, A. Poletti, G. Cardaci, S.M. Murgia and R. Catallotti, J. Organometal. Chem., 1973, 60, 157.

211. G. Paliani, S.M. Murgia, G. Cardaci and R. Cataclotti, J. Organometal. Chem., 1973, 63, 407.

212. J. Howard and T.C. Waddington, J.C.S. Faraday II, 1978, 74, 879.

213. M.J. Grogan and K. Nakamoto, J. Amer. Chem. Soc., 1966, 88, 5454.

214. M.J. Grogan and K. Nakamoto, J. Amer. Chem. Soc., 1968, 90, 918.

215. E J. Lanpher, J. Amer. Chem. Soc., 1957, 79, 5578.

216. J.W. Faller, D.F. Chodosh and D. Katahira, J. Organometal. Chem., 1980, 187, 227.

217. F. Dewans, J. Dewailly, J. Meunier-Piret and P. Piret, J. Organometal. Chem., 1974, 76, 53.

218. E.O. Fischer and H. Werner, Z. Chem., 1962, 2, 181.

219. C.E. Holloway, J.D. Kelley and M.H.B. Stiddard, J. Chem. Soc. A, 1969, 931.

220. B.J. Brisdon and G.F. Griffin, J.C.S. Dalton Trans., 1975, 1999.

221. G. Doyle, J. Organometal. Chem., 1977, 132, 243.

222. R.G. Hayter, J. Organometal. Chem., 1968, 13, P1.

223. H.D. Murdoch and R. Henzi, J. Organometal. Chem., 1966, 5, 552.

224. B.J. Brisdon, D.A. Edwards and J.W. White, J. Organometal. Chem., 1978, 156, 427.

225. A J. Graham,and R.H. Fenn, J. Organometal. Chem., 1969, 17, 405.

226. A.J. Graham and R.H. Fenn, J. Organometal. Chem., 1970, 25, 173.

227. A.J. Graham, D. Akrigg and B. Sheldrick, Cryst . Struct. Comm. 1977, 6, 253.

228. A.J. Graham, D. Akrigg and B. Sheldrick, Cryst. Struct. Comm., 1976, 5, 891.

229. M.G.B. Drew and G.F. Griffin, Acta Crystallogr., 1979, B35, 3036.

230. R.K. Breakell, S.J. Rettig, A. Storr and J. Trotter, Can. J. Chem. 1979, 57, 139.

231. K.S. Chong, S.J. Rettig, A. Storr and J. Trotter, Can. J. Chem., 1979, 57, 1335.

232. K.R. Breakell, S.J. Rettig, D.L. Singbeil, A. Storr and J. Trotter, Can. J. Chem., 1978, 56, 2099.

233. F.A. Cotton, C.A. Murillo and B.R. Stults, Inorg. Chim. Acta, 1977, 22, 75.

234. E.M. Holt, L. Smith and J.K. Watson, J.C.S. Dalton Trans., 1973, 2444.

235. F.A. Cotton, B.A. Frenz and A.G. Stanislowski, Inorg. Chim. Acta, 1973, 7, 503.

236. C.A. Kosky, P. Ganis and G. Avitabile, Acta Crystallogr., 1971, B27, 1859.

237. F.A. Cotton and V.W. Day, J.C.S. Chem. Comm., 1974, 415.

238. F.A. Cotton, T. LaCour and A.G. Stanislowski, J. Amer. Chem. Soc., 1974, 96, 754.

239. F.A. Cotton, B.A. Frenz, C.A. Murillo, J. Amer. Chem. Soc., 1975, 97, 2118.

240. M. Boyer, J.C . Daran and Y. Jeannin, J. Organometal. Chem., 1980, 190, 177.

241. M.G.B. Drew, B.J. Brisdon and M Cartwright, Inorg. Chim. Acta, 1979, 36, 127.

242. K.S. Chong and A. Storr, Can. J. Chem., 1979, 57, 167.

243. H. tom Dieck and H. Friedel, J. Organometal. Chem., 1968, 14, 375.

244. B.J. Brisdon and K.E. Paddick, J. Organometal. Chem., 1978, 149, 113.

245. A.T.T. Hsieh and B.O. West, J. Organometal. Chem., 1976, 112, 285.

246. S. Trofimenko, J. Amer. Chem. Soc., 1969, 91, 3183.

247. R.B. King and M.S. Saran, Inorg. Chem., 1974, 13, 2453.

248. J.W. Faller, C.-C. Chen, M.J. Mattina and A. Jakubowski, J. Organometal. Chem., 1973, 52, 361.

249. H. Friedel, I.W. Renk and H. tom Dieck, J. Organometal. Chem., 1971, 26, 247.

250. H. tom Dieck and H. Friedel, J.C.S. Chem. Comm., 1969, 411.

251. F. Hohmann, J. Organometal. Chem., 1977, 137, 315.

252. D.P. Tate, W.R. Knipple and J.M. Augl, Inorg. Chem., 1962, 1, 433.

253. F. Hohmann and H. tom Dieck, J. Organometal. Chem., 1975, 85, 47.

254. H. tom Dieck, F. Hohmann, M. Form, T. Mack and I.W. Renk, J. Less-Common Metals, 1977, 54, 221.

255. K.E. Paddick, Project Report 218, School of Chemistry, University of Bath, 1977.

256. B.J. Brisdon and M. Cartwright, J. Organometal. Chem., 1977, 128, C15.

257. B.J. Brisdon and M. Cartwright, J. Organometal. Chem., 1979, 164, 83.

258. R.S. Cahn, C. Ingold and V. Prelog, Angew. Chem. Int. Ed., Engl., 1966, 5, 385.

259. J. Lewis and R. Whyman, J. Chem. Soc., 1965, 6027.

260. P. Venkateswarlu, J. Chem. Phys., 1951, 19, 293.

261. P. Venkateswarlu, J. Chem. Phys., 1952, 20, 923.

262. B.N. Storhoff and H.C. Lewis, Co-ord. Chem. Rev., 1977, 23, 1.

263. R.A. Walton, Quart. Rev. Chem. Soc., 1965, 19, 126.

264. K.F. Purcell and R.S. Drago, J. Amer. Chem. Soc., 1966, 88, 919.

265. K.F. Purcell, J. Amer. Chem. Soc., 1967, 89, 247.

266. J.B. Milne, Can. J. Chem., 1970, 48, 75.

267. D.A. Edwards and J. Marshalsea, Syn. React. Inorg. Metal-Org. Chem., 1975, 5, 139.

268. J. Reedijk, A.P. Zuur and W.L. Groeneveld, Rec. Trav. Chim. Pays-Bas, 1967, 86, 1127.

269. P.S. Braterman, "Metal Carbonyl Spectra", Academic Press, London, 1975.

270. D.M. Adams, "Metal-Ligand and Related Vibrations", Edward Arnold Ltd., London, 1967.

271. C. Barbeau and J. Turcotte, Can. J. Chem., 1970, 48, 3583.

272. B.J. Brisdon, D.A. Edwards and J.W. White, J. Organometal. Chem., 1978, 161, 233.

273. I.E. Grey and P.W. Smith, Aust. J. Chem., 1969, 22, 1627.

274. B.J. Brisdon and M. Cartwright, Personal Communication.

275. R.J.H. Clark, Spectrochim. Acta, 1965, 21, 955.

276. B. Hutchinson and K. Nakamoto, Inorg. Chim. Acta, 1969, 3, 591.

277. R.A. Walton, Can. J. Chem., 1968, 46, 2347.

278. M.F. Farona, J.G. Grasselli and B.L. Ross, Spectrochim. Acta, 1967, 23A, 1875.

279. J.G. Dunn and D.A. Edwards, J. Organometal. Chem., 1971, 27, 73.

280. D.M. Byler and D.F. Shriver, Inorg. Chem., 1973, 12, 1412.

281. D.M. Byler and D.F. Shriver, Inorg. Chem., 1974, 13, 2697.

282. J. Reedijk and W.L. Groeneveld, Rec. Trav. Chim. Pays-Bas, 1968, 87, 1076.

283. J. Chatt and H.R..Watson, J. Chem. Soc., 1961, 4980.

284. A.M. Bond, R. Colton and J.J. Jackowski, Inorg. Chem., 1975, 14, 274.

285. A.P. Ginsberg and W.E. Lindsell, Inorg. Chem., 1973, 12, 1983.

286. J. Ellermann, H. Gäbelein and W. Uller, Z. anorg. Chem., 1975, 416, 117.

287. F.R. Young, R.A. Levenson, M.N. Memering and G.R. Dobson, Inorg. Chim. Acta, 1974, 8, 61.

288. J. Ellermann and H. Schössner, J. Organometal. Chem., 1976, 118, C69.

289. R. Colton and Q.N. Porter, Aust. J. Chem., 1968, 21, 2215.

290. R.B. King, J. Amer. Chem. Soc., 1968, 90, 1417.

291. M.S. Lupin and M. Cais, J. Chem. Soc. A, 1968, 3095.

292. R.J. Abraham, "The Analysis of High Resolution NMR Spectra", Elsevier, Amsterdam, 1971.

293. C. Sternhell, Quart. Rev. Chem. Soc., 1969, 23, 236.

294. R. Colton and C.J. Commons, Aust. J. Chem., 1973, 26, 1493.

295. C.J. Commons and B.F. Hoskins, Aust. J. Chem., 1975, 28, 1201.

296. R. Colton, Aust. J. Chem., 1976, 29, 1833.

297. M.W. Anker, R. Colton and I.B. Tomkins, Aust. J. Chem., 1968, 21, 1159.

298. R. Colton and M.J. McCormick, Aust. J. Chem., 1976, 29, 1657.

299. R. Colton and J.E. Gerrard, Aust. J. Chem., 1973, 26, 529.

300. R. Colton, Co-ord. Chem. Rev., 1971, 6, 269.

301. R. Colton and C.J. Rix, Aust. J. Chem., 1970, 23, 441.

302. M.G.B. Drew, A.W. Johans, A.P. Wolters and I.B. Tomkins, J.C.S. Chem. Comm., 1971, 819.

303. D.J. Bevan and R.J. Mawby, J.C.S. Dalton Trans., 1980, 1904.

304. G.M. Sheldrick, Personal Communication.

305. "International Tables for X-ray Crystallography", Kynoch Press, Birmingham, 1975, Vol. 4.

306. K. Fukushima, T. Miyamoto and Y. Saski, J. Organometal. Chem., 1976, 107, 265.

307. J.C. Dewan, K. Henrick, D.L. Kepert, K.R. Trigwell, A.H. White and S.B. Wild, J.C.S. Dalton Trans., 1975, 546.

308. R. Hoffmann, B.F. Beier, E.L. Muetterties and A.R. Rossi, Inorg. Chem., 1977, 16, 511.

309. M.G.B. Drew, Progr. Inorg. Chem., 1977, 23, 67.

310. M.A. Bush, A.D.V. Hardy, Lj. Manojlovic-Muir and G.A. Sim., J. Chem. Soc. A, 1971, 1003.

311. M.G.B. Drew, J.C.S. Dalton Trans., 1972, 1329.

312. F.W.B. Einstein and J.S. Field, J.C.S. Dalton Trans, 1975, 1628.

313. S. Chaiwasie and R.H. Fenn, Acta Crystallogr., 1968, 24B, 525.

314. S.S. Wreford, J.K. Kouba, J.F. Kirner, E.L. Muetterties, I. Travanaiepour and V.W. Day, J. Amer. Chem. Soc., 1980, 102, 1558.

315. A.D.U. Hardy and G.A. Sim, J.C.S. Dalton Trans., 1972, 1900.

316. I.B. Benson, S.A.R. Knox, P.J. Naish and A.J. Welch, J.C.S. Chem. Comm., 1978, 878.

317. C.A. Tolman, Chem. Rev., 1977, 77, 313.

318. A.R. Manning, J. Chem. Soc. A, 1967, 1984.

319. D. Steele, Quart. Rev. Chem. Soc., 1964, 18, 21.

320. P.S. Braterman, D.W. Milne, E.W. Randall and E. Rosenberg, J.C.S. Dalton Trans., 1973, 1027.

321. G.W. Flynn and J.D. Balderschwieler, J. Chem. Phys., 1963, 38, 226.

322. H.S. Gutowsky and C.H. Holm, J. Chem. Phys., 1956, 25, 1228.

323. S.O. Grim, Inorg. Nucl. Chem. Letts., 1968, 4, 187.

324. P. Meakin, L.J. Guggenberger, F.N. Tebbe and J.P. Jesson, Inorg. Chem., 1974, 13, 1025.

325. W.J. Geary, Co-ord. Chem. Rev., 1971, 7, 81.

326. S. Datta, B. Dezube, J.K. Kouba and S.S. Wreford, J. Amer. Chem. Soc., 1978, 100, 4404.

327. A.P. Ginsberg and M.E. Tully, J. Amer. Chem. Soc., 1973, 95, 4749.

328. L.D. Brown, S. Datta, J.K. Kouba, L.K. Smith and S.S. Wreford, Inorg. Chem., 1978, 17, 729.

329. J.O. Albright, S. Datta, J.K. Kouba, L.K. Smith, S.S. Wreford, J. Amer. Chem. Soc., 1979, 101, 611.

330. J.W. Byrne, J.R.M. Kress, J.A. Osborn, L. Ricard and R.E.Weiss, J.C.S. Chem. Comm., 1977, 662.

331. D. Britton and J.D. Dunitz, Acta Crystallogr., 1973, 29A, 362.

332. R.J. Gillespie, Can. J. Chem., 1960, 38, 818.

333. D. Britton, Can. J. Chem., 1963, 41, 1632.

334. T.A. Claxton and G.C. Benson, Can. J. Chem., 1966, 44, 157.

335. H.B. Thompson and L.S. Bartell, Inorg. Chem., 1968, 7, 488.

336. E.L. Muetterties and L.J. Guggenberger, J. Amer. Chem. Soc., 1974, 96, 1748.

337. F.G. Moers and J.G.A. Ruevers, Rec. Trav. Chim. Pays-Bas, 1974, 93, 246.

338. R.K. Harris, Can. J. Chem., 1964, 42, 2275.

339. R. Mattieu, Inorg. Chem., 1970, 9, 2030.

340. M. Arresta and A. Sacco, Gazz. Chim. Ital., 1972, 102, 755.

341. E.O. Fischer and E. Louis, J. Organometal. Chem., 1969, 18, P26.

342. M. Hidai, K. Tominari and Y. Uchida, J. Amer. Chem. Soc., 1972, 94, 110.

343. J.M. Jenkins and B.L. Shaw, J. Chem. Soc. A, 1966, 720.

344. R.D. Bertrand, P. Ogilivie and J.G. Verkade, J. Amer. Chem. Soc., 1970, 92, 1908.

345. F.B. Ogilivie, J.M. Jenkins and J.F. Verkade, J. Amer. Chem. Soc., 1970, 92, 1916.

346. C.A. McAuliffe and W. Levason, 'Phosphine, Arsine and Stibine Complexes of the Transition Elements', Elsevier, London 1979.

347. C.A. Streuli, Anal. Chem., 1960, 32, 985.

348. W. Strohmeier and F.J. Muller, Chem. Ber., 1967, 100, 2812.

349. M. Boyer, J.C. Daran and Y. Jeanin, Abstr., 9th International Conf. of Organometal. Chem. Dijon, France, September 3-7, 1979, No. P36W.

350. D.A. White, Organometal. Chem. Rev. Sec. A, 1968, 3, 497.

351. J.A. McCleverty and A.J. Murray, Transition Met. Chem., 1979, 4, 273.

352. D.A. Clark, D.L. Jones and R.J. Mawby, J.C.S. Dalton Trans., 1980, 565.

353. J.M. Jenkins, J.R. Moss and B.L. Shaw, J. Chem. Soc. A, 1969, 2796.

354. T.A. George and C.D. Seibold, Inorg. Chem., 1973, 12, 2548.

355. E.E. Isaacs and W.A.G. Graham, Inorg. Chem., 1975, 14, 2560.

356. B. Bell, J. Chatt and G.J. Leigh, J.C.S. Dalton Trans., 1972, 2492.

357. A. Finch, P.N. Gates, K. Radcliffe, F.N. Dickson and F.F. Bentley, 'Chemical Applications of Far Infrared Spectroscopy', Academic Press, 1970.

358. L.E. Orgel, Inorg Chem., 1962, 1, 25.

359. R. Poilblanc and M. Bigorgne, Bull. Soc. Chim. France, 1962, 1301.

360. F.A. Cotton, Inorg Chem., 1964, 3, 702.

361. R. Poilblanc and M. Bigorgne, J. Organometal. Chem., 1966, 5, 93.

362. F.A. Cotton, J. Organometal. Chem., 1966, 5, 293.

363. D.M. Adams and A. Squire, J. Chem. Soc. A, 1970, 814.

364. D.M. Adams and A. Squire, J. Organometal. Chem., 1973, 63, 381.

365. S.F.A. Kettle and I. Paul, J.C.S. Dalton Trans., 1974, 2293.

366. H. Gabelein and J. Ellermann, J. Organometal. Chem., 1978, 156, 389.

367. G.R. Dobson and R.A Brown, J. Inorg. Nucl. Chem., 1972, 34, 2785.

368. A.R. Manning, J. Chem. Soc. A , 1971, 106.

369. D.A. Edwards and J. Marshalsea, J. Organometal. Chem., 1977, 131, 73.

370. D.M. Adams, J. Chem. Soc., 1964, 1771.

371. J.A. Bowden, R. Colton and C.J. Commons, Aust. J. Chem., 1973, 26, 655.